

Tech Div

92-832



NATIONAL ADVISORY COMMITTEE FOR AERONAUTICS

REPORT No. 832

A SYSTEMATIC INVESTIGATION OF PRESSURE DISTRIBUTIONS AT HIGH SPEEDS OVER FIVE REPRESENTATIVE NACA LOW-DRAG AND CONVENTIONAL AIRFOIL SECTIONS

By DONALD J. GRAHAM, GERALD E. NITZBERG
and ROBERT N. OLSON



TECHNICAL LIBRARY
AIRESEARCH MANUFACTURING CO.
9851-9951 SEPULVEDA BLVD.
LOS ANGELES 45, CALIF.
CALIFORNIA

1945

AERONAUTIC SYMBOLS

1. FUNDAMENTAL AND DERIVED UNITS

	Symbol	Metric		English	
		Unit	Abbrevia- tion	Unit	Abbrevia- tion
Length.....	<i>l</i>	meter.....	m	foot (or mile).....	ft (or mi)
Time.....	<i>t</i>	second.....	s	second (or hour).....	sec (or hr)
Force.....	<i>F</i>	weight of 1 kilogram.....	kg	weight of 1 pound.....	lb
Power.....	<i>P</i>	horsepower (metric).....		horsepower.....	hp
Speed.....	<i>V</i>	{kilometers per hour..... meters per second.....	{kph mps	{miles per hour..... feet per second.....	{mph fps

2. GENERAL SYMBOLS

<p>W Weight=mg</p> <p>g Standard acceleration of gravity=9.80665 m/s^2 or 32.1740 ft/sec^2</p> <p>m Mass=$\frac{W}{g}$</p> <p>I Moment of inertia=mk^2. (Indicate axis of radius of gyration k by proper subscript.)</p> <p>μ Coefficient of viscosity</p>	<p>ν Kinematic viscosity</p> <p>ρ Density (mass per unit volume) Standard density of dry air, $0.12497 \text{ kg-m}^{-3}\text{-s}^2$ at 15° C and 760 mm; or $0.002378 \text{ lb-ft}^{-4} \text{ sec}^2$ Specific weight of "standard" air, 1.2255 kg/m^3 or 0.07651 lb/cu ft</p>
--	---

3. AERODYNAMIC SYMBOLS

<p>S Area</p> <p>S_w Area of wing</p> <p>G Gap</p> <p>b Span</p> <p>c Chord</p> <p>A Aspect ratio, $\frac{b^2}{S}$</p> <p>V True air speed</p> <p>q Dynamic pressure, $\frac{1}{2}\rho V^2$</p> <p>L Lift, absolute coefficient $C_L = \frac{L}{qS}$</p> <p>D Drag, absolute coefficient $C_D = \frac{D}{qS}$</p> <p>D_0 Profile drag, absolute coefficient $C_{D_0} = \frac{D_0}{qS}$</p> <p>D_i Induced drag, absolute coefficient $C_{D_i} = \frac{D_i}{qS}$</p> <p>D_p Parasite drag, absolute coefficient $C_{D_p} = \frac{D_p}{qS}$</p> <p>C Cross-wind force, absolute coefficient $C_C = \frac{C}{qS}$</p>	<p>i_w Angle of setting of wings (relative to thrust line)</p> <p>i_t Angle of stabilizer setting (relative to thrust line)</p> <p>Q Resultant moment</p> <p>Ω Resultant angular velocity</p> <p>R Reynolds number, $\rho \frac{Vl}{\mu}$ where l is a linear dimen- sion (e.g., for an airfoil of 1.0 ft chord, 100 mph, standard pressure at 15° C, the corresponding Reynolds number is 935,400; or for an airfoil of 1.0 m chord, 100 mps, the corresponding Reynolds number is 6,865,000)</p> <p>α Angle of attack</p> <p>ϵ Angle of downwash</p> <p>α_0 Angle of attack, infinite aspect ratio</p> <p>α_i Angle of attack, induced</p> <p>α_a Angle of attack, absolute (measured from zero- lift position)</p> <p>γ Flight-path angle</p>
--	---

REPORT No. 832

**A SYSTEMATIC INVESTIGATION OF PRESSURE
DISTRIBUTIONS AT HIGH SPEEDS OVER
FIVE REPRESENTATIVE NACA LOW-DRAG AND
CONVENTIONAL AIRFOIL SECTIONS**

**By DONALD J. GRAHAM, GERALD E. NITZBERG
and ROBERT N. OLSON**

**Ames Aeronautical Laboratory
Moffett Field, Calif.**

National Advisory Committee for Aeronautics

Headquarters, 1500 New Hampshire Avenue NW., Washington 25, D. C.

Created by act of Congress approved March 3, 1915, for the supervision and direction of the scientific study of the problems of flight (U. S. Code, title 49, sec. 241). Its membership was increased to 15 by act approved March 2, 1929. The members are appointed by the President, and serve as such without compensation.

JEROME C. HUNSAKER, Sc. D., Cambridge, Mass., *Chairman*

LYMAN J. BRIGGS, Ph. D., <i>Vice Chairman</i> , Director, National Bureau of Standards.	AUBREY W. FITCH, Vice Admiral, United States Navy, Deputy Chief of Naval Operations (Air), Navy Department.
CHARLES G. ABBOT, Sc. D., <i>Vice Chairman, Executive Committee</i> , Secretary, Smithsonian Institution.	WILLIAM LITTLEWOOD, M. E., Jackson Heights, Long Island, N. Y.
HENRY H. ARNOLD, General, United States Army, Commanding General, Army Air Forces, War Department.	FRANCIS W. REICHELDERFER, Sc. D., Chief, United States Weather Bureau.
WILLIAM A. M. BURDEN, Assistant Secretary of Commerce for Aeronautics.	LAWRENCE B. RICHARDSON, Rear Admiral, United States Navy, Assistant Chief, Bureau of Aeronautics. Navy Department.
VANNEVAR BUSH, Sc. D., Director, Office of Scientific Research and Development, Washington, D. C.	EDWARD WARNER, Sc. D., Civil Aeronautics Board, Washington, D. C.
WILLIAM F. DURAND, Ph. D. Stanford University, California.	ORVILLE WRIGHT, Sc. D., Dayton, Ohio.
OLIVER P. ECHOLS, Major General, United States Army, Chief of Matériel, Maintenance, and Distribution, Army Air Forces, War Department.	THEODORE P. WRIGHT, Sc. D., Administrator of Civil Aeronautics, Department of Commerce.

GEORGE W. LEWIS, Sc. D., *Director of Aeronautical Research*

JOHN F. VICTORY, LL. M., Secretary

HENRY J. E. REID, Sc. D., Engineer-in-Charge, Langley Memorial Aeronautical Laboratory, Langley Field, Va.

SMITH J. DEFRANCE, B. S., Engineer-in-Charge, Ames Aeronautical Laboratory, Moffett Field, Calif.

EDWARD R. SHARP, LL. B., Manager, Aircraft Engine Research Laboratory, Cleveland Airport, Cleveland, Ohio

CARLTON KEMPER, B. S., Executive Engineer, Aircraft Engine Research Laboratory, Cleveland Airport, Cleveland, Ohio

TECHNICAL COMMITTEES

AERODYNAMICS

OPERATING PROBLEMS

POWER PLANTS FOR AIRCRAFT

MATERIALS RESEARCH COORDINATION

AIRCRAFT CONSTRUCTION

Coordination of Research Needs of Military and Civil Aviation

Preparation of Research Programs

Allocation of Problems

Prevention of Duplication

LANGLEY MEMORIAL AERONAUTICAL LABORATORY

Langley Field, Va.

AMES AERONAUTICAL LABORATORY

Moffett Field, Calif.

AIRCRAFT ENGINE RESEARCH LABORATORY, Cleveland Airport, Cleveland, Ohio

Conduct, under unified control, for all agencies, of scientific research on the fundamental problems of flight

OFFICE OF AERONAUTICAL INTELLIGENCE, Washington, D. C.

Collection, classification, compilation, and dissemination of scientific and technical information on aeronautics

E R R A T A

NACA REPORT NO. 832

A SYSTEMATIC INVESTIGATION OF PRESSURE DISTRIBUTIONS AT HIGH SPEEDS OVER
FIVE REPRESENTATIVE NACA LOW-DRAG AND CONVENTIONAL AIRFOIL SECTIONS

By Donald J. Graham, Gerald E. Nitzberg, and Robert N. Olson

1945

Page 3, column 2, last line: Substitute "less" for "more".

Page 33, figure 6(f), key: Replace the last two lines with

▽ M = 0.760

△ M = 0.787

△ M = 0.818

REPORT No. 832

A SYSTEMATIC INVESTIGATION OF PRESSURE DISTRIBUTIONS AT HIGH SPEEDS OVER FIVE REPRESENTATIVE NACA LOW-DRAG AND CONVENTIONAL AIRFOIL SECTIONS

By DONALD J. GRAHAM, GERALD E. NITZBERG, and ROBERT N. OLSON

SUMMARY

Pressure distributions determined from high-speed wind-tunnel tests are presented for five NACA airfoil sections representative of both low-drag and conventional types. Section characteristics of lift, drag, and quarter-chord pitching moment are presented along with the measured pressure distributions for the NACA 65₂-215 ($a=0.5$), 66,2-215 ($a=0.6$), 0015, 23015, and 4415 airfoils for Mach numbers up to approximately 0.85. A critical study is made of the airfoil pressure distributions in an attempt to formulate a set of general criteria for defining the character of high-speed flows over typical airfoil shapes. Comparisons are made of the relative characteristics of the low-drag and conventional airfoils investigated insofar as they would influence the high-speed performance and the high-speed stability and control characteristics of airplanes employing these wing sections.

At Mach numbers where the local velocities over an airfoil are entirely subsonic, airfoil pressure distributions may generally be predicted satisfactorily from the corresponding low-speed pressure distributions by means of the Kármán-Tsien compressibility relation. At higher Mach numbers for which but limited regions of local supersonic flow exist, supercritical pressure distributions may be related qualitatively to the low-speed pressure distributions.

The low-drag-type airfoil, as exemplified in the present investigation by the NACA 65₂-215 ($a=0.5$) and 66,2-215 ($a=0.6$) sections, constitutes an improvement over the conventional type airfoil of equal thickness when employed on the wing sections of high-speed airplanes, in that it would promote more favorable airplane stability and control characteristics at supercritical speeds. Contrary to popular expectations, however, the low-drag airfoil is but slightly better than the conventional section as regards supercritical speed drag characteristics.

INTRODUCTION

Fundamental aerodynamic theory has been found to be fully adequate in defining the essential character of general low-speed air flows. Such a vast amount of engineering formulation has been amassed from research both theoretical and experimental on the characteristics of aerodynamic bodies subjected to low-speed air flows that the practical aerodynamicist has little difficulty in designing aircraft for efficient operation in this realm of flight. In the region of moderate- and high-speed flight, however, where fluid compressibility becomes an important factor, the extent of

knowledge of the character of air flows is very limited. The basic theory which treats low-speed flows so satisfactorily fails to define high-speed flows. Attempts have been made by many investigators to modify the classical aerodynamic theory for the effects of fluid compressibility so as to permit a logical understanding of high-speed air flows. The most familiar of these modifications are the Prandtl-Glauert and the Kármán-Tsien relations for predicting the velocity or pressure fields at compressibility speeds about airfoils from their known low-speed velocity or pressure distributions. These theoretical relations have been satisfactorily verified by experiments on airfoils at speeds up to their critical velocities, that is, the stream velocities corresponding to the first attainment of the velocity of sound locally on the airfoil surfaces. As the critical speed of an airfoil is exceeded, however, and the local velocities over the surface exceed the speed of sound, abrupt discontinuities occur in the flow which cause the basic theories and existing compressibility modifications thereof to fail. The critical speed, then, appears to be the upper limit of the speed range in which the Prandtl-Glauert and Kármán-Tsien modifications to the basic aerodynamic theory are applicable.

Although the character of low-speed flows is well understood and moderately high-speed flows can apparently be dealt with satisfactorily by means of existing modifications to classical theories, very little is known about the fundamental mechanism of air flows at supercritical velocities. Not only is the aerodynamicist at a loss to understand the character of supercritical speed flows, but until very recently the information available to him on the nature of the forces and moments on aerodynamic bodies subjected to such flows has been extremely meager. In recognition of the acute need for experimental data on the physical phenomena associated with the attainment of supercritical velocity flows over airfoils, and of the need for a more thorough understanding of the character of high subcritical velocity flows, the present investigation was undertaken.

Tests were made in the Ames 1- by 3½-foot high-speed wind tunnel to determine the pressure distributions at high speeds over the NACA 65₂-215 ($a=0.5$), 66,2-215 ($a=0.6$), 0015, 23015, and 4415 airfoil sections. The airfoils were selected as being representative of each of several types of airfoils widely employed in the design of aircraft; the NACA 65₂-215 ($a=0.5$) and 66,2-215 ($a=0.6$) being typical low-drag airfoils with different positions of minimum pressure;

the NACA 0015, a symmetrical conventional airfoil; the NACA 23015, a typical forward cambered conventional airfoil; and the NACA 4415, a typical highly positive cambered conventional airfoil. A critical study is made of the pressure distributions and aerodynamic characteristics of the airfoil sections investigated in the hope of obtaining a sufficient understanding of high-speed flows to permit the prediction of the behavior at supercritical speeds of other airfoil sections falling within the same general classification scheme.

SYMBOLS

a	mean line designation, fraction of chord from leading edge over which design load is uniform; in derivation of thickness distributions, basic length usually considered unity
c	airfoil chord
c_d	section drag coefficient
c_l	section lift coefficient
$c_{m_{c/4}}$	section moment coefficient about quarter-chord point
$dc_l/d\alpha_0$	section lift-curve slope, per degree
M	free-stream Mach number
p	local static pressure, pounds per square foot
p_0	free-stream static pressure, pounds per square foot
P	pressure coefficient $\left(\frac{p-p_0}{q_0}\right)$
P_l	local pressure coefficient on lower surface of airfoil section
P_u	local pressure coefficient on upper surface of airfoil section
q_0	free-stream dynamic pressure, pounds per square foot
x	distance along chord
α	angle of attack
α_0	section angle of attack

APPARATUS AND METHODS

The tests were conducted in the Ames 1- by 3½-foot high-speed wind tunnel, a low-turbulence, two-dimensional-flow wind tunnel powered by two electric motors of 1,000 horsepower—sufficient power to obtain choked flow with any size of model.

Six-inch-chord models of the NACA 65₂-215 ($a=0.5$), 66,2-215 ($a=0.6$), 0015, 23015, and 4415 airfoils were constructed of duralumin and steel for the tests. The models were equipped with from 30 to 32 pressure orifices of 0.008-inch diameter drilled perpendicularly to the airfoil surfaces at standard chordwise stations. The airfoils were mounted, as illustrated in figure 1, so as to span completely the 1-foot width of the tunnel test section, and were supported in tight-fitting plates contoured to the airfoil surfaces and sealed with rubber gaskets to eliminate air leakage about the ends of the airfoils. Wind-tunnel tests have indicated that end leakage must be prevented if two-dimensional-flow conditions are to be realized. To facilitate construction of the models, the plane of pressure measurements was chosen midway between one side wall and the center of the tunnel. Previous tests have shown no differences in airfoil pressures measured in this plane and in the plane of symmetry.

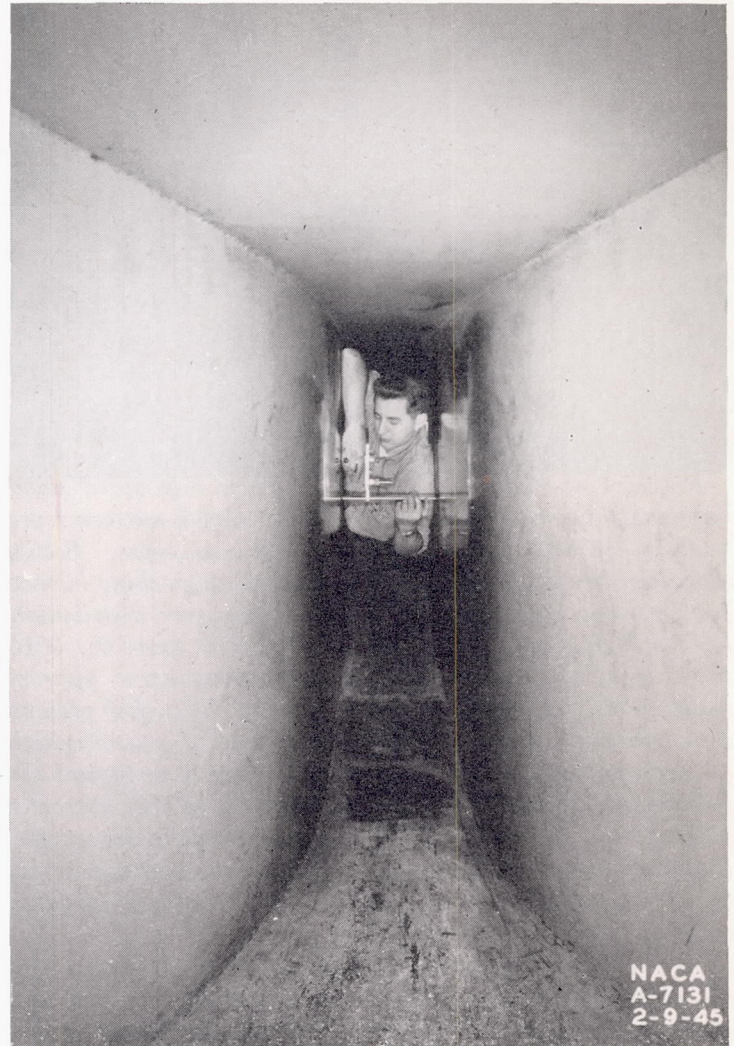


FIGURE 1.—Airfoil model mounted in the test section of the Ames 1- by 3½-foot high-speed wind tunnel.

Simultaneous measurements of airfoil pressure distribution, drag, and in the cases of the NACA 0015 and 4415 airfoils, lift and quarter-chord pitching moment were made for angles of attack ranging from -6° to 16° by 2° increments at speeds from 0.3 Mach number to approximately 0.85 Mach number, the choking speed of the wind tunnel for these tests. The corresponding Reynolds numbers ranged from approximately 1,000,000 to 2,000,000.

Airfoil pressures were measured by means of multiple-tube manometers, tetrabromoethane being used as the manometer fluid whenever possible to maintain a high degree of accuracy of measurement. For the higher pressures, mercury served as the manometer fluid. Liquid heights were recorded photographically to insure the simultaneous measurement of all pressures. Airfoil drag was measured by means of wake surveys made with a movable rake of total-head tubes.

In the cases of the NACA 0015 and 4415 airfoils, lift and quarter-chord pitching moments were obtained directly from measurements of the reactions on the tunnel walls of the forces experienced by the airfoils. Previous wind-tunnel tests have demonstrated very satisfactory agreement between characteristics determined from wall-reaction measurements and those derived from simultaneously measured airfoil pressure distributions.

TEST RESULTS

In figures 2 to 6, inclusive, appear the pressure distributions for the NACA 65₂-215 ($a=0.5$), 66,2-215 ($a=0.6$), 0015, 23015, and 4415 airfoil sections in that order. In these figures pressure coefficient P is plotted as a function of the chordwise location of the airfoil pressure orifices for constant angles of attack and varying Mach number. Corrections to the pressure coefficients and angles of attack for tunnel-wall-interference effects calculated by the method of reference 1 proved to be negligible for the size of model tested and have therefore not been applied to the pressure-distribution data. The stream velocities, however, have been corrected for tunnel-wall effects by the method of reference 1. Broken lines were used in figures 2 to 6 wherever the stream velocities were within 0.025 Mach number of the choking speed of the wind tunnel. Under such conditions, where present tunnel-wall-correction methods are invalid, it is doubtful whether the measured pressure distributions are truly representative of free-air characteristics.

For the convenience of the aircraft designer, values of the airfoil section load parameter $P=P_l-P_u$, where P_l and P_u are the local pressure coefficients on the upper and lower surfaces, respectively, at a given chordwise station of the airfoil, are tabulated for the five airfoils in tables I to V, inclusive, for the ranges of angles of attack and Mach numbers investigated.

In figures 7 through 11, pressure coefficients at the 2.5-percent-chord station for the surface having the minimum local pressure are plotted as a function of free-stream Mach number for angles of attack of -4° , -2° , 0° , 2° , 4° , and 8° for the NACA 65₂-215 ($a=0.5$), 66,2-215 ($a=0.6$), 0015, 23015, and 4415 airfoil sections, respectively. These figures are presented to show that a marked change in the character of the flow over an airfoil occurs after the airfoil critical speed has been exceeded.

The variation of section lift coefficient with Mach number at constant angles of attack from -6° to 10° is shown in figures 12 through 16 for the five airfoils in the previously mentioned sequence. For the NACA 65₂-215 ($a=0.5$), 66,2-215 ($a=0.6$), and 23015 profiles, the lift coefficients were obtained by integrating the measured pressure distributions. For the NACA 0015 and 4415 sections, the lift coefficients shown were calculated from wall-reaction force tests made simultaneously with the pressure-distribution measurements. This method, as mentioned previously, produces results as accurate as those derived from the pressure distributions without the tedious integration procedures involved in the latter method.

On each of the figures 12 through 16 are plotted theoretical airfoil critical speeds, taken from reference 2, for comparison with the experimental critical speeds determined from the measured pressure distributions by the method outlined in reference 3. In the belief that they are of greater significance than critical speeds in marking the onset of abrupt adverse changes in airfoil characteristics at compressibility speeds, Mach numbers of lift and drag divergence, appropriately defined hereinafter, are also plotted on each of these figures. The Mach number of lift divergence for a given angle of attack is defined in this report as the lowest value of the

Mach number corresponding to an inflection point on the curve of lift coefficient against Mach number. The value of the Mach number at which the slope of the curve of drag coefficient against Mach number becomes equal to 0.10 is arbitrarily defined as the Mach number of drag divergence.

The drag-divergence Mach numbers indicated in figures 12 through 16 were taken from the plots (figs. 17 to 21, incl.) of section drag coefficient against Mach number at constant angles of attack for the respective airfoils investigated. Drag coefficients were computed from the wake-survey measurements.

The variation of section quarter-chord pitching-moment coefficient with Mach number for the five airfoils is illustrated in figures 22 through 24 for angles of attack from -6° to 10° . Except in the case of the NACA 0015 and 4415 airfoils, where the pitching moments were determined from wall-reaction measurements, the values of section pitching-moment coefficients were derived from integrated pressure distributions.

The airfoil section characteristics of lift, drag, and pitching moment reported herein have been completely corrected for tunnel-wall interference by the method of reference 1. The dashed lines at the high-speed extremities of the curves of figures 12 to 24, inclusive, were used to indicate that characteristics observed in the vicinity of the choking velocity of the wind tunnel are of questionable validity.

In figures 25 through 29, cross plots of the variation of section lift coefficient with angle of attack at constant Mach number are shown for the respective airfoils. The variations of section drag and pitching-moment coefficients with section lift coefficient are presented in figures 30 to 34 and 35 to 39, respectively. Data obtained within 0.025 Mach number of the choking Mach number are again indicated by dashed lines.

DISCUSSION

The study of the large number of pressure distributions obtained in the course of the present investigation may perhaps be facilitated by considering the characteristic differences of flows which are entirely subsonic and those which consist of mixed subsonic and supersonic local velocities. As a first step in this direction several representative pressure distributions, shown in figure 2 (a), for the NACA 65₂-215 ($a=0.5$) airfoil at -6° angle of attack will be discussed. Considering the subcritical case, where the flow is entirely subsonic, the growth in pressure coefficient corresponding to the increase in Mach number from 0.300 to 0.501, for the pressure distributions of figure 2 (a), is in good agreement with what would be predicted by the Kármán-Tsien theory. The pressure coefficient at the lower surface 2.5-percent-chord station noted for the 0.501 Mach number corresponds to a local velocity which is slightly supersonic. Pressure distributions observed at Mach numbers above 0.50, then, fall within the supercritical category.

The characteristics of pressure distributions are more complex at supercritical than at subcritical Mach numbers. Referring again to figure 2 (a), as the Mach number rises to 0.626, the lower-surface minimum-pressure coefficient becomes more negative and attains a value which corresponds

less

to a local Mach number of about 1.5. At this free-stream Mach number the supersonic flow over the forward 10 percent of the airfoil chord on the lower surface is terminated by an abrupt pressure recovery, indicative of a shock wave. Over the remainder of the airfoil surface the flow is subsonic and the pressure coefficients are still in good agreement with those which would be predicted from the low-speed measurements. When the free-stream Mach number is increased still further, the lower-surface pressure-coefficient peak becomes less negative and the portion of the airfoil surface over which the local velocities are supersonic increases in length. At a Mach number of 0.757 the experimental pressure distribution shows that there are supersonic velocities over the forward 50 percent of the lower surface, and over the upper surface from the 40- to the 60-percent-chord stations. The pressure coefficients measured behind these supersonic regions are somewhat more negative than would be predicted by the Kármán-Tsien theory, a difference which becomes greater when the free-stream Mach number is increased above 0.757.

The description which has just been presented applies to a specific airfoil section at a specific angle of attack. Figures 2 through 6 show that the variation of the pressure distributions with Mach number is considerably different for other airfoil sections and angles of attack. In all these cases, however, the effect of compressibility at subcritical speeds is to change the pressure distribution with Mach number in a manner which is adequately represented, except very near the airfoil leading edge, by the Kármán-Tsien compressibility correction. It can therefore be said that a satisfactory understanding of airfoil pressure distributions at subcritical Mach numbers has been achieved.

The nature of supersonic flow being fundamentally different from subsonic flow, the pressure distribution over that portion of the airfoil where the local flow velocities are supersonic cannot be expected to be directly related to the local low-speed pressure distribution. A study of the pressure-distribution data presented in this report reveals that, outside the local region of supersonic flow, there is a general resemblance between the supercritical and the subcritical pressure distributions for the same airfoil. This fact provides valuable assistance in studying those pressure distributions, characteristic of small angles of attack, for which the region of supersonic flow does not begin until some distance from the airfoil leading edge. Another factor of assistance in the analysis at these angles is a general similarity of the shape of the supersonic portion of the pressure distribution for all five airfoils investigated.

An analysis of the particular type of pressure distribution characteristic of small angles of attack revealed that the subsonic portion of supercritical pressure distributions could be related to the subcritical pressure distribution for the same airfoil at a reduced angle of attack. This relationship is not surprising since figures 12 through 16 indicate that marked changes in the airfoil circulation occur after the critical speed is exceeded. At small angles of attack the shape of the supersonic portion of the supercritical pressure distribution resembles that which would be calculated by the Prandtl-Meyer supersonic theory; however, the magni-

tude of the measured chordwise pressure variation is less than that calculated. Such theoretical calculations are invalid at subsonic-stream Mach numbers where the local supersonic region is of limited extent. Development of a theory treating the effects of supersonic regions of limited extent is beyond the scope of the present report.

A major difficulty arises in the treatment of pressure distributions at large angles of attack in that supersonic velocities occur in the immediate vicinity of the airfoil leading edge in which region, as has been mentioned, available theories are inadequate. An understanding of the nature of the variation of pressure coefficients with Mach number in the immediate vicinity of the airfoil leading edge at supercritical Mach numbers is basic to a quantitative analysis of supercritical pressure distributions. In order to study conditions near the airfoil leading edge, consider the variation of pressure coefficient with Mach number at the 2½-percent-chord station, the most forward station at which pressure coefficients were measured in the present study. These data are shown in figures 7 through 11. It is observed in every case that, at free-stream Mach numbers somewhat above the critical, a relatively constant local Mach number is maintained while the free-stream Mach number is increasing. This constant local Mach number apparently can be either subsonic or supersonic but there is no evident relationship between its magnitude and the value of the low-speed pressure coefficient. No satisfactory explanation has as yet been developed to permit a quantitative assessment of this behavior. However, the data of the present investigation are sufficient to permit a qualitative formulation of the characteristics of supercritical pressure distributions.

In studying supercritical pressure distributions it soon becomes apparent that the pressure coefficients over the rear portion of the airfoils at large Mach numbers are affected by some factor not previously considered. It was observed that a marked decrease occurs in the pressures over the rear portion of the airfoil with increasing Mach number only after the drag coefficient exceeds a value of about 0.05. A similar change in pressure distributions occurs at low speeds for increasing angles of attack in the vicinity of maximum lift. This latter change is known to be the result of a marked local increase in boundary-layer thickness. Moreover, the low-speed drag coefficient at maximum lift is of the magnitude of 0.05 for Reynolds numbers comparable to those of the present tests (1,000,000 to 2,000,000). It therefore seems likely that the local pressure distribution changes over the rear portion of airfoils at high supercritical speeds are a result of marked local boundary-layer growth. Because of the complexity of this phenomenon, the following discussion will be restricted to those Mach numbers for which boundary-layer effects are of secondary importance.

The general behavior with increasing Mach number of the supersonic region of the pressure distributions over the airfoils tested appears to be directly related to the shape of the pressure distribution at the critical Mach number. The shapes of pressure distributions at the critical speed can be classified into five types: (1) a sharp pressure peak with moderate minimum pressure at the nose of the airfoil, typical for low-drag airfoils at lift coefficients immediately

outside the low-drag-coefficient range; (2) nearly constant pressures over the forward portion of the airfoil, typical for low-drag airfoils at lift coefficients within the low-drag-coefficient range; (3) large negative pressure coefficients at the nose of the airfoil, typical for large additional lift coefficients; (4) minimum pressure ahead of about the quarter-chord station followed by gentle pressure recovery, typical for conventional airfoils at small angles of attack; and (5) rounded pressure peak at airfoil nose, typical for conventional airfoils at moderate angles of attack. The characteristics of each of these types will now be discussed individually. It should be borne in mind that the analysis is based only on measurements at moderate Reynolds numbers on airfoil sections of 15-percent-chord thickness so that numerical values stated may be different for thinner or thicker sections.

The abrupt forward peak of the type 1 pressure distribution occurs for low-drag airfoils at moderate positive and negative angles of attack and for conventional airfoils with camber far forward, such as the NACA 23015, at moderate negative angles of attack. The following table lists the cases of this type found in the figures of the present data together with the experimentally determined critical Mach number and also the upper limit of Mach number for which this pressure distribution classification can be used, namely, the Mach number M_1 at which the drag coefficient attains the value of 0.05:

Airfoil Section	Angle of Attack (deg)	Fig. No.	Critical Mach Number, M_{cr}	Mach Number	
				M_1 for $c_d=0.05$	M_1-M_{cr}
65 ₂ -215	-6	2(a)	0.46	0.73	0.27
65 ₂ -215	-4	2(b)	.57	.78	.21
65 ₂ -215	8	2(h)	.47	.66	.19
66, 2-215	-6	3(a)	.46	.74	.28
66, 2-215	-4	3(b)	.58	.79	.21
66, 2-215	6	3(g)	.52	.71	.19
66, 2-215	8	3(h)	.46	.68	.22
23015	-6	5(a)	.50	.73	.23
23015	-4	5(b)	.56	.79	.23

It is seen that for type 1 pressure distributions the critical Mach number is low, in the neighborhood of 0.5, and with increasing Mach number the drag rises relatively slowly so that M_1 is between 0.19 and 0.28 above the critical Mach number. Within this supercritical Mach number range, as the Mach number is increased the minimum pressure coefficient becomes less negative and the chordwise extent of the supersonic portion of the pressure distribution increases until at M_1 the pressure coefficients over the forward third or half of the airfoil are relatively constant.

The low-drag pressure distribution of type 2 has the same general shape at supercritical speeds as at subcritical speeds. The following configurations are of this type:

Airfoil Section	Angle of Attack (deg)	Fig. No.	Critical Mach Number, M_{cr}	Mach Number	
				M_1 for $c_d=0.05$	M_1-M_{cr}
65 ₂ -215	-2	2 (e)	0.66	0.80	0.14
65 ₂ -215	0	2 (d)	.67	.81	.14
65 ₂ -215	2	2 (e)	.65	.77	.12
65 ₂ -215	4	2 (f)	.62	.72	.10
66, 2-215	-2	3 (e)	.70	.80	.10
66, 2-215	0	3 (d)	.69	.81	.12
66, 2-215	2	3 (e)	.67	.82	.15
66, 2-215	4	3 (f)	.62	.74	.12

For pressure distributions of this type the critical Mach number is high, and above this critical Mach number the drag rises rather rapidly so that M_1 is only about 0.10 to 0.15 above the critical Mach number.

For the airfoils tested the type 3 pressure distribution occurred only at angles of attack above 10°. The relatively low test Reynolds numbers and the variation of Reynolds number with Mach number do not permit any definite conclusions for this type. It appears that the trend is for the general shape of the pressure distribution to remain the same, while the magnitude of the nose pressure peak decreases with increasing Mach numbers.

The type 4 conventional-airfoil-section pressure distribution for moderate angles of attack has, at subcritical speeds, minimum pressure near the airfoil nose followed by a more or less gentle pressure recovery. At supercritical speeds the minimum pressure point moves rearward and the length of the supersonic velocity region increases with increasing Mach number. Examples of this variation are found in the figures listed in the following table:

Airfoil Section	Angle of Attack (deg)	Fig. No.	Critical Mach Number, M_{cr}	Mach Number	
				M_1 for $c_d=0.05$	M_1-M_{cr}
0015	0	4 (a)	0.70	0.81	0.11
0015	-2	4 (b)	.65	.80	.15
0015	-4	4 (c)	.58	.73	.15
23015	0	5 (d)	.64	.80	.16
23015	2	5 (e)	.59	.75	.16
23015	4	5 (f)	.53	.68	.15
4415	-2	6 (c)	.63	.76	.13
4415	0	6 (d)	.62	.75	.13
4415	2	6 (e)	.59	.71	.12
4415	4	6 (f)	.56	.66	.10

The Mach number M_1 is from 0.10 to 0.16, above the critical Mach number. At M_1 the supersonic portion of the pressure distribution terminates somewhere between 30 and 60 percent of the airfoil chord from the nose, depending upon the subcritical pressure-recovery gradient. The less rapid the pressure recovery behind minimum pressure at subcritical speeds the more extensive will be the length of the supersonic flow region at M_1 .

The type 5 pressure distribution for conventional airfoils at moderate angles of attack has a nose pressure peak at subcritical speeds which is less abrupt than that of type 1, but what seems to be more important is the fact that the peak is not followed by a region of relatively constant pressure as it is for type 1. At slightly supercritical speeds the type 5 pressure peak rounds off so that the supersonic region is from 10 to 30 percent of the chord in length. At increasingly supercritical speeds, the length of the supersonic region remains constant at this limited value. Type 5 pressure distributions occur in the following configurations of the present investigation: NACA 0015 at -8° and NACA 23015 and 4415 airfoils at 8° and 10° angles of attack. For these cases the critical Mach number is about 0.45 and the value of M_1 is between 0.08 and 0.16 above the critical Mach number.

Of course there is no abrupt change in the shape of the pressure distribution with changing angle of attack. Therefore, it is to be expected that there will be borderline cases in which the behavior of the pressure distribution at super-

critical Mach numbers is between two of the types previously discussed. The experimental pressure distributions indicate that this overlap is limited to an angle-of-attack range of only 1° or 2° . In the following table the pressure distributions presented in the present report are classified according to the type of variation with Mach number of the supersonic portion of the pressure distributions for the surface on which the local velocity of sound is first attained:

Angle of Attack (deg)	NACA Airfoils				
	65 ₂ -215	66,2-215	0015	23015	4415
-10	-----	-----	3-5	-----	-----
-8	-----	-----	5	-----	-----
-6	1	1	5-4	1	3-5
-4	1	1	4	1	5-4
-2	2	2	4	1-4	4
0	2	2	4	4	4
2	2	2	4	4	4
4	2	2	4	4	4
6	2-1	1	4-5	4-5	4-5
8	1	1	5	5	5
10	1-3	1-3	5-3	5	5

This table shows that at positive angles of attack the low-drag airfoils have one pattern which is different from that of all the conventional airfoil sections. At moderate and large negative angles of attack this simple differentiation does not hold, differences in type of camber line having as much effect as type of thickness distribution.

As the pressure distribution over an airfoil changes with Mach number there is naturally a resultant variation of the airfoil-section characteristics. A parameter which would be expected to affect this variation is the critical Mach number, at which value sonic velocity is first attained at some point on the airfoil surface. The surprising thing is that no changes are observed in the variation of section lift and drag coefficients with Mach number at the critical Mach number. It has therefore been necessary to introduce two other parameters, denoted as the lift- and drag-divergence Mach numbers, which satisfactorily locate the change in variation of lift and drag coefficient with Mach number. It is seen in figures 12 through 16 that for all the airfoil sections and most of the angles of attack investigated the lift-divergence Mach number is the same as the drag-divergence Mach number, and has a value somewhat larger than the critical Mach number. The increment of the lift- and drag-divergence Mach number above the critical Mach number was studied for each airfoil and angle of attack in terms of the classification scheme for the type of pressure distribution. The following facts were noted: For types 2, 4, and 5 pressure distributions, lift and drag divergence occur at a Mach number about 0.05 above the critical Mach number, while for types 1 and 3 this Mach number increment is about 0.15 to 0.20. In the description of the pressure-distribution classification it was pointed out that for each type there was an approximate value for the difference between the critical Mach number and the Mach number M_1 at which the drag coefficient attains the value of 0.05. The numerical values for this Mach number difference were given as: type 1 from 0.19 to 0.28, type 2 from 0.10 to 0.15, type 3 undetermined because of insufficient data, type 4 from 0.10 to 0.16, and type 5 from 0.08 to 0.16. This information together with that for the drag-divergence Mach

number permits an estimate of the rapidity of the increase in drag coefficient at supercritical Mach numbers.

The method of classifying pressure distributions which has been presented appears to be of value in estimating the general differences in pressure-distribution variation with Mach number and also some changes in section characteristics at supercritical Mach number as determined by the airfoil shape and angle of attack.

The variation with Mach number in the character of the flow over airfoils, which has been discussed in the preceding sections, is accompanied by profound changes in the forces and moments acting on the airfoils, the detailed discussion of which will not be undertaken here. The treatment will be confined instead to a discussion of the extent to which the characteristics of the several broad classifications of airfoils investigated are affected by compressibility.

LIFT CHARACTERISTICS

From figures 12 through 16 of the variation of section lift coefficient with Mach number at constant incidence for the NACA 65₂-215 ($a=0.5$), 66,2-215 ($a=0.6$), 0015, 23015, and 4415 airfoils, the subcritical behavior is seen to be sensibly the same for all five airfoils. Except at high angles of attack the lift coefficient increases with Mach number approximately in the ratio $1/\sqrt{1-M^2}$ until the critical speed has been appreciably exceeded. At supercritical speeds the lift characteristics of the low-drag airfoils are definitely superior to those of the conventional airfoils investigated on several counts. For moderate and high angles of attack, the Mach numbers of lift divergence are considerably higher for the low-drag airfoils than for the conventional sections. Moreover, upon exceeding the lift-divergence velocity at high angles of attack the conventional airfoils experience a more severe loss in lift than do the NACA 65₂-215 ($a=0.5$) and 66,2-215 ($a=0.6$) sections.

Perhaps the most important difference in the supercritical characteristics of the low-drag and conventional profiles lies in the changes in lift-curve slope beyond the lift-divergence Mach numbers of the respective airfoils. Although all the airfoils experience a reduction in lift-curve slope upon exceeding their lift-divergence velocities, the conventional sections suffer particularly in this respect. The variation in lift-curve slope with Mach number at 0.2 lift coefficient shown in figure 40 for all five airfoils illustrates this fact. The slope of the lift curve is of particular significance because it is one of the principal factors affecting airplane stability. Excessively low slopes tend to promote extreme airplane stability, a very undesirable characteristic. The NACA low-drag sections, then, possess a definite advantage in this regard over the conventional sections at supercritical speeds.

Another parameter of great importance in airplane control is the angle of zero lift. Figure 41 depicts the variation with Mach number in the angle of zero lift for all five airfoils. It is noted that the low-drag and cambered conventional sections alike experience marked positive shifts in their respective angles of zero lift at supercritical speeds. The change for the NACA 4415 airfoil is particularly severe but should be regarded as being characteristic of highly cam-

bered rather than conventional airfoils alone. This positive shift in the angle of zero lift is detrimental in that it alters airplane trim in a direction to promote an airplane diving tendency upon exceeding the Mach number of lift divergence. Disregarding the NACA 4415 section as a special case, the low-drag and conventional profiles exhibit this undesirable characteristic to approximately the same degree. The constant positive angle of zero lift noted in the figure for the NACA 0015 airfoil is attributed to imperfect model construction and not to any aerodynamic phenomenon.

One additional item of interest regarding the comparative lift characteristics of the low-drag and the conventional airfoils is the variation of the maximum lift coefficient with Mach number which may be seen in figures 25 to 29. Although the Reynolds numbers of the present tests were too low to permit an accurate quantitative assessment of the maximum lift coefficients, the results are of qualitative value in indicating the trend of the changes in this parameter with Mach number. For the low-drag NACA 65₂-215 ($a=0.5$) and 66,2-215 ($a=0.6$) airfoils the maximum lift coefficient first decreases slightly with Mach number, then rises appreciably at moderately high speeds and finally declines gradually at the highest Mach numbers. The over-all variation is not very great, however. In contrast to this behavior, the maximum lift coefficients for the conventional NACA 0015 and 23015 sections fall off at first sharply, and later, decreasingly with Mach number. The character of the variation of maximum lift coefficient with Mach number for the NACA 4415 airfoil lies in between the other two types except at the higher Mach numbers where it resembles more closely the variation for the conventional profiles. At high subcritical and all supercritical speeds, then, the low-drag airfoils are superior to the conventional sections in this respect.

DRAG CHARACTERISTICS

The high-speed performance of airplanes is largely determined by the drag characteristics of the airfoil sections composing the principal lifting surfaces. The variation of section drag coefficient with Mach number illustrated in figures 17 to 21 for the representative airfoils investigated then becomes of particular interest. Except at moderately high positive angles of attack the general character of the variation in drag coefficient with Mach number is the same for both the low-drag and conventional airfoils. At the higher positive angles of attack the low-drag airfoils exhibit a peculiar decrease in drag beyond the critical speed which is apparent as a dip in the curve of drag coefficient against Mach number. This phenomenon, believed to be associated with flow separation was not observed for the conventional airfoils.

The drag characteristics of the several airfoil types can best be compared in figure 42 where the section drag coefficient at 0.2 lift coefficient is shown as a function of Mach number for all five airfoils. It is readily apparent from an examination of this figure that the low-drag airfoils possess no advantage over the conventional airfoil sections insofar as supercritical speed performance is concerned. The NACA 4415 airfoil appears to be definitely inferior to the other airfoils investigated.

MOMENT CHARACTERISTICS

Airfoil pitching moments are of interest here only insofar as they affect airplane stability characteristics at supercritical speeds. The variation with Mach number of the quarter-chord pitching-moment coefficient seen in figures 22 to 24 for the NACA 65₂-215 ($a=0.5$), 66,2-215 ($a=0.6$), 23015, 0015, and 4415 airfoil sections, respectively, is too small for all the airfoils investigated, except possibly the NACA 4415 at high angles of attack, to appreciably affect airplane trim.

CONCLUSIONS

From the results of pressure distribution and drag measurements at high speeds and moderate Reynolds numbers (1,000,000 to 2,000,000) for a representative group of 15-percent-chord-thick low-drag and conventional airfoil sections several conclusions regarding the characteristics of airfoils at subcritical and supercritical velocities are drawn. It should be emphasized that the following conclusions apply specifically to airfoils of thicknesses in the vicinity of 15 percent of the airfoil chord and do not necessarily apply in the general case.

1. At subcritical velocities the Kármán-Tsien modification of potential theory for compressibility satisfactorily predicts the variation of the local pressure coefficient with Mach number on an airfoil surface except in the vicinity of the leading edge. One consequence of this result is the very satisfactory agreement noted in the present investigation between experimental and theoretical critical Mach numbers at other than large angles of attack.

2. At supercritical speeds the variation of pressure distribution with Mach number for both low-drag and conventional airfoils appears to be directly related to the form of the corresponding low-speed pressure distributions. Although this relationship is purely qualitative it permits a more rational understanding of the character of supercritical speed flows.

3. At subcritical Mach numbers there appears to be little to choose between the lift characteristics of the low-drag and the conventional airfoils except insofar as the maximum lift coefficient is concerned, where the conventional sections hold the advantage at low speeds and the low-drag profiles are favored at the higher velocities. For low-drag and conventional airfoils alike, the lift, and consequently the lift-curve slope, increases with Mach number approximately in the ratio $1/\sqrt{1-M^2}$ until the critical speed has been exceeded.

4. The supercritical speed lift characteristics of the low-drag airfoils, as represented by the NACA 65₂-215 ($a=0.5$) and 66,2-215 ($a=0.6$) sections, are definitely superior to the corresponding characteristics of the conventional profiles investigated in that the lift-curve slopes of the former are not nearly as drastically reduced beyond the Mach numbers of lift divergence as are the slopes of the latter sections. Moreover, the lift-divergence velocities at the higher angles of attack are greater for the low-drag than for the conventional airfoils, enhancing the high-speed maneuverability of airplanes employing the former sections.

5. The low-drag and moderately cambered conventional airfoils exhibit an equally unfavorable positive shift in the angle of zero lift at high supercritical speeds. The NACA

4415 airfoil, a special case as a highly cambered section, exhibits particularly undesirable characteristics in this respect.

6. At supercritical speeds in the normal lift-coefficient range, the drag characteristics of the low-drag and conventional airfoils are sensibly the same, no advantage being discernible for the low-drag type in this range. Although the critical speeds for the conventional sections are considerably lower than those for the low-drag type, in the vicinity of the design lift coefficient the drag-divergence Mach numbers are approximately equal for both types.

7. The variation of airfoil pitching-moment coefficients with Mach number for the low-drag and conventional airfoils alike is such as to have but small detrimental effects on the performance characteristics of airplanes at high speeds.

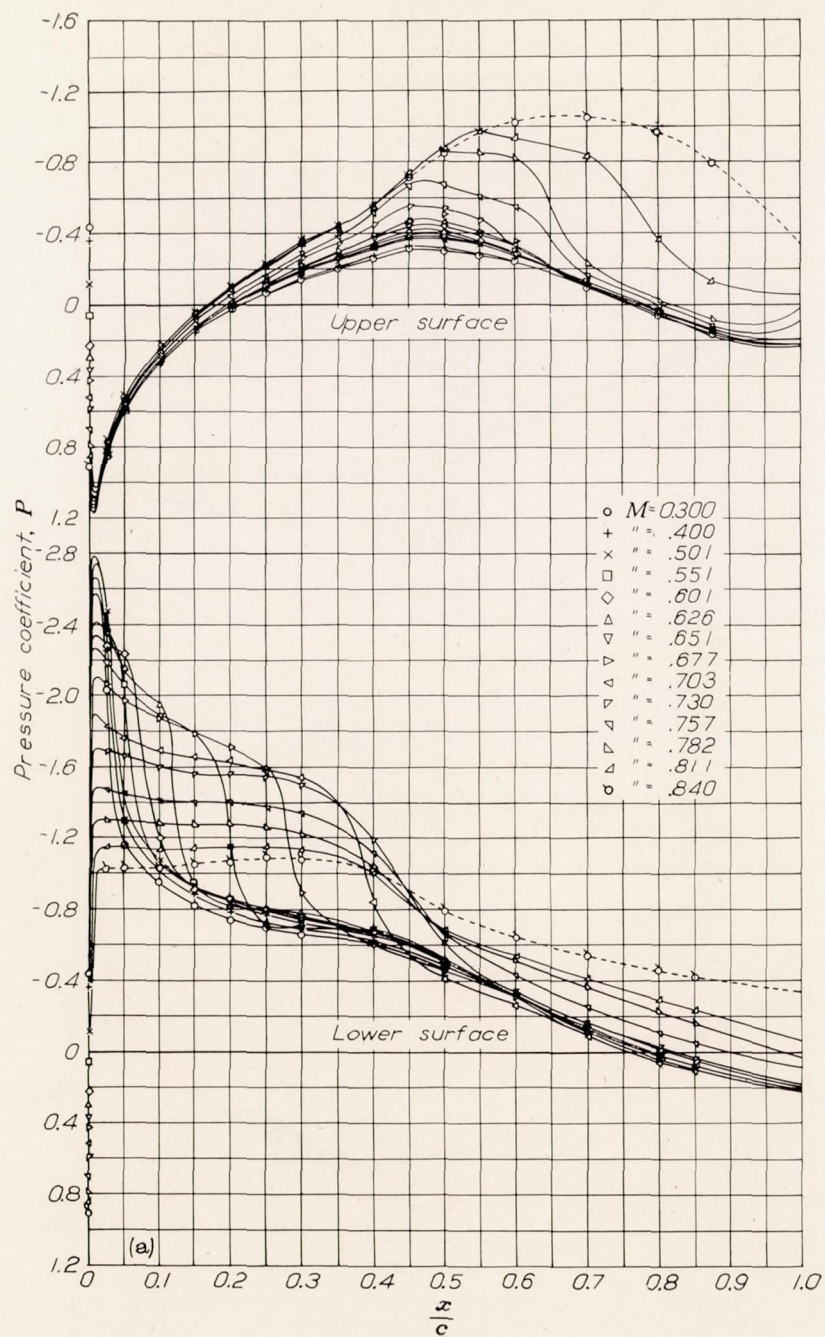
8. Although the low-drag airfoil would appear to possess small advantage over the conventional section as far as high-

speed performance is concerned, it appears definitely superior to the latter in the matter of airplane stability and control at supercritical speeds.

AMES AERONAUTICAL LABORATORY,
NATIONAL ADVISORY COMMITTEE FOR AERONAUTICS,
MOFFETT FIELD, CALIF.

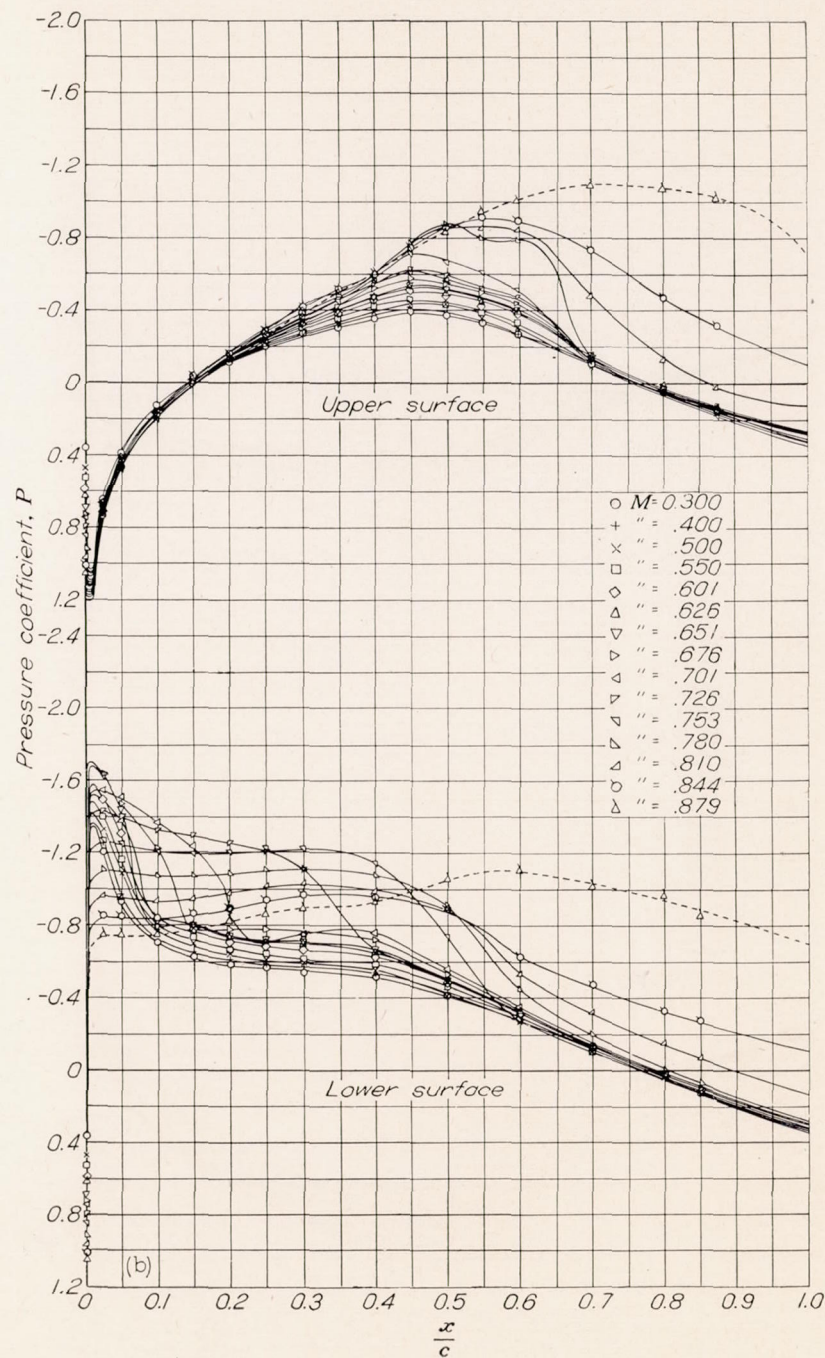
REFERENCES

1. Allen, H. Julian, and Vincenti, Walter G.: Wall Interference in a Two-Dimensional-Flow Wind Tunnel With Consideration of the Effects of Compressibility. NACA Rep. No. 782, 1944.
2. Heaslet, Max. A.: Critical Mach Numbers of Various Airfoil Sections. NACA ACR No. 4G18, 1944.
3. von Kármán, Th.: Compressibility Effects in Aerodynamics. Jour. Aero. Sci. vol. 8, no. 9, July 1941, pp. 337-356.



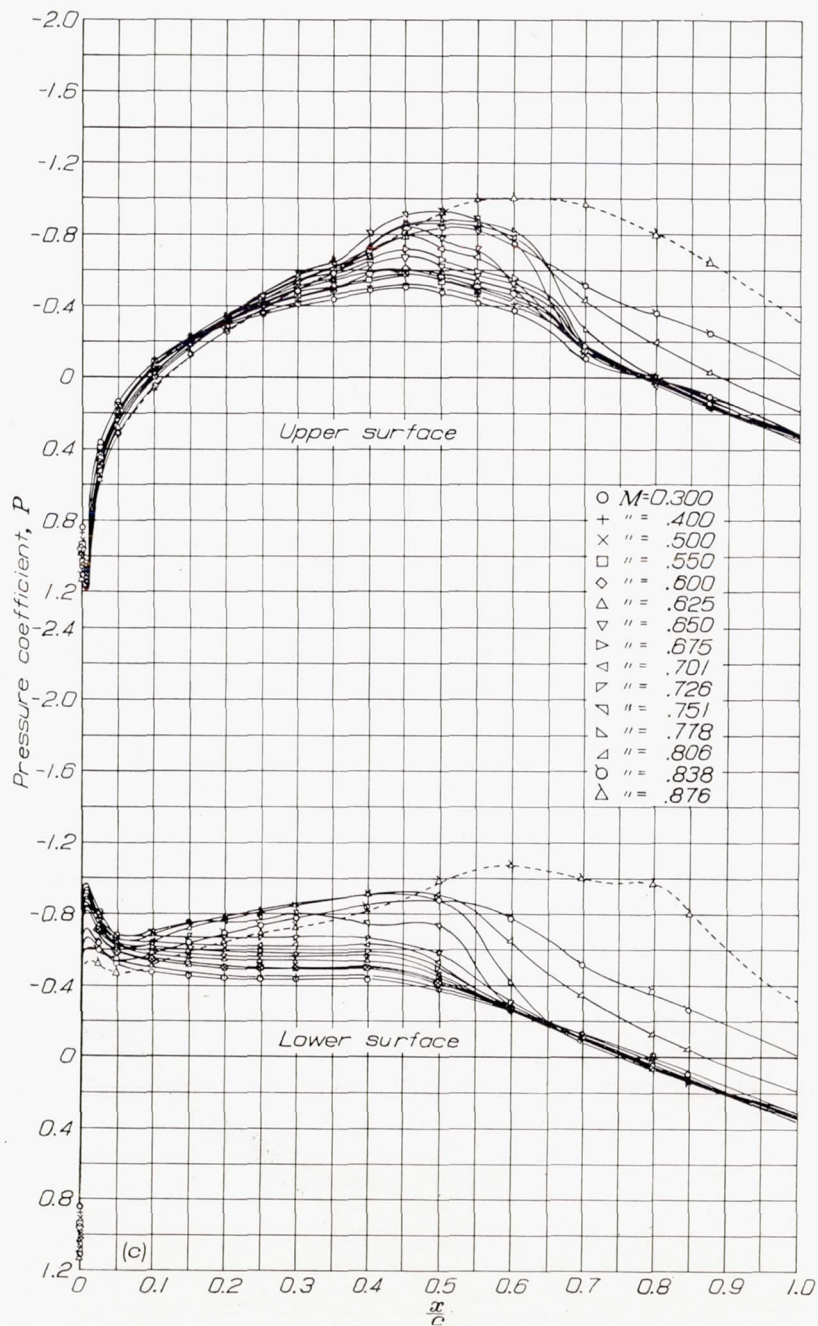
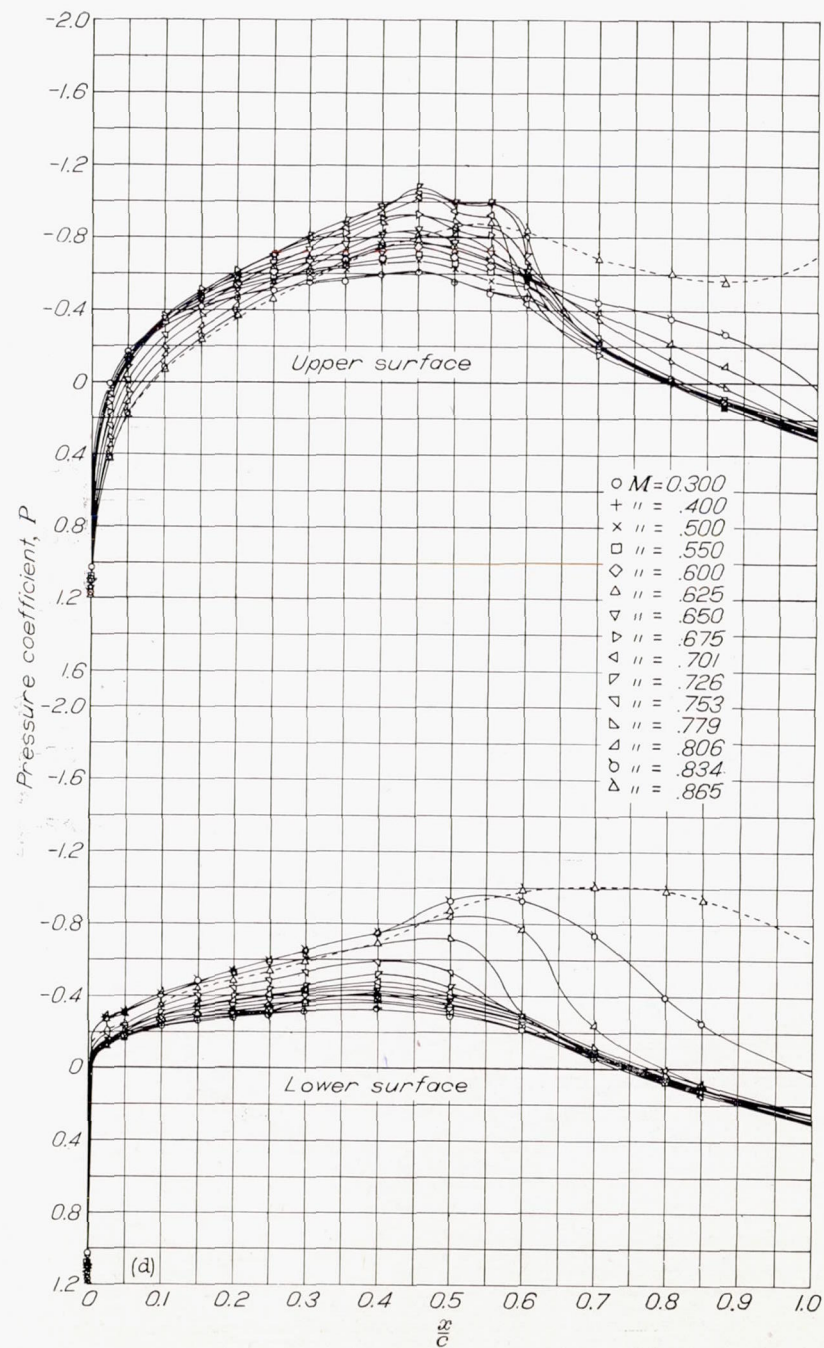
(a) Section angle of attack, $\alpha_0 = -6^\circ$.

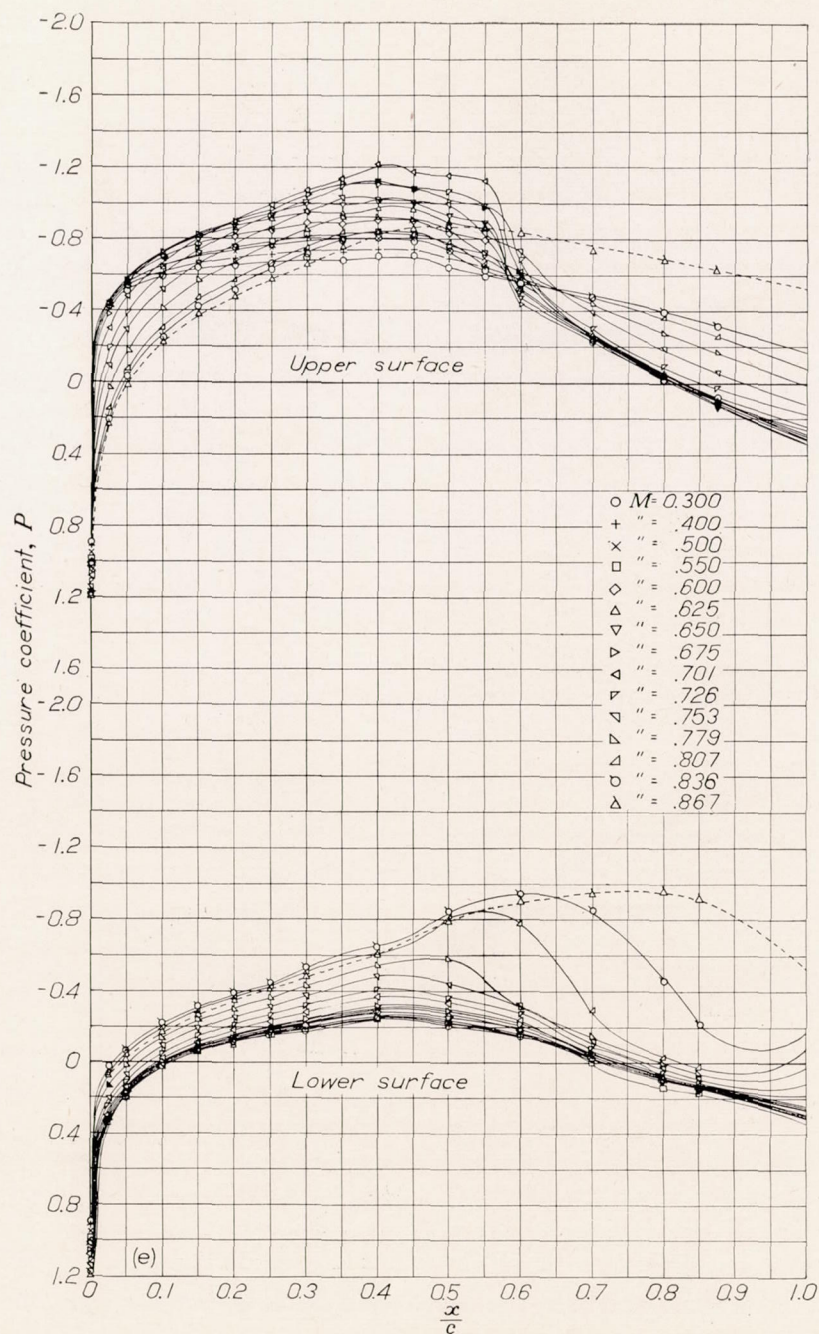
FIGURE 2.—Pressure distribution over the NACA 652-215 ($a=0.5$) airfoil section with constant angle of attack and varying Mach number.



(b) Section angle of attack, $\alpha_0 = -4^\circ$.

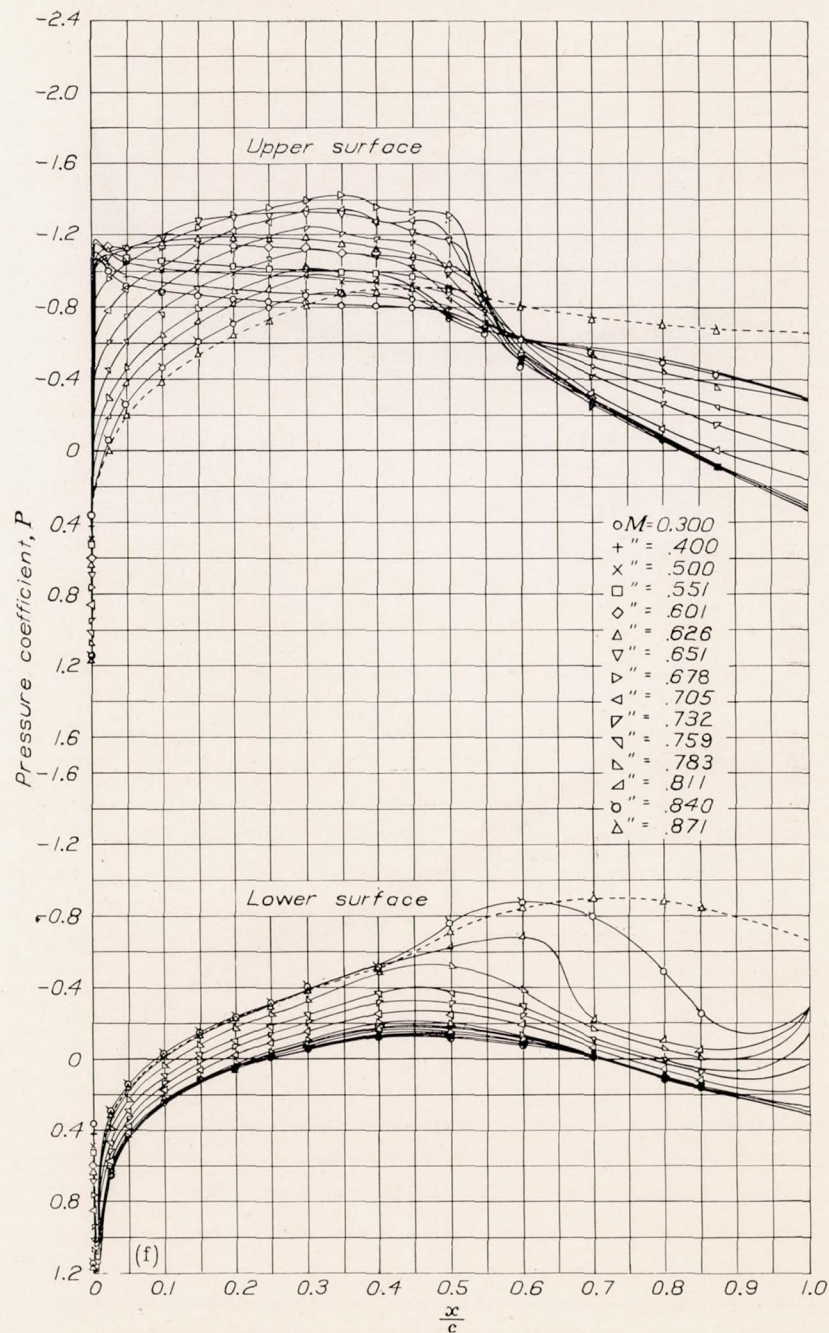
FIGURE 2.—Continued. NACA 652-215 ($a=0.5$) airfoil section.

(c) Section angle of attack, $\alpha_0 = -2^\circ$.FIGURE 2.—Continued. NACA 652-215 ($a=0.5$) airfoil section.(d) Section angle of attack, $\alpha_0 = 0^\circ$.FIGURE 2.—Continued. NACA 652-215 ($a=0.5$) airfoil section.



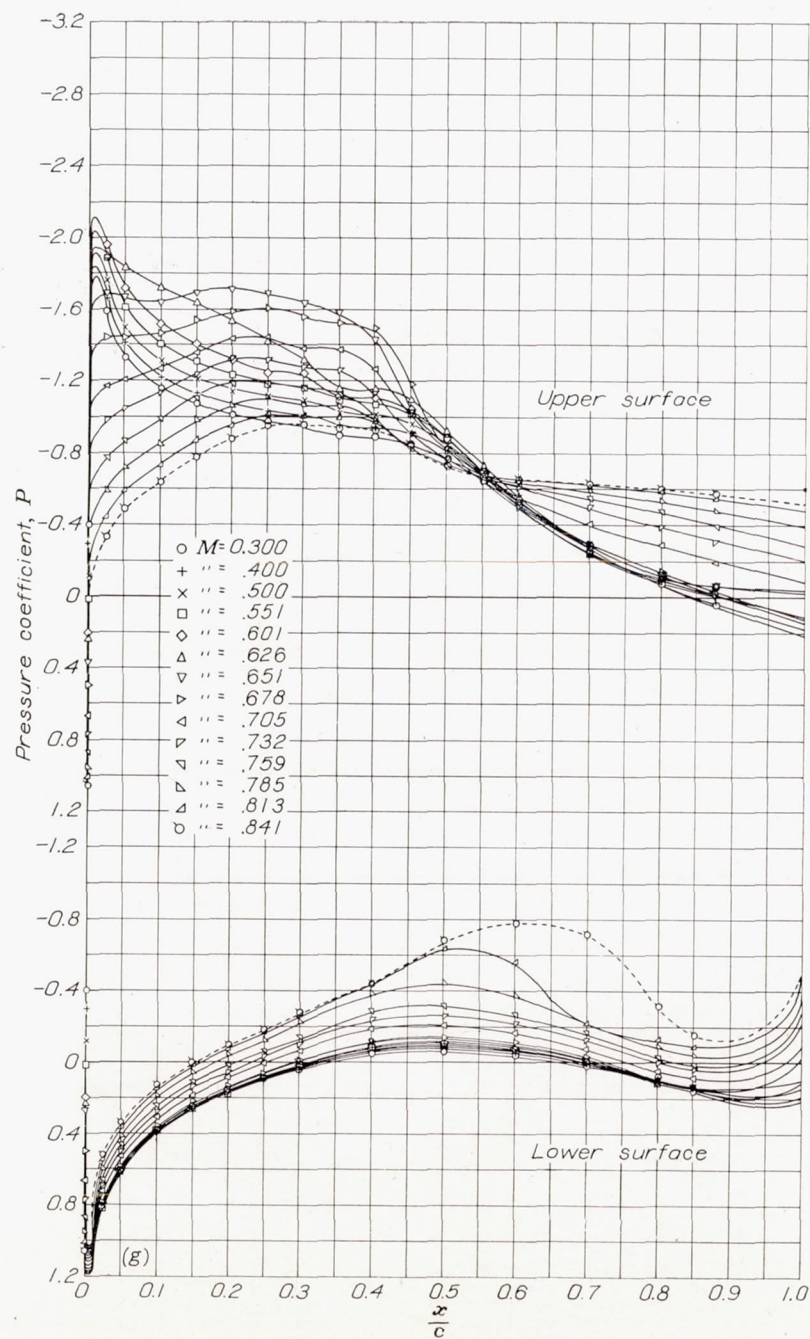
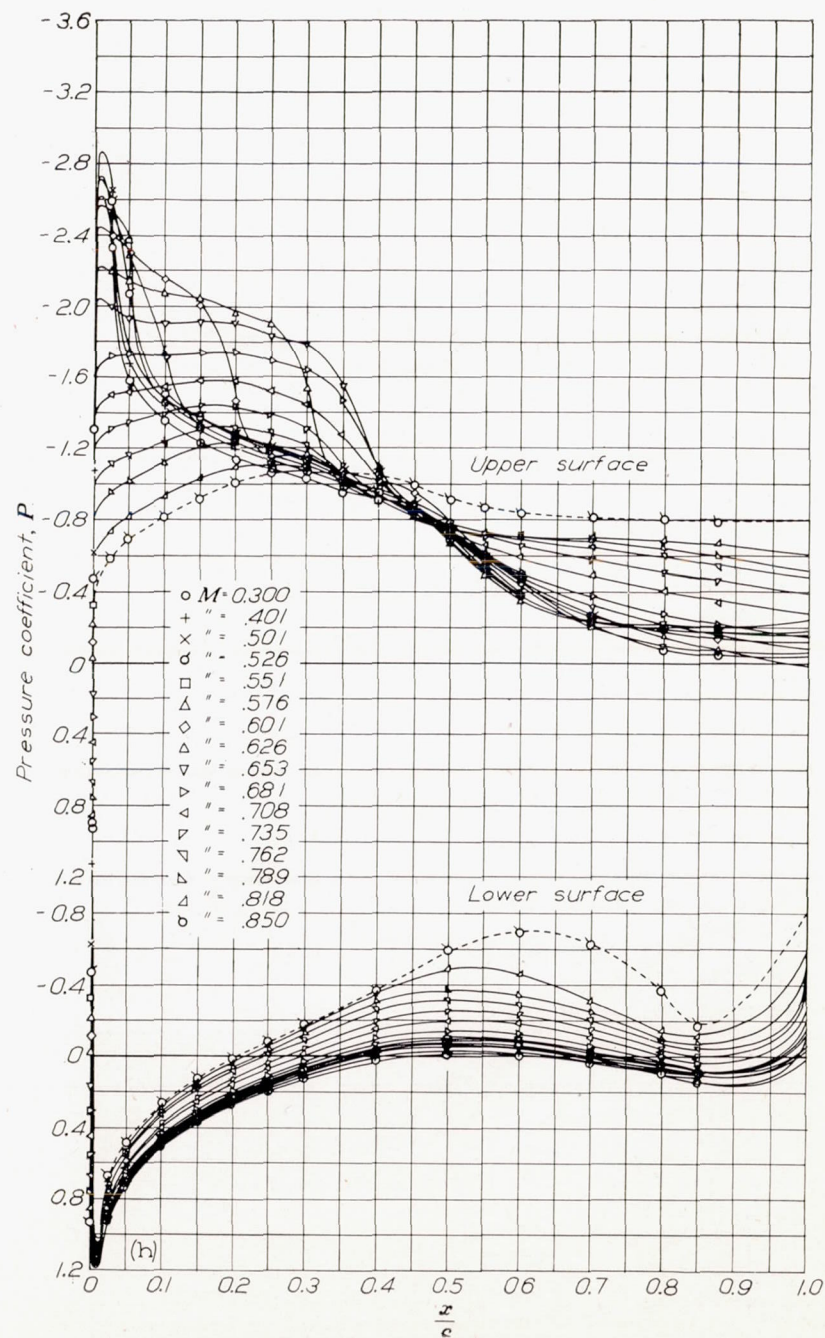
(e) Section angle of attack, $\alpha_0 = 2^\circ$.

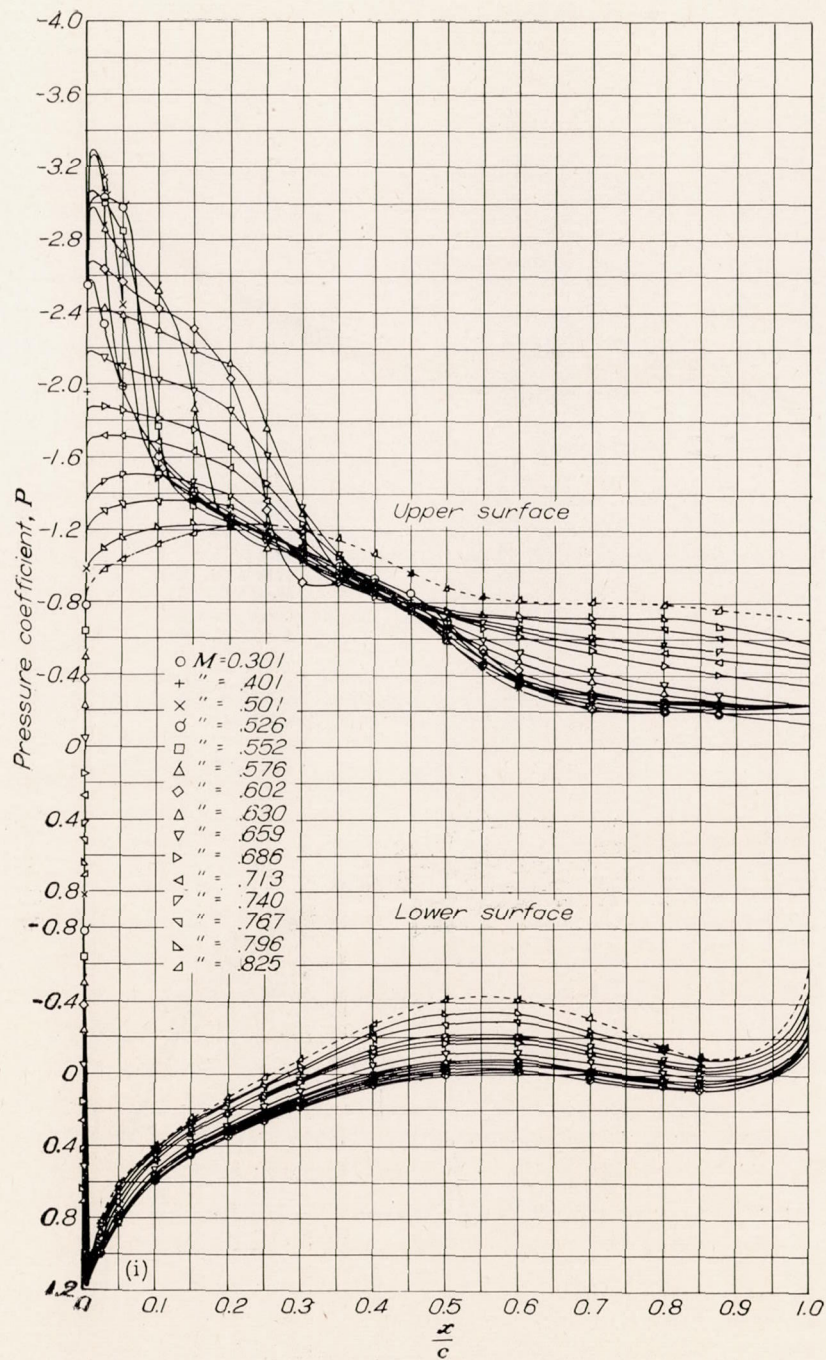
FIGURE 2.—Continued. NACA 65₂-215 ($a=0.5$) airfoil section.



(f) Section angle of attack, $\alpha_0 = 4^\circ$.

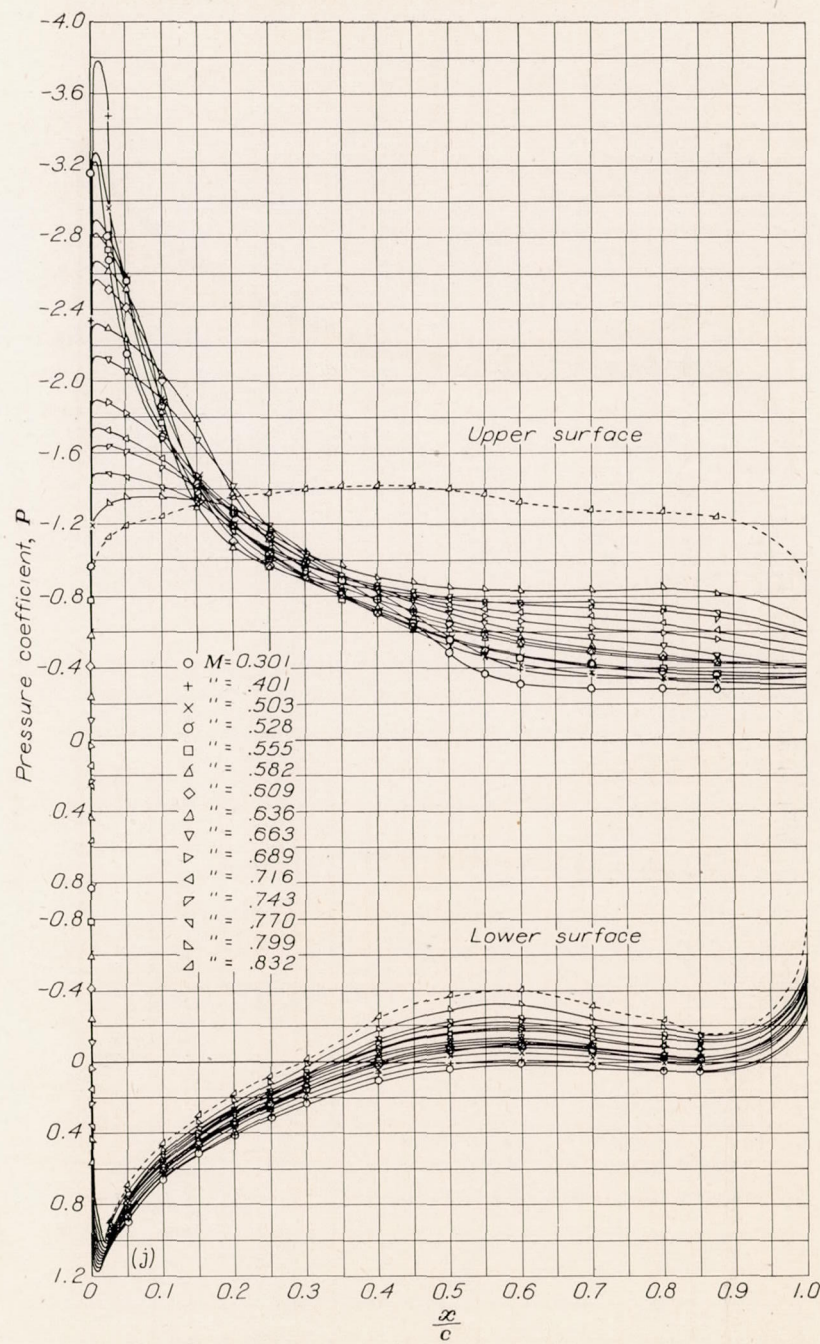
FIGURE 2.—Continued. NACA 65₂-215 ($a=0.5$) airfoil section.

(g) Section angle of attack, $\alpha_0 = 6^\circ$.FIGURE 2.—Continued. NACA 65-215 ($a=0.5$) airfoil section.(h) Section angle of attack, $\alpha_0 = 8^\circ$.FIGURE 2.—Continued. NACA 65-215 ($a=0.5$) airfoil section.



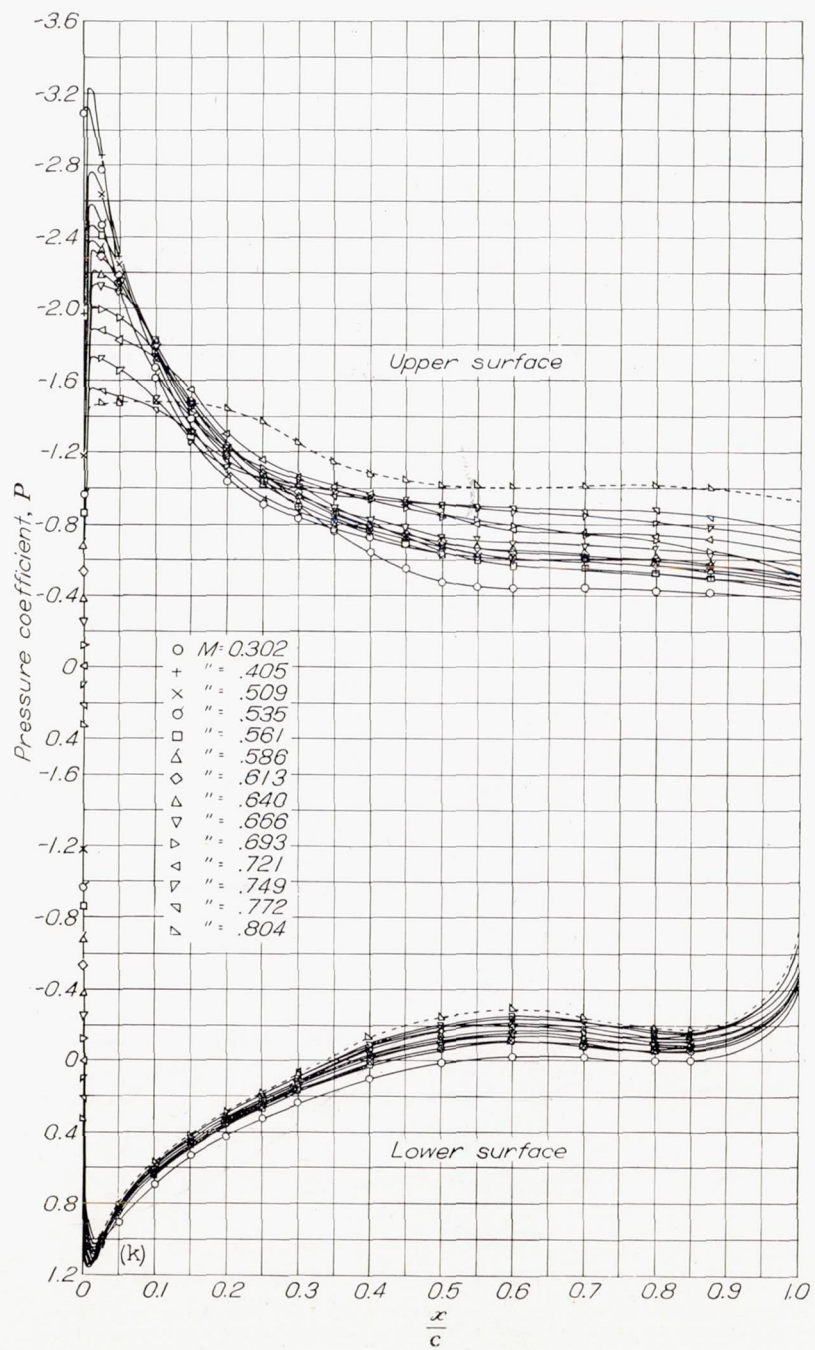
(i) Section angle of attack, $\alpha_0=10^\circ$.

FIGURE 2.—Continued. NACA 652-215 ($a=0.5$) airfoil section.

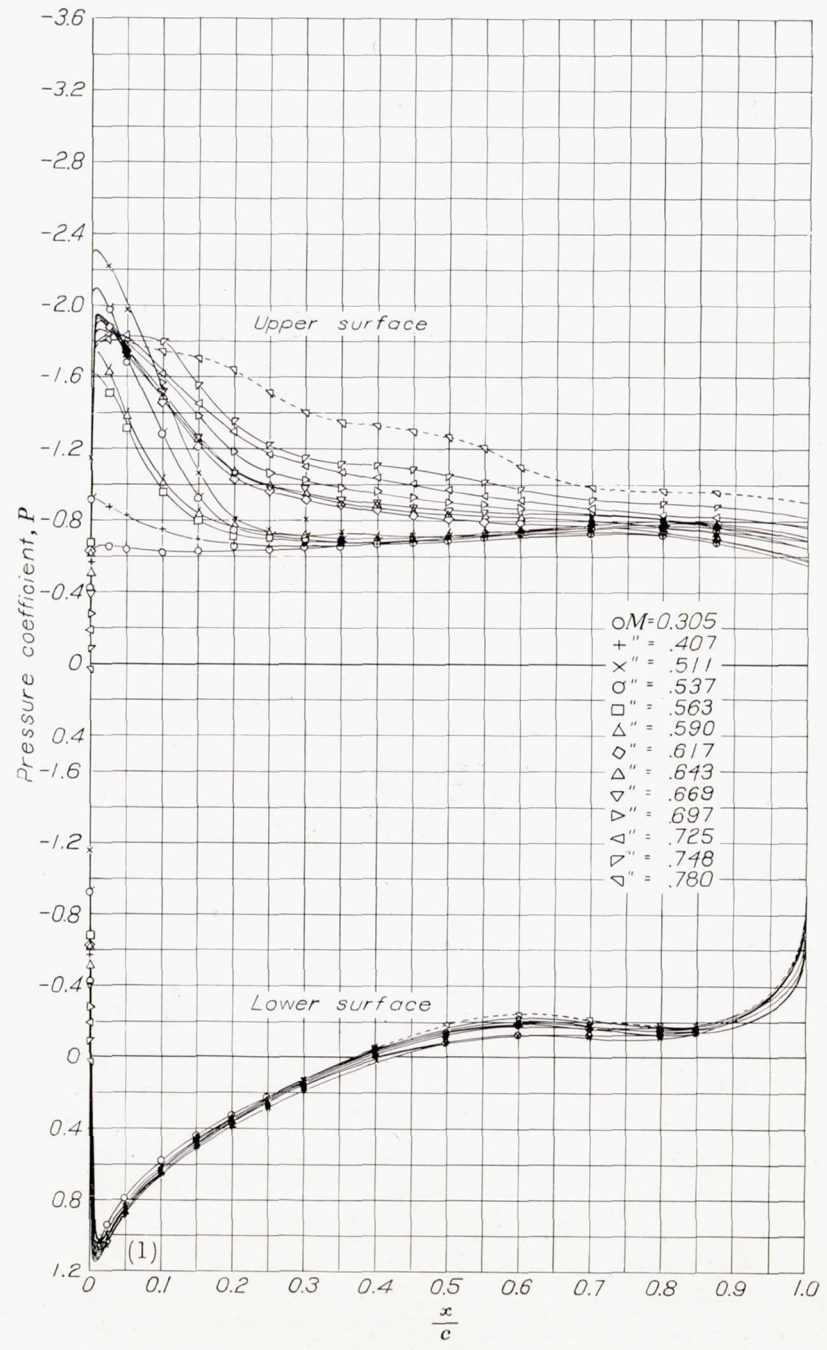


(j) Section angle of attack, $\alpha_0=12^\circ$.

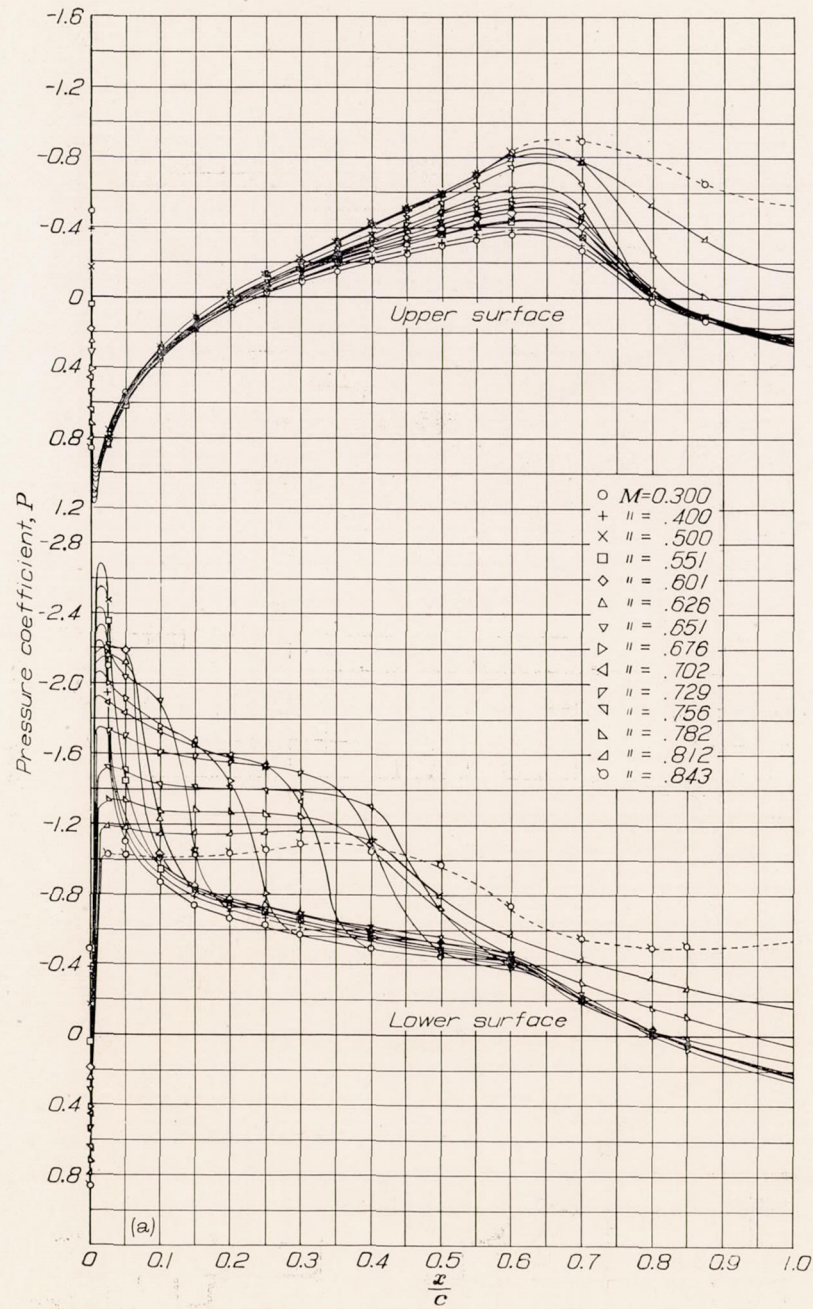
FIGURE 2.—Continued. NACA 652-215 ($a=0.5$) airfoil section.



(k) Section angle of attack, $\alpha_0=14^\circ$.
 FIGURE 2.—Continued. NACA 65-215 ($\alpha=0.5$) airfoil section.

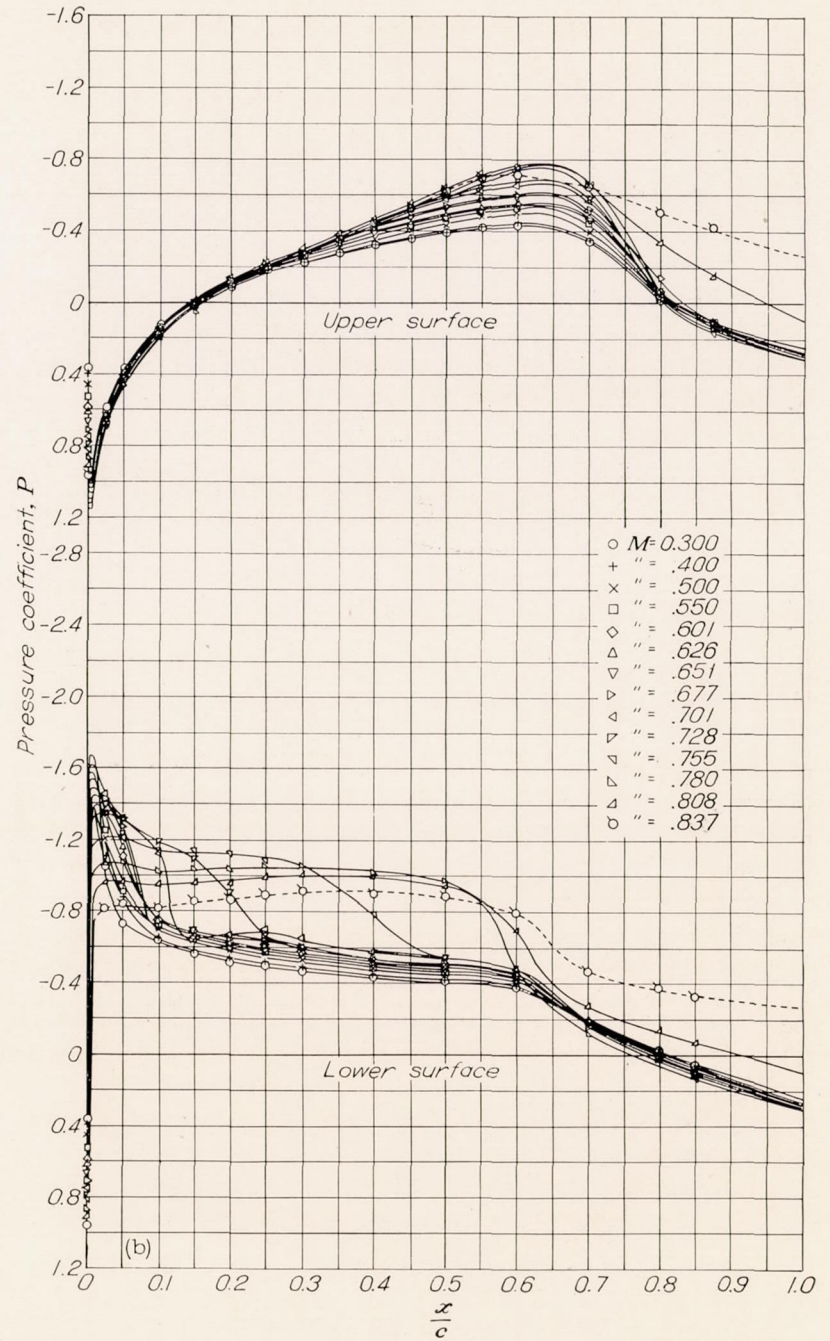


(l) Section angle of attack, $\alpha_0=16^\circ$.
 FIGURE 2.—Concluded. NACA 65-215 ($\alpha=0.5$) airfoil section.



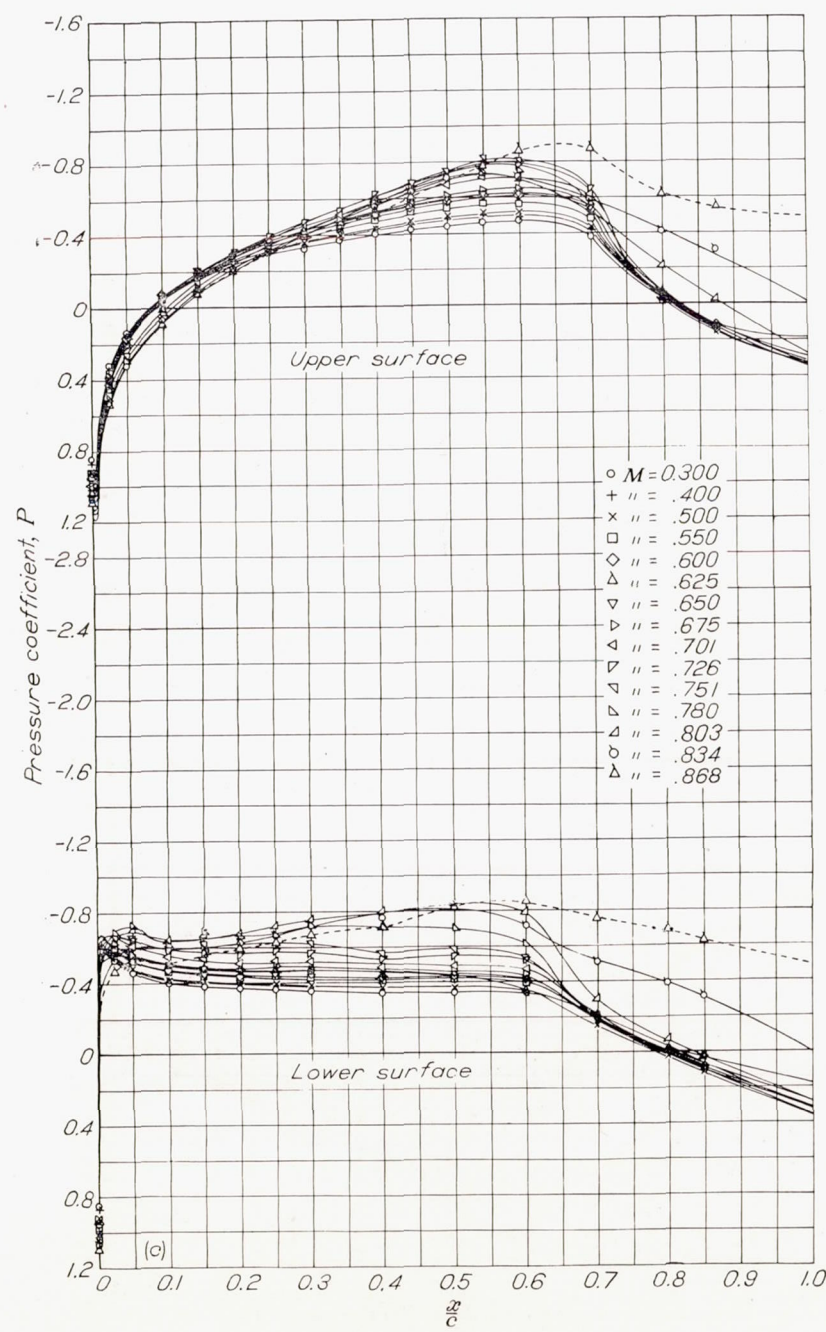
(a) Section angle of attack, $\alpha_0 = -6^\circ$.

FIGURE 3.—Pressure distribution over the NACA 66, 2-215 ($a=0.6$) airfoil section with constant angle of attack and varying Mach number.



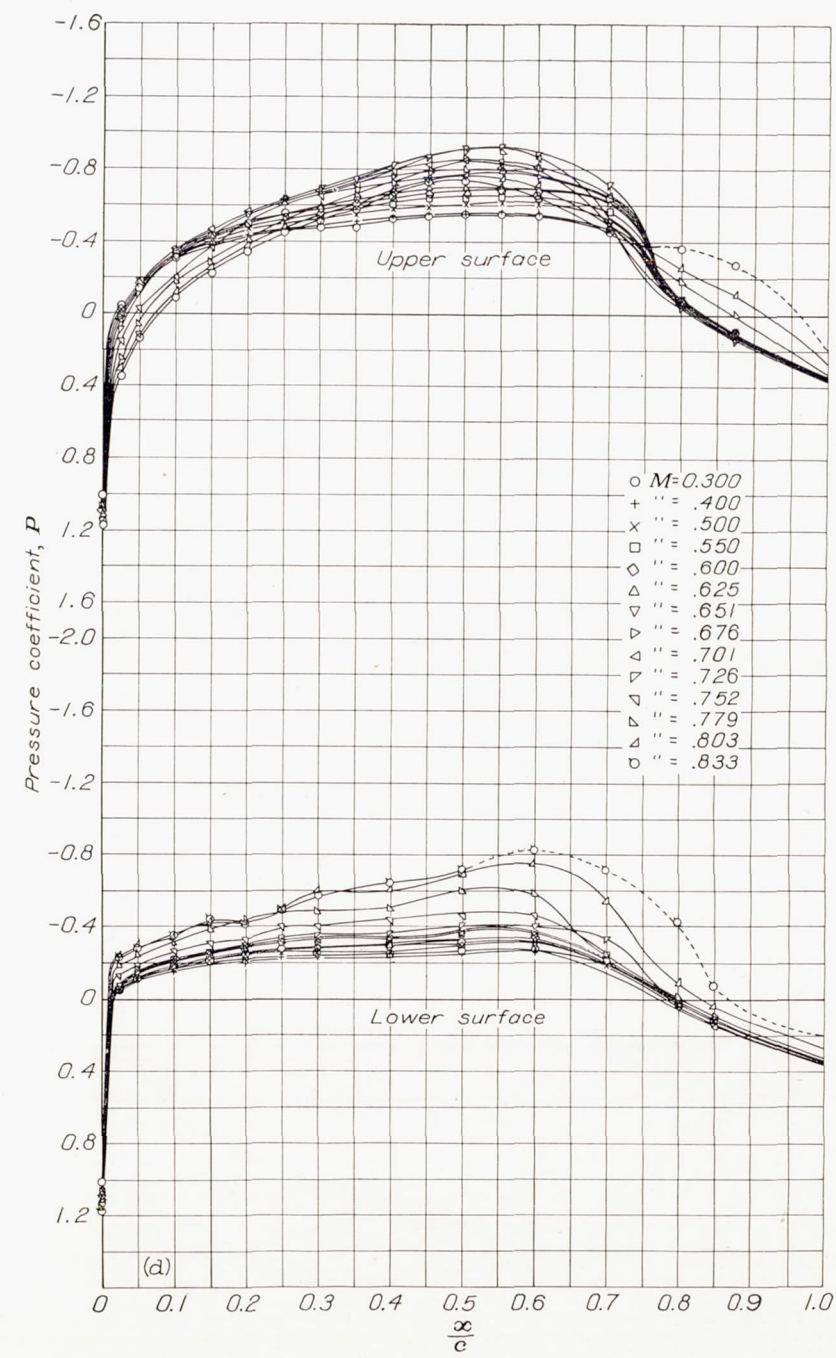
(b) Section angle of attack, $\alpha_0 = -4^\circ$.

FIGURE 3.—Continued. NACA 66, 2-215 ($a=0.6$) airfoil section.



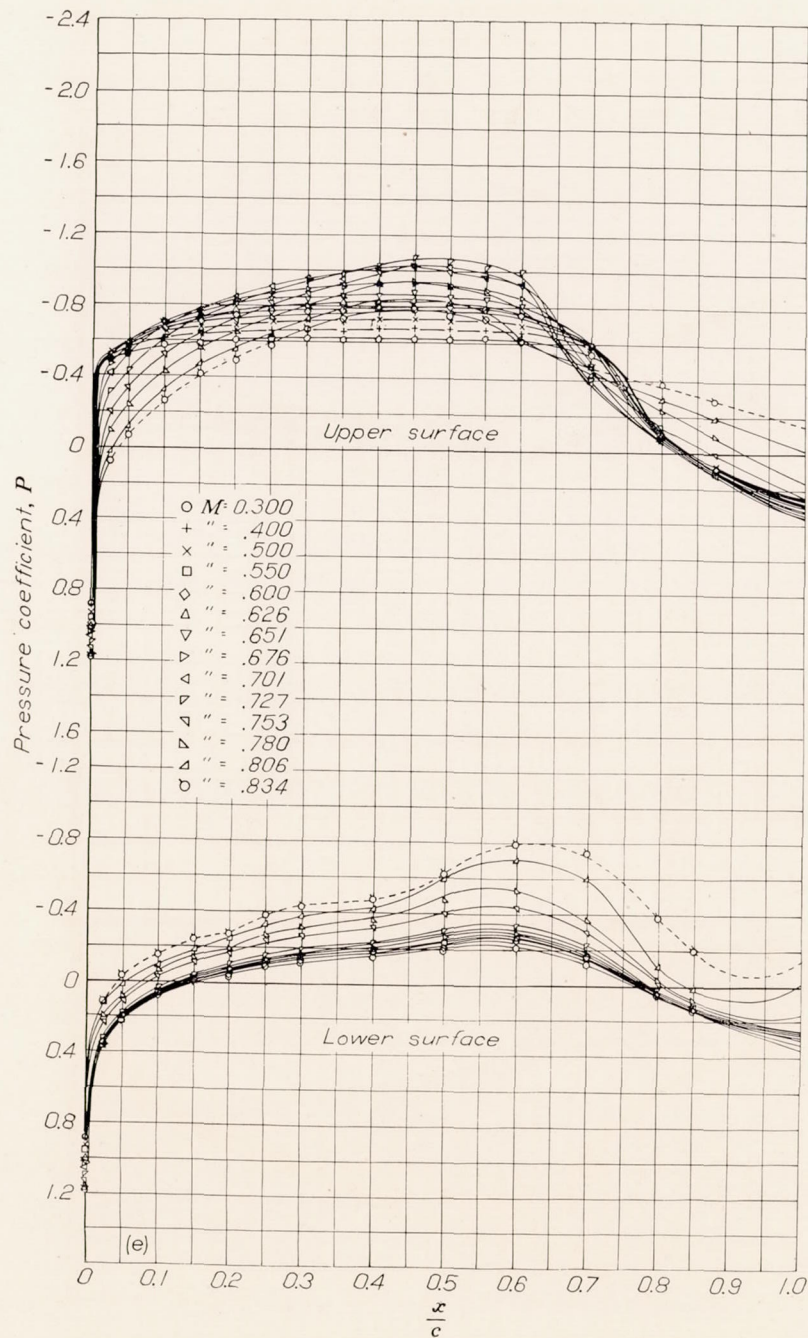
(c) Section angle of attack, $\alpha_0 = -2^\circ$.

FIGURE 3.—Continued. NACA 66, 2-215 ($\alpha=0.6$) airfoil section.



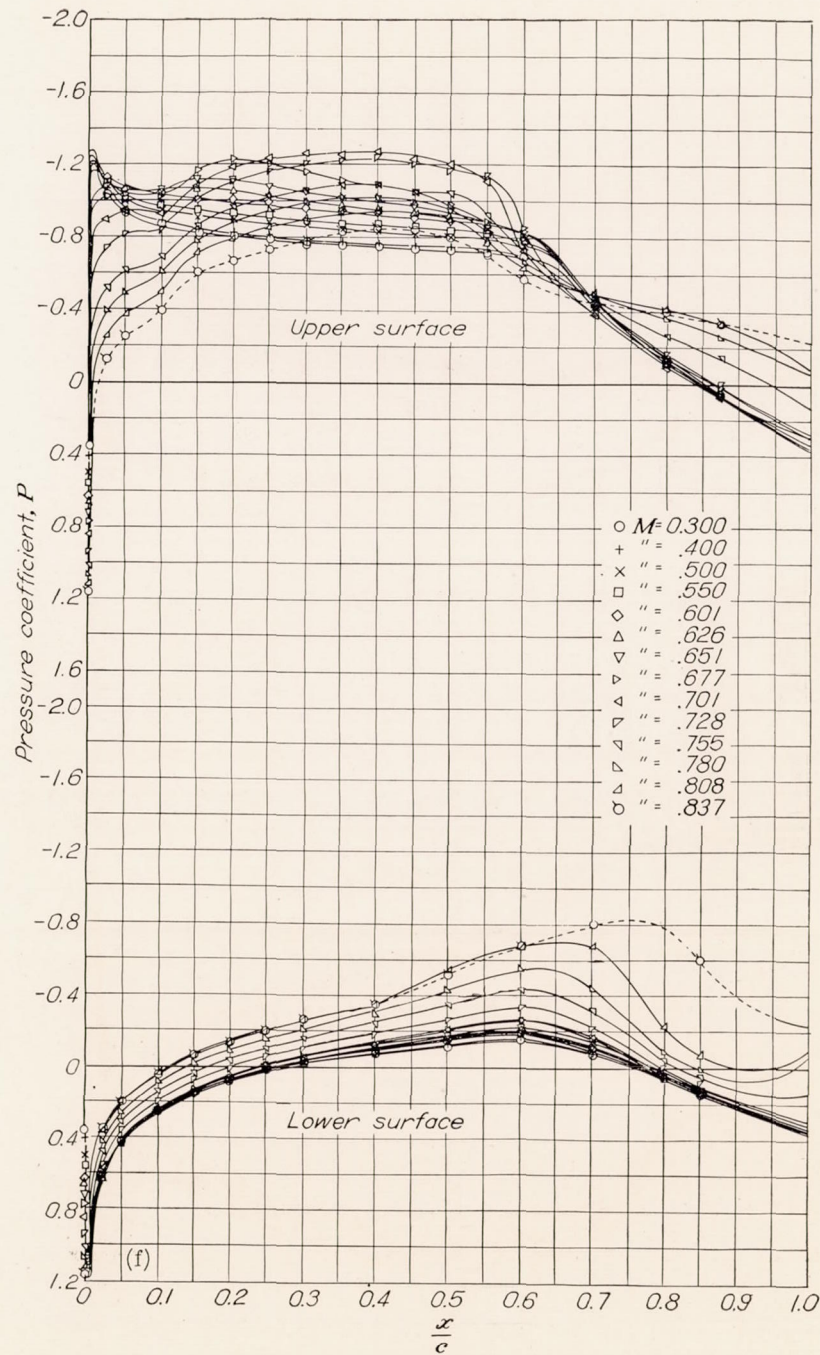
(d) Section angle of attack, $\alpha_0 = 0^\circ$.

FIGURE 3.—Continued. NACA 66, 2-215 ($\alpha=0.6$) airfoil section.



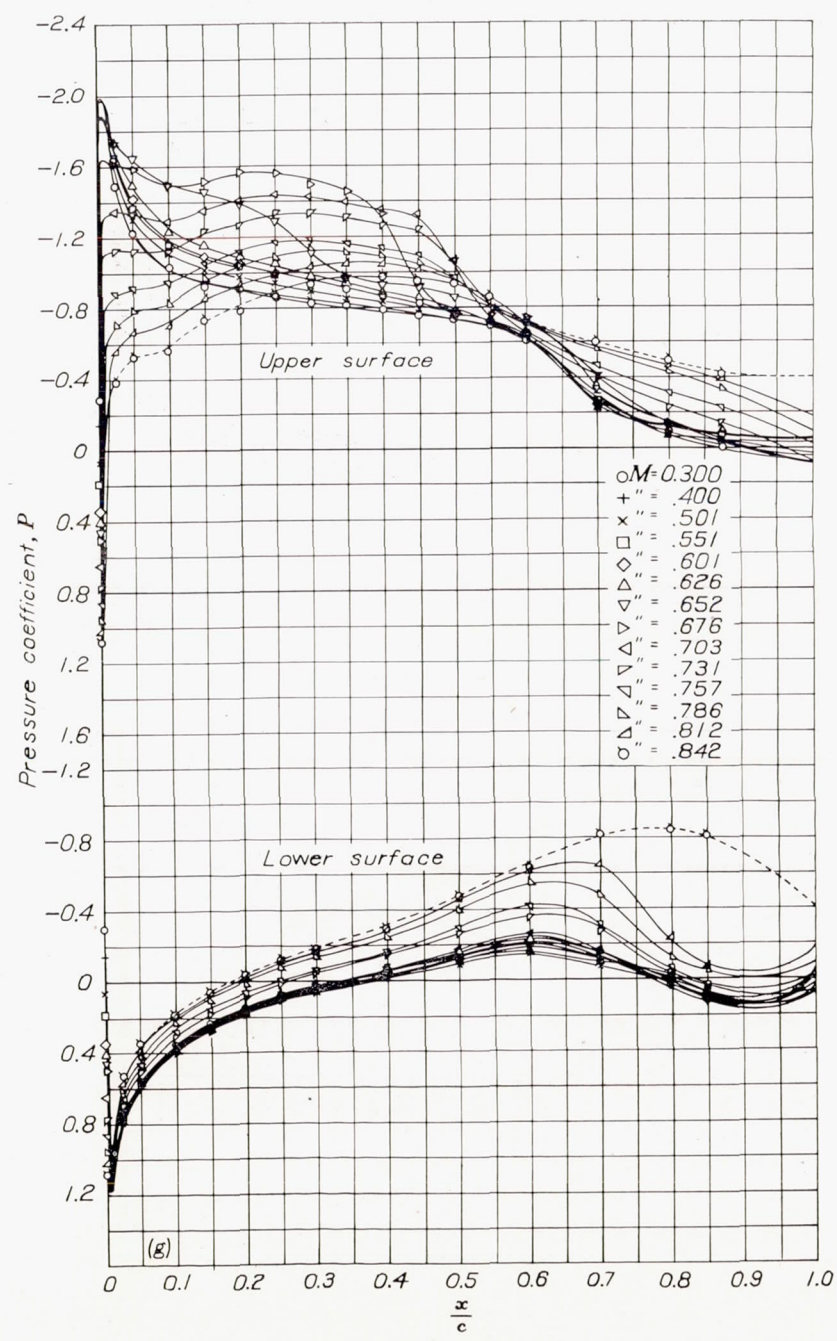
(e) Section angle of attack, $\alpha_0 = 2^\circ$.

FIGURE 3.—Continued. NACA 66, 2-215 ($a=0.6$) airfoil section.



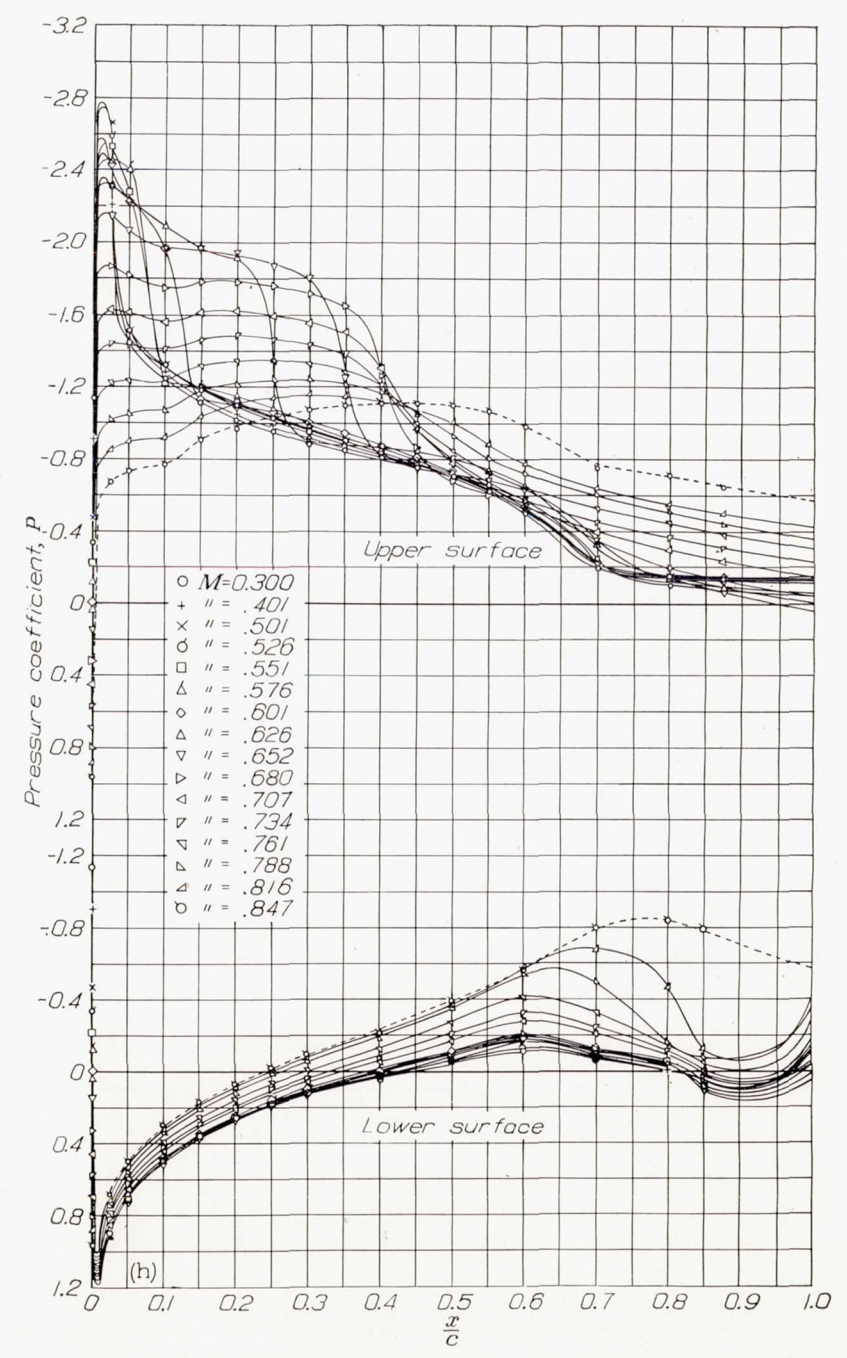
(f) Section angle of attack, $\alpha_0 = 4^\circ$.

FIGURE 3.—Continued. NACA 66, 2-215 ($a=0.6$) airfoil section.



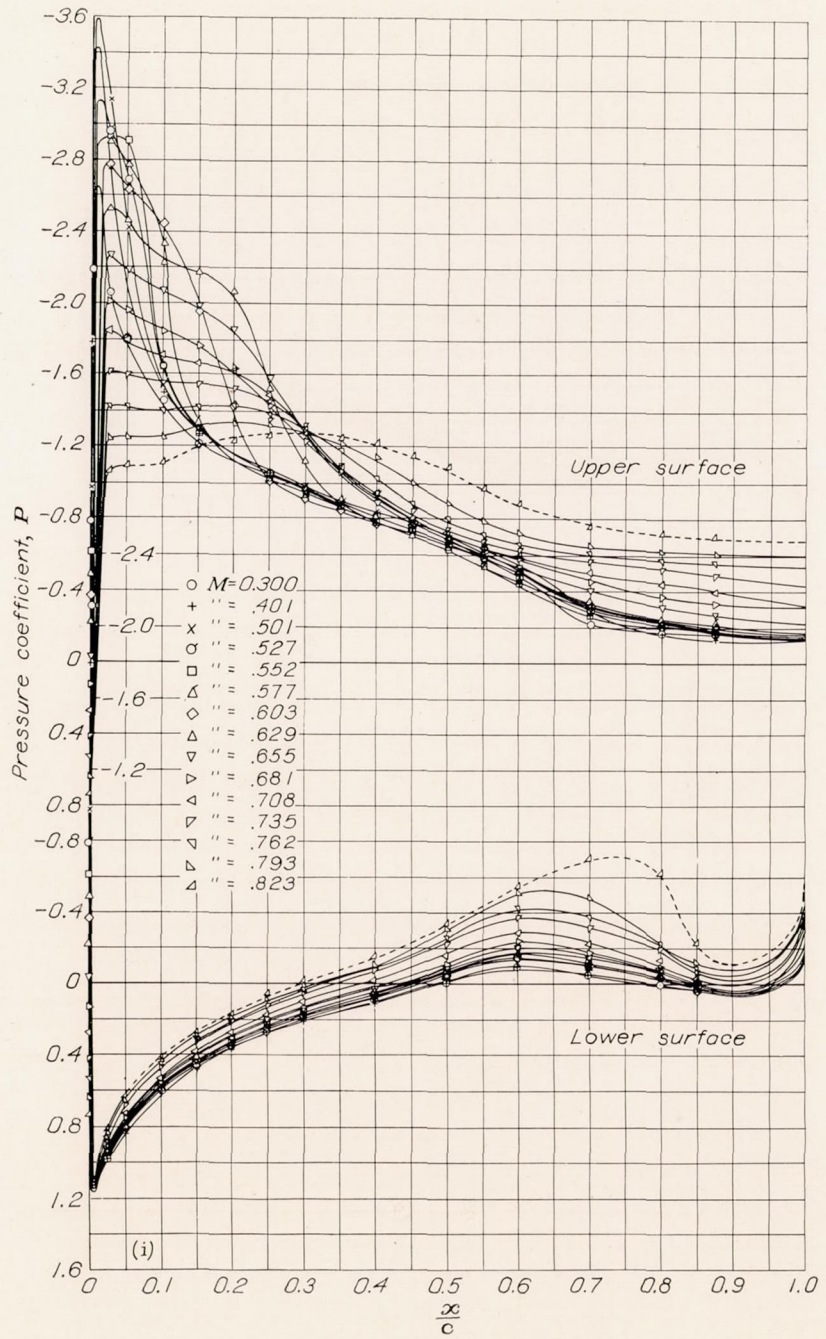
(g) Section angle of attack, $\alpha_0=6^\circ$.

FIGURE 3.—Continued. NACA 66, 2-215 ($a=0.6$) airfoil section.

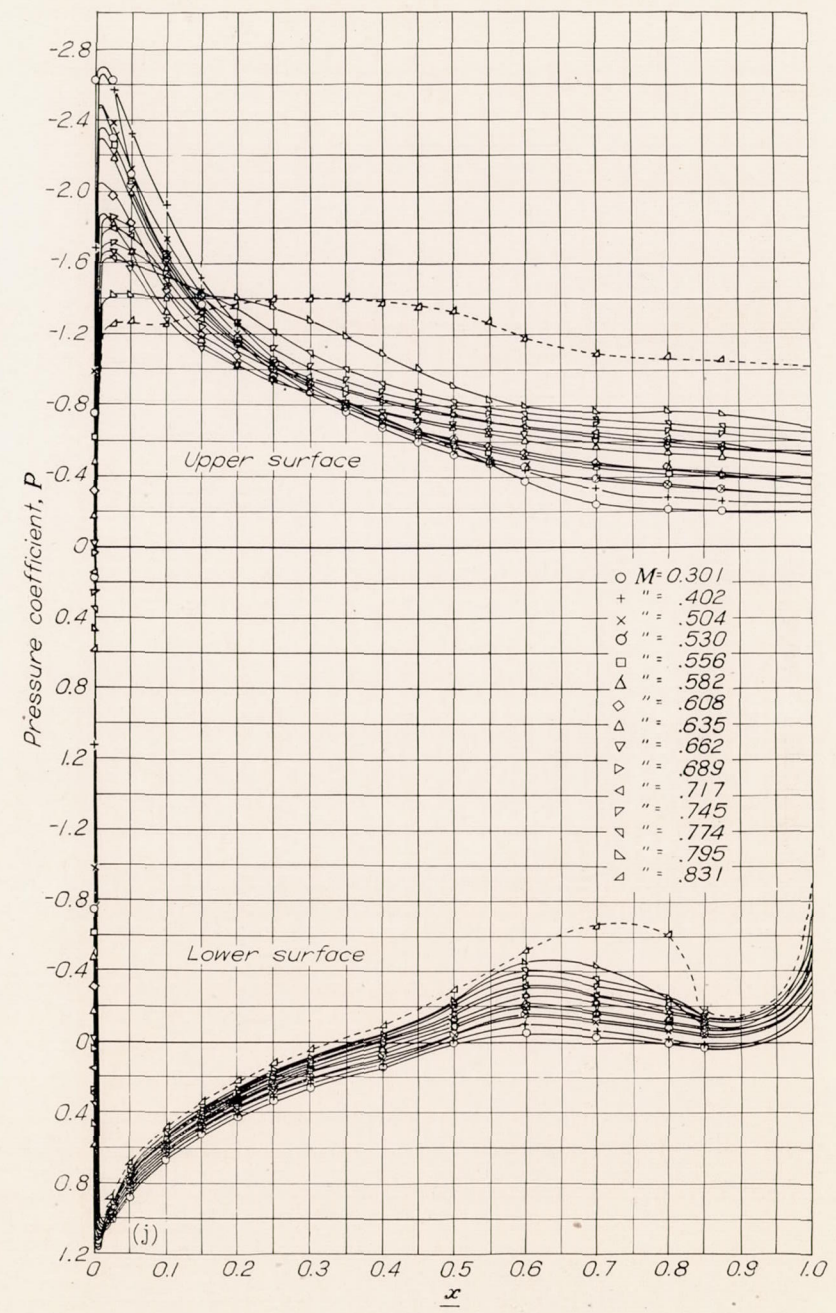


(h) Section angle of attack, $\alpha_0=8^\circ$.

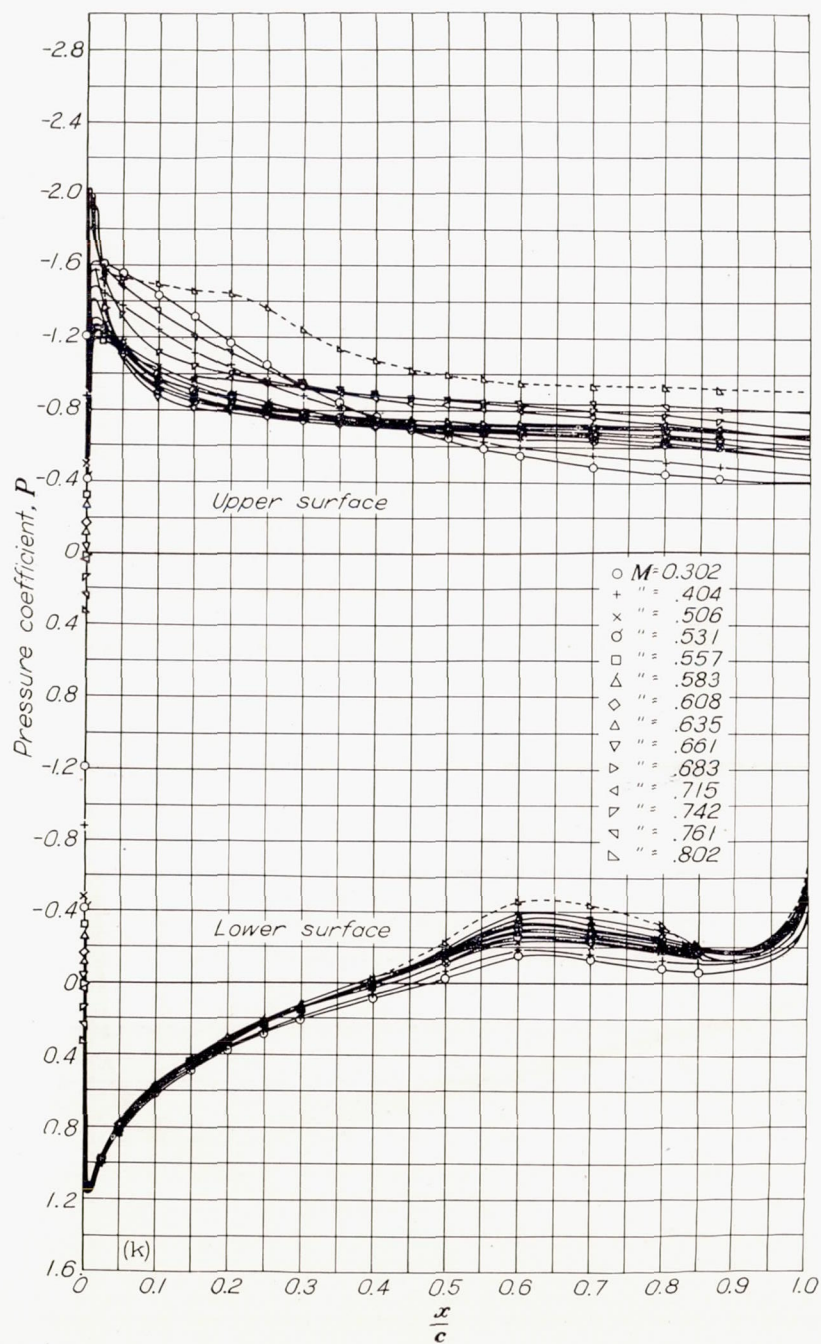
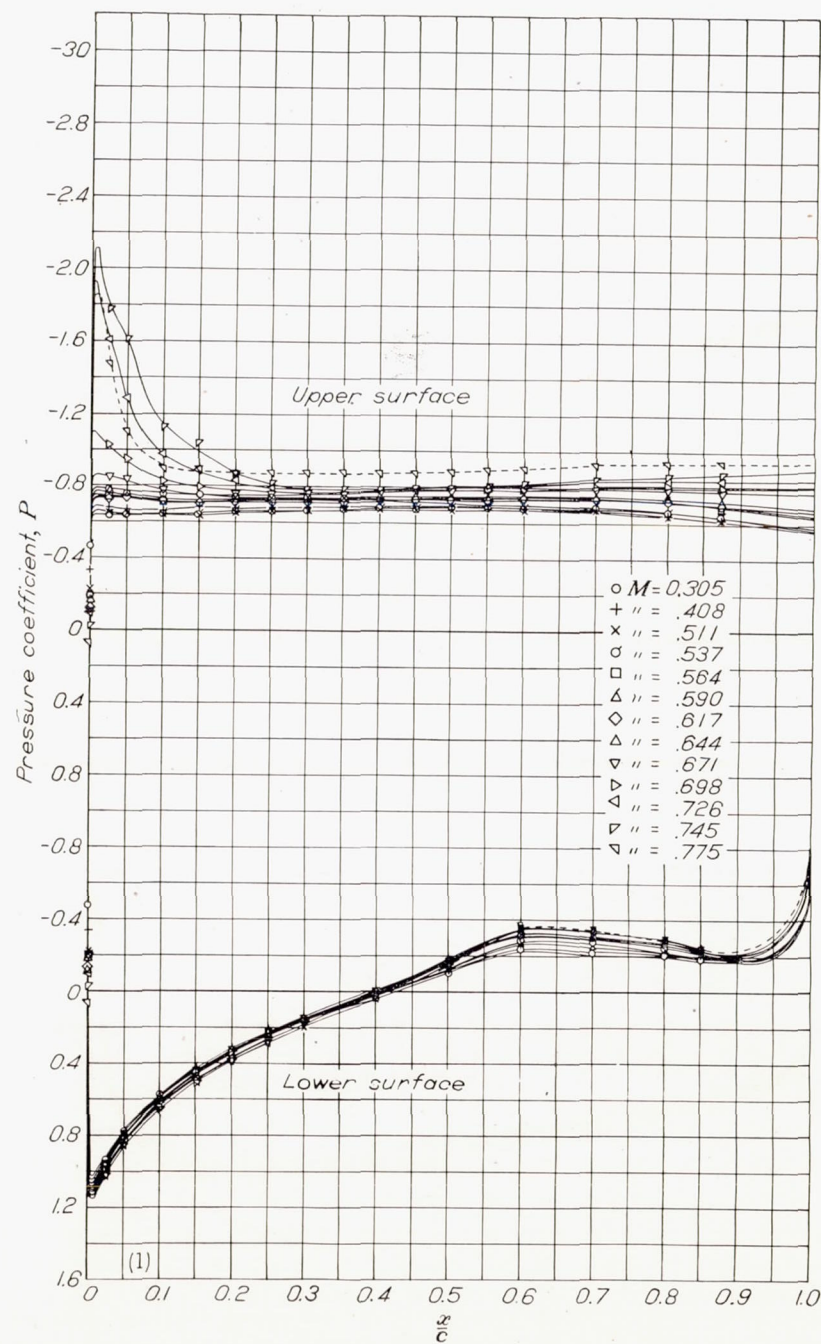
FIGURE 3.—Continued. NACA 66, 2-215 ($a=0.6$) airfoil section.

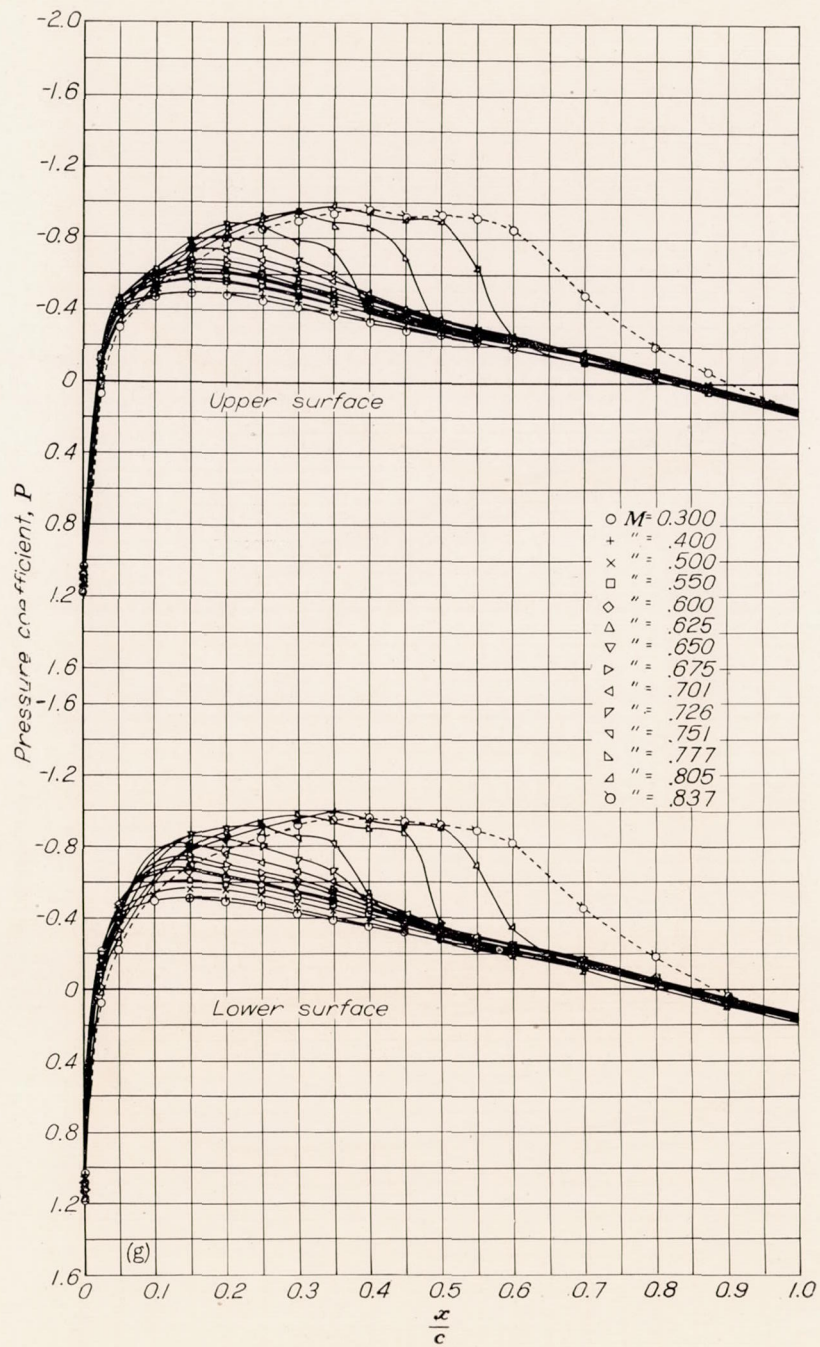


(i) Section angle of attack, $\alpha_0=10^\circ$.
 FIGURE 3.—Continued. NACA 66, 2-215 ($a=0.6$) airfoil section.



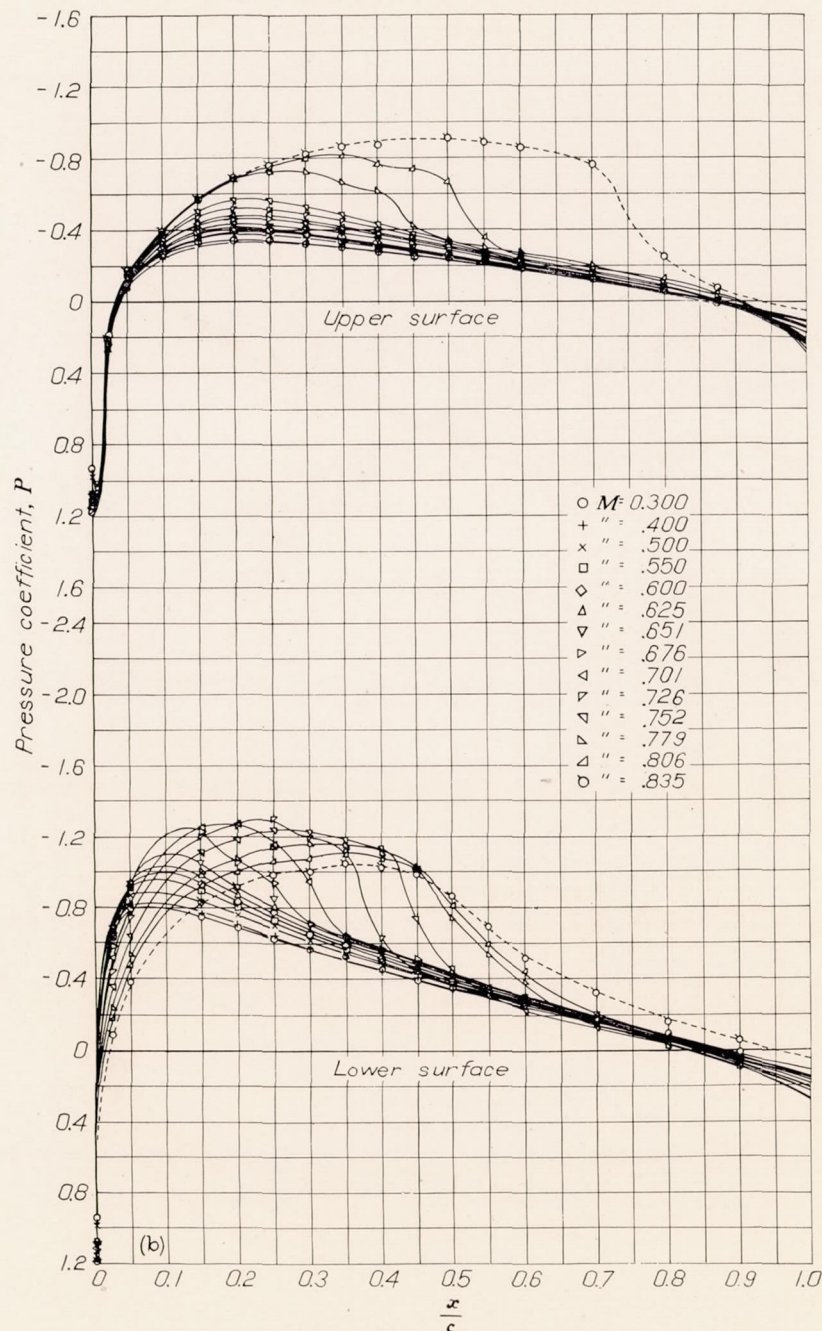
(j) Section angle of attack, $\alpha_0=12^\circ$.
 FIGURE 3.—Continued. NACA 66, 2-215 ($a=0.6$) airfoil section.

(k) Section angle of attack, $\alpha_0=14^\circ$.FIGURE 3.—Continued. NACA 66, 2-215 ($a=0.6$) airfoil section.(l) Section angle of attack, $\alpha_0=16^\circ$.FIGURE 3.—Concluded. NACA 66, 2-215 ($a=0.6$) airfoil section.



(a) Section angle of attack, $\alpha_0=0^\circ$.

FIGURE 4.—Pressure distribution over the NACA 0015 airfoil section with constant angle of attack and varying Mach number.



(b) Section angle of attack, $\alpha_0=-2^\circ$.

FIGURE 4.—Continued. NACA 0015 airfoil section.

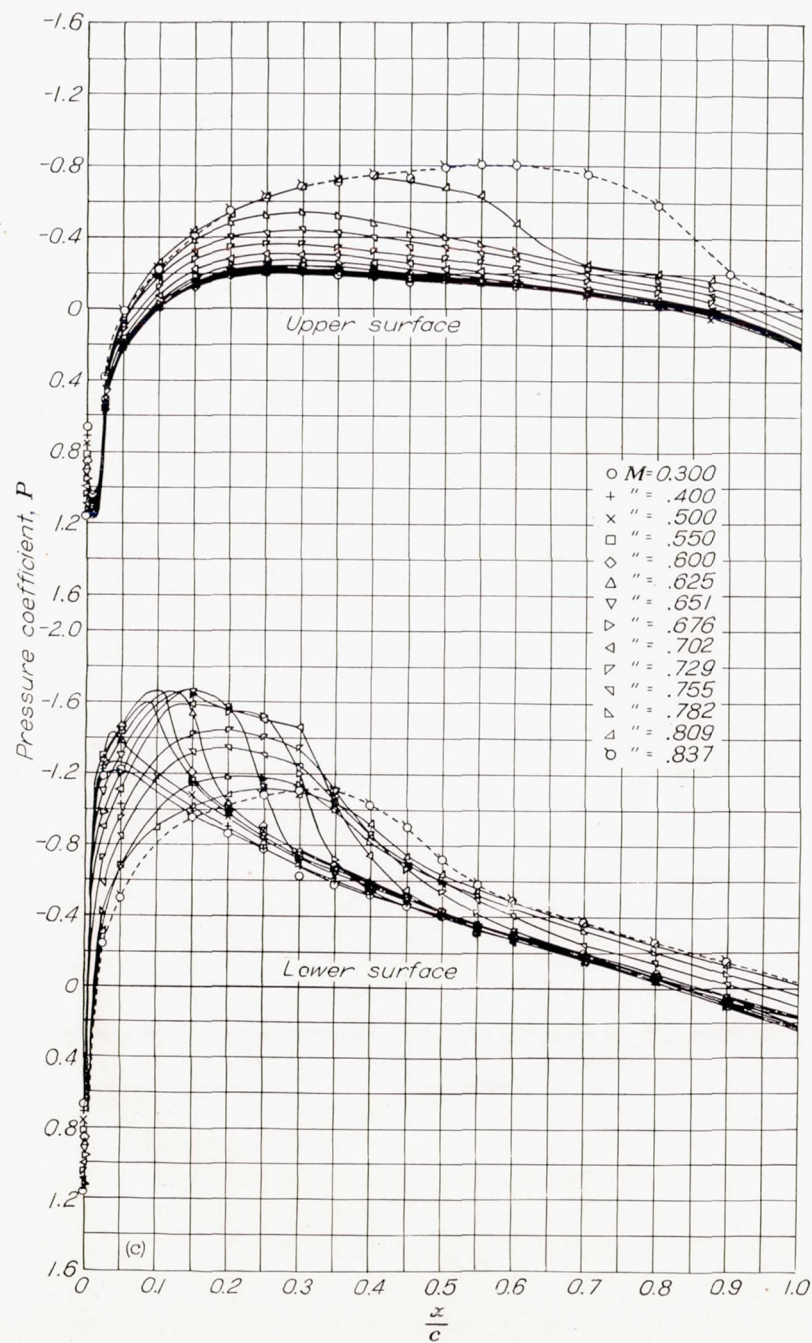
(c) Section angle of attack, $\alpha_0 = -4^\circ$.

FIGURE 4.—Continued. NACA 0015 airfoil section.

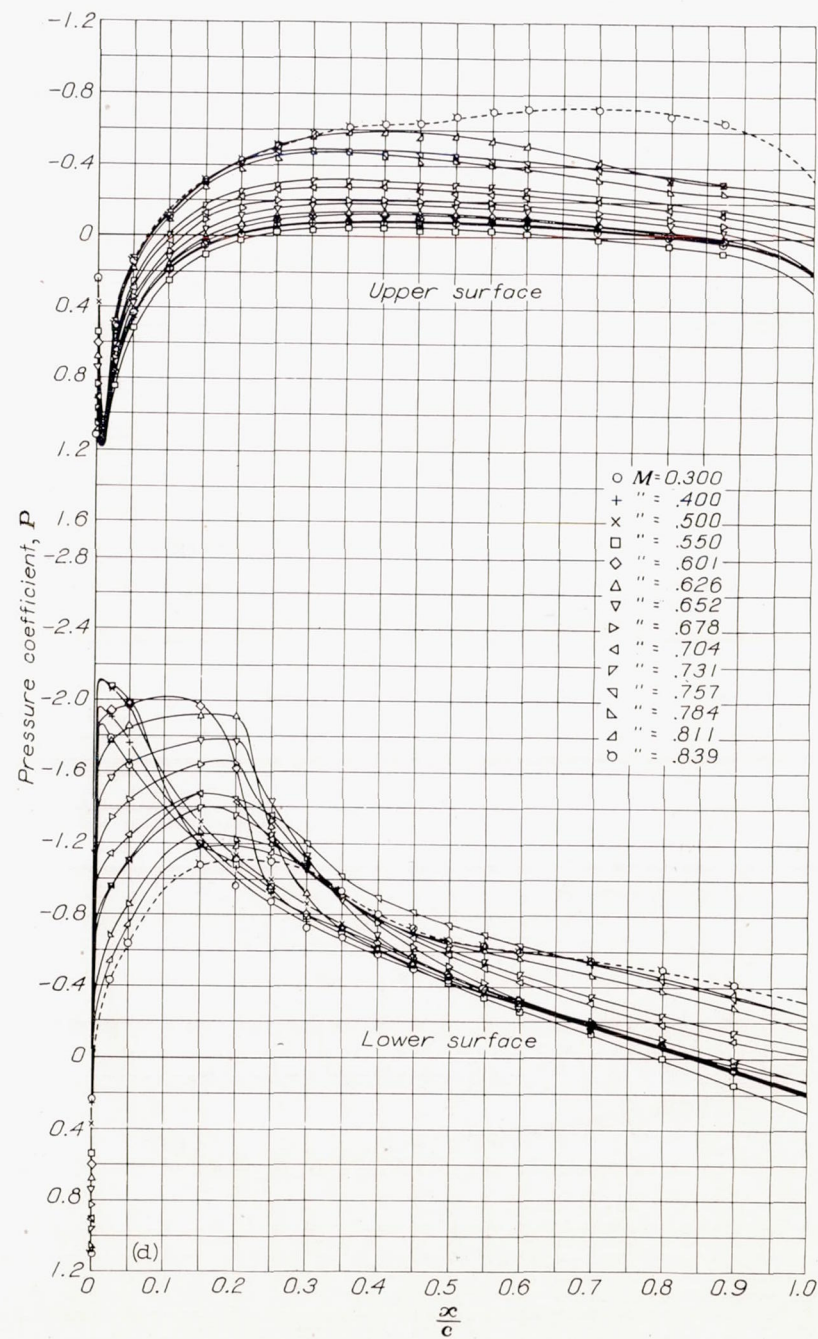
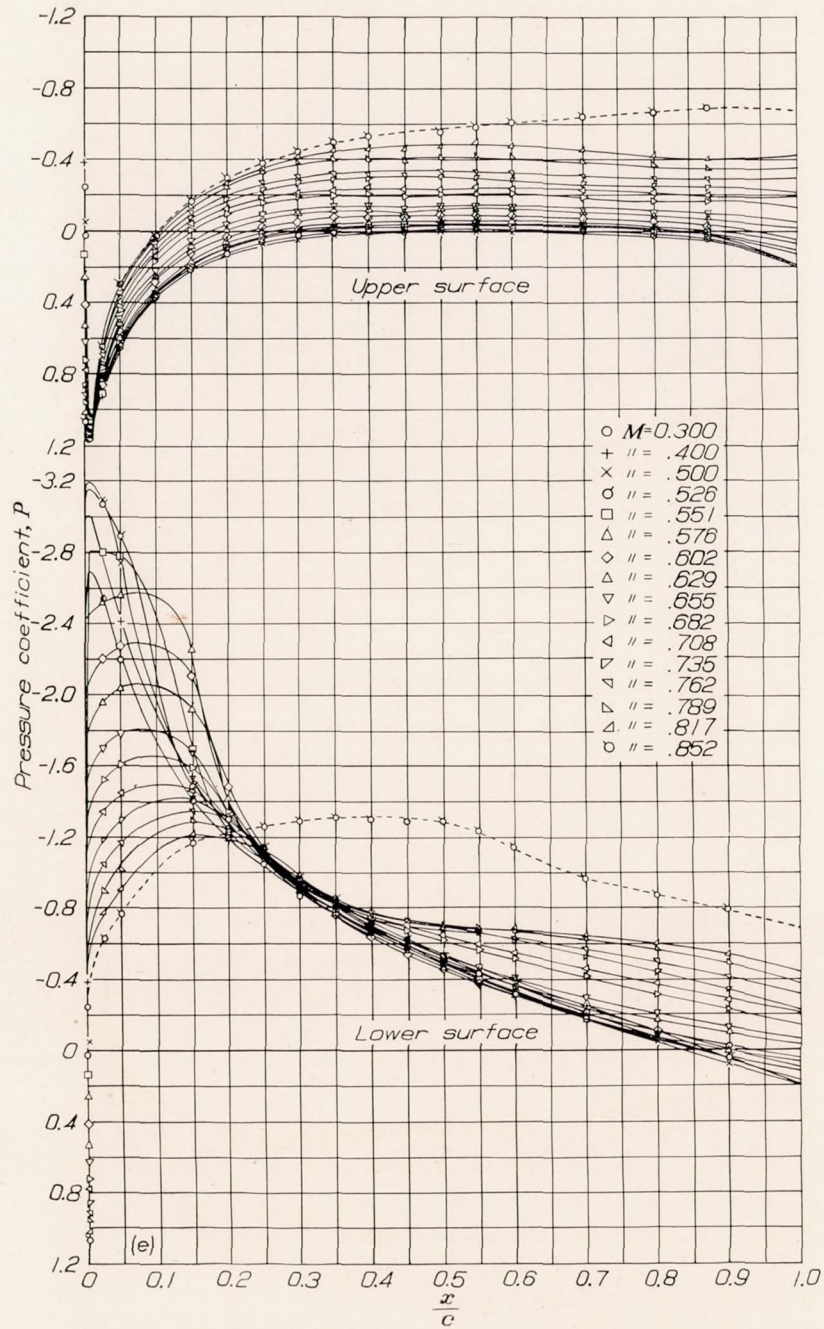
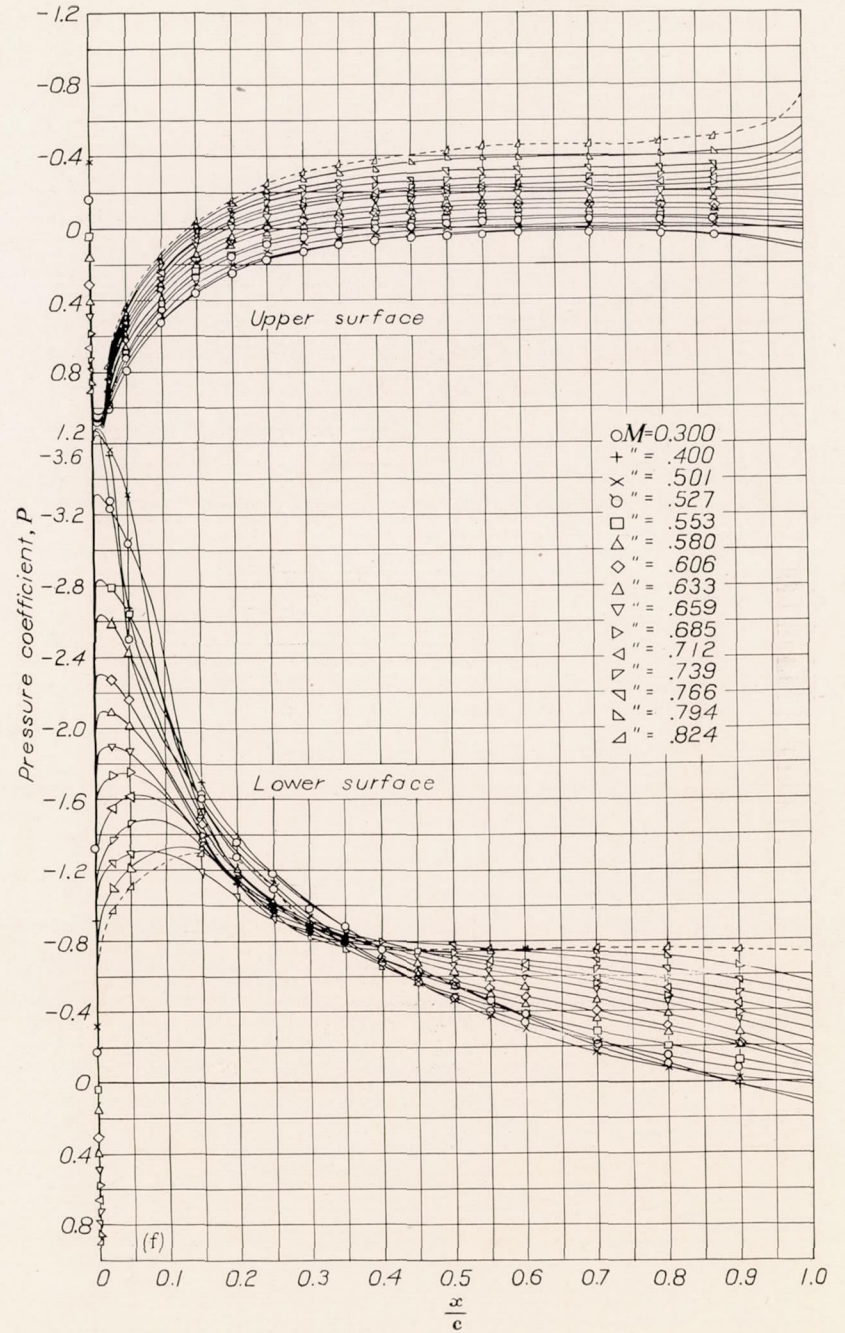
(d) Section angle of attack, $\alpha_0 = -6^\circ$.

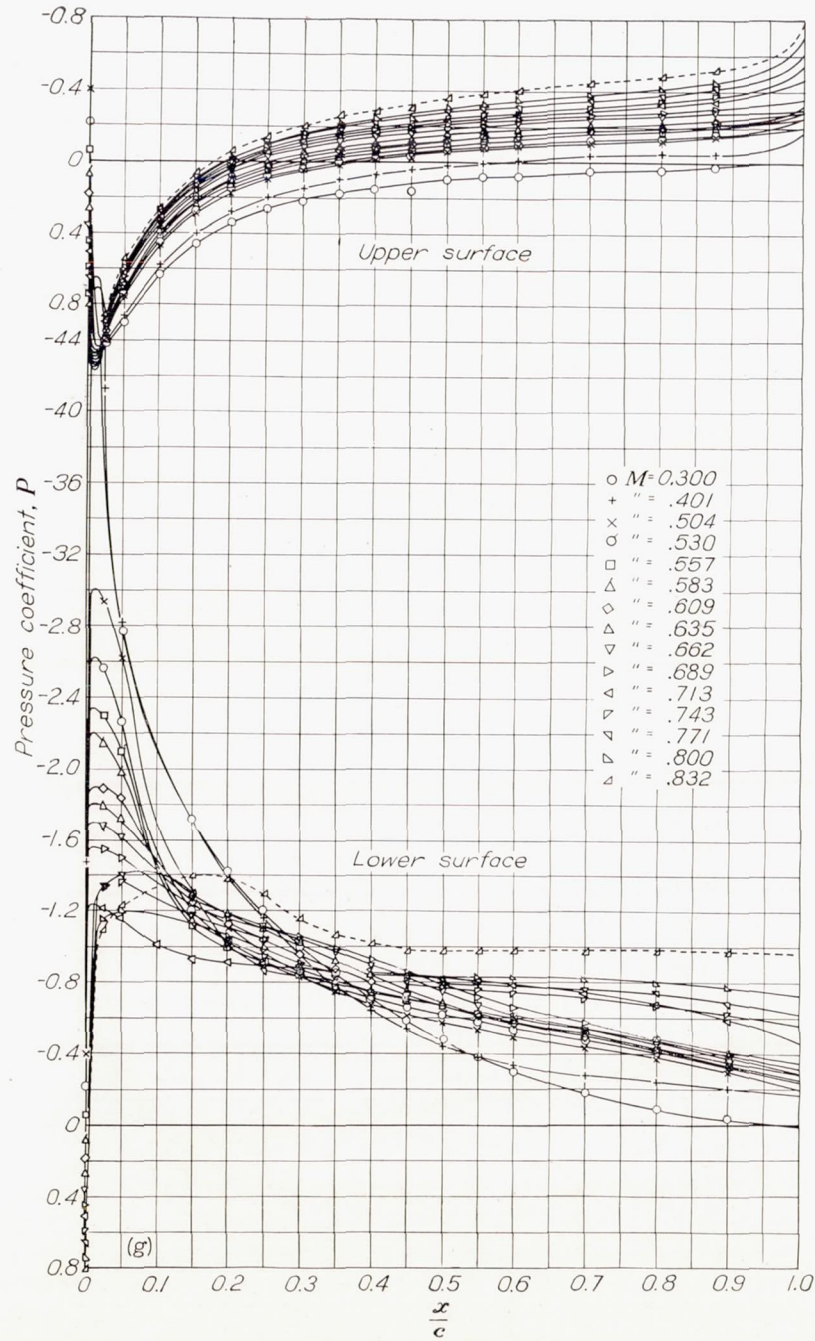
FIGURE 4.—Continued. NACA 0015 airfoil section.



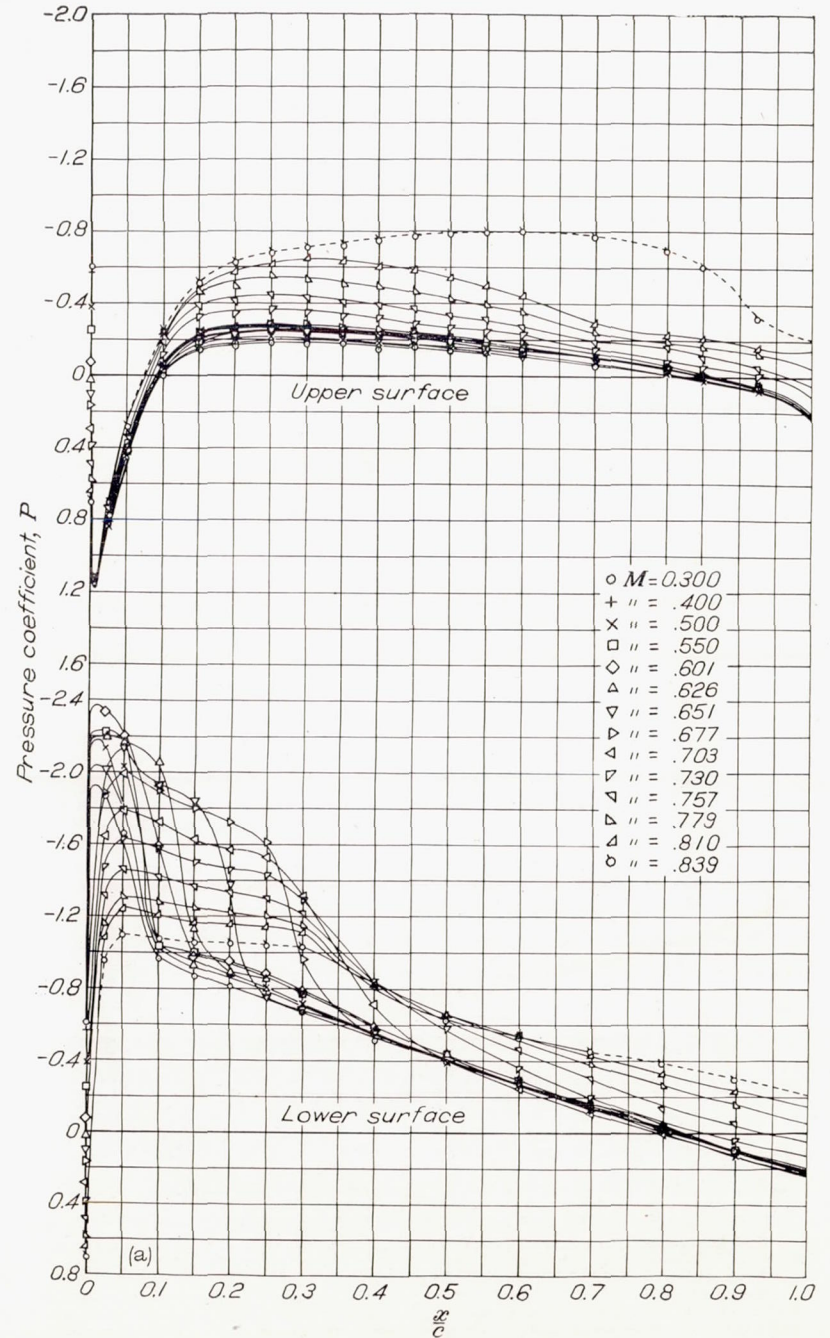
(e) Section angle of attack, $\alpha_0 = -8^\circ$.
 FIGURE 4.—Continued. NACA 0015 airfoil section.



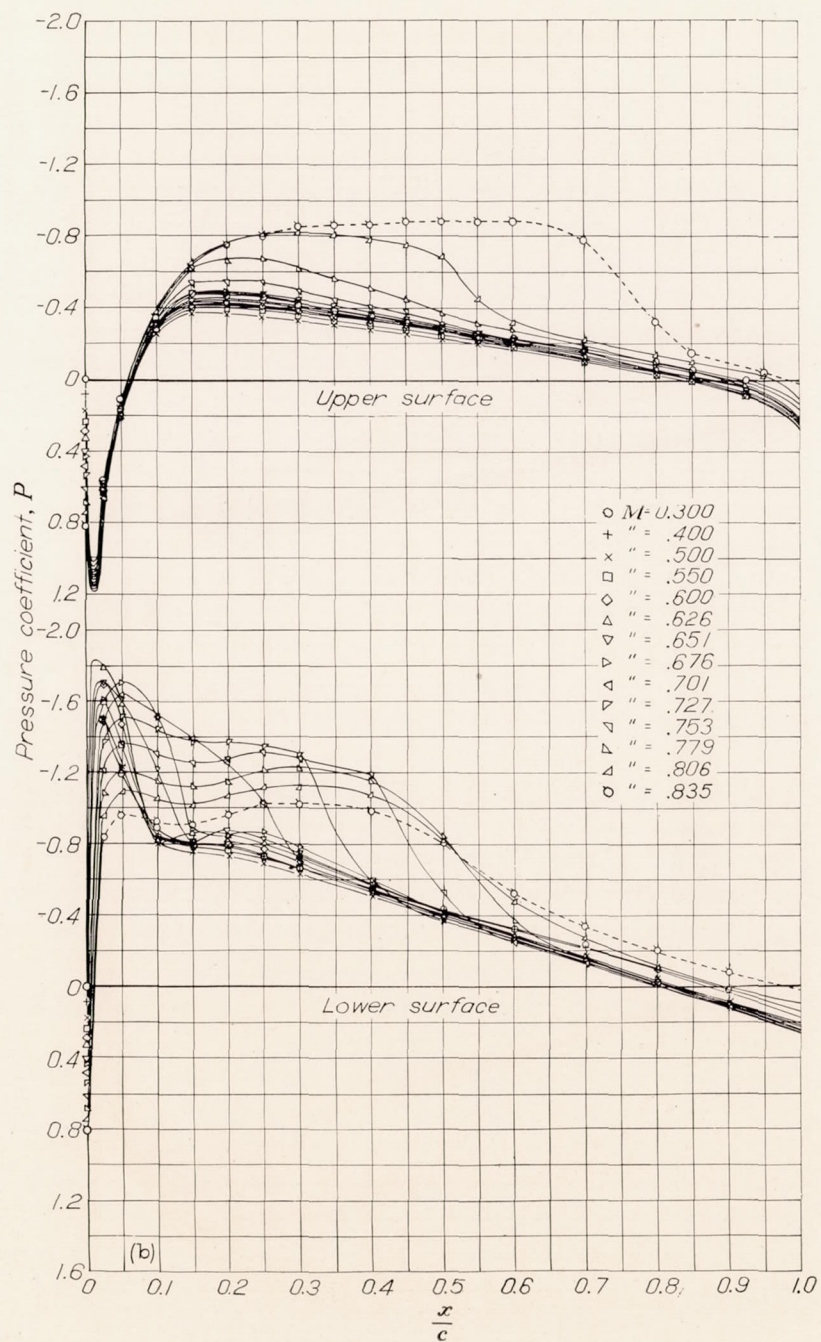
(f) Section angle of attack, $\alpha_0 = -10^\circ$.
 FIGURE 4.—Continued. NACA 0015 airfoil section.



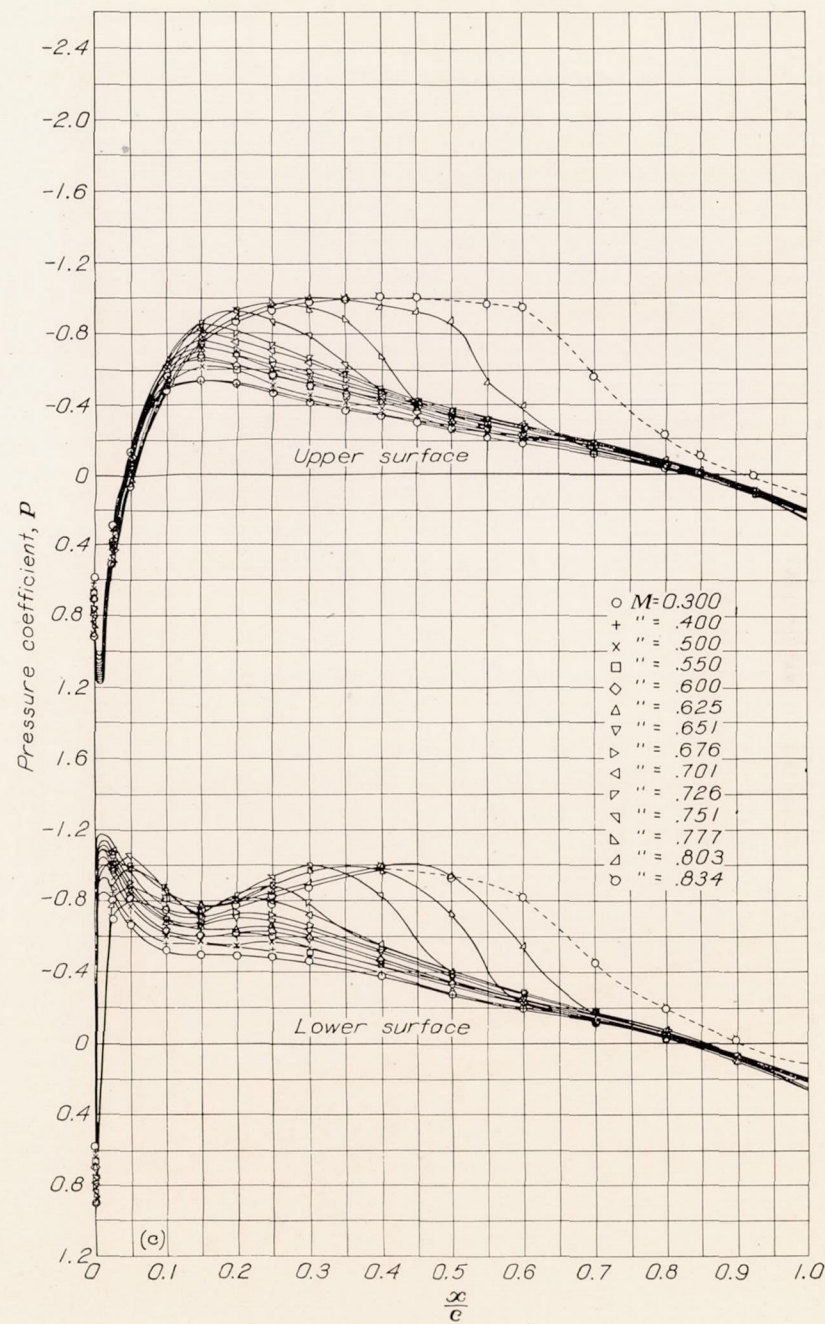
(g) Section angle of attack, $\alpha_0 = -12^\circ$.
 FIGURE 4.—Concluded. NACA 0015 airfoil section.



(a) Section angle of attack, $\alpha_0 = -6^\circ$.
 FIGURE 5.—Pressure distribution over the NACA 23015 airfoil section with constant angle of attack and varying Mach number.



(b) Section angle of attack $\alpha_0 = -4^\circ$.
 FIGURE 5.—Continued. NACA 23015 airfoil section.



(c) Section angle of attack $\alpha_0 = -2^\circ$.
 FIGURE 5.—Continued. NACA 23015 airfoil section.

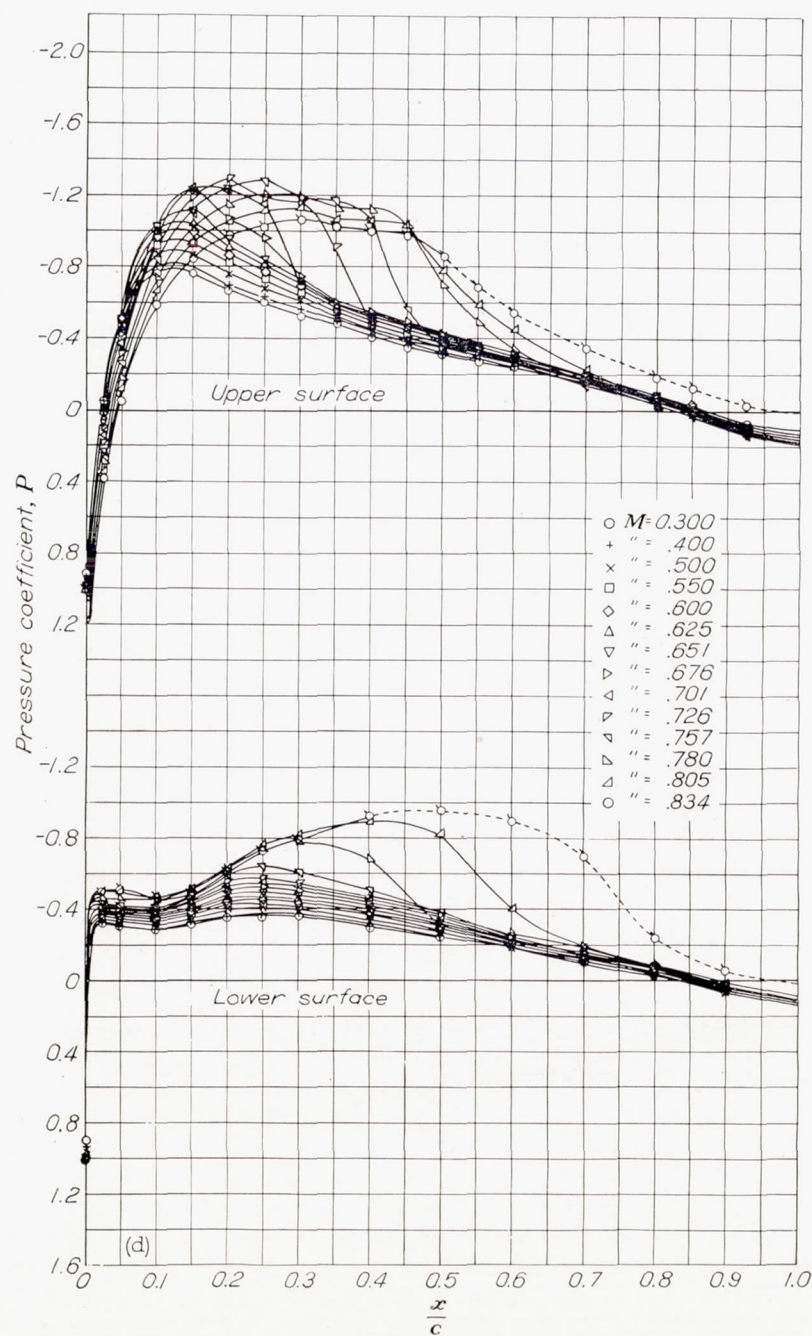
(d) Section angle of attack $\alpha_0 = 0^\circ$.

FIGURE 5.—Continued. NACA 23015 airfoil section.

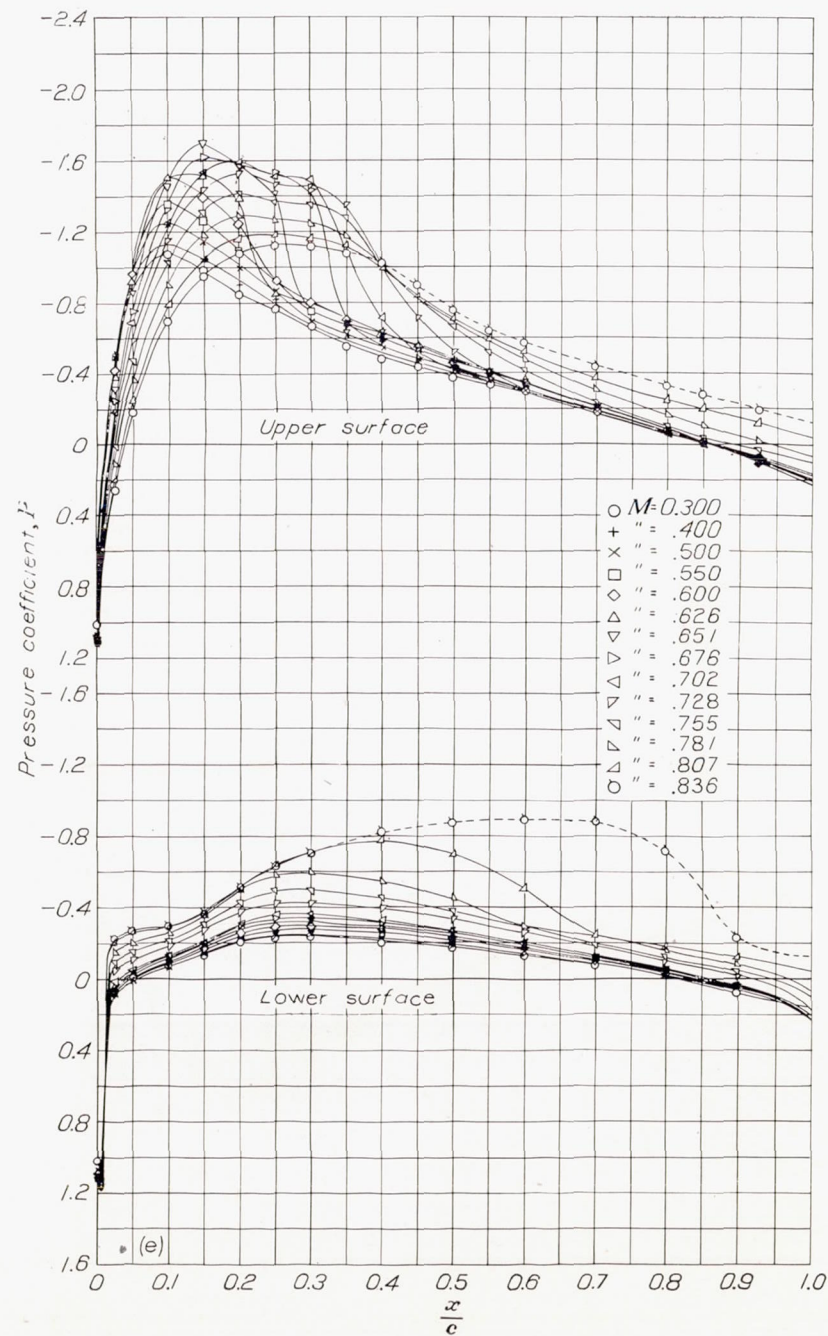
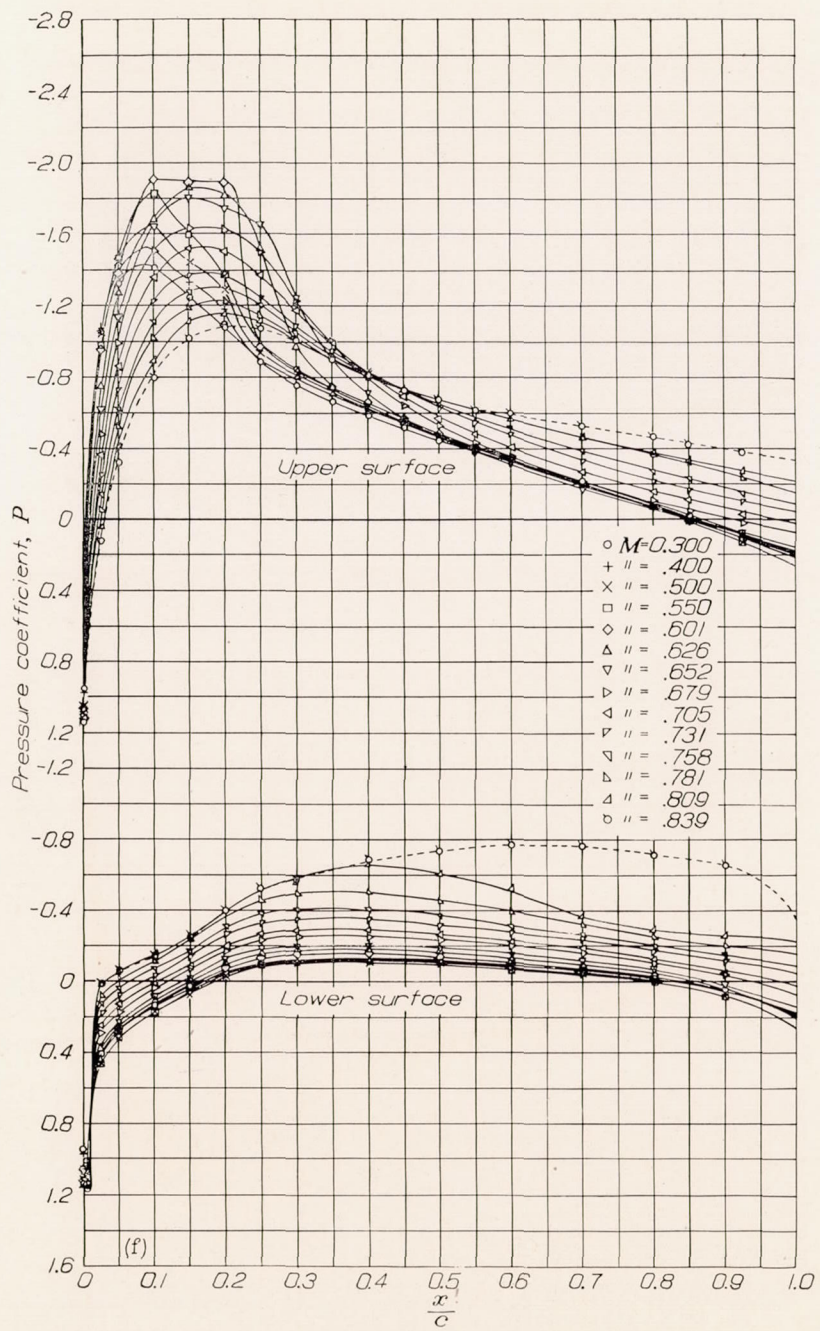
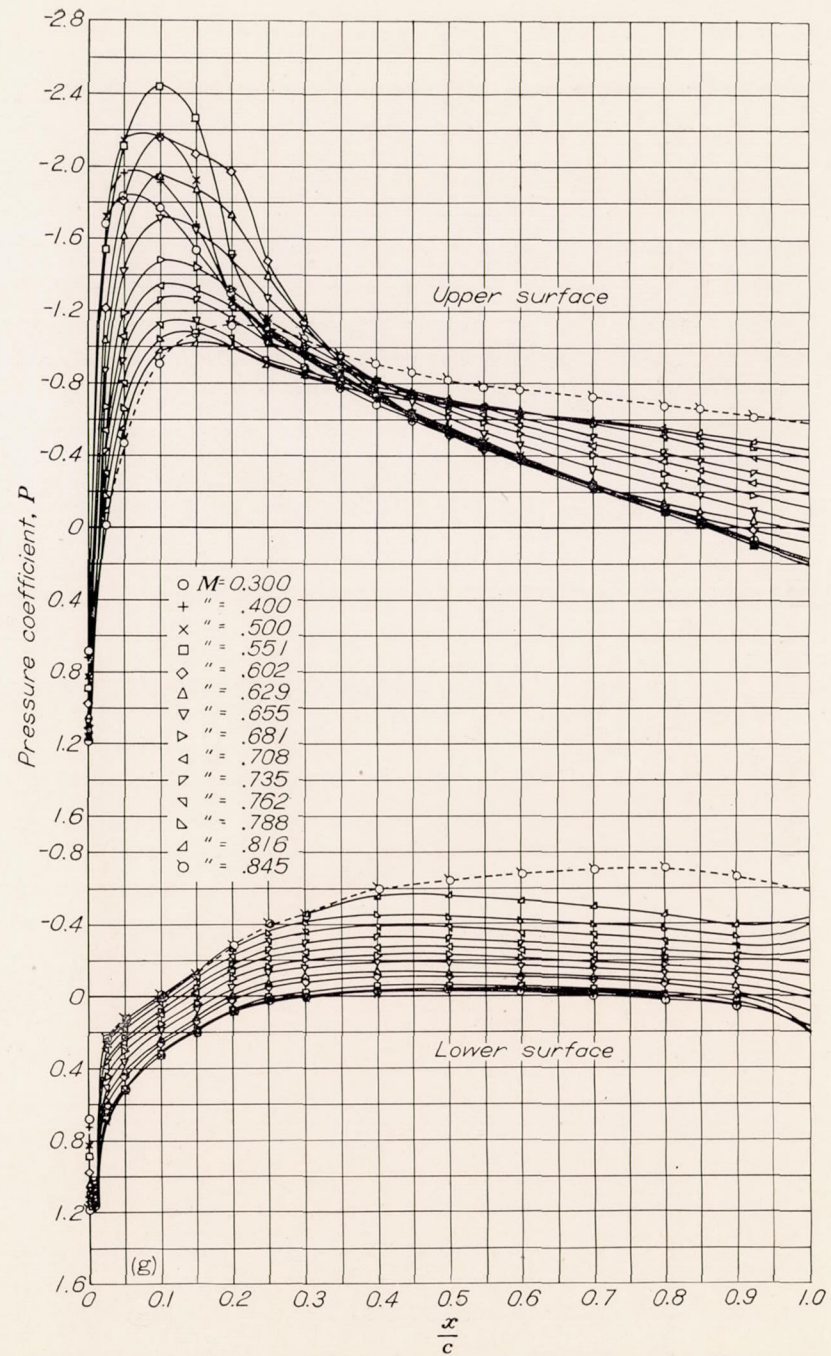
(e) Section angle of attack, $\alpha_0 = 2^\circ$.

FIGURE 5.—Continued. NACA 23015 airfoil section.



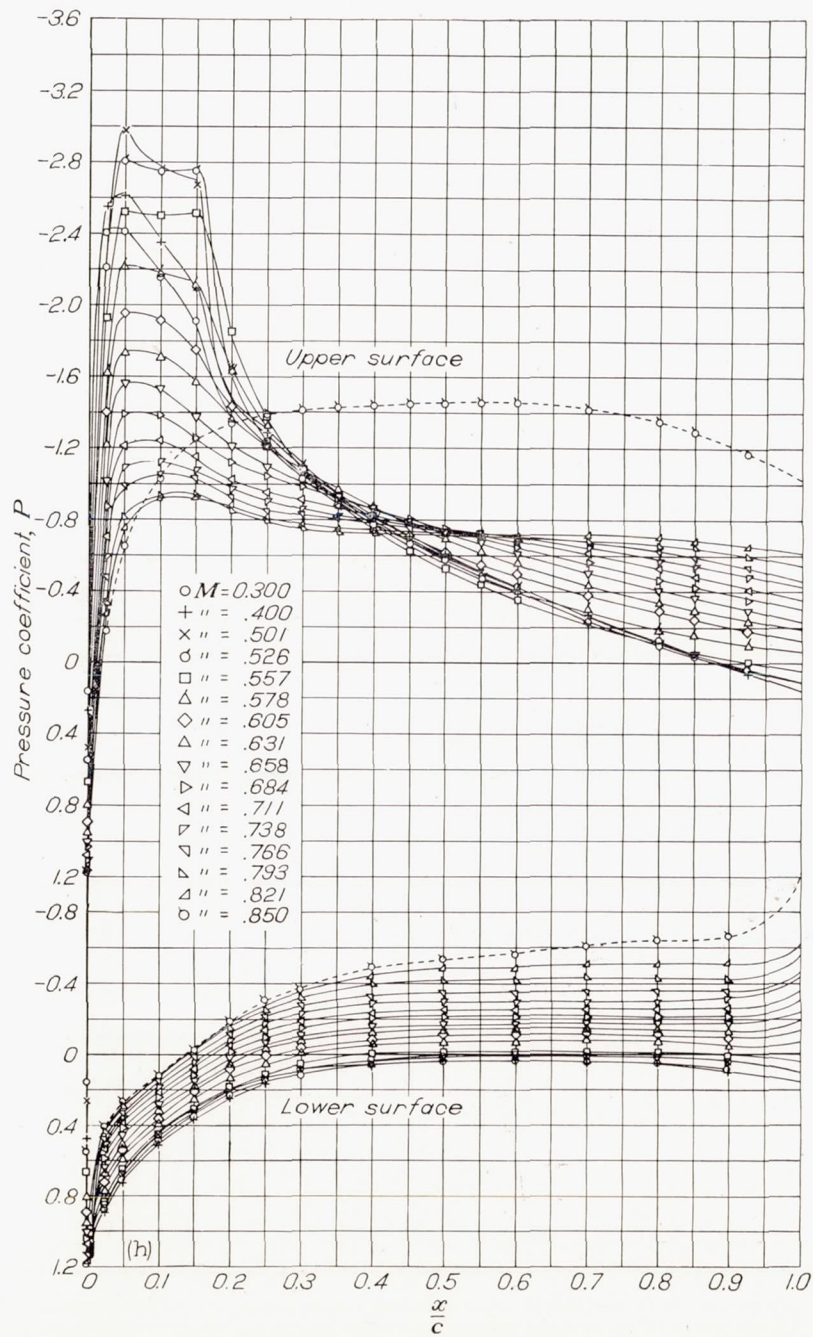
(f) Section angle of attack $\alpha_0 = 4^\circ$.

FIGURE 5.—Continued. NACA 23015 airfoil section.



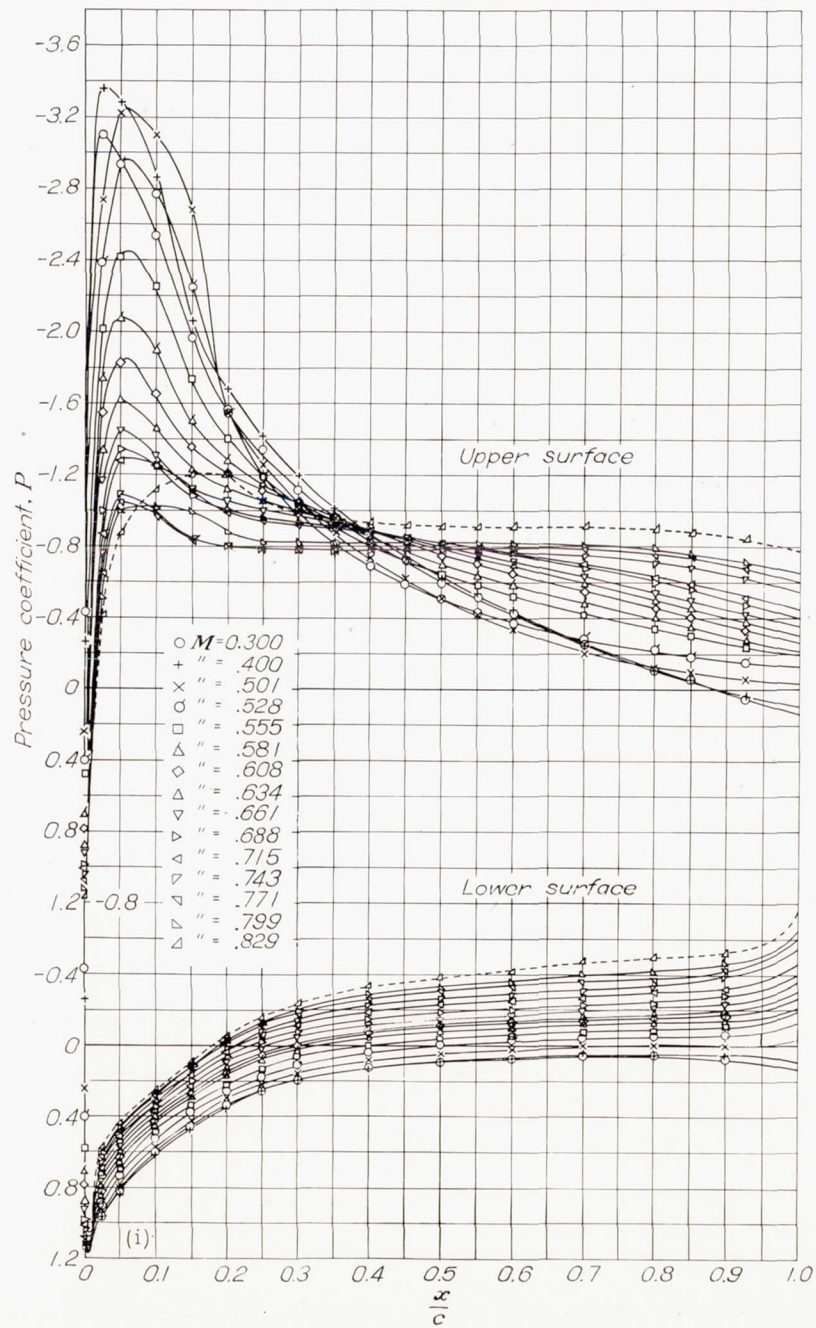
(g) Section angle of attack, $\alpha_0 = 6^\circ$.

FIGURE 5.—Continued. NACA 23015 airfoil section.



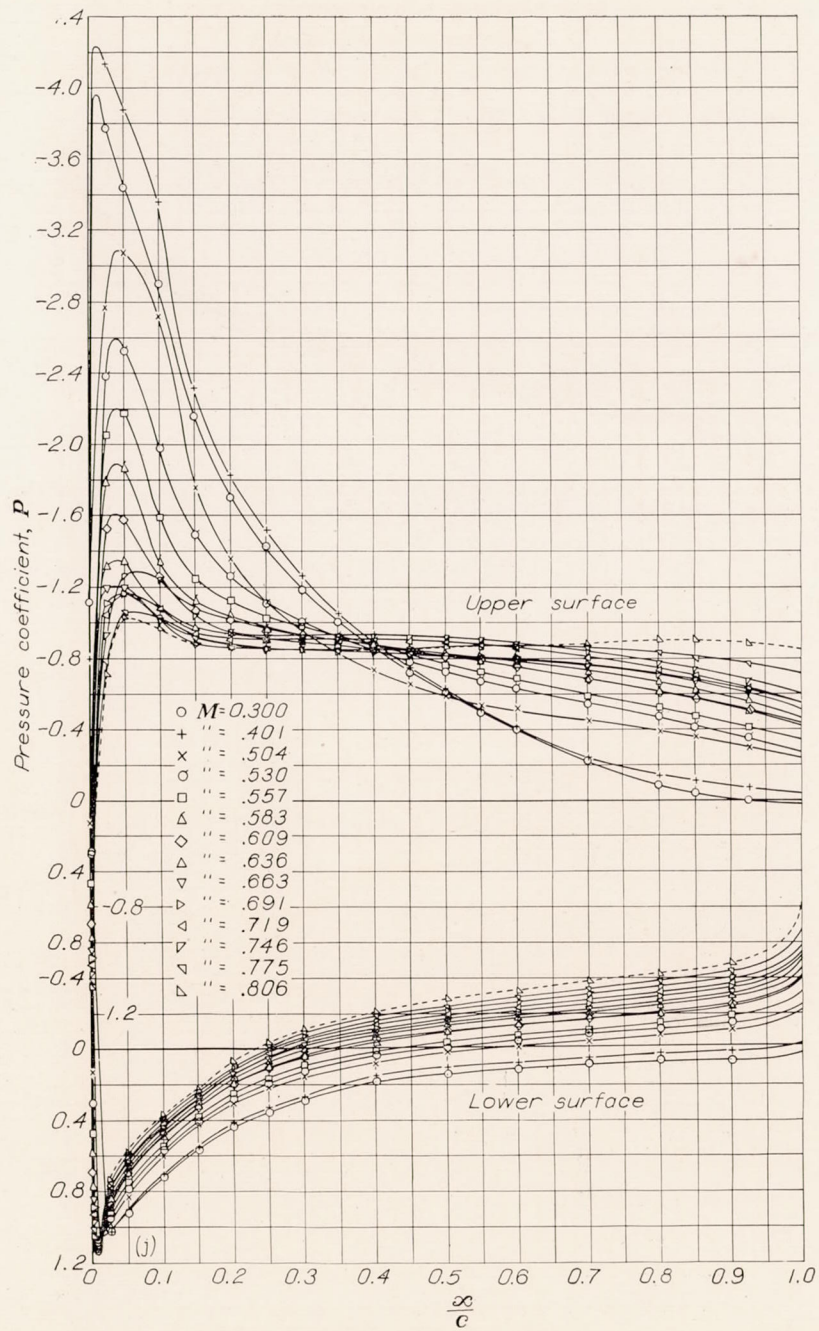
(h) Section angle of attack $\alpha_0=8^\circ$.

FIGURE 5.—Continued. NACA 23015 airfoil section.

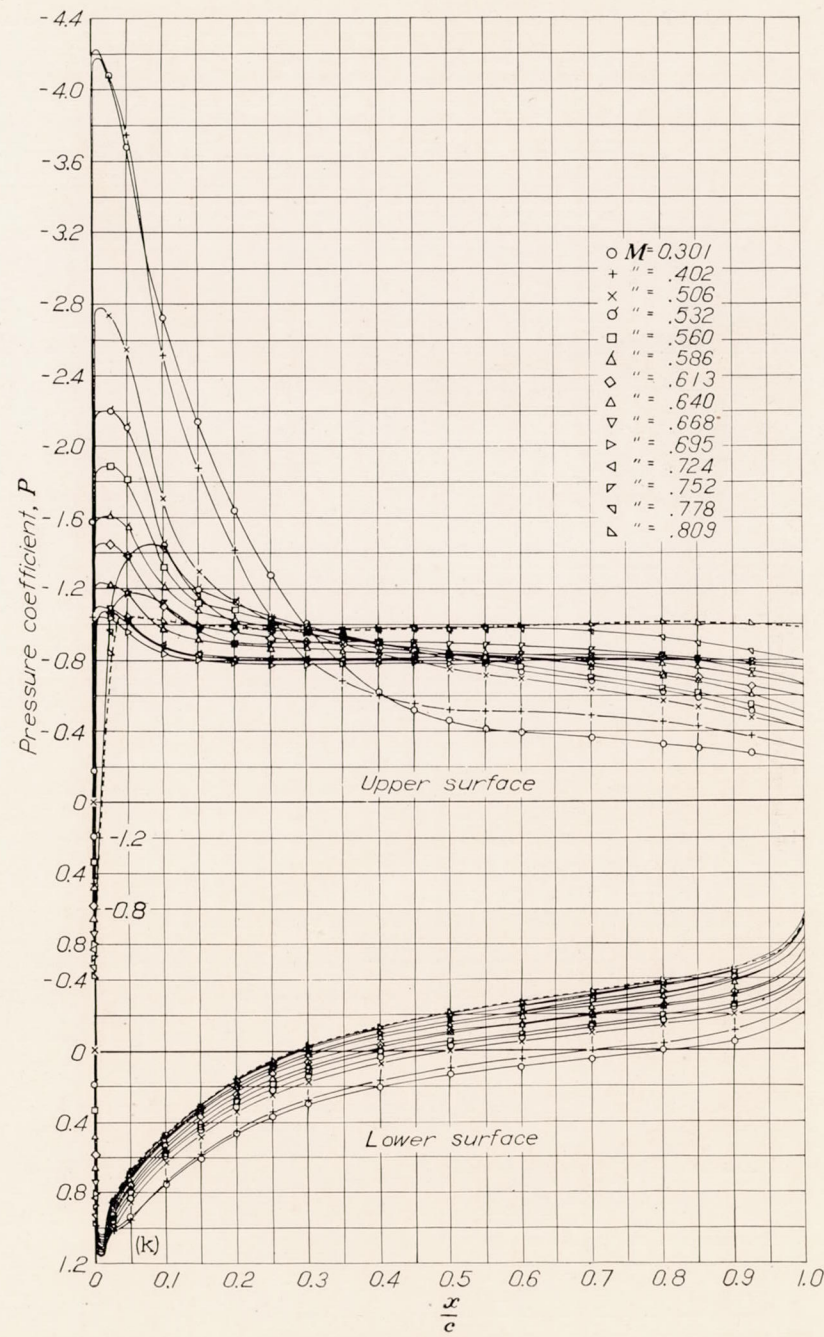


(i) Section angle of attack $\alpha_0=10^\circ$.

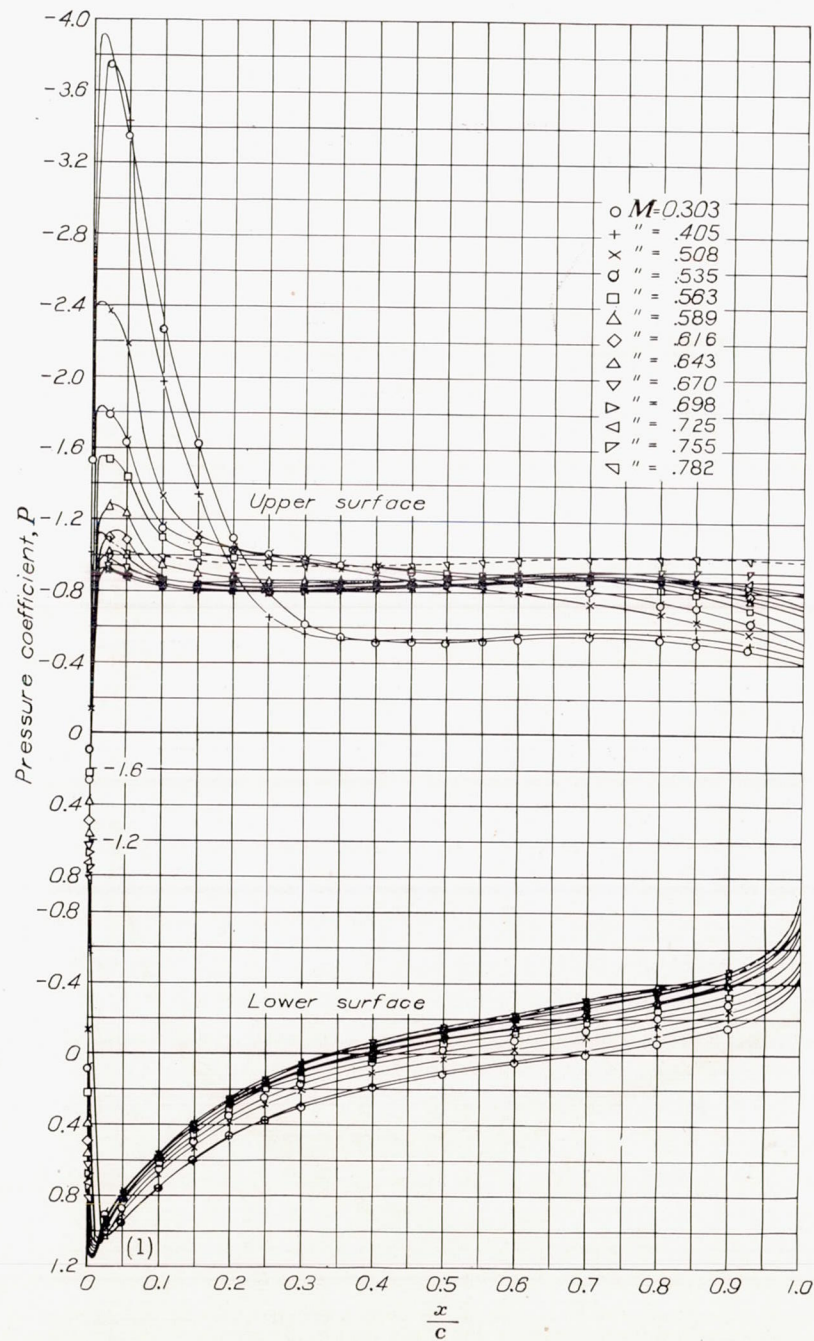
FIGURE 5.—Continued. NACA 23015 airfoil section.



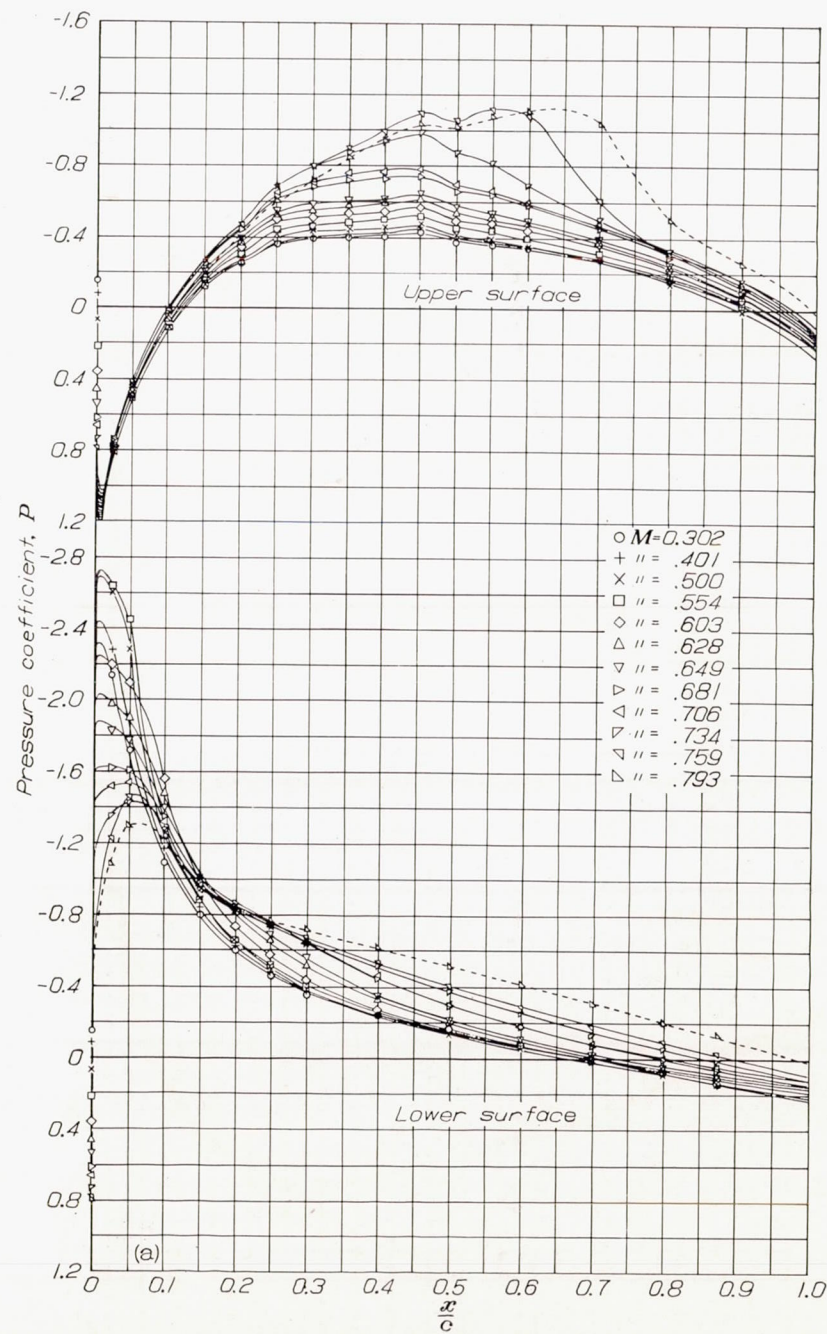
(j) Section angle of attack, $\alpha_0=12^\circ$.
 FIGURE 5.—Continued. NACA 23015 airfoil section.



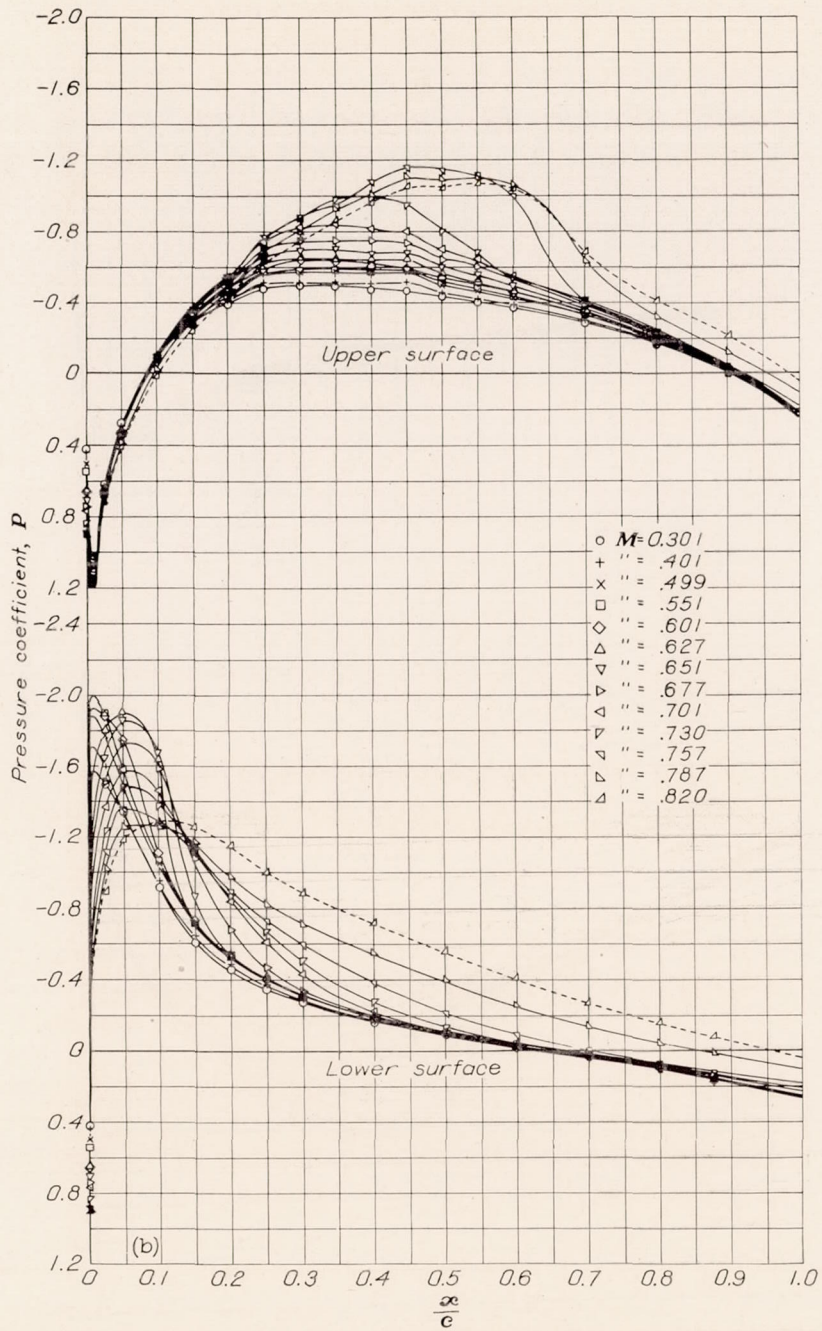
(k) Section angle of attack, $\alpha_0=14^\circ$.
 FIGURE 5.—Continued. NACA 23015 airfoil section.



(1) Section angle of attack, $\alpha_0=16^\circ$.
 FIGURE 5.—Concluded. NACA 23015 airfoil section.

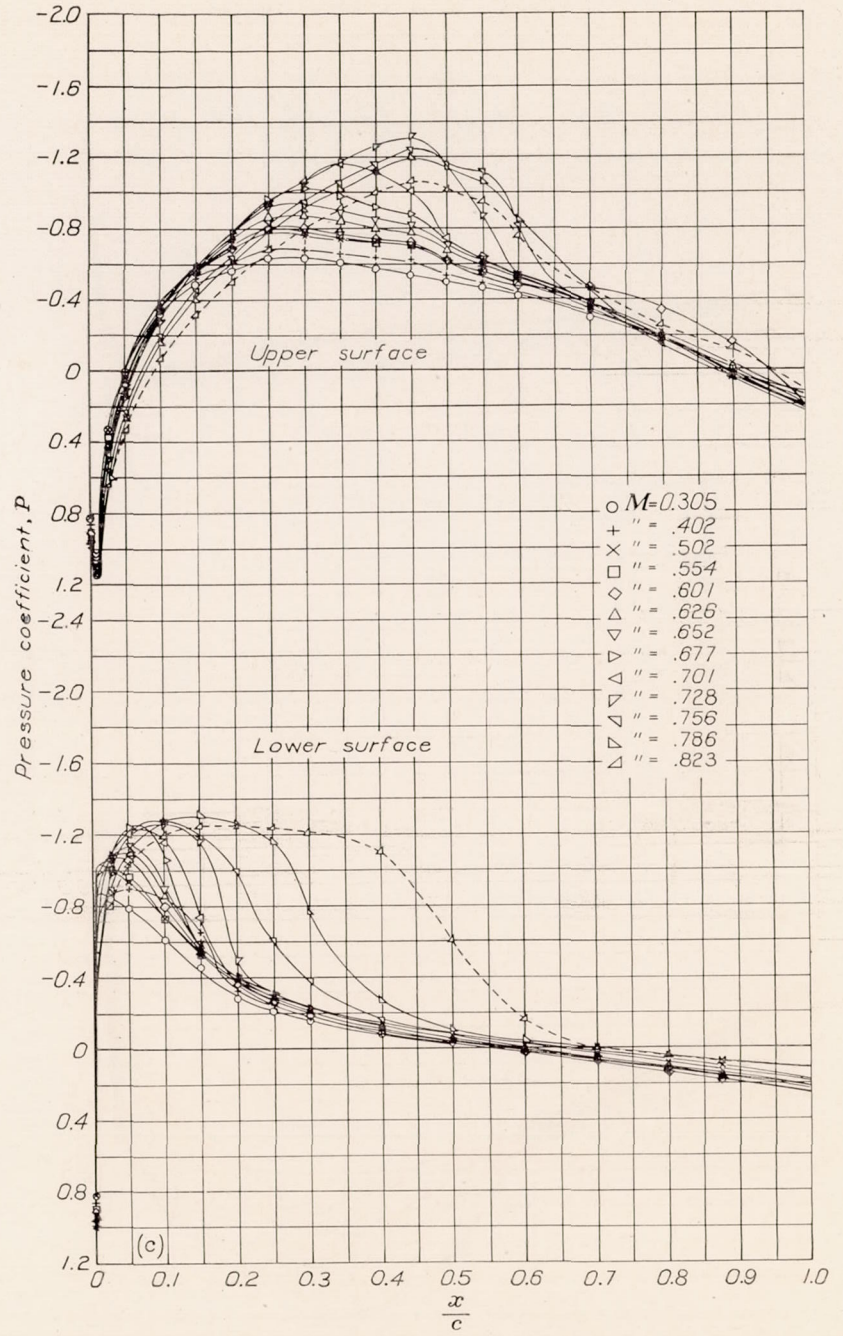


(a) Section angle of attack, $\alpha_0=-6^\circ$.
 FIGURE 6.—Pressure distribution over the NACA 4415 airfoil section with constant angle of attack and varying Mach number.



(b) Section angle of attack, $\alpha_0 = -4^\circ$.

FIGURE 6.—Continued. NACA 4415 airfoil section.



(c) Section angle of attack, $\alpha_0 = -2^\circ$.

FIGURE 6.—Continued. NACA 4415 airfoil section.

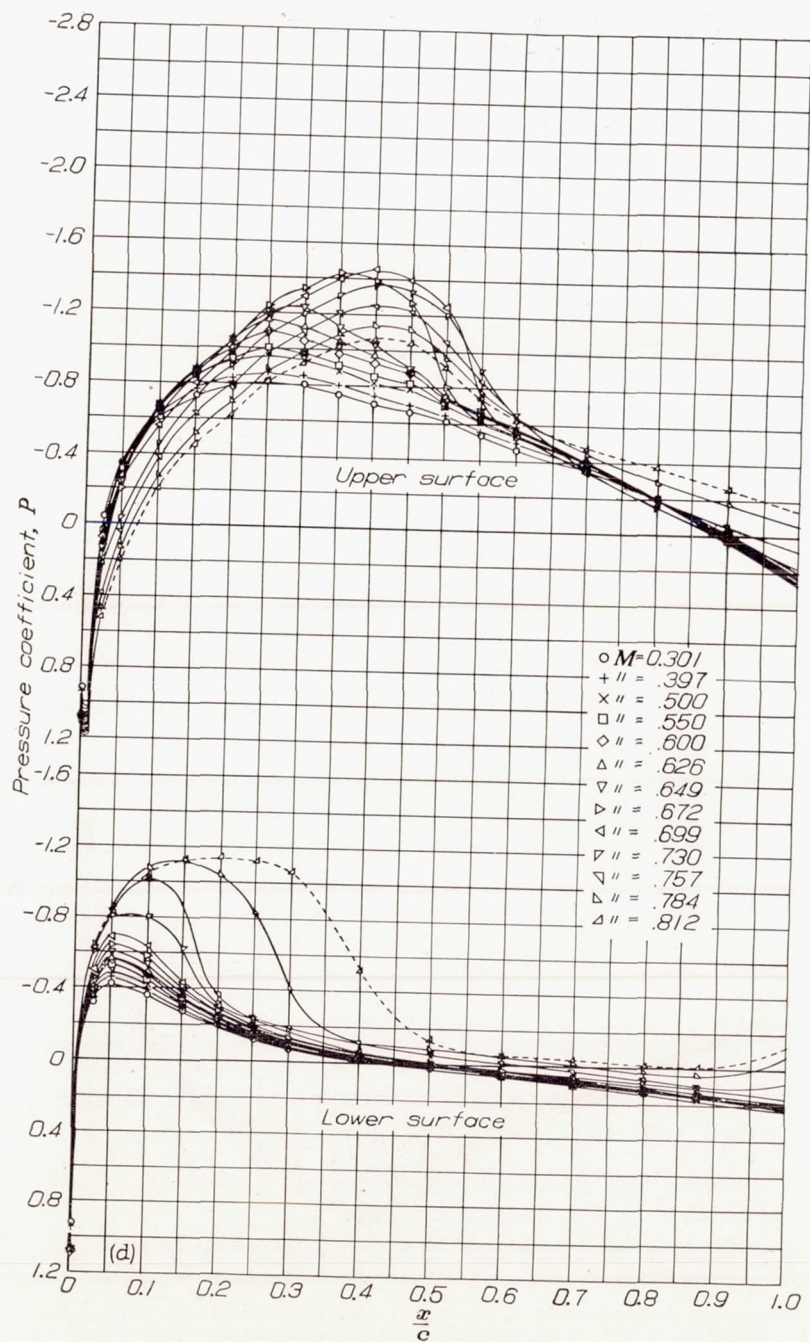
(d) Section angle of attack, $\alpha_0=0^\circ$.

FIGURE 6.—Continued. NACA 4415 airfoil section.

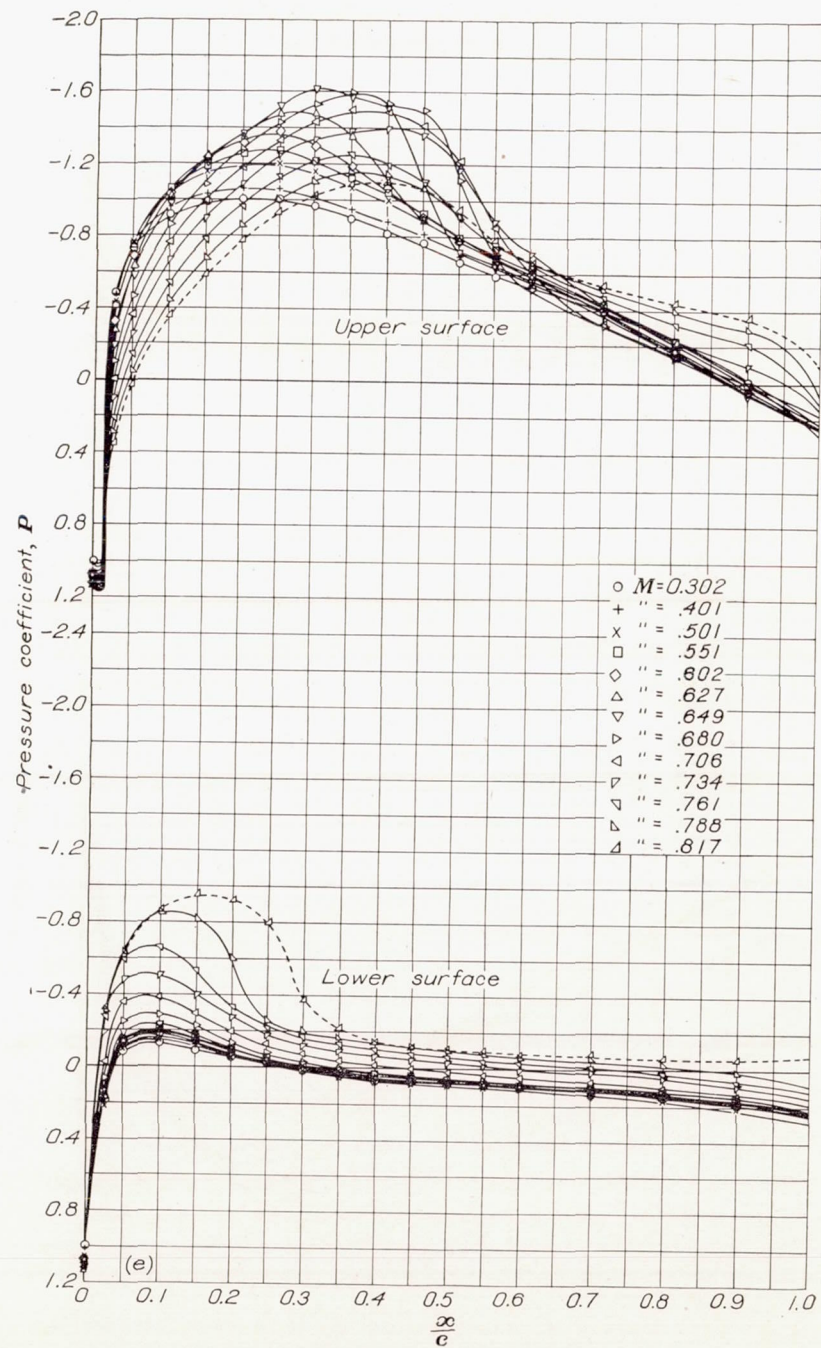
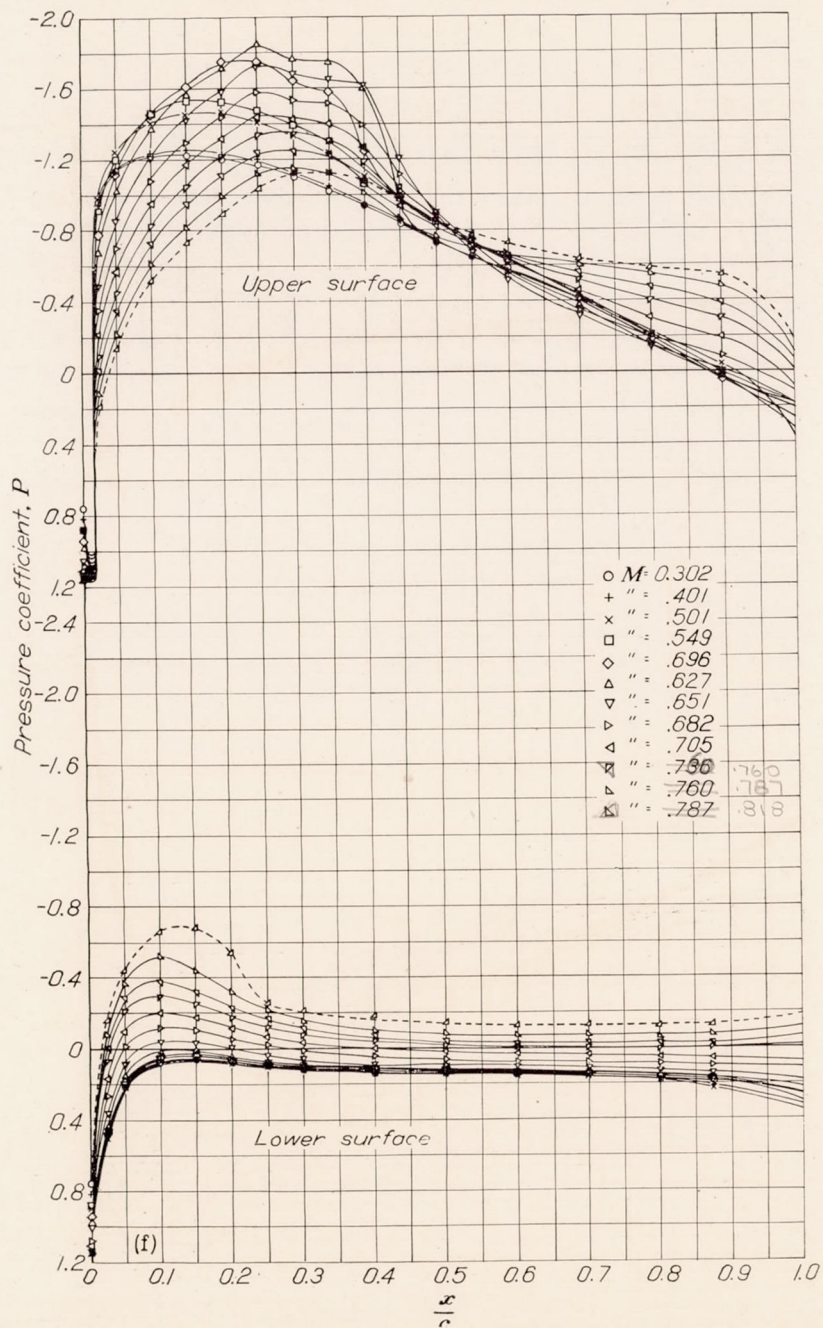
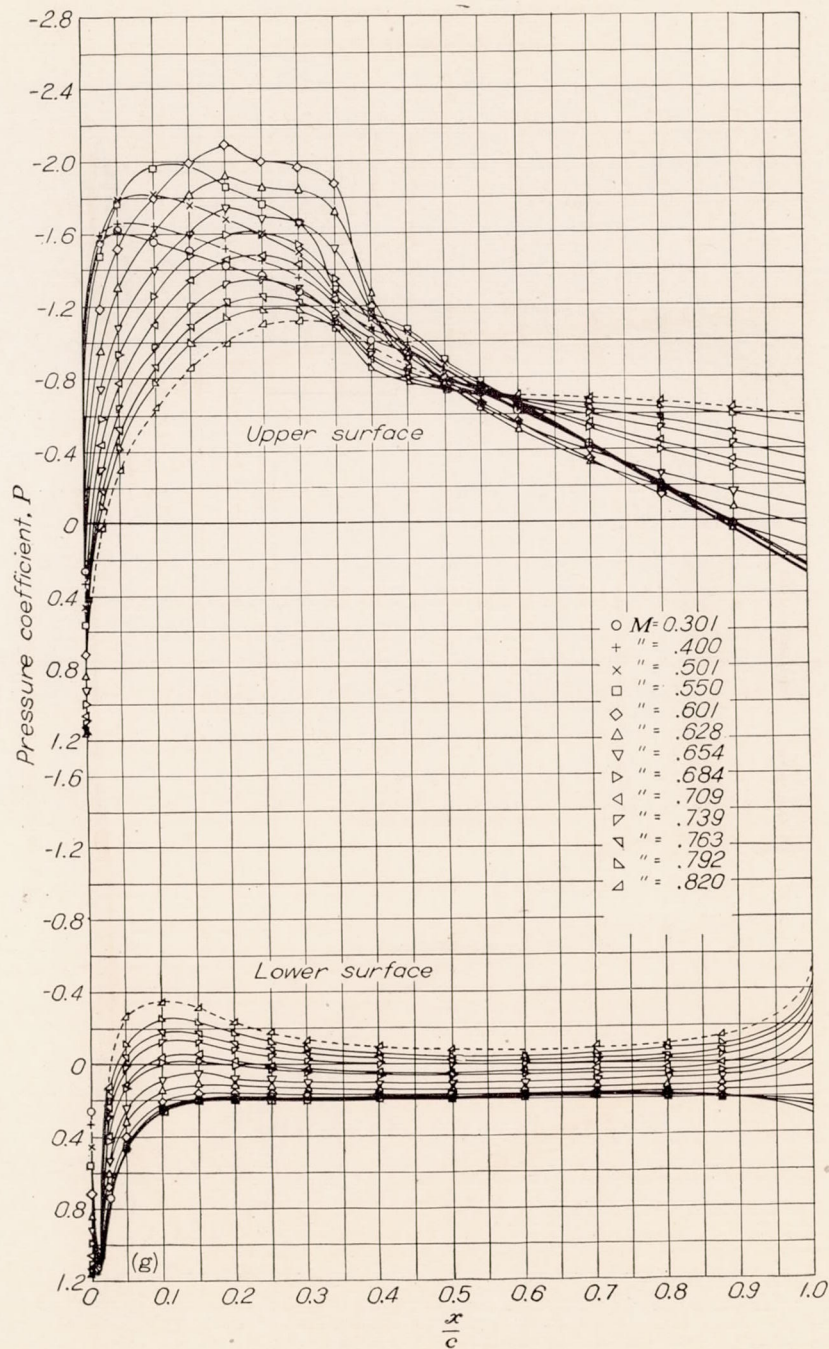
(e) Section angle of attack $\alpha_0=2^\circ$.

FIGURE 6.—Continued. NACA 4415 airfoil section.



(f) Section angle of attack, $\alpha_0=4^\circ$.
 FIGURE 6.—Continued. NACA 4415 airfoil section.



(g) Section angle of attack $\alpha_0=6^\circ$.
 FIGURE 6.—Continued. NACA 4415 airfoil section.

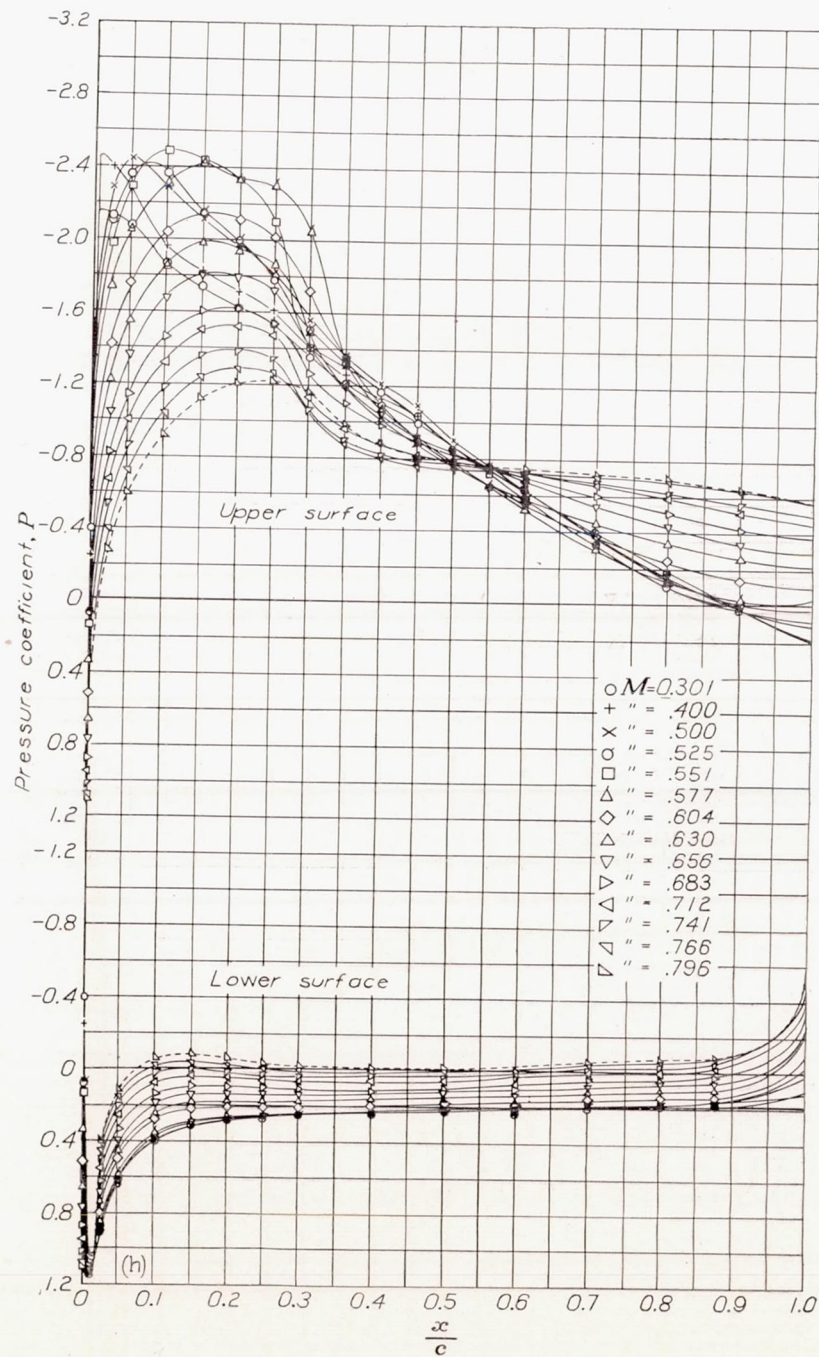
(h) Section angle of attack, $\alpha_0=8^\circ$.

FIGURE 6.—Continued. NACA 4415 airfoil section.

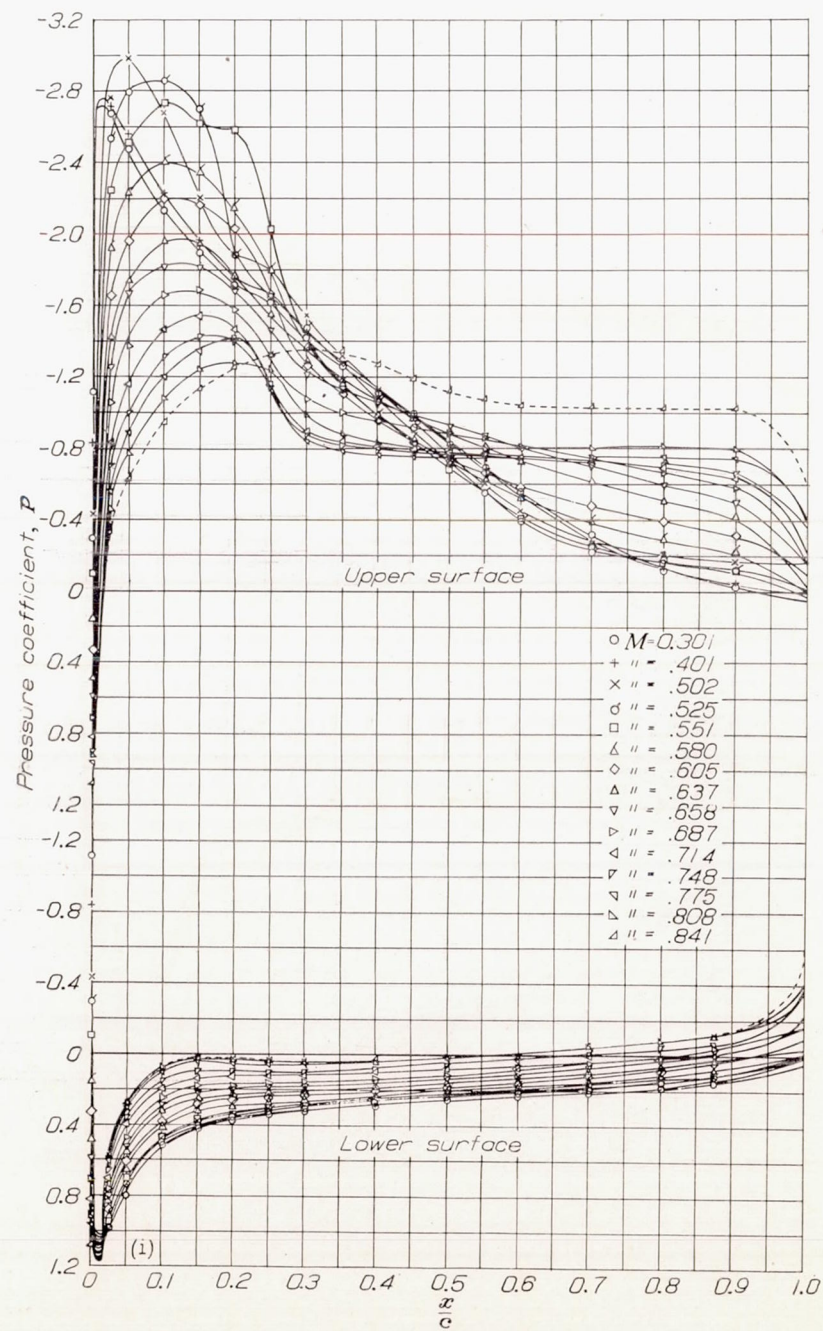
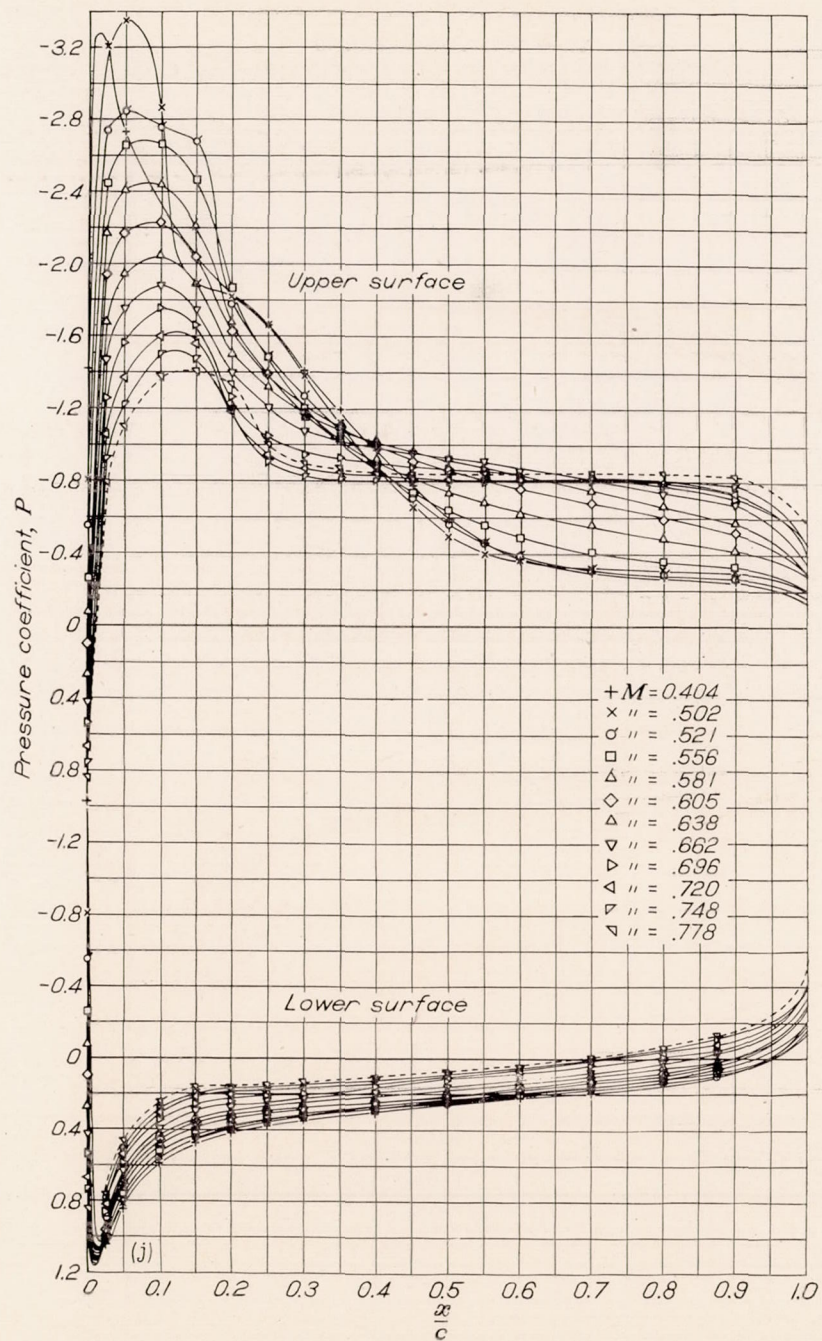
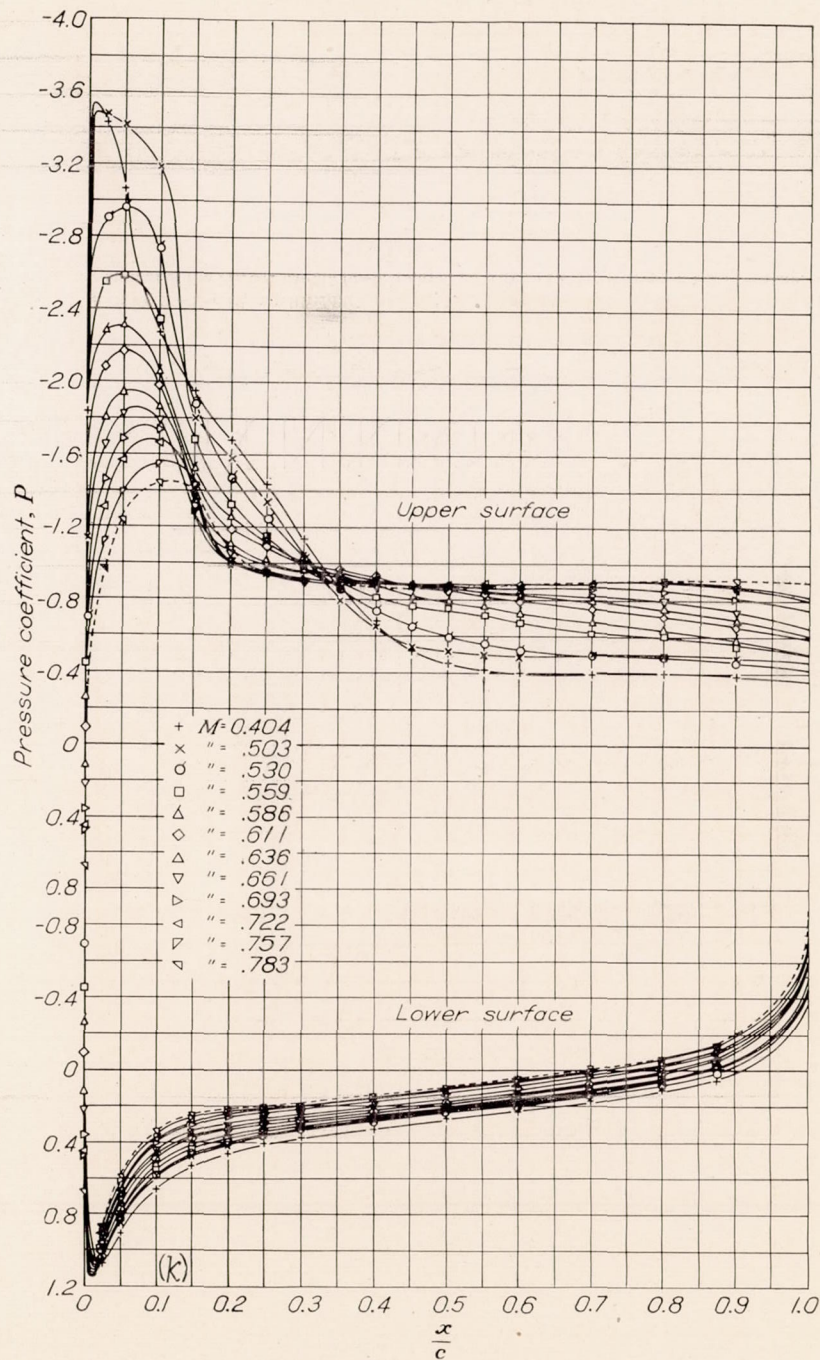
(i) Section angle of attack, $\alpha_0=10^\circ$.

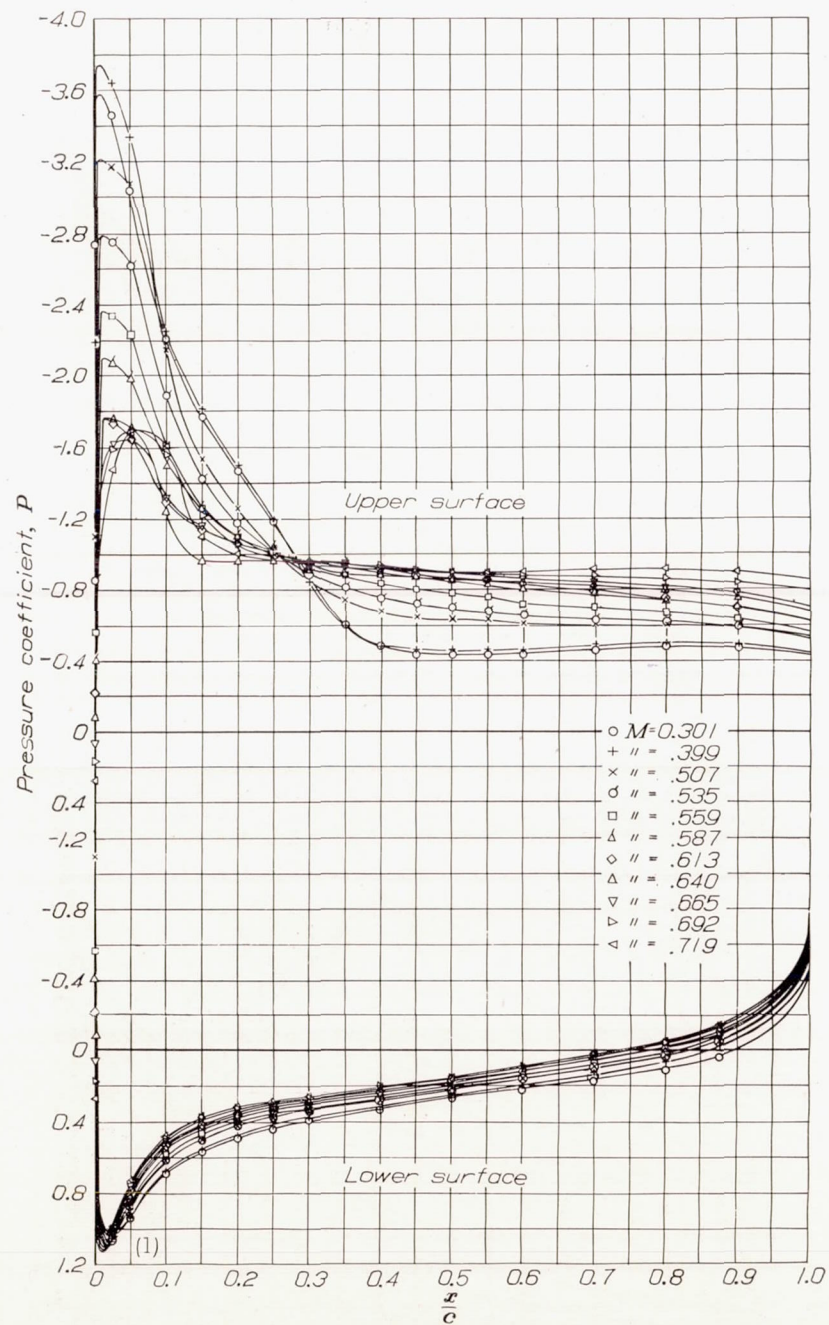
FIGURE 6.—Continued. NACA 4415 airfoil section.



(j) Section angle of attack, $\alpha_0 = 12^\circ$.
 FIGURE 6.—Continued. NACA 4415 airfoil section.



(k) Section angle of attack $\alpha_0 = 14^\circ$.
 FIGURE 6.—Continued. NACA 4415 airfoil section.



(1) Section angle of attack, $\alpha_0=16^\circ$.

FIGURE 6.—Concluded. NACA 4415 airfoil section.

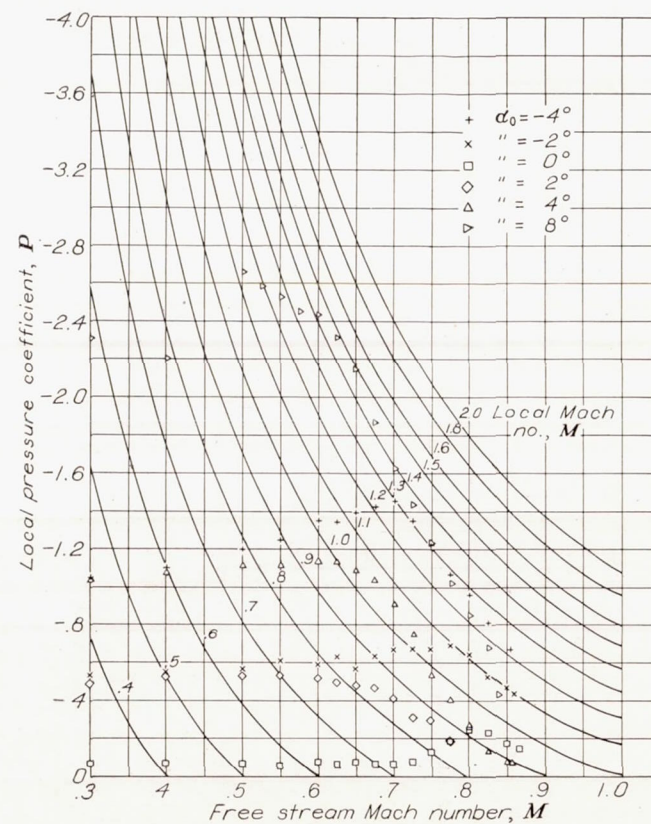


FIGURE 7.—Variation with Mach number of pressure coefficient at the 2.5-percent-chord station of the NACA 65-215 ($a=0.5$) airfoil for surface having minimum local pressure.

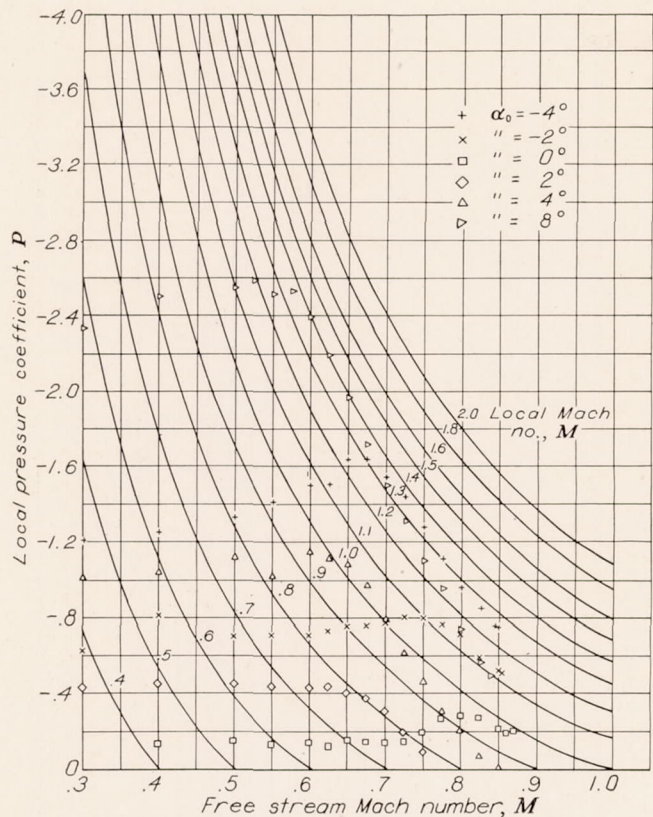


FIGURE 8.—Variation with Mach number of pressure coefficient at the 2.5-percent-chord station of the NACA 66, 2-215 ($\alpha=0.6$) airfoil for surface having minimum local pressure.

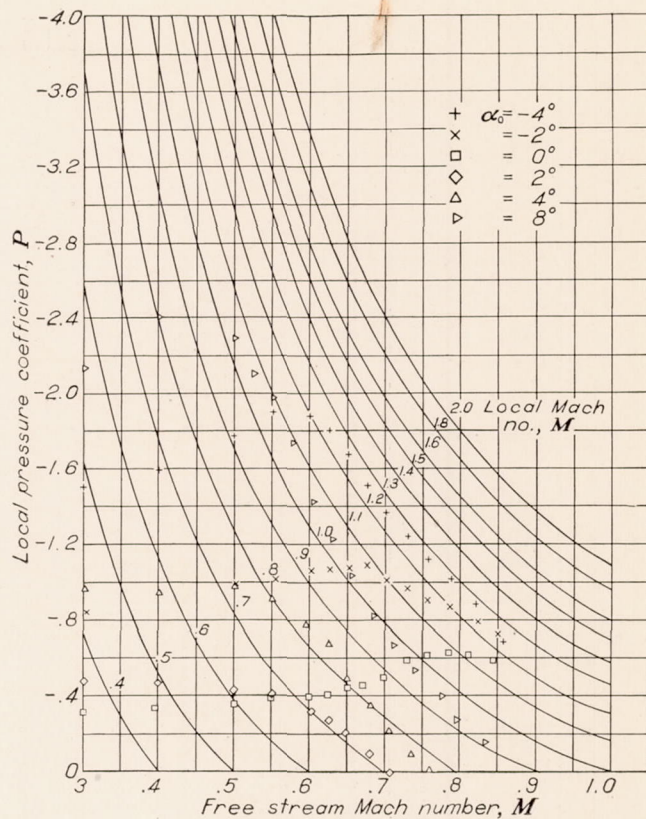


FIGURE 10.—Variation with Mach number of pressure coefficient at the 2.5-percent-chord station of the NACA 23015 airfoil for surface having minimum local pressure.

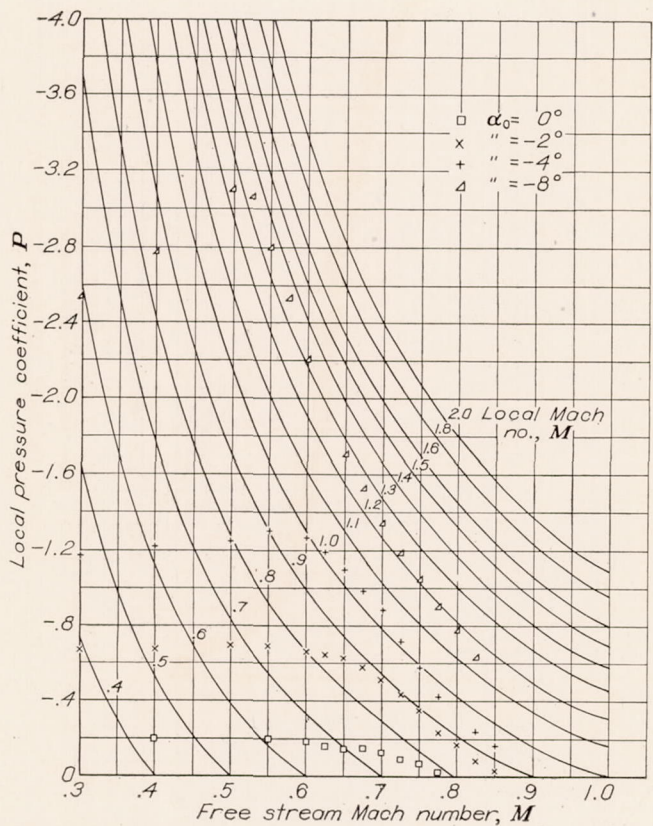


FIGURE 9.—Variation with Mach number of pressure coefficient at the 2.5-percent-chord station of the NACA 0015 airfoil for surface having minimum local pressure.

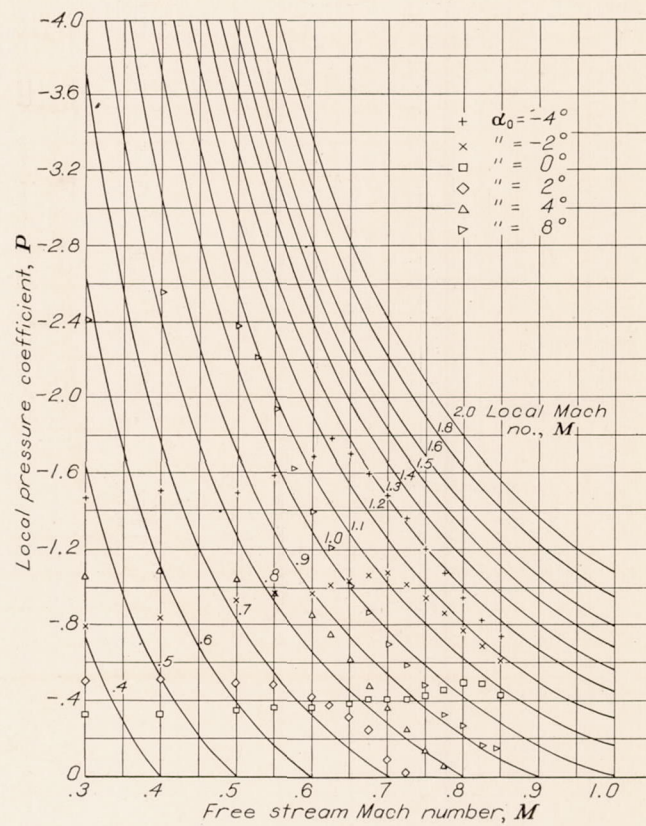


FIGURE 11.—Variation with Mach number of pressure coefficient at the 2.5-percent-chord station of the NACA 4415 airfoil for surface having minimum local pressure.

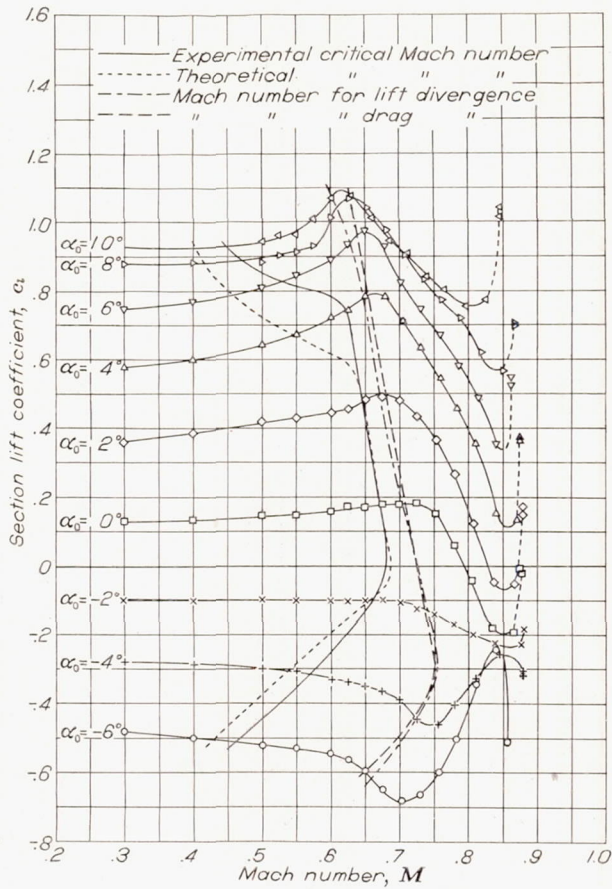


FIGURE 12.—Section lift coefficient vs Mach number for the NACA 65-215 ($a=0.5$) airfoil.

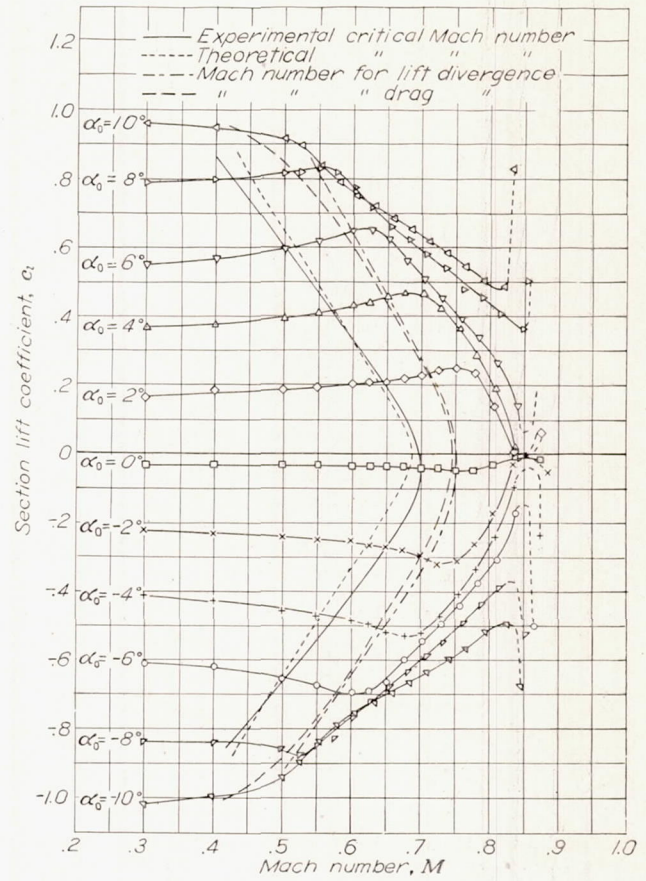


FIGURE 14.—Section lift coefficient vs Mach number for the NACA 0015 airfoil.

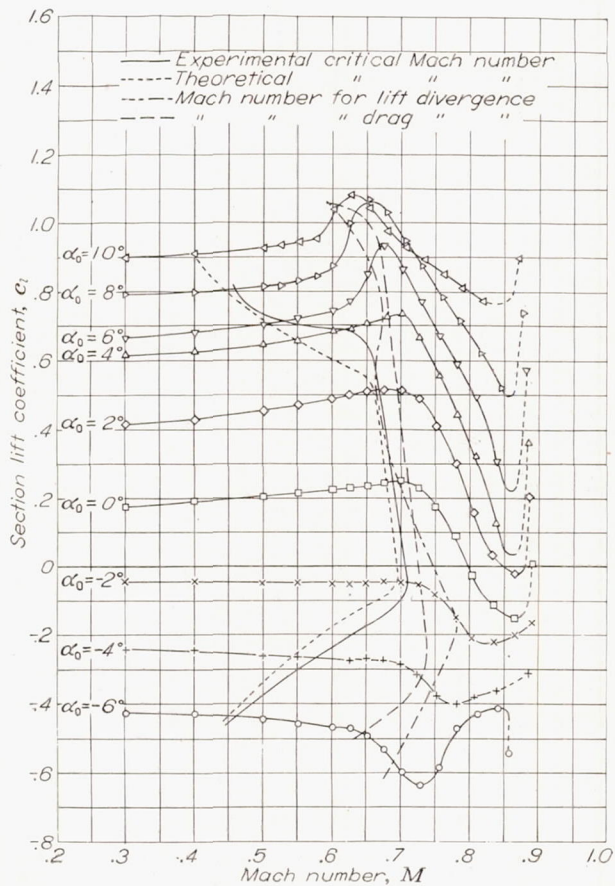


FIGURE 13.—Section lift coefficient vs Mach number for the NACA 66, 2-215 ($a=0.6$) airfoil.

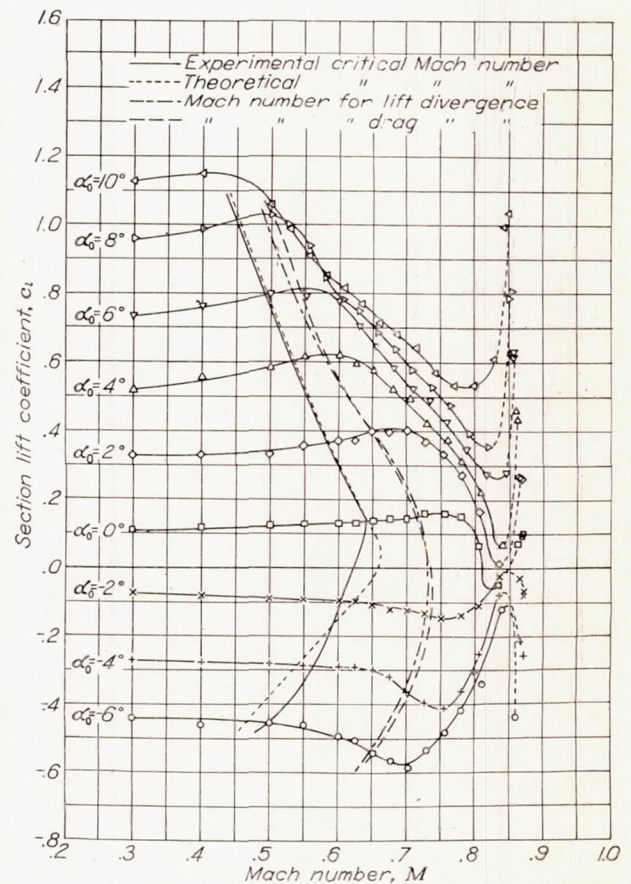


FIGURE 15.—Section lift coefficient vs Mach number for the NACA 23015 airfoil.

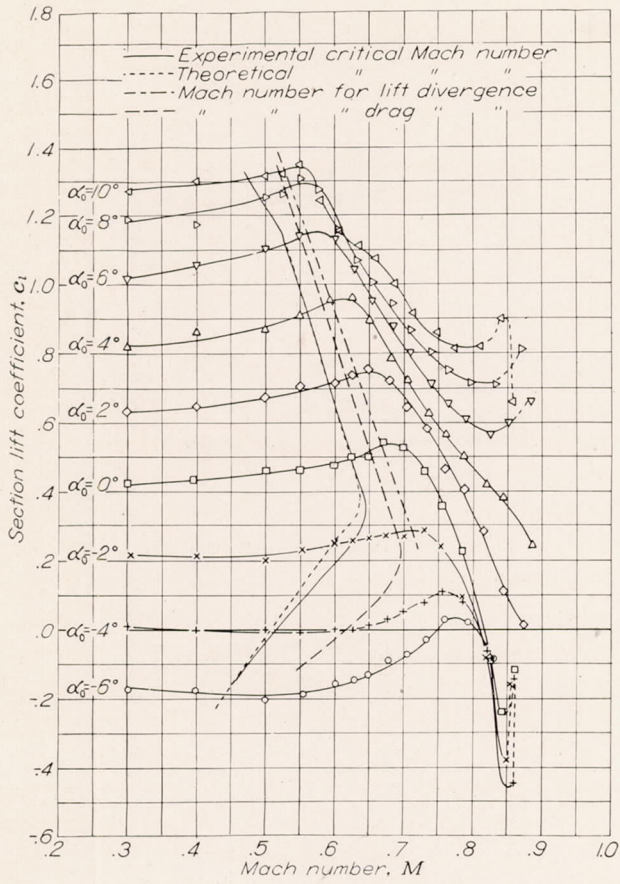


FIGURE 16.—Section lift coefficient vs Mach number for the NACA 4415 airfoil.

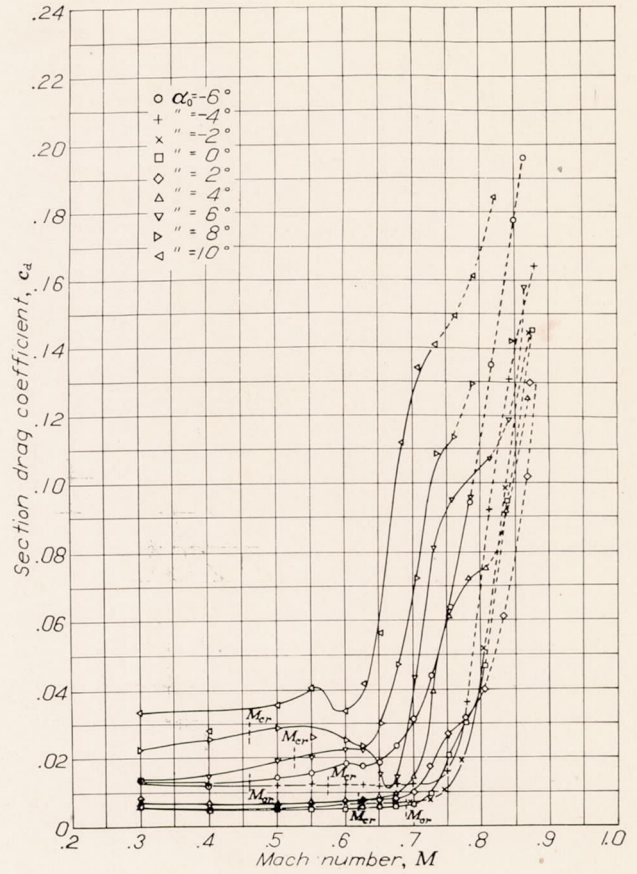


FIGURE 18.—Section drag coefficient vs Mach number for the NACA 66, 2-215 ($a=0.6$) airfoil.

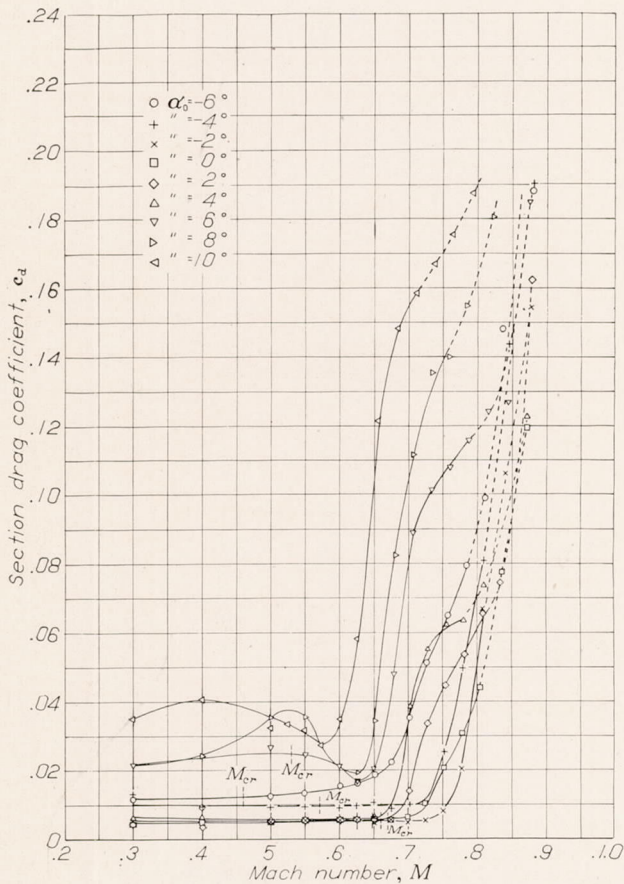


FIGURE 17.—Section drag coefficient vs Mach number for the NACA 65-215 ($a=0.5$) airfoil.

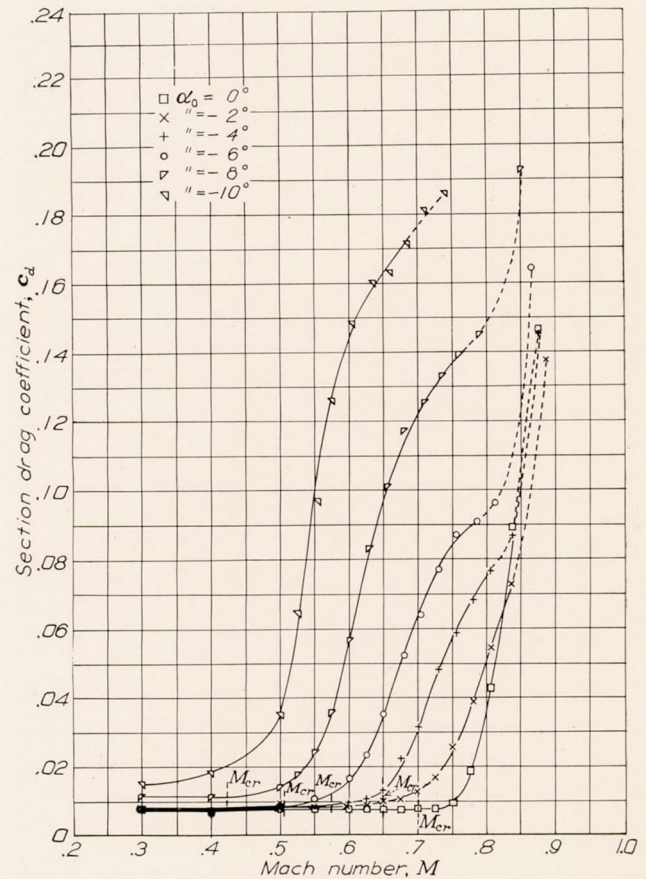


FIGURE 19.—Section drag coefficient vs Mach number for the NACA 0015 airfoil.

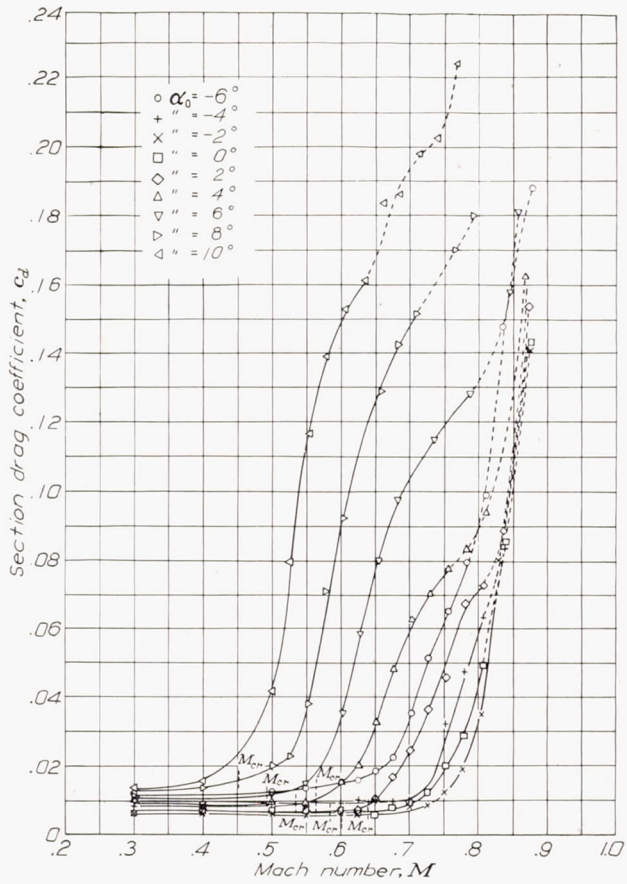


FIGURE 20.—Section drag coefficient vs Mach number for the NACA 23015 airfoil.

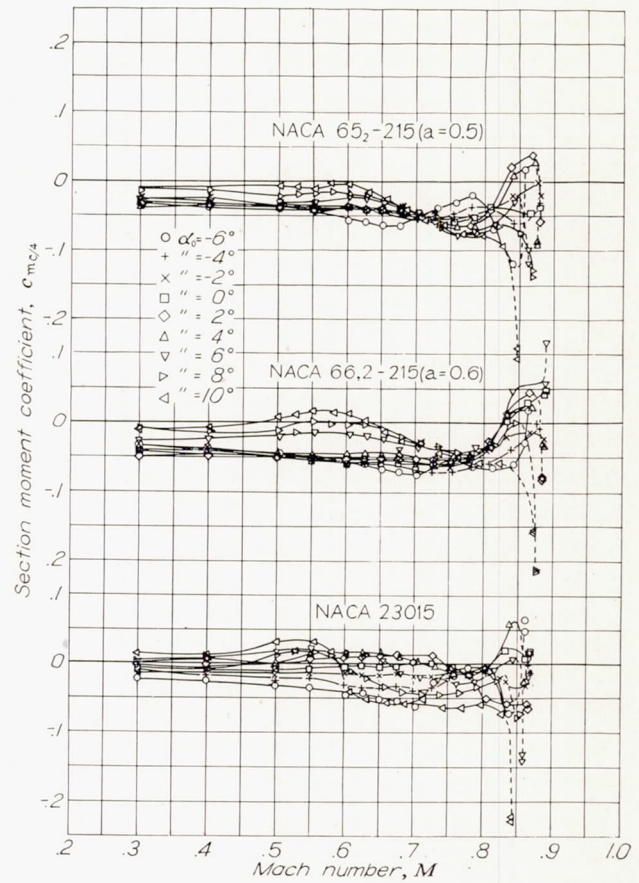


FIGURE 22.—Section moment coefficient vs Mach number for the NACA 65₂-215 ($a=0.5$), 66₂-215 ($a=0.6$) and 23015 airfoils.

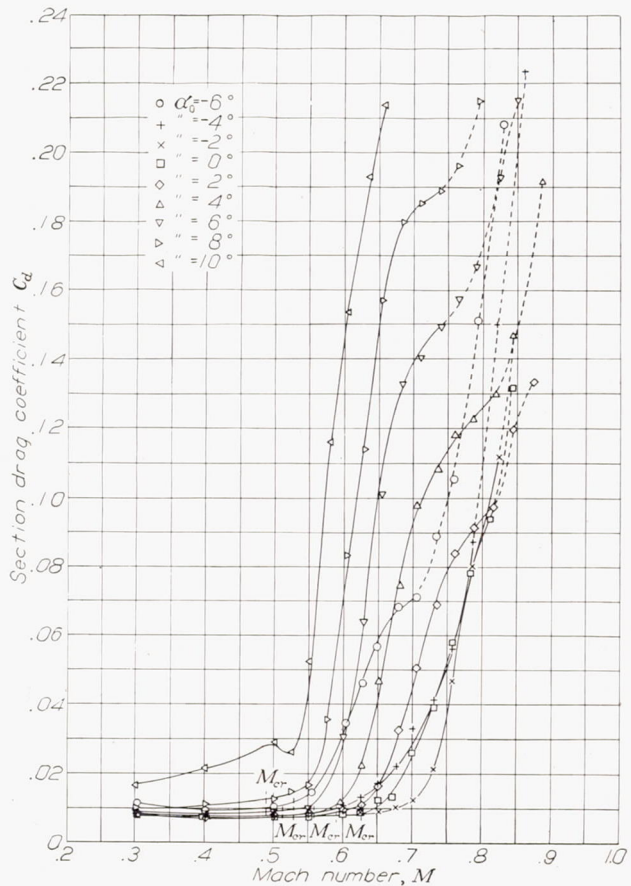


FIGURE 21.—Section drag coefficient vs Mach number for the NACA 4415 airfoil.

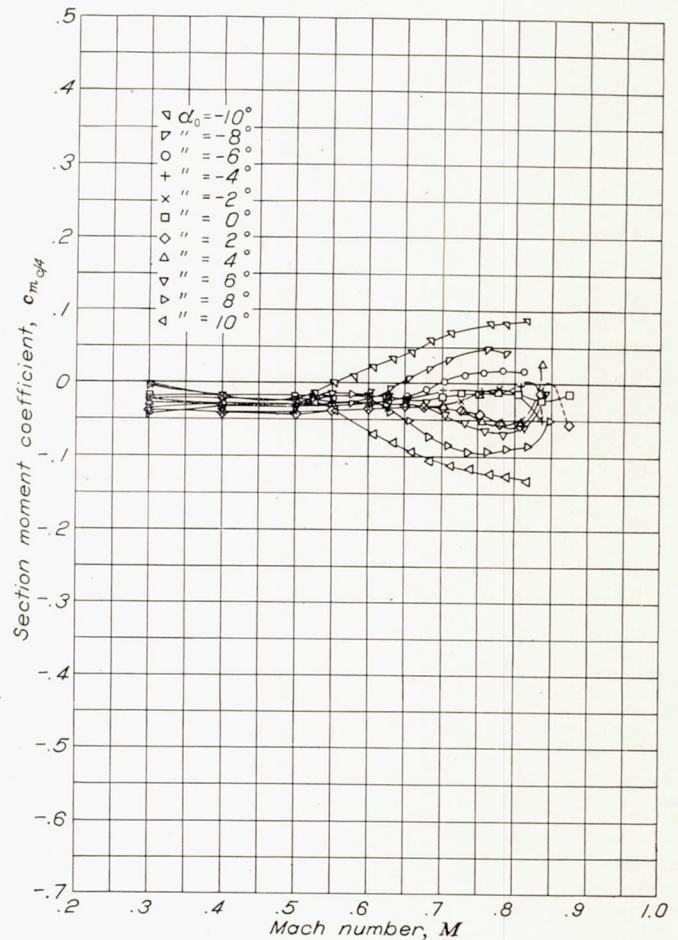


FIGURE 23.—Section moment coefficient vs Mach number for the NACA 0015 airfoil.

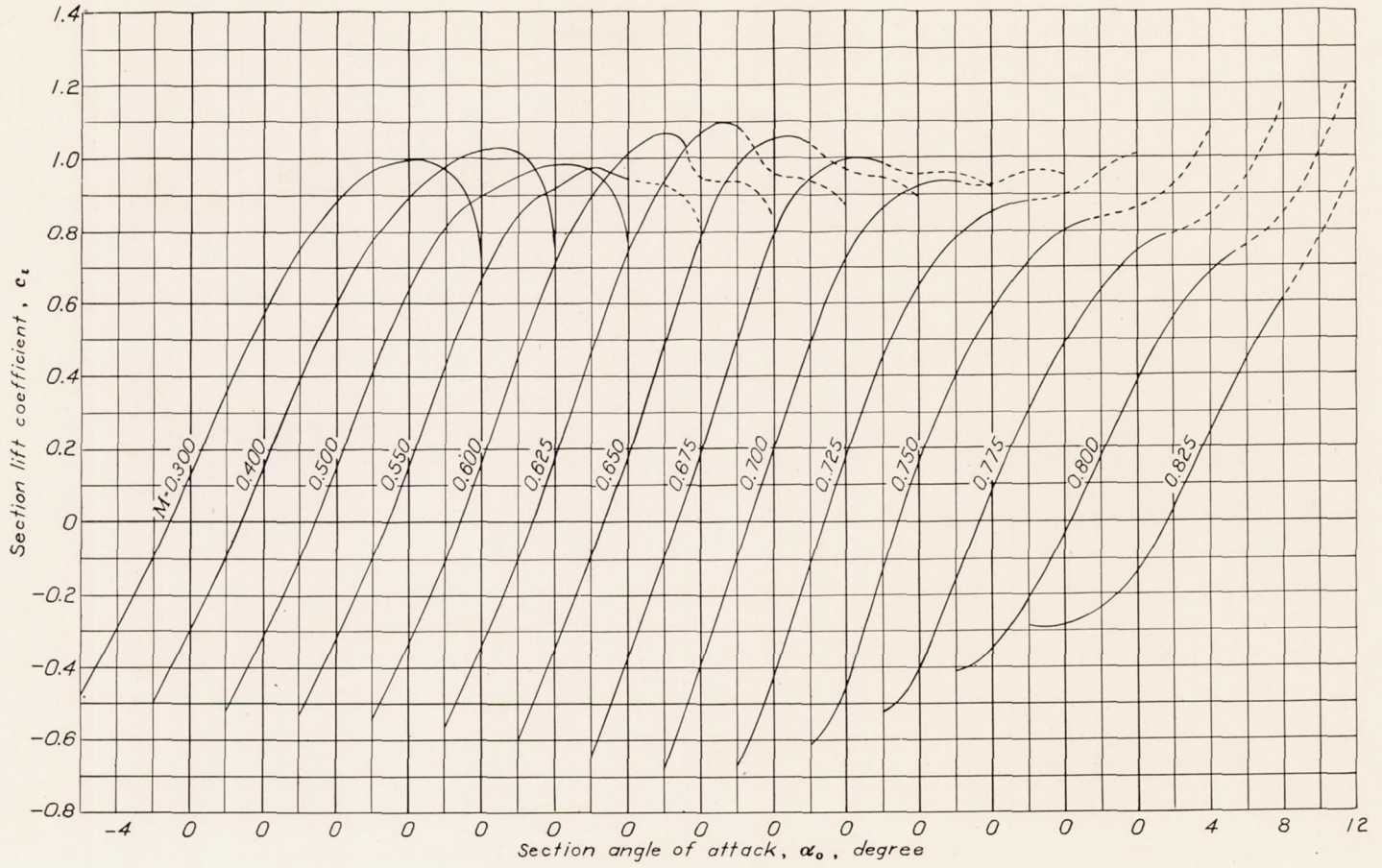


FIGURE 25.—Variation of section lift coefficient with angle of attack at various Mach numbers for the NACA 65₂-215 ($\alpha=0.5$) airfoil.

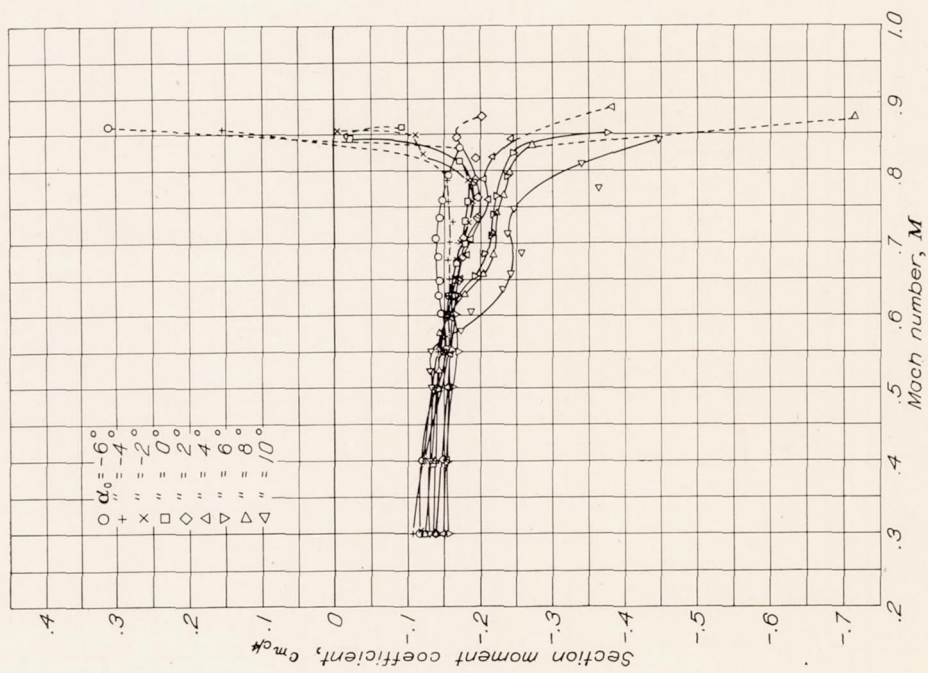


FIGURE 24.—Section moment coefficient vs Mach number for the NACA 4415 airfoil.

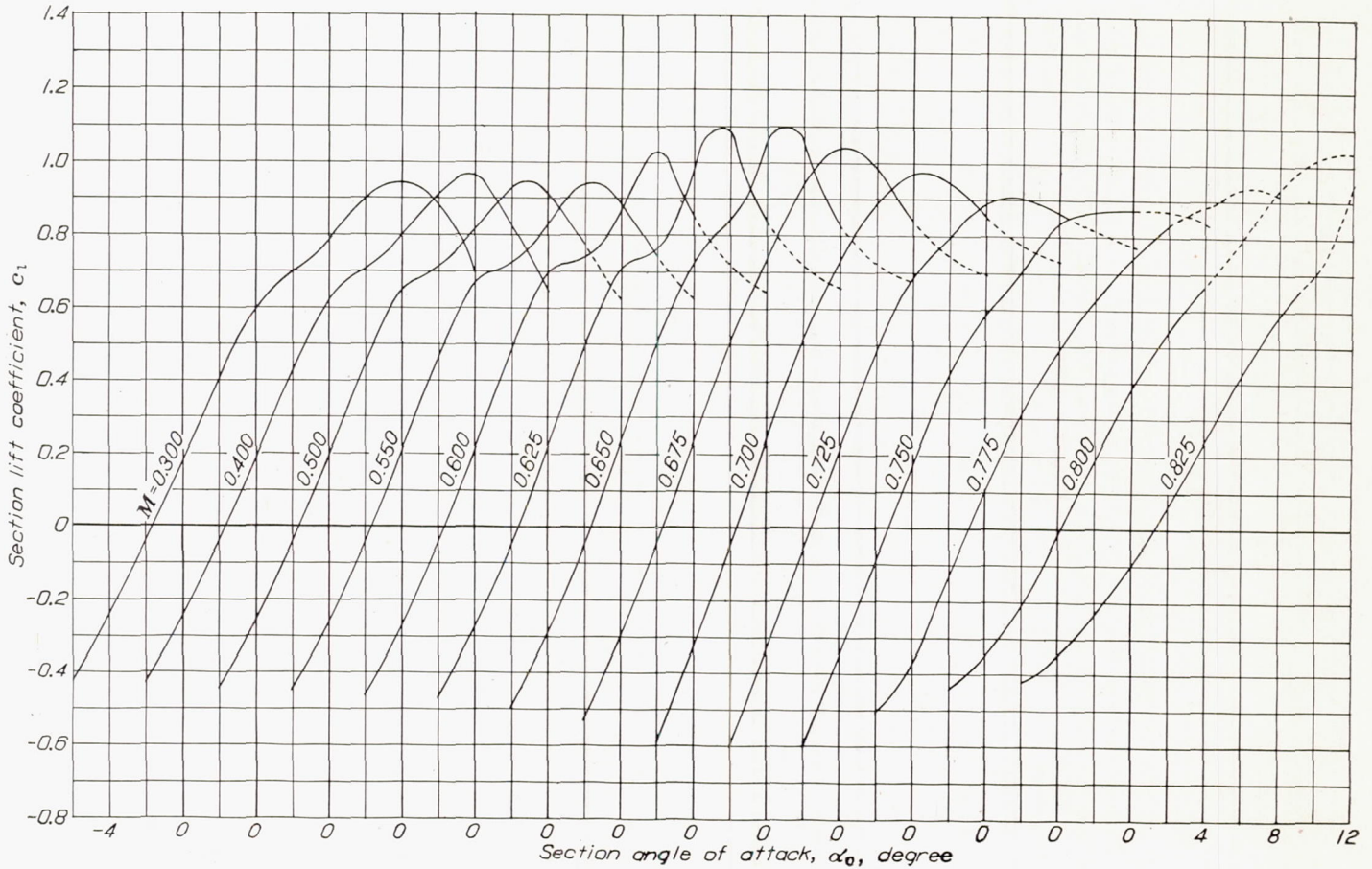


FIGURE 26.—Variation of section lift coefficient with angle of attack at various Mach numbers for the NACA 66, 2-215 ($a=0.6$) airfoil.

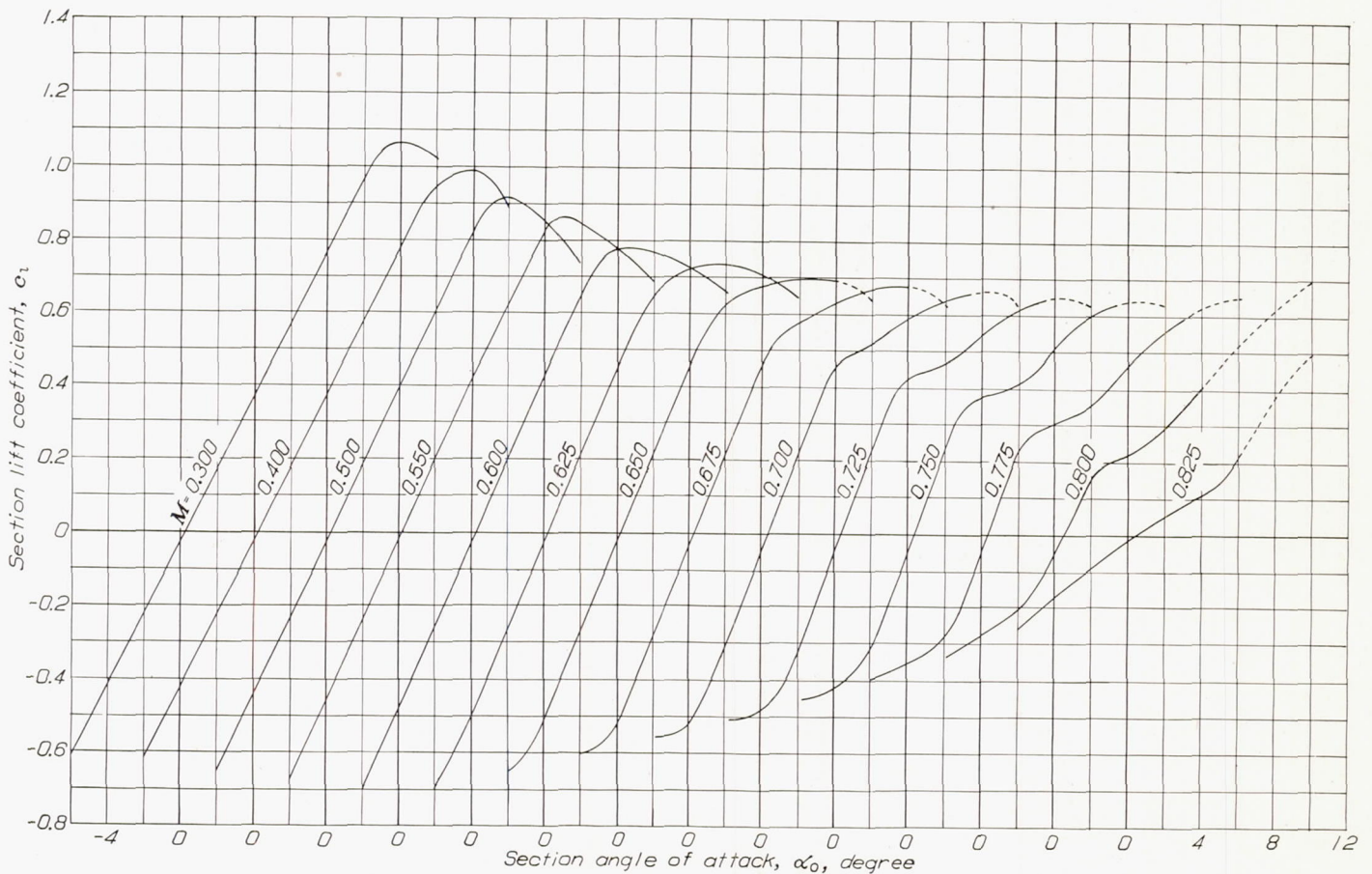


FIGURE 27.—Variation of section lift coefficient with angle of attack at various Mach numbers for the NACA 0015 airfoil.

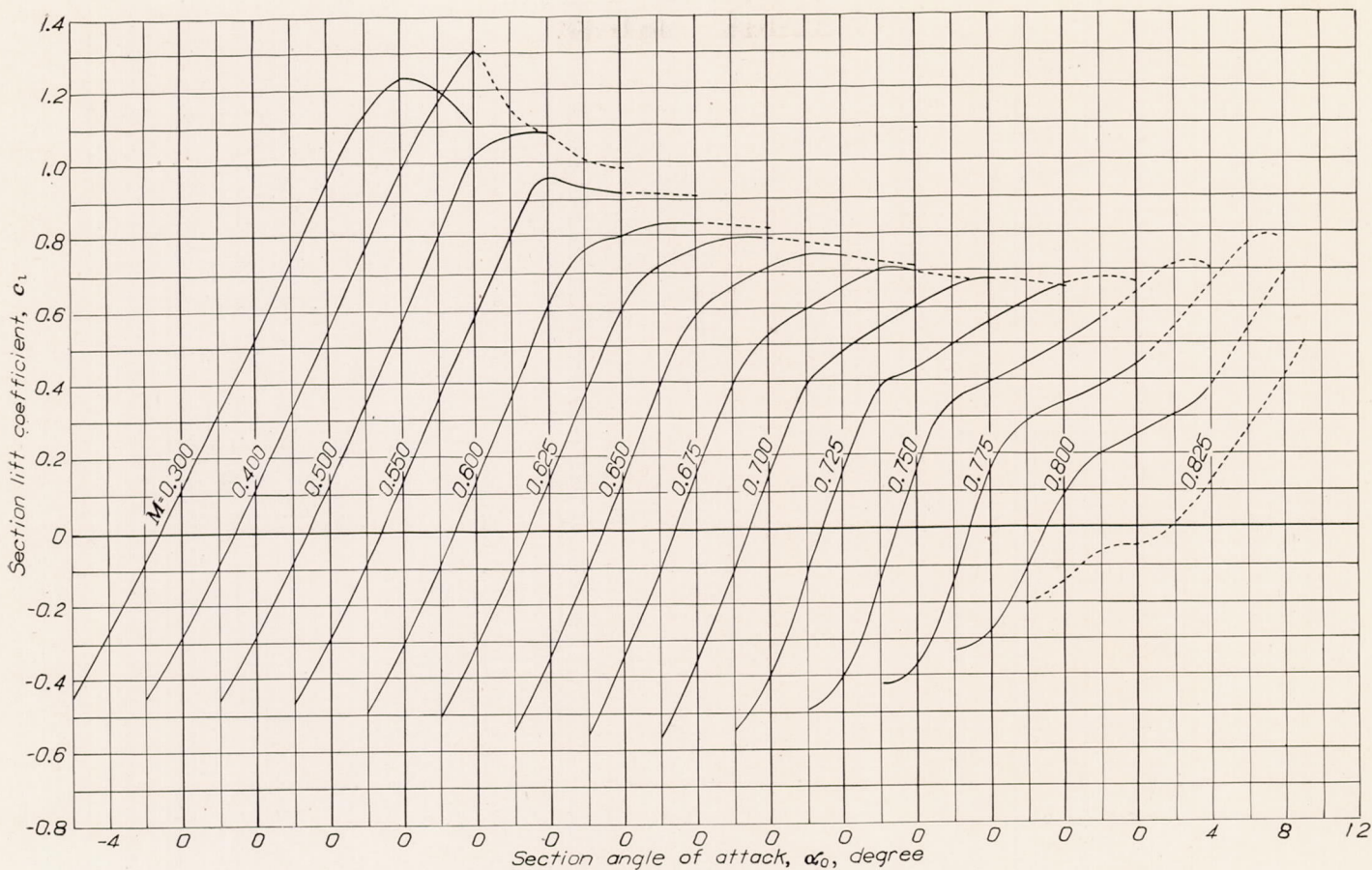


FIGURE 28.—Variation of section lift coefficient with angle of attack at various Mach numbers for the NACA 23015 airfoil.

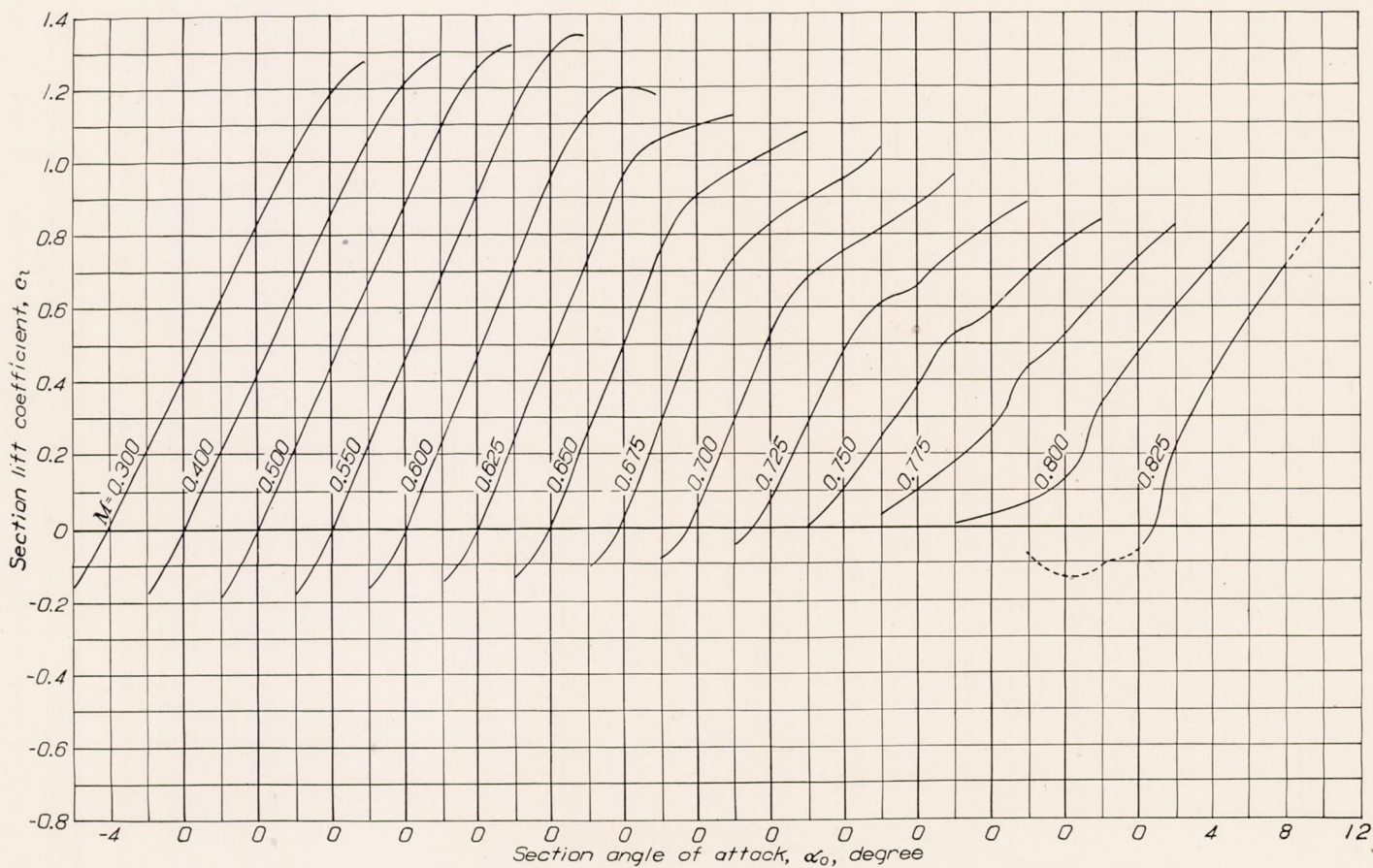


FIGURE 29.—Variation of section lift coefficient with section angle of attack at various Mach numbers for the NACA 4415 airfoil.

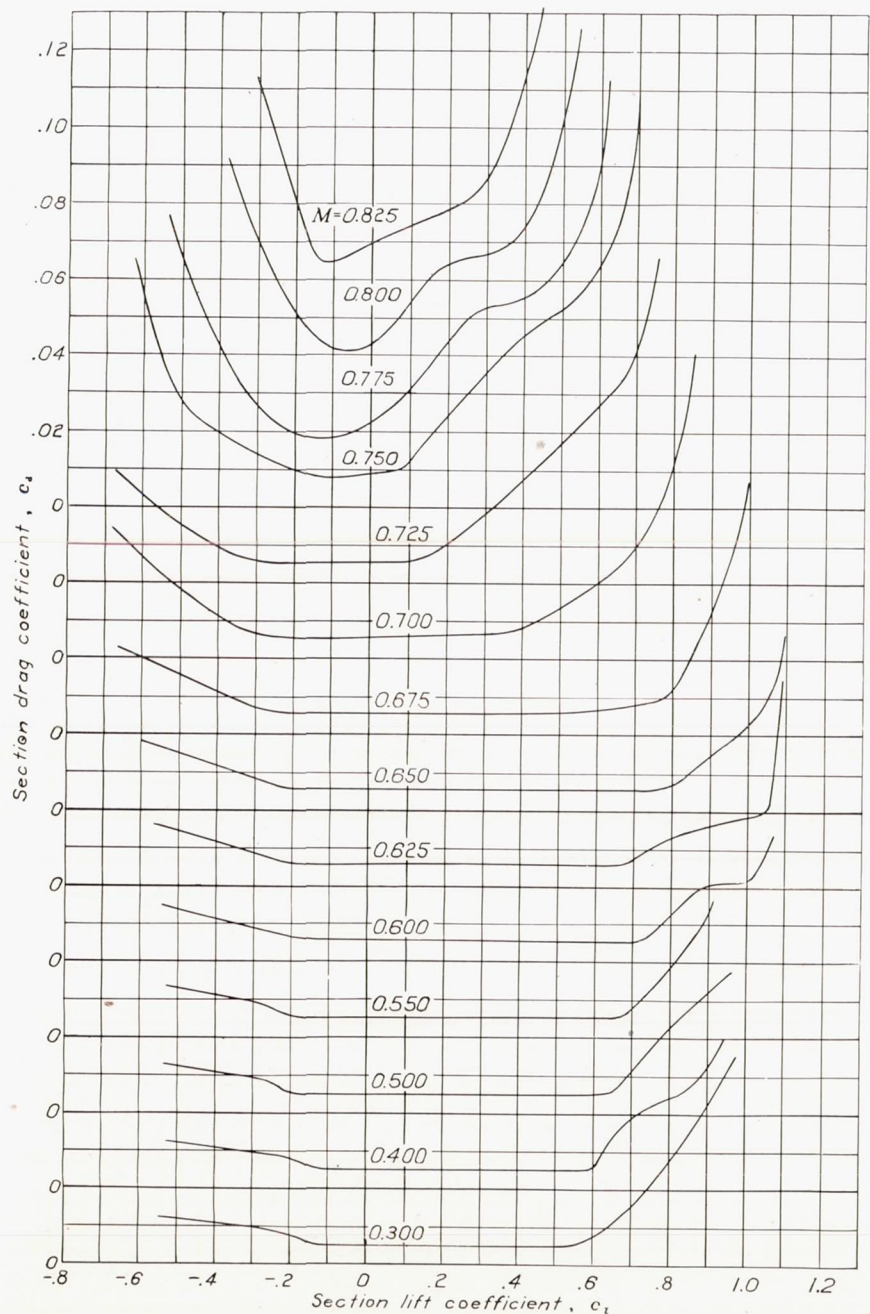


FIGURE 30.—Variation of section drag coefficient with lift coefficient for the NACA 65₂-215 ($\alpha=0.5$) airfoil.

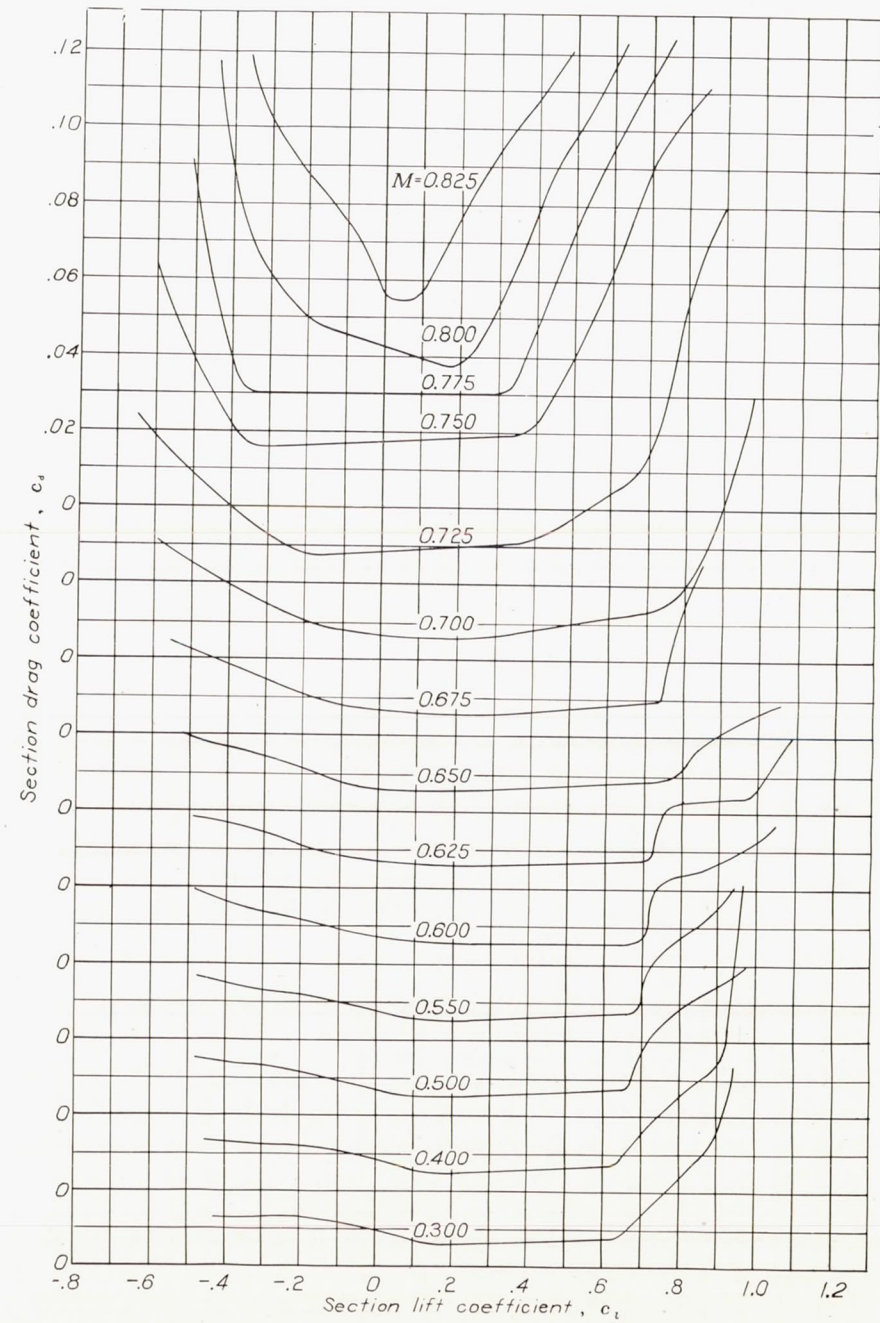


FIGURE 31.—Variation of section drag coefficient with lift coefficient for the NACA 66, 2-215 ($\alpha=0.6$) airfoil.

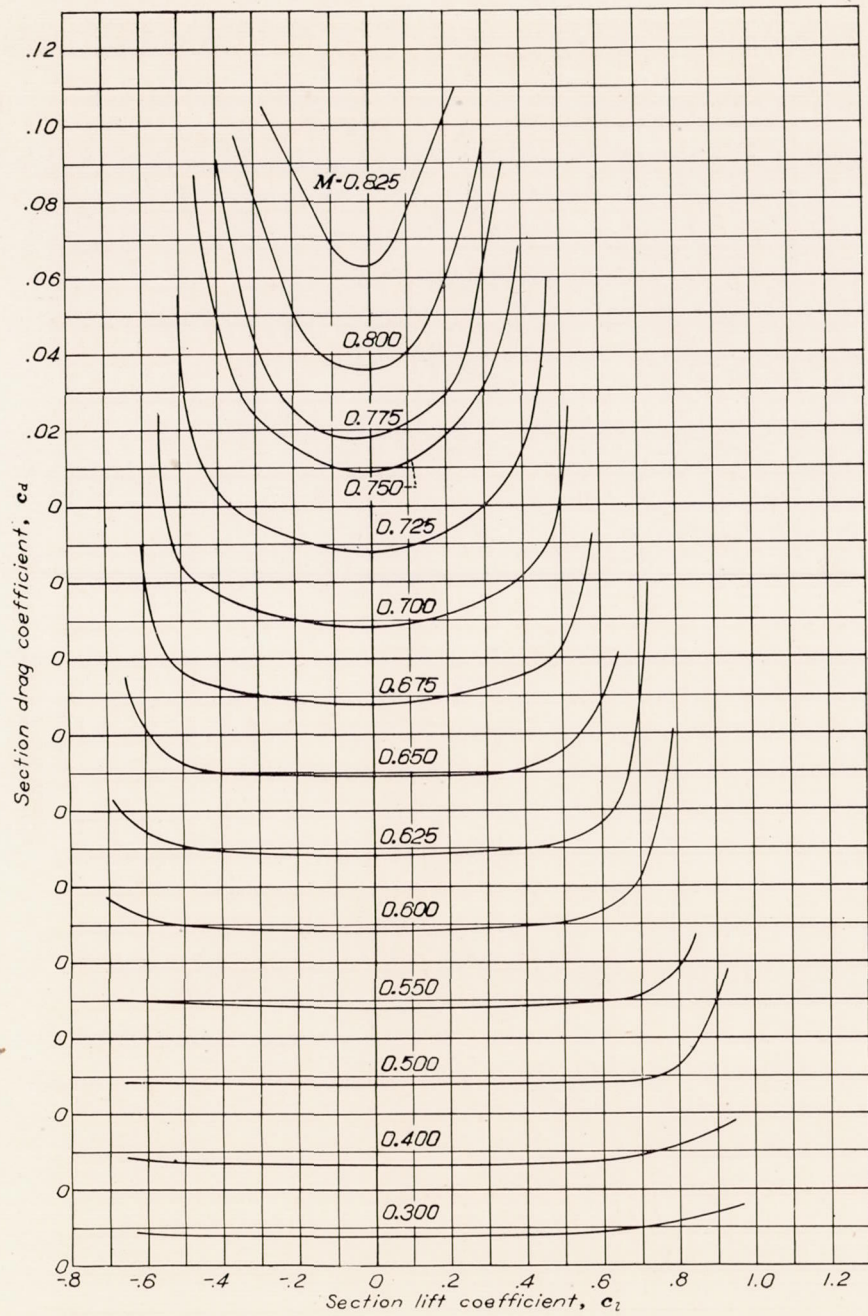


FIGURE 32.—Variation of section drag coefficient with lift coefficient for the NACA 0015 airfoil.

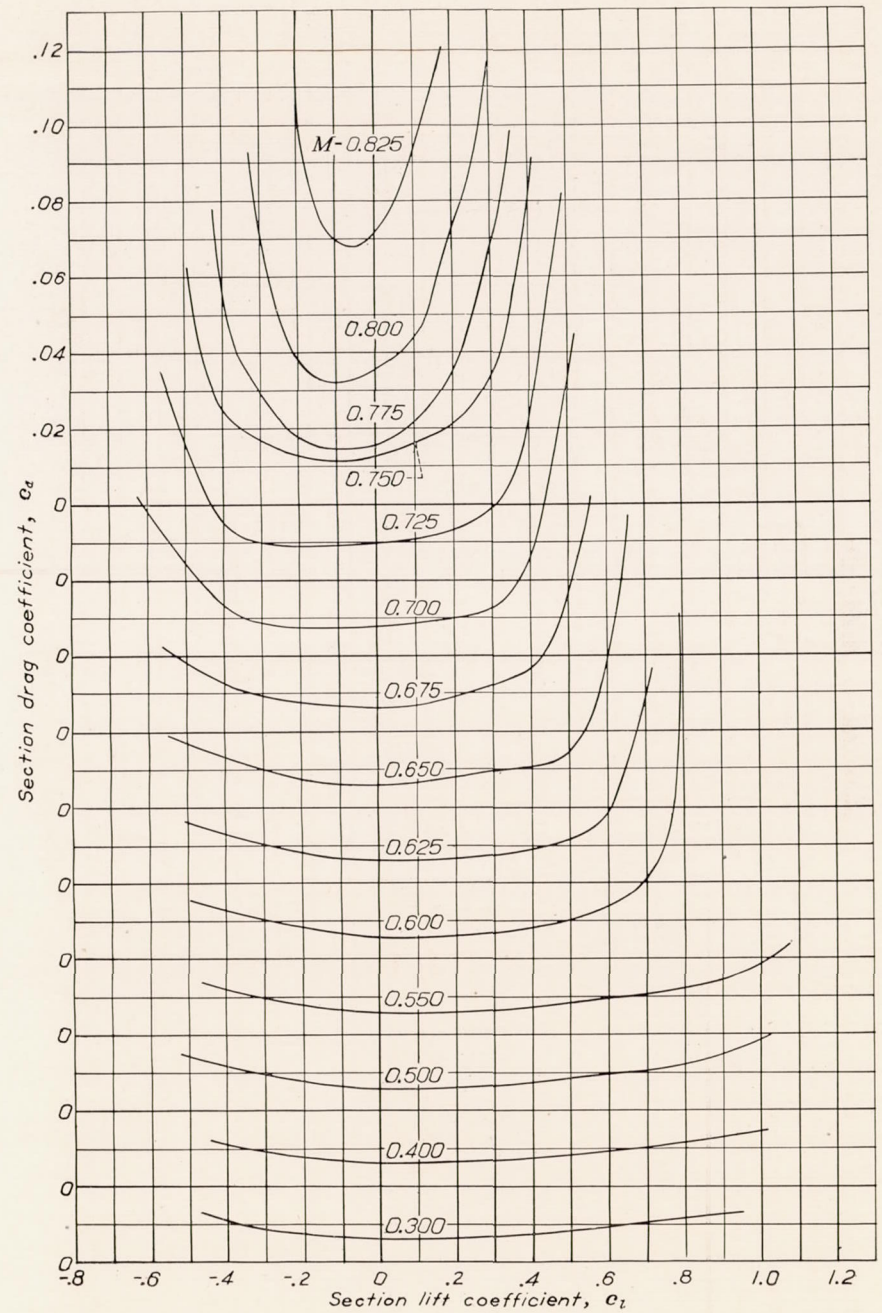


FIGURE 33.—Variation of section drag coefficient with lift coefficient for the NACA 23015 airfoil.

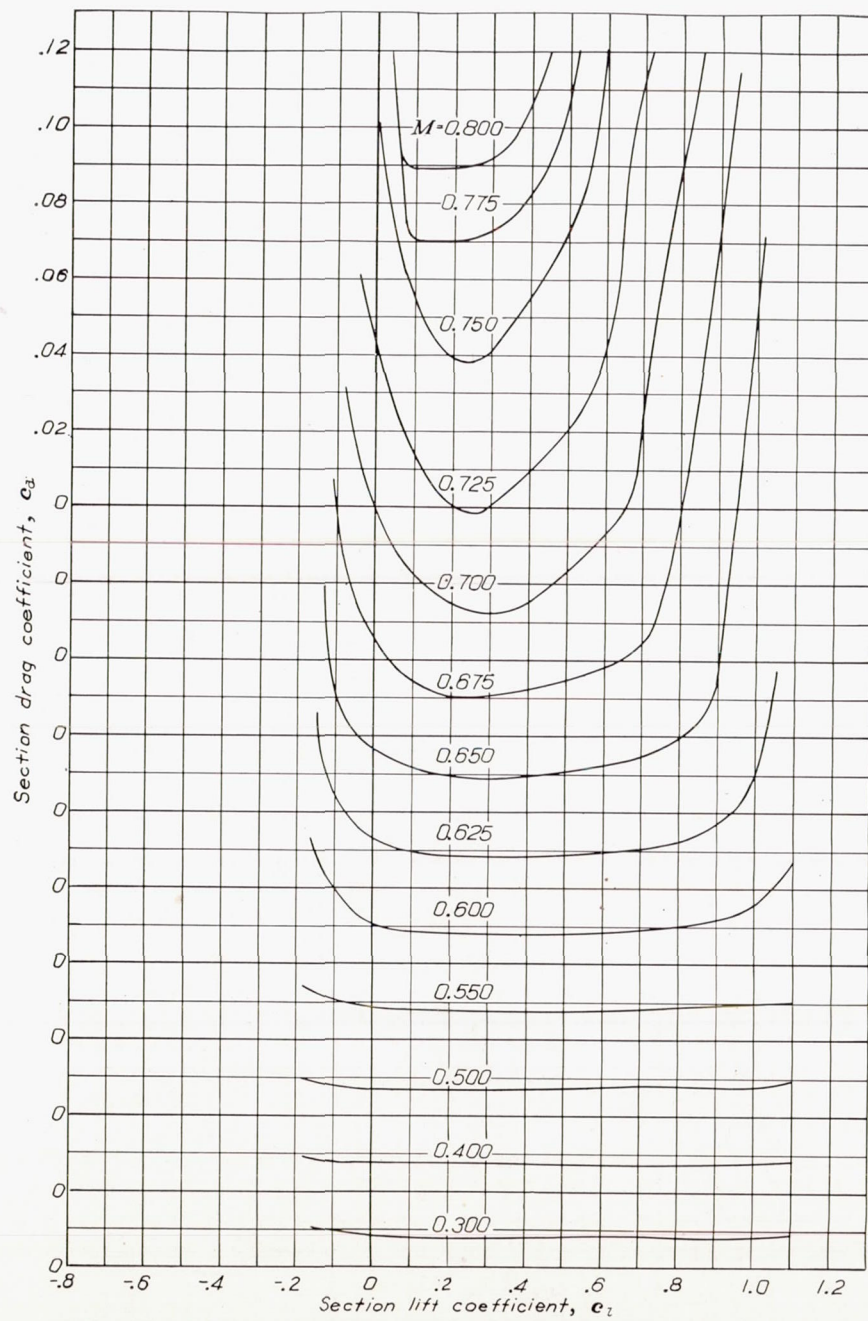


FIGURE 34.—Variation of section drag coefficient with lift coefficient for the NACA 4415 airfoil.

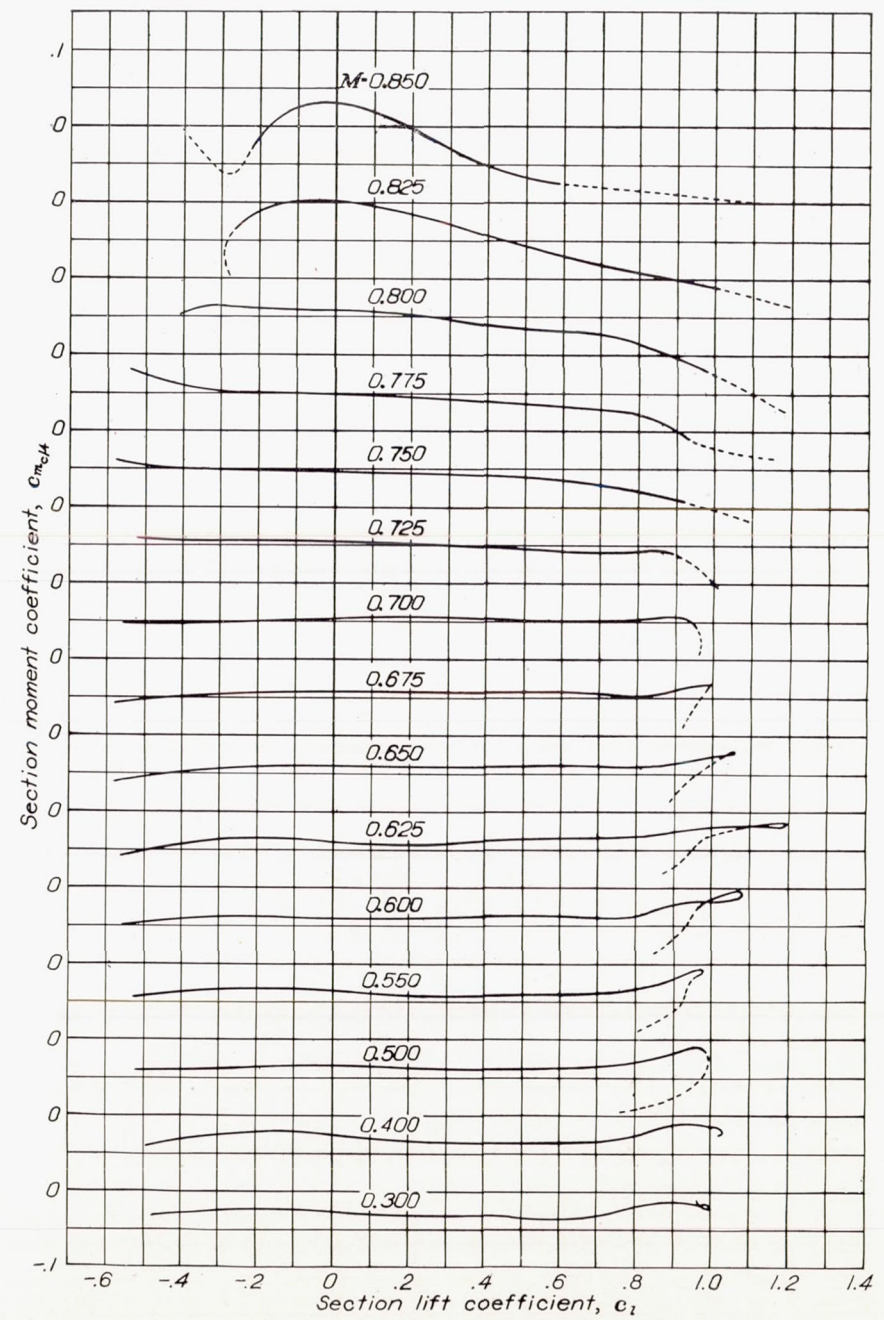


FIGURE 35.—Variation of section quarter-chord moment coefficient with lift coefficient for the NACA 652-215 ($\alpha=0.5$) airfoil.

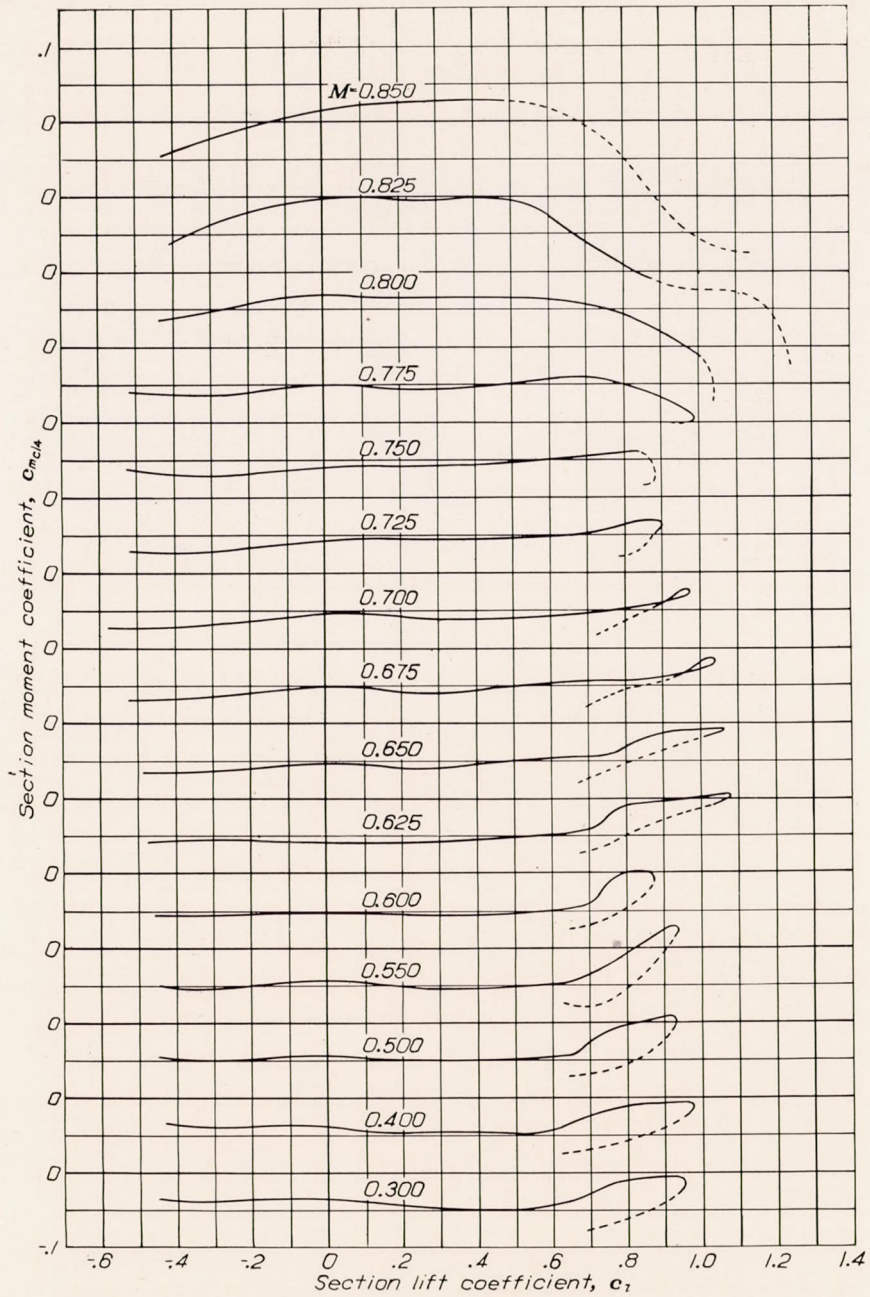


FIGURE 36.—Variation of section quarter-chord moment coefficient with lift coefficient for the NACA 66, 2-215 ($a=0.6$) airfoil.

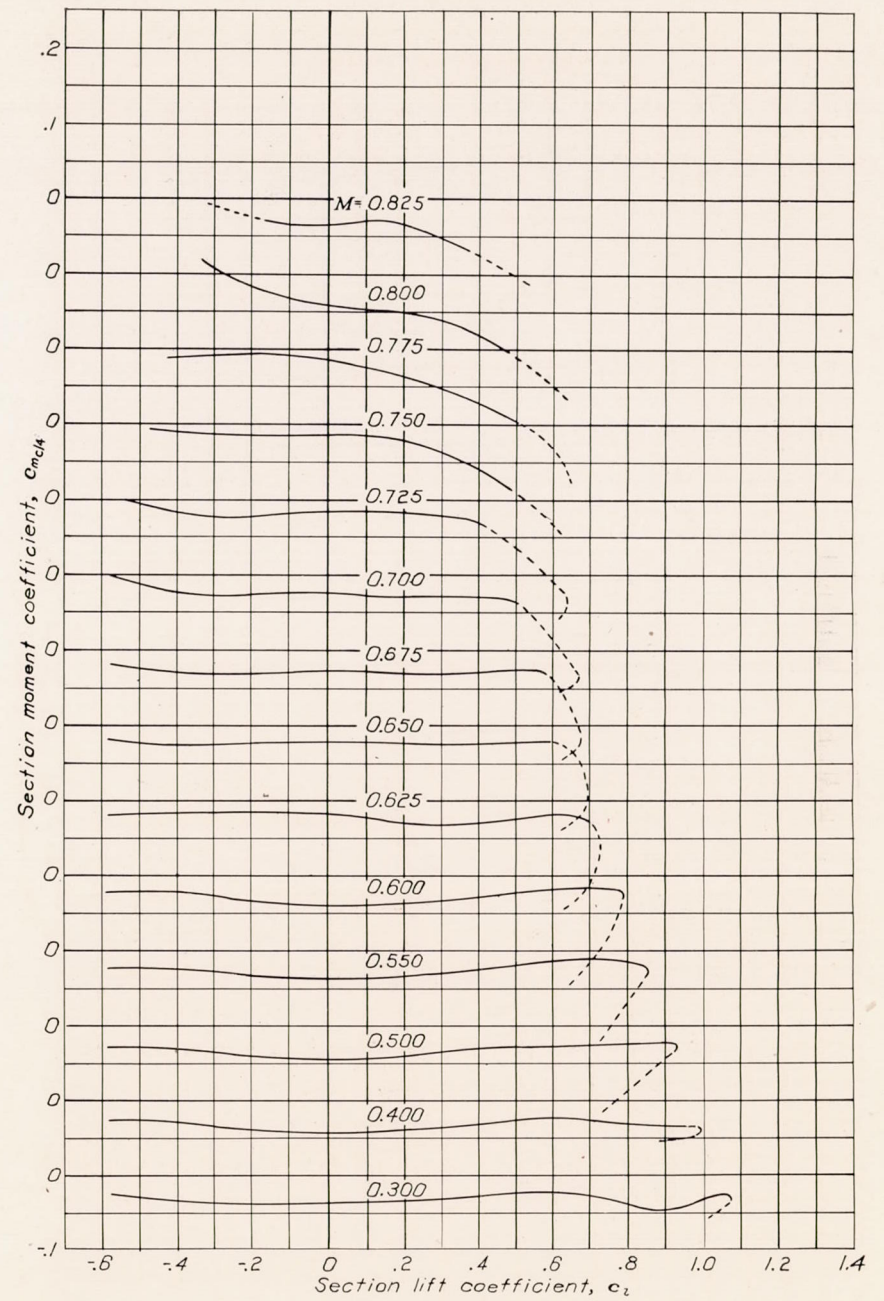


FIGURE 37.—Variation of section quarter chord moment coefficient with lift coefficient for the NACA 0015 airfoil.

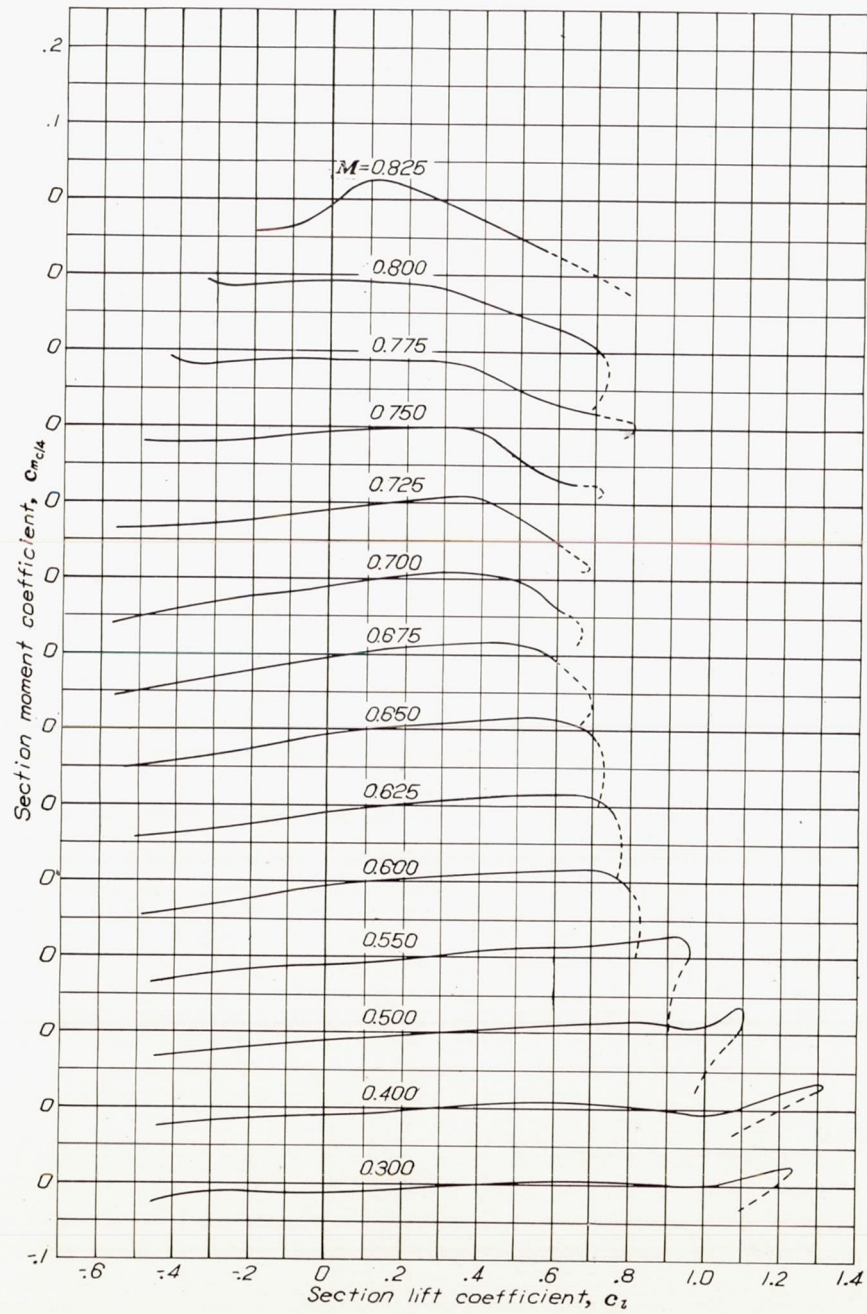


FIGURE 38.—Variation of section quarter-chord moment coefficient with lift coefficient for the NACA 23015 airfoil.

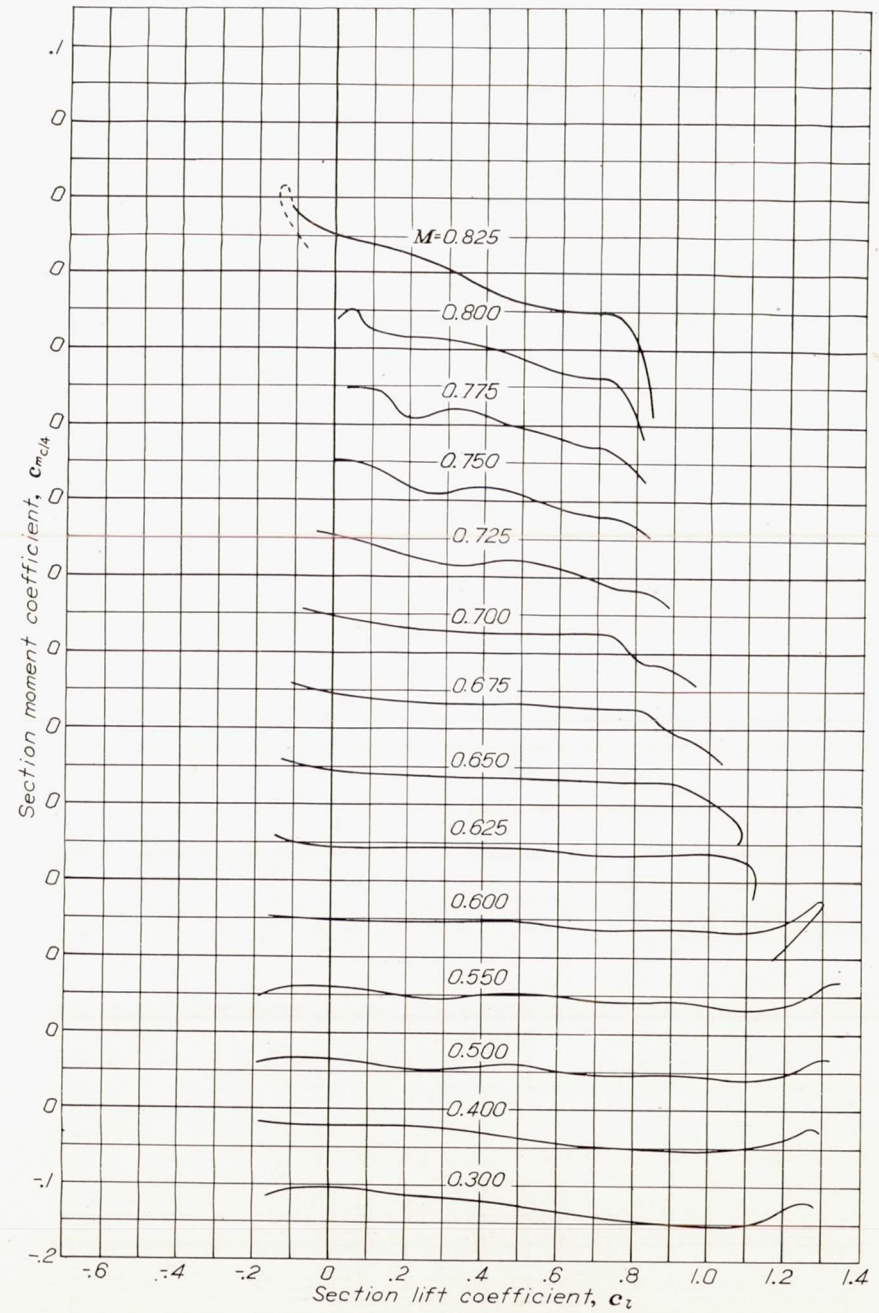


FIGURE 39.—Variation of section quarter-chord moment coefficient with lift coefficient for the NACA 4415 airfoil.

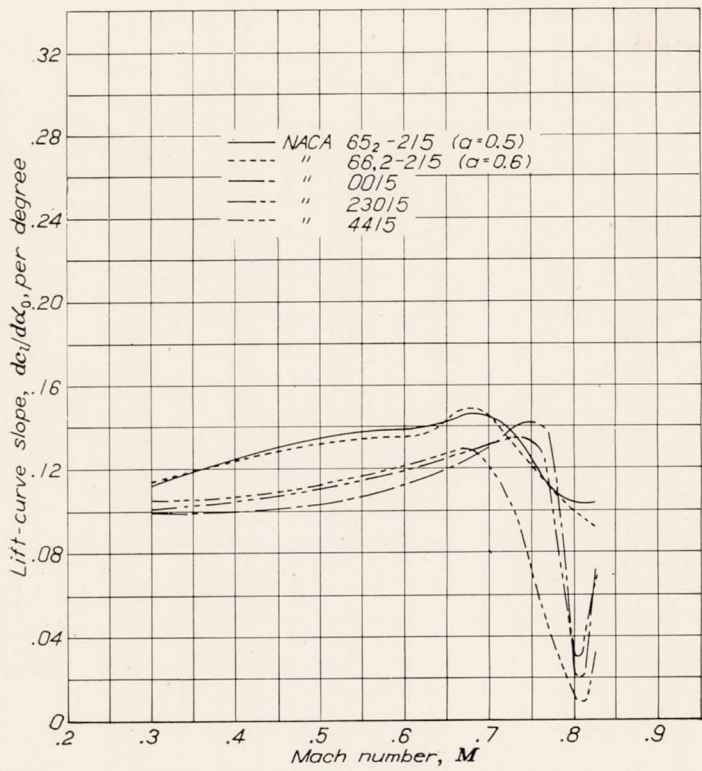


FIGURE 40.—Variation of lift-curve slope with Mach number at $\alpha=0.20$ for the NACA 65₂-215 ($\alpha=0.5$) 66, 2-215 ($\alpha=0.6$) 0015, 23015, and 4415 airfoils.

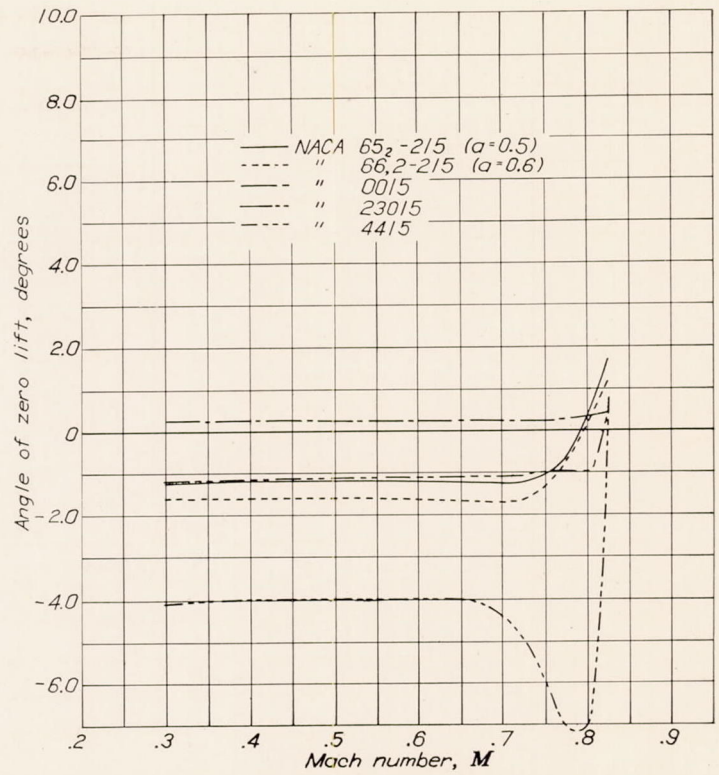


FIGURE 41.—Variation of angle of zero lift with Mach number for the NACA 65₂-215 ($\alpha=0.5$) 66, 2-215 ($\alpha=0.6$) 0015, 23015, and 4415 airfoils.

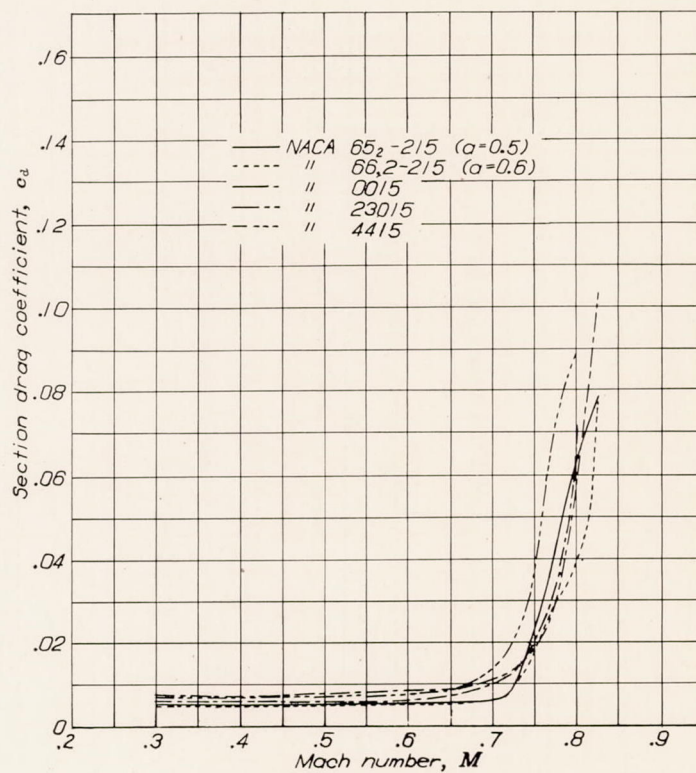


FIGURE 42.—Variation of section drag coefficient with Mach number at $C_l=0.20$ for the NACA 65₂-215 ($\alpha=0.5$) 66, 2-215 ($\alpha=0.6$) 0015, 23015, and 4415 airfoils.

TABLE Ia.—EXPERIMENTAL LOAD DATA

[NACA 65₂-215 ($\alpha=0.5$) Section Angle of Attack, $\alpha_0=-6^\circ$]

Station	Values of load parameter, $P=P_l-P_u$, for different Mach numbers														
	x/c	0.300	0.400	0.501	0.551	0.601	0.626	0.651	0.677	0.703	0.730	0.757	0.782	0.811	0.840
0	0	0	0	0	0	0	0	0	0	0	0	0	0	0	0
.025	-2.880	-3.120	-3.320	-3.210	-3.130	-3.228	-3.035	-2.920	-2.685	-2.530	-2.280	-2.100	-1.920	-1.800	-1.800
.050	-1.750	-1.885	-1.900	-2.660	-2.840	-2.758	-2.670	-2.580	-2.370	-2.250	-2.010	-1.840	-1.670	-1.550	-1.550
.100	-1.270	-1.340	-1.390	-1.375	-1.520	-2.278	-2.210	-2.200	-2.020	-1.910	-1.690	-1.540	-1.370	-1.260	-1.260
.150	-.960	-1.030	-1.065	-1.080	-1.040	-1.050	-1.920	-1.930	-1.805	-1.690	-1.490	-1.340	-1.180	-1.100	-1.100
.200	-.760	-.820	-.845	-.860	-.860	-.820	-1.160	-1.710	-1.660	-1.540	-1.350	-1.200	-1.060	-.970	-.970
.250	-.630	-.675	-.680	-.700	-.710	-.710	-.595	-1.480	-1.480	-1.400	-1.220	-1.050	-.920	-.870	-.870
.300	-.520	-.526	-.550	-.560	-.560	-.580	-.480	-.670	-1.330	-1.240	-1.050	-.880	-.770	-.730	-.730
.350	-.428	-.461	-.449	-.453	-.458	-.481	-.410	-.404	-1.108	-1.048	-.874	-.729	-.655	-.632	-.632
.400	-.350	-.340	-.340	-.340	-.330	-.350	-.320	-.230	-.460	-.740	-.600	-.490	-.440	-.490	-.490
.450	-.233	-.241	-.224	-.213	-.203	-.196	-.180	-.059	-.068	-.338	-.219	-.109	-.090	-.202	-.202
.500	-.170	-.170	-.150	-.130	-.120	-.120	-.070	.050	.050	.070	.010	.190	.200	.060	.060
.550	-.113	-.111	-.073	-.073	-.068	-.061	-.030	.011	.067	.042	.076	.266	.370	.248	.248
.600	-.080	-.080	-.060	-.050	-.020	-.025	.020	.020	.080	.010	.120	.310	.400	.380	.380
.700	-.010	-.020	-.035	-.020	-.020	.030	-.030	-.050	-.020	-.040	-.080	-.110	-.200	.510	.510
.800	-.060	-.040	-.010	-.020	-.010	.030	0	-.030	.020	.050	-.080	-.110	-.200	.510	.510
.850	-.082	-.044	-.031	-.032	-.007	-.019	-.010	-.021	-.012	-.062	-.121	-.206	-.085	.452	.452
.875	-.053	-.056	-.044	-.053	-.043	-.041	-.055	-.054	-.078	-.073	-.144	-.204	-.075	.388	.388

TABLE Ib.—EXPERIMENTAL LOAD DATA

[NACA 65₂-215 ($\alpha=0.5$) Section Angle of Attack, $\alpha_0=-4^\circ$]

Station	Values of load parameter, $P=P_l-P_u$, for different Mach numbers															
	x/c	0.300	0.400	0.500	0.550	0.601	0.626	0.651	0.676	0.701	0.726	0.753	0.780	0.810	0.844	0.879
0	0	0	0	0	0	0	0	0	0	0	0	0	0	0	0	0
.025	-1.850	-1.930	-2.020	-2.110	-2.215	-2.210	-2.370	-2.365	-2.280	-2.180	-2.010	-1.825	-1.655	-1.540	-1.450	-1.450
.050	-1.320	-1.380	-1.520	-1.510	-1.760	-1.825	-1.900	-1.940	-1.970	-1.880	-1.735	-1.560	-1.390	-1.290	-1.200	-1.200
.100	-.830	-.850	-.920	-.960	-1.000	-1.000	-.970	-1.400	-1.540	-1.530	-1.415	-1.250	-1.100	-1.010	-.930	-.930
.150	-.600	-.640	-.690	-.730	-.770	-.790	-.810	-.765	-1.230	-1.320	-1.215	-1.070	-.920	-.830	-.770	-.770
.200	-.465	-.490	-.520	-.550	-.575	-.600	-.620	-.640	-.750	-.760	-.685	-.580	-.480	-.400	-.340	-.340
.250	-.370	-.380	-.400	-.430	-.450	-.480	-.490	-.530	-.460	-.460	-.385	-.280	-.190	-.110	-.050	-.050
.300	-.260	-.290	-.300	-.310	-.340	-.360	-.380	-.400	-.385	-.385	-.260	-.160	-.080	-.010	.010	.010
.350	-.228	-.241	-.244	-.253	-.268	-.286	-.305	-.339	-.343	-.343	-.245	-.145	-.060	-.010	.010	.010
.400	-.155	-.160	-.160	-.171	-.170	-.175	-.200	-.200	-.220	-.220	-.120	-.020	-.020	-.020	-.020	-.020
.450	-.063	-.070	-.044	-.068	-.063	-.051	-.050	-.054	-.048	-.048	-.052	-.264	-.030	-.035	-.020	-.220
.500	-.030	-.030	.030	-.030	0	0	.020	.020	.010	.095	-.070	-.580	-.254	-.195	-.182	-.264
.550	-.003	-.011	.026	.012	.027	.044	.050	.071	.052	.122	-.070	-.151	-.131	.115	.148	-.154
.600	-.010	-.020	.040	.040	.070	.070	.085	.120	.120	.160	.240	.340	.320	.270	.270	-.095
.700	-.010	-.040	-.020	0	.010	0	.020	.020	0	0	-.020	-.050	-.160	.270	.080	.080
.800	-.020	0	0	0	.010	.005	.010	.035	.010	-.015	-.010	-.020	-.020	.145	.110	.110
.850	-.027	-.024	-.006	-.012	-.007	-.039	-.020	-.021	-.012	-.008	-.021	-.061	-.050	.102	.194	.194
.875	-.003	-.021	.006	.002	.017	.014	0	-.004	.002	-.038	-.049	-.029	-.050	.078	.176	.176

TABLE Ic.—EXPERIMENTAL LOAD DATA

[NACA 65₂-215 ($\alpha=0.5$) Section Angle of Attack, $\alpha_0=-2^\circ$]

Station	Values of load parameter, $P=P_l-P_u$, for different Mach numbers															
	x/c	0.300	0.400 ^a	0.500	0.550	0.600	0.625	0.650	0.675	0.701	0.726	0.751	0.778	0.806	0.838	0.876
0	0	0	0	0	0	0	0	0	0	0	0	0	0	0	0	0
.025	-1.002	-1.010	-1.119	-1.115	-1.160	-1.195	-1.233	-1.234	-1.288	-1.312	-1.320	-1.318	-1.270	-1.167	-1.092	-1.092
.050	-.665	-.690	-.740	-.753	-.774	-.816	-.850	-.852	-.894	-.920	-.940	-.940	-.920	-.852	-.782	-.782
.100	-.390	-.410	-.447	-.450	-.497	-.518	-.550	-.553	-.610	-.631	-.680	-.682	-.624	-.627	-.580	-.580
.150	-.240	-.260	-.284	-.308	-.325	-.341	-.364	-.392	-.409	-.467	-.550	-.572	-.539	-.513	-.469	-.469
.200	-.159	-.160	-.182	-.182	-.195	-.228	-.240	-.258	-.286	-.329	-.428	-.478	-.470	-.438	-.390	-.390
.250	-.080	-.089	-.100	-.100	-.110	-.125	-.140	-.149	-.171	-.215	-.330	-.387	-.395	-.367	-.330	-.330
.300	-.025	-.026	-.030	-.040	-.022	-.040	-.057	-.042	-.076	-.100	-.230	-.292	-.319	-.300	-.288	-.288
.350	.002	.004	-.004	-.010	.004	-.001	-.015	.001	-.013	-.048	-.139	-.239	-.232	-.232	-.192	-.192
.400	.050	.040	.049	.052	.073	.060	.070	.070	-.080	.073	.061	-.192	-.180	-.163	-.162	-.162
.450	.097	.099	.126	.112	.127	.084	.120	.146	.187	.222	.164	-.049	-.060	-.063	-.089	-.089
.500	.110	.107	.130	.128	.128	.136	.151	.158	.190	.230	.188	0	-.051	-.042	-.070	-.070
.550	.097	.119	.141	.132	.157	.184	.210	.208	.282	.272	.371	.137	.028	-.030	-.062	-.062
.600	.118	.140	.170	.167	.208	.222	.247	.273	.357	.357	.452	.400	.130	-.030	-.080	-.080
.700	-.032	-.011	-.028	.048	.050	.062	.069	.060	.079	.056	.029	.170	.080	0	-.042	-.042
.800	-.023	-.020	.027	0	.028	.024	.025	.040	.038	.020	.010	.053	.072	-.012	-.182	-.182
.850	-.003	.051	.034	.028	.023	.021	.024	.019	.018	.018	.009	.032	.033	.022	-.102	-.102
.875	.017	.029	.020	-.006	.007	.007	-.016	.009	.001	-.003	-.004	.031	.032	.013	-.074	-.074

TABLE Id.—EXPERIMENTAL LOAD DATA

[NACA 65₂-215 ($a=0.5$) Section Angle of Attack, $\alpha_0=0^\circ$]

Station x/c	Values of load parameter, $P=P_1-P_u$, for different Mach numbers														
	0.300	0.400	0.500	0.550	0.601	0.626	0.651	0.676	0.701	0.726	0.753	0.779	0.806	0.834	0.865
0	0	0	0	0	0	0	0	0	0	0	0	0	0	0	0
.025	-.160	-.178	-.195	-.209	-.226	-.207	-.247	-.244	-.282	-.320	-.438	-.580	-.640	-.690	-.638
.050	0	-.012	-.031	-.040	-.038	-.036	-.054	-.060	-.089	-.130	-.230	-.351	-.426	-.477	-.430
.100	.110	.090	.093	.089	.082	.088	.066	.074	.058	.014	-.090	-.208	-.272	-.321	-.282
.150	.152	.143	.165	.182	.158	.180	.159	.120	.143	.120	.020	-.095	-.170	-.234	-.212
.200	.188	.183	.203	.218	.232	.230	.228	.244	.230	.194	.095	-.036	-.120	-.160	-.118
.250	.220	.220	.242	.249	.260	.281	.282	.306	.288	.260	.155	-.043	-.050	-.085	-.086
.300	.240	.245	.269	.243	.308	.318	.332	.360	.358	.353	.194	.058	-.025	-.073	-.041
.350	.234	.246	.264	.262	.287	.309	.337	.374	.392	.405	.306	.141	.034	-.022	.006
.400	.260	.263	.290	.302	.320	.348	.383	.443	.444	.435	.375	.192	.067	0	.039
.450	.287	.301	.333	.346	.367	.391	.436	.484	.562	.580	.466	.206	.025	-.094	.034
.500	.267	.262	.310	.334	.350	.367	.396	.440	.520	.539	.440	.167	-.023	-.183	-.020
.550	.237	.257	.296	.315	.337	.349	.385	.454	.562	.620	.586	.259	-.100	-.286	-.066
.600	.247	.259	.316	.292	.310	.327	.324	.231	.137	.412	.531	.361	-.190	-.354	-.148
.700	.128	.128	.130	.154	.130	.143	.140	.056	.140	.083	.150	.216	-.140	-.297	-.322
.800	.072	.071	.070	.080	.067	.068	.082	.070	.070	.048	.075	.155	.229	-.040	-.382
.850	.043	.048	.054	.078	.055	.071	.060	.049	.068	.078	.064	.114	.093	-.045	-.364
.875	.040	.041	.054	.022	.034	.039	.040	.048	.022	.001	.056	.091	.202	.078	-.354

TABLE Ie.—EXPERIMENTAL LOAD DATA

[NACA 65₂-215 ($a=0.5$) Section Angle of Attack, $\alpha_0=2^\circ$]

Station x/c	Values of load parameter, $P=P_1-P_u$, for different Mach numbers														
	0.300	0.400	0.500	0.550	0.600	0.625	0.650	0.675	0.701	0.726	0.753	0.779	0.807	0.836	0.867
0	0	0	0	0	0	0	0	0	0	0	0	0	0	0	0
.025	.713	.739	.751	.770	.756	.748	.738	.705	.592	.439	.298	.069	-.081	-.177	-.157
.050	.661	.683	.726	.733	.742	.754	.744	.720	.630	.500	.367	.200	.036	-.031	-.030
.100	.590	.620	.672	.682	.715	.728	.747	.729	.671	.550	.430	.273	.114	.036	.056
.150	.572	.596	.648	.659	.696	.727	.747	.740	.700	.602	.470	.330	.170	.107	.108
.200	.532	.570	.620	.658	.692	.720	.757	.768	.719	.625	.508	.369	.210	.132	.130
.250	.514	.555	.602	.638	.670	.716	.750	.772	.750	.658	.540	.400	.235	.190	.173
.300	.518	.548	.628	.630	.676	.715	.778	.808	.783	.683	.576	.422	.238	.187	.182
.350	.485	.528	.566	.585	.635	.679	.720	.821	.812	.725	.600	.436	.265	.188	.213
.400	.480	.500	.554	.590	.624	.670	.727	.793	.841	.714	.535	.377	.225	.130	.220
.450	.473	.504	.544	.562	.614	.669	.680	.747	.807	.675	.516	.331	.148	.063	.163
.500	.440	.468	.510	.542	.583	.613	.670	.740	.820	.700	.550	.284	-.032	-.108	.077
.550	.427	.454	.504	.522	.577	.619	.640	.721	.835	.652	.451	.259	-.180	-.277	.009
.600	.410	.415	.373	.370	.331	.309	.285	.242	.375	.404	.410	.305	-.200	-.380	-.071
.700	.141	.189	.238	.246	.240	.235	.234	.219	.185	.230	.280	.292	-.172	-.372	-.215
.800	.138	.129	.130	.172	.122	.123	.120	.120	.100	.144	.218	.278	.330	-.060	-.273
.850	.088	.078	.093	.123	.093	.071	.092	.099	.048	.108	.181	.259	.316	.122	-.276
.875	.067	.047	.060	.072	.047	.059	.030	.031	.060	.102	.174	.248	.299	.176	-.247

TABLE If.—EXPERIMENTAL LOAD DATA

[NACA 65₂-215 ($a=0.5$) Section Angle of Attack, $\alpha_0=4^\circ$]

Station x/c	Values of load parameter, $P=P_1-P_u$, for different Mach numbers														
	0.300	0.400	0.500	0.551	0.601	0.626	0.651	0.678	0.705	0.732	0.759	0.783	0.811	0.840	0.871
0	0	0	0	0	0	0	0	0	0	0	0	0	0	0	0
.025	1.625	1.670	1.745	1.765	1.800	1.770	1.735	1.595	1.360	1.130	.925	.685	.535	.365	.310
.050	1.345	1.410	1.490	1.530	1.595	1.590	1.585	1.480	1.285	1.090	.910	.695	.555	.410	.365
.100	1.120	1.165	1.245	1.305	1.385	1.420	1.435	1.360	1.195	1.030	.865	.680	.575	.430	.375
.150	.990	1.040	1.140	1.180	1.280	1.310	1.425	1.365	1.210	1.050	.890	.720	.600	.465	.410
.200	.895	.945	1.050	1.095	1.200	1.235	1.355	1.340	1.210	1.055	.910	.725	.610	.480	.425
.250	.835	.885	.970	1.020	1.125	1.160	1.295	1.320	1.190	1.060	.900	.730	.610	.490	.440
.300	.785	.840	.915	.970	1.075	1.120	1.245	1.290	1.195	1.045	.880	.705	.600	.470	.430
.350	.727	.774	.851	.897	.987	1.024	1.190	1.271	1.142	.947	.796	.596	.505	.438	.436
.400	.690	.730	.805	.860	.940	.960	1.105	1.155	.935	.870	.720	.515	.420	.360	.390
.450	.677	.724	.791	.832	.912	.919	1.040	1.121	1.022	.842	.636	.396	.325	.233	.306
.500	.630	.665	.735	.765	.850	.880	1.000	1.120	.940	.665	.475	.240	.120	-.015	.195
.550	.587	.609	.656	.667	.737	.724	.625	.686	.642	.492	.381	.201	0	-.192	.036
.600	.400	.410	.440	.440	.440	.445	.425	.375	.430	.390	.335	.240	-.050	-.290	-.040
.700	.260	.260	.275	.285	.290	.280	.275	.235	.265	.330	.390	.370	.360	-.240	-.155
.800	.190	.190	.185	.190	.185	.185	.165	.155	.190	.295	.350	.380	.470	.010	-.175
.850	.123	.131	.134	.128	.133	.131	.140	.119	.163	.263	.334	.394	.420	.192	-.156
.875	.117	.114	.106	.102	.097	.099	.085	.096	.182	.252	.316	.361	.380	.243	-.144

TABLE Ig.—EXPERIMENTAL LOAD DATA

[NACA 65₂-215 ($\alpha=0.5$) Section Angle of Attack, $\alpha_0=6^\circ$]

Station x/c	Values of load parameter, $P=P_l-P_u$, for different Mach numbers													
	0.300	0.400	0.500	0.551	0.601	0.626	0.651	0.678	0.705	0.732	0.759	0.785	0.813	0.841
0	0	0	0	0	0	0	0	0	0	0	0	0	0	0
0.025	2.390	2.480	2.590	2.705	2.770	2.720	2.500	2.230	1.900	1.670	1.430	1.190	.990	.850
.050	1.930	2.020	2.110	2.230	2.330	2.445	2.270	2.030	1.730	1.550	1.330	1.135	.960	.830
.100	1.540	1.600	1.700	1.790	1.900	2.100	2.010	1.820	1.580	1.420	1.330	1.040	.880	.770
.150	1.330	1.380	1.460	1.570	1.660	1.890	1.940	1.755	1.550	1.380	1.220	1.040	.890	.780
.200	1.180	1.230	1.310	1.410	1.480	1.690	1.860	1.720	1.520	1.380	1.210	1.020	.880	.790
.250	1.078	1.130	1.210	1.270	1.330	1.510	1.750	1.675	1.445	1.290	1.130	.980	.855	.770
.300	1.000	1.050	1.125	1.190	1.260	1.340	1.640	1.545	1.320	1.180	1.020	.850	.740	.680
.350	.897	.949	1.011	1.067	1.082	1.119	1.510	1.451	1.237	1.082	.926	.756	.640	.578
.400	.845	.880	.940	.990	1.020	1.070	1.310	1.370	1.070	.890	.710	.600	.535	.490
.450	.797	.834	.881	.927	.942	.989	.900	1.041	.792	.652	.511	.401	.300	.283
.500	.710	.735	.755	.770	.770	.805	.700	.690	.590	.510	.410	.281	.100	.050
.550	.597	.609	.616	.617	.597	.624	.570	.506	.472	.442	.381	.256	.055	-.072
.600	.481	.470	.470	.450	.440	.465	.450	.380	.390	.390	.360	.270	.100	-.130
.700	.300	.270	.270	.240	.240	.260	.280	.250	.330	.370	.380	.375	.395	.090
.800	.160	.160	.180	.200	.220	.220	.240	.240	.335	.390	.450	.450	.460	.280
.850	.143	.146	.154	.208	.203	.191	.170	.199	.308	.378	.434	.449	.470	.422
.875	.147	.139	.186	.222	.207	.179	.150	.171	.282	.352	.421	.451	.455	.413

TABLE Ih.—EXPERIMENTAL LOAD DATA

[NACA 65₂-215 ($\alpha=0.5$) Section Angle of Attack, $\alpha_0=8^\circ$]

Station x/c	Values of load parameter, $P=P_l-P_u$, for different Mach numbers														
	0.300	0.401	0.501	0.526	0.551	0.576	0.601	0.626	0.653	0.681	0.708	0.735	0.762	0.789	0.818
0	0	0	0	0	0	0	0	0	0	0	0	0	0	0	0
0.025	3.265	3.430	3.470	3.520	3.435	3.440	3.310	3.110	2.800	2.590	2.330	2.120	1.880	1.700	1.440
.050	2.315	2.410	2.260	2.800	3.090	2.990	3.020	2.860	2.620	2.400	2.150	1.960	1.725	1.570	1.340
.100	1.865	1.945	1.970	1.990	1.940	2.200	2.630	2.570	2.360	2.160	1.945	1.770	1.560	1.430	1.210
.150	1.600	1.660	1.680	1.730	1.720	1.650	2.350	2.395	2.240	2.040	1.840	1.670	1.500	1.370	1.170
.200	1.410	1.460	1.480	1.520	1.515	1.515	1.715	2.220	2.120	1.940	1.735	1.560	1.400	1.290	1.140
.250	1.275	1.310	1.330	1.360	1.340	1.345	1.310	2.070	1.960	1.800	1.590	1.430	1.280	1.180	1.050
.300	1.155	1.175	1.190	1.210	1.200	1.220	1.240	1.640	1.840	1.665	1.440	1.290	1.130	1.050	.940
.350	1.032	1.054	1.046	1.049	1.052	1.040	1.072	.994	1.535	1.426	1.192	.982	.876	.821	.800
.400	.940	.950	.935	.935	.930	.910	1.000	.890	.990	1.000	.870	.740	.650	.600	.570
.450	.857	.859	.826	.814	.812	.805	.877	.809	.750	.741	.687	.555	.490	.466	.410
.500	.730	.705	.660	.635	.600	.580	.720	.710	.610	.570	.461	.467	.452	.416	.240
.550	.582	.549	.486	.464	.442	.410	.517	.534	.485	.461	.380	.380	.420	.405	.280
.600	.450	.390	.325	.300	.270	.255	.400	.420	.390	.380	.310	.380	.430	.440	.240
.700	.245	.210	.230	.230	.220	.205	.270	.280	.280	.310	.300	.395	.460	.520	.250
.800	.165	.170	.240	.230	.240	.240	.260	.245	.280	.300	.380	.460	.520	.550	.400
.850	.158	.181	.264	.271	.278	.275	.283	.231	.280	.299	.398	.468	.514	.529	.550
.875	.157	.189	.276	.269	.352	.345	.232	.169	.240	.301	.372	.457	.506	.521	.530

TABLE Ii.—EXPERIMENTAL LOAD DATA

[NACA 65₂-215 ($\alpha=0.5$) Section Angle of Attack, $\alpha_0=10^\circ$]

Station x/c	Values of load parameter, $P=P_l-P_u$, for different Mach numbers												
	0.501	0.526	0.552	0.576	0.602	0.630	0.659	0.686	0.713	0.740	0.767	0.796	0.825
0	0	0	0	0	0	0	0	0	0	0	0	0	0
0.025	4.160	4.036	4.006	3.856	3.640	3.396	3.110	2.800	2.636	2.376	2.160	1.940	1.810
.050	3.280	3.790	3.680	3.520	3.380	3.170	2.860	2.570	2.430	2.205	2.000	1.800	1.660
.100	2.130	2.075	2.350	3.090	3.010	2.860	2.560	2.290	2.165	1.950	1.790	1.630	1.520
.150	1.820	1.810	1.750	2.280	2.760	2.590	2.350	2.090	1.960	1.780	1.640	1.505	1.430
.200	1.585	1.580	1.565	1.540	2.380	2.430	2.145	1.885	1.770	1.600	1.500	1.380	1.360
.250	1.390	1.380	1.390	1.320	1.550	1.970	1.790	1.590	1.480	1.350	1.300	1.260	1.260
.300	1.220	1.210	1.220	1.190	1.070	1.405	1.425	1.280	1.200	1.075	1.030	1.030	1.110
.350	1.066	1.014	1.062	1.020	.972	1.039	1.095	1.021	.947	.852	.821	.821	.975
.400	.910	.890	.880	.865	.880	.830	.950	.820	.770	.700	.630	.630	.800
.450	.786	.719	.747	.745	.727	.714	.705	.681	.652	.592	.551	.501	.605
.500	.570	.550	.540	.560	.620	.580	.580	.565	.570	.520	.475	.430	.470
.550	.426	.424	.412	.415	.457	.479	.480	.491	.497	.482	.446	.401	.410
.600	.310	.300	.290	.325	.390	.400	.410	.445	.465	.460	.430	.390	.405
.700	.260	.270	.285	.285	.310	.340	.360	.430	.450	.460	.480	.485	.500
.800	.280	.290	.285	.280	.300	.335	.350	.410	.460	.500	.540	.570	.640
.850	.284	.291	.288	.295	.273	.321	.295	.419	.468	.508	.549	.614	.680
.875	.286	.279	.332	.295	.217	.279	.290	.386	.427	.457	.541	.606	.680

TABLE Ij.—EXPERIMENTAL LOAD DATA

[NACA 65₂-215 ($\alpha=0.5$) Section Angle of Attack, $\alpha_0=12^\circ$]

Station x/c	Values of load parameter, $P=P_l-P_u$, for different Mach numbers													
	0.301	0.401	0.528	0.555	0.582	0.609	0.636	0.663	0.689	0.716	0.743	0.770	0.799	0.832
0	0	0	0	0	0	0	0	0	0	0	0	0	0	0
0.025	3.695	4.490	3.820	3.750	3.610	3.520	3.300	3.100	2.860	2.700	2.600	2.440	2.225	2.020
.050	3.055	3.090	3.400	3.405	3.340	3.230	3.050	2.860	2.605	2.470	2.390	2.225	2.075	1.885
.100	2.350	2.357	2.470	2.380	2.425	2.595	2.615	2.445	2.240	2.120	2.050	1.935	1.855	1.705
.150	1.955	1.954	1.915	1.820	1.750	1.880	2.220	2.084	1.875	1.805	1.780	1.705	1.685	1.615
.200	1.675	1.684	1.550	1.515	1.420	1.445	1.700	1.715	1.555	1.485	1.470	1.430	1.510	1.530
.250	1.440	1.448	1.285	1.270	1.220	1.210	1.330	1.390	1.315	1.250	1.225	1.190	1.300	1.455
.300	1.255	1.258	1.075	1.060	1.070	1.060	1.080	1.130	1.100	1.070	1.045	0.985	1.070	1.385
.350	1.192	1.053	.894	.862	.875	.897	.819	.945	.916	.912	.897	.841	.886	1.285
.400	.885	.891	.710	.720	.750	.780	.760	.795	.770	.770	.760	.700	.720	1.165
.450	.852	.752	.604	.592	.630	.667	.664	.690	.666	.672	.662	.626	.636	1.095
.500	.530	.590	.490	.500	.555	.565	.575	.590	.575	.600	.600	.560	.560	1.030
.550	.517	.482	.424	.422	.480	.492	.499	.525	.521	.552	.562	.536	.521	.980
.600	.325	.385	.370	.380	.450	.440	.450	.475	.485	.525	.535	.520	.515	.925
.700	.325	.374	.370	.360	.440	.440	.440	.480	.495	.545	.565	.577	.585	.975
.800	.345	.385	.380	.380	.440	.430	.435	.495	.510	.560	.590	.590	.660	1.045
.850	.338	.382	.346	.358	.430	.418	.421	.475	.499	.543	.588	.614	.694	1.130
.875	.242	.350	.379	.357	.405	.402	.399	.435	.481	.532	.560	.581	.671	1.100

TABLE Ik.—EXPERIMENTAL LOAD DATA

[NACA 65₂-215 ($\alpha=0.5$) Section Angle of Attack, $\alpha_0=14^\circ$]

Station x/c	Values of load parameter, $P=P_l-P_u$, for different Mach numbers												
	0.405	0.509	0.535	0.561	0.586	0.613	0.640	0.666	0.693	0.721	0.749	0.772	0.804
0	0	0	0	0	0	0	0	0	0	0	0	0	0
0.025	3.851	3.660	3.480	3.450	3.360	3.330	3.210	3.150	3.020	2.890	2.730	2.540	2.460
.050	3.149	3.125	2.990	3.080	2.990	3.030	2.970	2.940	2.780	2.670	2.500	2.320	2.290
.100	2.377	2.350	2.250	2.470	2.410	2.410	2.410	2.420	2.350	2.330	2.090	2.030	2.050
.150	1.882	1.790	1.770	1.940	1.930	1.940	1.930	1.940	1.860	2.000	1.680	1.750	1.880
.200	1.523	1.440	1.460	1.570	1.565	1.600	1.580	1.580	1.515	1.620	1.420	1.460	1.730
.250	1.303	1.220	1.165	1.300	1.290	1.300	1.310	1.330	1.330	1.390	1.240	1.270	1.560
.300	1.092	1.030	1.000	1.080	1.260	1.120	1.100	1.150	1.170	1.180	1.130	1.100	1.330
.350	.985	.906	.852	.872	.890	.897	.899	.920	1.006	1.032	.982	.961	1.116
.400	.841	.780	.740	.770	.755	.770	.765	.790	.870	.895	.880	.850	.950
.450	.724	.696	.654	.632	.650	.667	.669	.670	.771	.782	.797	.781	.846
.500	.599	.605	.570	.570	.570	.600	.570	.600	.675	.680	.720	.700	.780
.550	.507	.536	.494	.472	.495	.517	.519	.530	.626	.602	.672	.671	.751
.600	.469	.510	.495	.470	.470	.490	.510	.525	.590	.560	.630	.640	.720
.700	.474	.510	.530	.480	.475	.500	.520	.520	.580	.470	.640	.660	.770
.800	.471	.520	.530	.470	.480	.510	.520	.550	.580	.600	.650	.710	.840
.850	.432	.494	.491	.438	.465	.503	.481	.535	.549	.578	.643	.714	.829
.875	.451	.481	.479	.407	.445	.472	.459	.500	.526	.552	.612	.671	.821

TABLE II.—EXPERIMENTAL LOAD DATA

[NACA 65₂-215 ($\alpha=0.5$) Section Angle of Attack, $\alpha_0=16^\circ$]

Station x/c	Values of load parameter, $P=P_l-P_u$, for different Mach numbers										
	0.511	0.537	0.563	0.590	0.617	0.643	0.669	0.697	0.725	0.748	0.780
0	0	0	0	0	0	0	0	0	0	0	0
0.025	3.270	3.020	2.545	2.670	2.930	2.930	2.930	2.890	2.890	2.940	2.860
.050	2.855	2.555	2.190	2.250	2.620	2.605	2.620	2.680	2.715	2.700	2.670
.100	2.190	1.920	1.600	1.650	2.120	2.145	2.175	2.220	2.270	2.450	2.395
.150	1.570	1.395	1.270	1.320	1.715	1.700	1.750	1.875	1.950	2.050	2.200
.200	1.200	1.120	1.090	1.130	1.400	1.450	1.430	1.555	1.440	1.730	2.020
.250	1.030	.970	.940	.980	1.240	1.250	1.250	1.335	1.440	1.490	1.770
.300	.990	.880	.825	.860	1.080	1.110	1.130	1.185	1.265	1.315	1.550
.350	.856	.769	.742	.755	.937	.949	.970	1.021	1.112	1.162	1.391
.400	.740	.660	.660	.670	.830	.870	.870	.935	1.010	1.070	1.280
.450	.696	.619	.612	.635	.737	.764	.790	.831	.902	.992	1.186
.500	.645	.580	.570	.580	.690	.710	.720	.770	.820	.895	1.090
.550	.616	.559	.552	.575	.637	.669	.685	.721	.747	.822	.991
.600	.605	.550	.555	.575	.620	.640	.660	.680	.715	.760	.860
.700	.635	.600	.580	.600	.605	.640	.655	.670	.690	.725	.780
.800	.670	.635	.620	.615	.600	.615	.640	.640	.680	.740	.790
.850	.654	.616	.618	.595	.563	.586	.600	.629	.673	.728	.799
.875	.636	.589	.602	.625	.527	.559	.590	.591	.632	.692	.771

TABLE IIa.—EXPERIMENTAL LOAD DATA

[NACA 66,2-215 ($\alpha=0.6$) Section Angle of Attack, $\alpha_0=-6^\circ$]

Station	Values of load parameter, $P=P_l-P_u$, for different Mach numbers													
x/c	0.300	0.400	0.500	0.551	0.601	0.626	0.651	0.676	0.702	0.729	0.756	0.782	0.812	0.843
0	0	0	0	0	0	0	0	0	0	0	0	0	0	0
0.025	-2.905	-2.765	-3.290	-3.195	-3.025	-2.975	-3.050	-2.830	-2.710	-2.550	-2.330	-2.115	-1.950	-1.790
.050	-1.690	-1.780	-1.770	-2.060	-2.790	-2.715	-2.630	-2.525	-2.435	-2.310	-2.100	-1.895	-1.740	-1.580
.100	-1.195	-1.245	-1.305	-1.290	-1.370	-1.555	-2.220	-2.110	-2.055	-1.935	-1.745	-1.560	-1.420	-1.295
.150	-.915	-.985	-1.000	-1.015	-1.005	-.970	-1.195	-1.840	-1.840	-1.745	-1.570	-1.405	-1.270	-1.150
.200	-.730	-.750	-.780	-.800	-.820	-.780	-.725	-1.500	-1.625	-1.585	-1.425	-1.255	-1.120	-1.025
.250	-.600	-.630	-.640	-.670	-.670	-.665	-.640	-.750	-1.470	-1.440	-1.290	-1.135	-1.030	-.940
.300	-.485	-.505	-.530	-.550	-.540	-.545	-.530	-.430	-1.170	-1.335	-1.205	-1.025	-.940	-.875
.350	-.378	-.381	-.399	-.423	-.433	-.411	-.410	-.344	-.468	-1.148	-1.079	-.879	-.830	-.792
.400	-.295	-.310	-.310	-.300	-.310	-.300	-.295	-.260	-.180	-.770	-.945	-.660	-.695	-.635
.450	-.213	-.221	-.219	-.228	-.218	-.181	-.195	-.179	-.078	-.278	-.559	-.369	-.440	-.522
.500	-.160	-.160	-.140	-.130	-.140	-.110	-.125	-.105	.035	0	-.180	-.130	-.200	-.385
.550	-.103	-.101	-.069	-.068	-.038	-.011	-.015	-.009	.097	.162	.126	.126	.040	-.172
.600	-.040	-.035	-.002	.005	.045	.045	.075	.075	.125	.240	.335	.365	.215	.090
.700	.060	.115	.115	.145	.185	.185	.220	.235	.245	.320	.435	.480	.340	.345
.800	.050	.015	.020	.010	-.020	.020	.025	.020	.015	-.015	0	.095	.210	.285
.850	-.057	-.059	-.035	-.022	-.032	-.024	-.035	.014	-.007	-.002	-.051	-.051	.025	.187
.875	-.043	-.026	-.024	-.043	-.033	-.021	-.020	-.014	-.048	-.043	-.069	-.059	.110	.158

TABLE IIb.—EXPERIMENTAL LOAD DATA

[NACA 66,2-215 ($\alpha=0.6$) Section Angle of Attack, $\alpha_0=-4^\circ$]

Station	Values of load parameter, $P=P_l-P_u$, for different Mach numbers													
x/c	0.300	0.400	0.500	0.550	0.600	0.626	0.651	0.676	0.701	0.726	0.752	0.782	0.807	0.839
0	0	0	0	0	0	0	0	0	0	0	0	0	0	0
0.025	-1.635	-1.705	-1.825	-1.870	-2.000	-1.990	-2.030	-2.080	-2.115	-2.020	-1.900	-1.750	-1.625	-1.485
.050	-1.095	-1.260	-1.355	-1.295	-1.510	-1.575	-1.640	-1.700	-1.745	-1.770	-1.675	-1.530	-1.405	-1.290
.100	-.755	-.785	-.840	-.850	-.900	-.910	-.875	-.855	-1.280	-1.370	-1.335	-1.220	-1.125	-1.010
.150	-.575	-.585	-.665	-.645	-.680	-.670	-.695	-.700	-.630	-.610	-1.110	-1.080	-.980	-.890
.200	-.405	-.440	-.460	-.460	-.500	-.500	-.525	-.535	-.520	-.795	-1.020	-.940	-.845	-.775
.250	-.320	-.345	-.375	-.365	-.410	-.410	-.430	-.450	-.480	-.460	-.905	-.870	-.770	-.690
.300	-.240	-.260	-.280	-.290	-.305	-.320	-.305	-.320	-.350	-.315	-.790	-.800	-.710	-.645
.350	-.163	-.176	-.179	-.178	-.193	-.201	-.200	-.214	-.228	-.193	-.569	-.689	-.620	-.547
.400	-.110	-.115	-.120	-.100	-.120	-.115	-.115	-.120	-.120	-.145	-.350	-.580	-.500	-.440
.450	-.058	-.051	-.059	-.053	-.063	-.051	-.040	-.039	-.028	-.003	-.099	-.474	-.410	-.352
.500	-.015	-.025	-.020	0	-.010	0	.020	.055	.040	.030	.060	-.370	-.290	-.260
.550	.027	.019	.046	.052	.057	.069	.090	.101	.112	.182	.161	-.149	-.130	-.142
.600	.060	.065	.085	.100	.120	.120	.150	.165	.180	.200	.295	.290	.060	-.080
.700	.160	.165	.210	.270	.280	.310	.340	.370	.390	.410	.455	.550	.380	.190
.800	.020	.005	.035	.065	.060	.040	.080	.165	.080	.050	.035	.105	.210	.130
.850	-.032	-.014	-.011	.008	.013	.026	.030	.049	-.003	.008	.064	.034	.155	.112
.875	-.018	-.021	-.004	.012	.007	.004	.020	.001	.012	-.008	.009	.036	-.120	.103

TABLE IIc.—EXPERIMENTAL LOAD DATA

[NACA 66,2-215 ($\alpha=0.6$) Section Angle of Attack, $\alpha_0=-2^\circ$]

Station	Values of load parameter, $P=P_l-P_u$, for different Mach numbers													
x/c	0.300	0.400	0.500	0.550	0.600	0.625	0.650	0.675	0.701	0.726	0.751	0.780	0.803	0.834
0	0	0	0	0	0	0	0	0	0	0	0	0	0	0
.025	-.853	-.895	-.930	-.990	-.980	-1.025	-.975	-1.055	-1.095	-1.115	-1.145	-1.195	-1.165	0
.050	-.598	-.620	-.655	-.695	-.695	-.730	-.760	-.785	-.815	-.860	-.920	-1.015	-1.015	-1.055
.100	-.338	-.353	-.370	-.410	-.400	-.450	-.455	-.485	-.505	-.555	-.600	-.650	-.700	-.660
.150	-.219	-.240	-.255	-.275	-.260	-.305	-.255	-.305	-.360	-.395	-.485	-.580	-.600	-.545
.200	-.120	-.131	-.140	-.155	-.140	-.185	-.175	-.190	-.205	-.250	-.310	-.425	-.460	-.415
.250	-.063	-.072	-.075	-.100	-.095	-.115	-.115	-.125	-.145	-.185	-.265	-.335	-.415	-.370
.300	-.034	-.036	-.025	-.040	-.045	-.055	-.055	-.055	-.075	-.100	-.185	-.310	-.360	-.345
.350	.022	.017	.016	.017	.027	.019	.005	.006	.002	-.013	-.079	-.229	-.305	-.322
.400	.063	.056	.060	.060	.085	.085	.075	.080	.090	.090	.030	-.140	-.240	-.220
.450	.087	.089	.102	.102	.117	.119	.115	.131	.132	.142	.106	-.049	-.165	-.177
.500	.098	.109	.130	.125	.145	.150	.150	.160	.185	.190	.165	.030	-.125	-.115
.550	.126	.134	.146	.152	.177	.219	.220	.196	.222	.252	.246	.116	-.040	-.047
.600	.137	.145	.170	.165	.195	.270	.195	.210	.245	.250	.265	.140	-.080	0
.700	.168	.245	.290	.295	.330	.345	.370	.365	.420	.440	.455	.400	.225	.085
.800	.020	.025	.060	.045	.045	.040	.045	.045	.035	.030	.035	.085	.155	.025
.850	.023	.011	.049	.028	.018	.006	.020	.034	.018	.013	.034	-.076	.115	.012
.875	-.005	.003	-.016	.002	.012	.014	-.005	-.029	-.008	-.003	.001	-.064	.110	.013

TABLE II*d*.—EXPERIMENTAL LOAD DATA

[NACA 66,2-215 ($\alpha=0.6$) Section Angle of Attack, $\alpha_0=0^\circ$]

Station	Values of load parameter, $P=P_l-P_u$, for different Mach numbers													
	0.300	0.400	0.500	0.550	0.600	0.625	0.651	0.676	0.701	0.726	0.752	0.779	0.803	0.833
0	0	0	0	0	0	0	0	0	0	0	0	0	0	0
.025	-.030	-.035	-.035	-.040	-.065	-.065	-.070	-.080	-.100	-.160	-.285	-.429	-.540	-.575
.050	-.060	-.060	-.045	-.050	-.050	-.025	-.046	0	-.010	-.050	-.161	-.302	-.420	-.415
.100	-.145	-.165	-.160	-.155	-.145	-.155	-.140	-.148	-.145	-.098	-.080	-.132	-.222	-.270
.150	-.175	-.195	-.185	-.205	-.210	-.215	-.210	-.192	-.204	-.167	-.060	-.085	-.173	-.225
.200	-.210	-.230	-.245	-.255	-.255	-.270	-.278	-.280	-.278	-.243	-.167	-.040	-.047	-.075
.250	-.220	-.240	-.245	-.250	-.265	-.280	-.297	-.296	-.310	-.288	-.200	-.046	-.023	-.050
.300	-.225	-.250	-.270	-.270	-.295	-.305	-.317	-.360	-.348	-.330	-.250	-.108	-.045	-.057
.350	-.227	-.289	-.296	-.287	-.312	-.334	-.385	-.386	-.379	-.382	-.281	-.141	-.010	-.039
.400	-.270	-.300	-.305	-.320	-.340	-.375	-.380	-.430	-.448	-.450	-.368	-.216	0	0
.450	-.272	-.309	-.316	-.322	-.342	-.374	-.420	-.429	-.472	-.482	-.401	-.228	-.107	-.068
.500	-.275	-.300	-.315	-.330	-.360	-.390	-.393	-.418	-.475	-.490	-.450	-.250	-.067	-.010
.550	-.272	-.309	-.301	-.327	-.347	-.384	-.440	-.409	-.447	-.515	-.421	-.192	-.001	-.092
.600	-.265	-.290	-.300	-.320	-.340	-.365	-.385	-.390	-.438	-.468	-.400	-.211	-.050	-.175
.700	-.285	-.335	-.350	-.380	-.425	-.420	-.418	-.428	-.448	-.185	-.275	-.234	-.085	-.255
.800	-.110	-.105	-.085	-.090	-.095	-.090	-.109	-.088	-.105	-.067	-.070	-.164	-.165	-.070
.850	-.048	-.071	-.054	-.068	-.073	-.086	-.045	-.049	-.062	-.036	-.034	-.139	-.195	-.047
.875	-.072	-.059	-.051	-.037	-.032	-.034	-.055	-.041	-.060	-.022	-.069	-.146	-.200	-.283

TABLE II*e*.—EXPERIMENTAL LOAD DATA

[NACA 66,2-215 ($\alpha=0.6$) Section Angle of Attack, $\alpha_0=2^\circ$]

Station	Values of load parameter, $P=P_l-P_u$, for different Mach numbers													
	0.300	0.400	0.500	0.550	0.600	0.626	0.651	0.676	0.701	0.727	0.753	0.780	0.806	0.834
0	0	0	0	0	0	0	0	0	0	0	0	0	0	0
.025	.818	.834	.865	.858	.885	.870	.830	.830	.760	.630	.430	.280	.088	.030
.050	.700	.727	.755	.780	.791	.800	.770	.770	.720	.610	.440	.320	.120	.030
.100	.637	.656	.700	.728	.730	.760	.770	.770	.740	.640	.500	.365	.220	.110
.150	.575	.618	.650	.688	.700	.720	.740	.760	.744	.680	.530	.420	.280	.170
.200	.560	.570	.630	.660	.695	.715	.750	.760	.760	.690	.550	.460	.300	.210
.250	.515	.540	.595	.626	.656	.690	.715	.740	.755	.712	.565	.460	.300	.190
.300	.502	.526	.575	.600	.630	.670	.670	.730	.780	.755	.600	.490	.350	.240
.350	.487	.509	.554	.582	.610	.629	.670	.721	.757	.767	.631	.511	.370	.268
.400	.470	.509	.550	.590	.620	.650	.670	.730	.795	.790	.670	.562	.410	.305
.450	.439	.488	.536	.567	.592	.624	.665	.696	.762	.812	.676	.521	.350	.258
.500	.430	.460	.492	.530	.580	.580	.610	.660	.750	.750	.590	.430	.210	.130
.550	.405	.429	.481	.502	.522	.529	.560	.596	.660	.672	.521	.346	.100	-.012
.600	.402	.419	.460	.480	.500	.520	.520	.570	.630	.660	.490	.250	-.070	-.171
.700	.423	.430	.431	.435	.422	.420	.380	.310	.180	.175	.160	.100	-.170	-.280
.800	.150	.160	.150	.150	.140	.150	.149	.130	.120	.107	.130	.200	.190	-.200
.850	.068	.046	.054	.063	.078	.091	.100	.109	.113	.118	.139	.209	.245	-.078
.875	.102	.114	.096	.087	.072	.059	.059	.044	.042	.052	.131	.211	.250	-.178

TABLE III*f*.—EXPERIMENTAL LOAD DATA

[NACA 66,2-215 ($\alpha=0.6$) Section Angle of Attack, $\alpha_0=4^\circ$]

Station	Values of load parameter, $P=P_l-P_u$, for different Mach numbers													
	0.300	0.400	0.500	0.550	0.601	0.626	0.651	0.677	0.701	0.728	0.755	0.780	0.808	0.837
0	0	0	0	0	0	0	0	0	0	0	0	0	0	0
.025	1.650	1.685	1.720	1.730	1.750	1.770	1.705	1.630	1.500	1.300	1.010	.820	.625	.485
.050	1.350	1.378	1.423	1.445	1.500	1.510	1.490	1.470	1.375	1.180	.925	.760	.585	.460
.100	1.125	1.144	1.197	1.225	1.300	1.315	1.310	1.270	1.170	1.040	.830	.695	.540	.440
.150	.980	.993	1.055	1.100	1.150	1.220	1.270	1.300	1.220	1.080	.905	.770	.655	.553
.200	.890	.914	.969	1.010	1.070	1.130	1.175	1.280	1.250	1.120	.930	.805	.655	.545
.250	.815	.838	.894	.940	1.005	1.040	1.075	1.190	1.230	1.105	.925	.800	.655	.535
.300	.770	.775	.842	.855	.925	.970	1.005	1.100	1.205	1.100	.910	.780	.640	.530
.350	.717	.727	.785	.807	.877	.904	.930	1.016	1.152	1.077	.891	.761	.630	.533
.400	.685	.700	.744	.770	.845	.870	.915	.960	1.155	1.060	.845	.725	.580	.505
.450	.647	.659	.695	.727	.772	.799	.820	.881	1.052	.982	.751	.621	.475	.403
.500	.615	.612	.650	.680	.720	.745	.770	.770	.990	.905	.690	.535	.350	.280
.550	.577	.574	.616	.637	.677	.684	.685	.641	.877	.837	.531	.336	.145	.098
.600	.540	.533	.557	.580	.615	.620	.590	.550	.470	.490	.295	.115	-.040	-.105
.700	.380	.345	.345	.340	.325	.340	.290	.270	.210	.150	.140	.055	-.190	-.330
.800	.160	.177	.171	.185	.175	.175	.145	.145	.140	.125	.210	.265	.180	-.390
.850	.123	.121	.108	.113	.113	.126	.135	.119	.173	.118	.219	.309	.290	-.233
.875	.137	.114	.131	.127	.137	.099	.110	.141	.072	.132	.231	.301	.310	-.142

TABLE IIg.—EXPERIMENTAL LOAD DATA

[NACA 66,2-215 ($\alpha=0.6$) Section Angle of Attack, $\alpha_0=6^\circ$]

Station	Values of load parameter, $P=P_1-P_u$, for different Mach numbers														
	x/c	0.300	0.400	0.501	0.551	0.601	0.626	0.652	0.676	0.703	0.731	0.757	0.786	0.812	0.842
0	0	0	0	0	0	0	0	0	0	0	0	0	0	0	0
0.025	2.245	2.300	2.390	2.430	2.415	2.510	2.505	2.400	2.100	1.820	1.540	1.320	1.130	.930	
.050	1.790	1.800	1.875	1.930	1.990	2.065	2.235	2.180	1.880	1.630	1.385	1.210	1.050	.880	
.100	1.390	1.420	1.480	1.530	1.525	1.600	1.870	1.890	1.660	1.430	1.230	1.055	.915	.745	
.150	1.160	1.220	1.270	1.290	1.345	1.410	1.710	1.790	1.585	1.415	1.215	1.080	.935	.800	
.200	1.060	1.085	1.150	1.185	1.215	1.255	1.555	1.745	1.560	1.360	1.185	1.055	.920	.750	
.250	.955	.980	1.030	1.060	1.085	1.130	1.370	1.655	1.515	1.340	1.160	1.005	.885	.760	
.300	.870	.890	.930	.955	.980	1.000	1.140	1.540	1.440	1.285	1.120	.985	.870	.750	
.350	.842	.829	.866	.912	.912	.944	.965	1.436	1.377	1.207	1.061	.915	.830	.723	
.400	.755	.760	.800	.795	.835	.825	.875	1.285	1.280	1.115	.975	.850	.760	.665	
.450	.692	.709	.716	.742	.752	.779	.820	.826	1.207	1.042	.866	.736	.650	.558	
.500	.620	.630	.640	.630	.645	.625	.715	.610	.890	.800	.670	.560	.510	.460	
.550	.547	.549	.546	.547	.522	.529	.615	.556	.497	.502	.411	.311	.270	.293	
.600	.500	.470	.445	.420	.410	.385	.500	.515	.345	.300	.245	.140	.100	.100	
.700	.270	.230	.175	.130	.140	.080	.195	.275	.180	.150	.150	.075	-.060	-.215	
.800	.050	.050	.065	.075	.120	.105	.150	.190	.175	.190	.250	.300	.235	-.345	
.850	.118	.156	.141	.178	.203	.161	.180	.204	.178	.213	.274	.319	.345	-.363	
.875	.162	.149	.171	.202	.192	.214	.160	.131	.142	.202	.271	.311	.339	-.342	

TABLE IIh.—EXPERIMENTAL LOAD DATA

[NACA 66,2-215 ($\alpha=0.6$) Section Angle of Attack, $\alpha_0=8^\circ$]

Station	Values of load parameter, $P=P_1-P_u$, for different Mach numbers														
	x/c	0.300	0.401	0.501	0.526	0.551	0.576	0.601	0.626	0.652	0.680	0.707	0.734	0.761	0.788
0	0	0	0	0	0	0	0	0	0	0	0	0	0	0	0
0.025	3.210	3.105	3.570	3.490	3.435	3.340	3.320	3.230	3.065	2.750	2.480	2.255	2.010	1.760	1.560
.050	2.150	2.215	2.180	2.220	2.990	3.100	2.915	2.940	2.790	2.520	2.260	2.060	1.830	1.605	1.430
.100	1.740	1.790	1.810	1.805	1.790	1.700	2.445	2.585	2.480	2.250	2.000	1.830	1.620	1.410	1.240
.150	1.470	1.480	1.540	1.540	1.560	1.540	1.480	2.340	2.340	2.145	1.920	1.745	1.570	1.385	1.230
.200	1.280	1.320	1.360	1.365	1.365	1.405	1.340	2.180	2.215	2.040	1.830	1.680	1.505	1.330	1.180
.250	1.140	1.165	1.190	1.190	1.200	1.240	1.220	1.530	2.060	1.940	1.710	1.560	1.410	1.250	1.130
.300	1.010	1.045	1.055	1.055	1.060	1.080	1.100	1.010	1.935	1.820	1.610	1.470	1.320	1.185	1.080
.350	.927	.944	.946	.964	.962	.975	1.007	.929	1.290	1.691	1.502	1.132	1.216	1.091	1.000
.400	.850	.850	.850	.850	.845	.860	.870	.890	.860	1.275	1.250	1.135	1.060	.990	.920
.450	.752	.764	.756	.769	.762	.745	.767	.804	.690	.806	.862	.822	.801	.791	.760
.500	.665	.655	.630	.610	.610	.610	.625	.700	.635	.575	.610	.600	.580	.585	.640
.550	.572	.544	.496	.479	.497	.490	.512	.594	.530	.436	.412	.402	.371	.361	.430
.600	.460	.420	.345	.310	.340	.330	.350	.470	.490	.340	.275	.250	.230	.180	.200
.700	.200	.150	.110	.095	.110	.100	.095	.210	.240	.220	.190	.200	.200	.105	-.040
.800	.100	.110	.110	.090	.080	.100	.105	.095	.130	.170	.200	.250	.300	.350	-.080
.850	.123	.166	.189	.186	.208	.195	.203	.241	.255	.229	.278	.318	.359	.384	.390
.875	.127	.149	.276	.264	.242	.235	.242	.169	.145	.206	.292	.337	.401	.371	.430

TABLE IIi.—EXPERIMENTAL LOAD DATA

[NACA 66,2-215 ($\alpha=0.6$) Section Angle of Attack $\alpha_0=10^\circ$]

Station	Values of load parameter $P=P_1-P_u$ for different Mach numbers														
	x/c	0.300	0.401	0.501	0.527	0.552	0.577	0.603	0.629	0.655	0.681	0.708	0.735	0.762	0.793
0	0	0	0	0	0	0	0	0	0	0	0	0	0	0	0
0.025	3.040	3.737	4.060	3.940	3.905	3.875	3.760	3.510	3.220	2.940	2.770	2.510	2.285	2.085	1.890
.050	2.600	2.652	3.185	3.495	2.700	3.570	3.450	3.265	2.955	2.710	2.520	2.290	2.095	1.900	1.725
.100	2.050	2.112	2.090	2.240	2.220	2.910	3.040	2.880	2.630	2.380	2.240	2.030	1.860	1.695	1.530
.150	1.670	1.739	1.700	1.740	1.720	1.775	2.415	2.630	2.405	2.170	2.045	1.890	1.745	1.620	1.480
.200	1.495	1.531	1.470	1.515	1.490	1.460	1.775	2.420	2.175	1.950	1.895	1.755	1.650	1.530	1.410
.250	1.305	1.346	1.290	1.315	1.290	1.270	1.315	1.780	1.800	1.635	1.665	1.580	1.500	1.430	1.325
.300	1.160	1.189	1.110	1.140	1.130	1.100	1.105	1.310	1.420	1.370	1.380	1.380	1.340	1.300	1.270
.350	1.042	1.049	1.041	1.009	.977	.975	.927	.989	.985	1.131	1.122	1.097	1.146	1.176	1.170
.400	.920	.948	.870	.885	.850	.845	.850	.845	.920	.940	.930	.880	.940	1.045	1.070
.450	.797	.833	.791	.739	.707	.720	.689	.755	.781	.712	.712	.692	.726	.816	.915
.500	.675	.704	.620	.615	.580	.580	.610	.595	.600	.610	.580	.530	.550	.590	.760
.550	.532	.560	.511	.464	.417	.425	.457	.444	.435	.456	.407	.362	.356	.376	.535
.600	.385	.445	.350	.345	.290	.290	.360	.350	.325	.340	.410	.320	.240	.220	.345
.700	.165	.233	.180	.195	.165	.190	.225	.245	.255	.280	.270	.260	.240	.170	.070
.800	.165	.172	.145	.165	.160	.195	.205	.205	.230	.265	.300	.325	.355	.410	.165
.850	.198	.180	.159	.216	.203	.210	.243	.246	.290	.339	.383	.438	.474	.499	.470
.875	.197	.167	.246	.214	.202	.245	.212	.214	.285	.326	.387	.447	.501	.516	.560

TABLE IIj.—EXPERIMENTAL LOAD DATA

[NACA 66,2-215 ($\alpha=0.6$) Section Angle of Attack $\alpha_0=12^\circ$]

Station	Values of load parameter, $P=P_l-P_u$, for different Mach numbers															
	x/c	0.301	0.402	0.504	0.530	0.556	0.582	0.608	0.635	0.662	0.689	0.717	0.745	0.774	0.795	0.831
0	0	0	0	0	0	0	0	0	0	0	0	0	0	0	0	0
0.025	3.625	3.571	3.385	3.300	3.245	3.165	2.955	2.765	2.620	2.810	2.735	2.650	2.570	2.340	2.140	2.140
.050	2.962	3.176	2.950	2.865	2.855	2.800	2.615	2.455	2.350	2.555	2.510	2.410	2.325	2.155	1.960	1.960
.100	2.325	2.558	2.345	2.250	2.200	2.160	2.030	1.890	1.850	2.030	2.090	2.090	2.050	1.915	1.745	1.745
.150	1.930	2.026	1.925	1.855	1.780	1.760	1.640	1.595	1.550	1.655	1.695	1.810	1.825	1.785	1.675	1.675
.200	1.590	1.682	1.580	1.550	1.510	1.480	1.410	1.350	1.360	1.440	1.485	1.555	1.640	1.670	1.599	1.599
.250	1.360	1.379	1.335	1.285	1.270	1.250	1.210	1.170	1.150	1.230	1.260	1.300	1.380	1.510	1.525	1.525
.300	1.180	1.150	1.110	1.080	1.060	1.065	1.040	1.010	1.010	1.075	1.080	1.115	1.190	1.375	1.445	1.445
.350	1.017	.993	.946	.904	.912	.905	.862	.884	.865	.911	.927	.987	1.016	1.206	1.380	1.380
.400	.890	.870	.809	.770	.780	.775	.730	.775	.775	.820	.820	.850	.890	1.050	1.280	1.280
.450	.742	.717	.666	.614	.637	.635	.602	.609	.640	.686	.652	.722	.751	.881	1.170	1.170
.500	.610	.553	.515	.495	.510	.515	.530	.555	.565	.590	.590	.590	.600	.680	1.035	1.035
.550	.457	.439	.386	.369	.382	.375	.392	.444	.460	.451	.447	.447	.436	.471	.870	.870
.600	.325	.337	.300	.290	.310	.295	.325	.340	.380	.365	.365	.360	.345	.345	.675	.675
.700	.210	.274	.270	.250	.295	.285	.310	.340	.370	.370	.380	.375	.370	.335	.430	.430
.800	.215	.266	.290	.275	.310	.315	.335	.370	.400	.410	.405	.415	.430	.510	.450	.450
.850	.238	.277	.289	.286	.318	.335	.353	.391	.430	.439	.463	.498	.554	.649	.875	.875
.875	.242	.287	.306	.289	.332	.330	.327	.389	.410	.431	.447	.502	.536	.666	.900	.900

TABLE IIk.—EXPERIMENTAL LOAD DATA

[NACA 66,2-215 ($\alpha=0.6$) Section Angle of Attack, $\alpha_0=14^\circ$]

Station	Values of load parameter, $P=P_l-P_u$, for different Mach numbers														
	x/c	0.302	0.404	0.506	0.531	0.557	0.583	0.608	0.635	0.661	0.683	0.715	0.742	0.761	0.802
0	0	0	0	0	0	0	0	0	0	0	0	0	0	0	0
0.025	2.575	2.410	2.210	2.210	2.160	2.220	2.180	2.240	2.225	2.350	2.520	2.550	2.585	2.530	2.530
.050	2.390	2.195	1.990	1.970	1.920	1.940	1.905	1.935	1.885	1.940	1.975	2.130	2.310	2.330	2.330
.100	2.060	1.860	1.615	1.580	1.545	1.540	1.490	1.495	1.455	1.510	1.690	1.720	1.950	2.080	2.080
.150	1.800	1.580	1.410	1.360	1.350	1.310	1.290	1.270	1.240	1.295	1.435	1.500	1.660	1.880	1.880
.200	1.540	1.410	1.230	1.210	1.190	1.160	1.130	1.130	1.110	1.170	1.330	1.340	1.470	1.760	1.760
.250	1.330	1.220	1.065	1.055	1.040	1.020	.990	1.010	.990	1.030	1.185	1.195	1.270	1.580	1.580
.300	1.140	1.070	.930	.930	.930	.910	.880	.890	.890	.925	1.080	1.090	1.095	1.380	1.380
.350	.977	.939	.846	.824	.837	.805	.797	.819	.800	.826	.967	.962	.951	1.191	1.191
.400	.850	.825	.765	.750	.750	.730	.710	.725	.730	.755	.895	.895	.885	1.050	1.050
.450	.722	.714	.666	.669	.662	.650	.642	.649	.650	.676	.752	.787	.776	.910	.910
.500	.620	.600	.580	.580	.580	.560	.550	.550	.555	.580	.670	.685	.670	.780	.780
.550	.507	.494	.491	.489	.472	.460	.457	.479	.456	.471	.542	.552	.546	.611	.611
.600	.400	.416	.420	.410	.410	.390	.390	.390	.381	.400	.460	.460	.450	.500	.500
.700	.370	.400	.415	.410	.430	.420	.410	.410	.421	.430	.470	.465	.485	.500	.500
.800	.360	.380	.430	.425	.440	.440	.440	.450	.455	.480	.480	.510	.545	.590	.590
.850	.378	.396	.459	.451	.468	.460	.473	.471	.490	.499	.503	.548	.624	.779	.779
.875	.362	.374	.451	.459	.447	.450	.467	.494	.505	.501	.522	.552	.621	.791	.791

TABLE III.—EXPERIMENTAL LOAD DATA

[NACA 66,2-215 ($\alpha=0.6$) Section Angle of Attack, $\alpha_0=16^\circ$]

Station	Values of load parameter, $P=P_l-P_u$, for different Mach numbers													
	x/c	0.305	0.408	0.511	0.537	0.564	0.590	0.617	0.644	0.671	0.698	0.726	0.745	0.775
0	0	0	0	0	0	0	0	0	0	0	0	0	0	0
0.025	1.720	1.625	1.605	1.600	1.695	1.710	1.710	1.710	1.755	1.835	2.030	2.615	2.805	2.500
.050	1.540	1.455	1.435	1.433	1.530	1.530	1.530	1.570	1.650	1.780	2.130	2.465	2.465	1.955
.100	1.330	1.245	1.230	1.220	1.295	1.315	1.310	1.330	1.380	1.450	1.610	1.790	1.790	1.545
.150	1.200	1.130	1.080	1.095	1.150	1.140	1.155	1.175	1.200	1.290	1.385	1.555	1.555	1.400
.200	1.080	1.010	.990	.990	1.045	1.065	1.040	1.070	1.100	1.160	1.210	1.255	1.255	1.270
.250	.975	.920	.895	.895	.945	.945	.945	.970	.990	1.040	1.050	1.095	1.095	1.160
.300	.900	.840	.825	.830	.870	.875	.865	.890	.900	.960	.945	.980	.980	1.070
.350	.857	.784	.761	.764	.812	.810	.797	.809	.835	.846	.847	.842	.842	.986
.400	.765	.720	.690	.700	.730	.740	.730	.745	.765	.805	.810	.820	.820	.920
.450	.687	.649	.621	.624	.672	.680	.662	.679	.690	.696	.702	.702	.702	.836
.500	.620	.580	.540	.553	.570	.575	.574	.585	.605	.640	.630	.640	.640	.730
.550	.517	.489	.461	.474	.477	.485	.457	.474	.500	.506	.512	.522	.522	.641
.600	.470	.430	.400	.400	.420	.420	.415	.420	.440	.460	.450	.465	.465	.530
.700	.470	.445	.420	.413	.435	.440	.425	.450	.455	.490	.480	.500	.500	.570
.800	.360	.420	.410	.415	.445	.435	.450	.465	.490	.540	.540	.580	.580	.640
.850	.523	.431	.424	.431	.473	.465	.473	.491	.540	.579	.588	.618	.618	.679
.875	.437	.429	.426	.434	.482	.485	.482	.504	.550	.571	.607	.647	.647	.701

TABLE IIIa.—EXPERIMENTAL LOAD DATA

[NACA 23015 Section Angle of Attack, $\alpha_0 = -6^\circ$]

Station	Values of load parameter, $P = P_1 - P_u$, for different Mach numbers														
	x/c	0.300	0.400	0.500	0.550	0.601	0.626	0.651	0.677	0.703	0.730	0.757	0.779	0.810	0.839
0	0	0	0	0	0	0	0	0	0	0	0	0	0	0	0
0.025	-2.650	-2.810	-2.960	-3.060	-3.150	-3.000	-2.830	-2.690	-2.470	-2.260	-2.060	-1.900	-1.790	-1.660	-1.660
.050	-2.070	-2.230	-2.460	-2.620	-2.610	-2.585	-2.560	-2.430	-2.200	-2.010	-1.800	-1.630	-1.490	-1.380	-1.380
.100	-.960	-1.020	-1.030	-1.020	-1.535	-2.000	-1.910	-1.840	-1.660	-1.460	-1.240	-1.070	-.970	-.830	-.830
.150	-.720	-.760	-.780	-.820	-.760	-.910	-1.640	-1.560	-1.390	-1.170	-.980	-.785	-.670	-.540	-.540
.200	-.655	-.690	-.700	-.730	-.720	-.650	-1.140	-1.460	-1.300	-1.120	-.920	-.730	-.590	-.430	-.430
.250	-.565	-.590	-.590	-.610	-.630	-.585	-.500	-1.330	-1.240	-1.060	-.850	-.650	-.530	-.360	-.360
.300	-.490	-.510	-.520	-.530	-.540	-.510	-.440	-.680	-1.040	-.940	-.790	-.615	-.460	-.320	-.320
.350	-.421	-.431	-.434	-.450	-.456	-.442	-.392	-.419	-.748	-.738	-.619	-.464	-.310	-.217	-.217
.400	-.360	-.370	-.370	-.365	-.349	-.370	-.340	-.290	-.470	-.520	-.450	-.330	-.220	-.060	-.060
.450	-.304	-.301	-.299	-.299	-.274	-.272	-.260	-.229	-.288	-.408	-.354	-.284	-.165	-.078	-.078
.500	-.260	-.260	-.240	-.250	-.240	-.230	-.220	-.190	-.195	-.320	-.305	-.240	-.120	-.060	-.060
.550	-.213	-.201	-.194	-.209	-.184	-.176	-.165	-.129	-.138	-.218	-.226	-.192	-.110	-.050	-.050
.600	-.160	-.170	-.145	-.150	-.130	-.110	-.110	-.100	-.080	-.135	-.190	-.170	-.110	-.060	-.060
.700	-.110	-.100	-.065	-.060	-.051	-.050	-.040	-.030	-.010	-.050	-.110	-.140	-.140	-.100	-.100
.800	-.010	-.030	.020	.030	.019	-.020	.030	.020	.040	.020	.030	.070	.100	.310	.310
.850	-.037	-.029	.037	.042	.116	.047	.052	.051	.063	.042	.066	.049	.070	.263	.263
.900	.055	.063	.074	.068	.078	.069	.080	.069	.075	.068	.029	-.016	-.049	.137	.137

TABLE IIIb.—EXPERIMENTAL LOAD DATA

[NACA 23015 Section Angle of Attack, $\alpha_0 = -4^\circ$]

Station	Values of load parameter, $P = P_1 - P_u$, for different Mach numbers														
	x/c	0.300	0.400	0.500	0.550	0.600	0.626	0.651	0.676	0.701	0.727	0.753	0.779	0.806	0.835
0	0	0	0	0	0	0	0	0	0	0	0	0	0	0	0
0.025	-2.040	-2.080	-2.125	-2.220	-2.320	-2.420	-2.355	-2.240	-2.160	-2.040	-1.870	-1.710	-1.555	-1.440	-1.440
.050	-1.300	-1.355	-1.420	-1.550	-1.650	-1.760	-1.815	-1.900	-1.850	-1.740	-1.560	-1.420	-1.260	-1.130	-1.130
.100	-.570	-.530	-.540	-.560	-.540	-.500	-.930	-1.180	-1.220	-1.150	-.980	-.790	-.670	-.580	-.580
.150	-.350	-.380	-.380	-.410	-.415	-.410	-.370	-.400	-.915	-.890	-.710	-.500	-.385	-.280	-.280
.200	-.350	-.380	-.370	-.410	-.390	-.415	-.450	-.360	-.785	-.900	-.730	-.480	-.320	-.210	-.210
.250	-.310	-.320	-.330	-.350	-.350	-.360	-.400	-.390	-.565	-.870	-.770	-.540	-.310	-.220	-.220
.300	-.290	-.300	-.310	-.320	-.320	-.330	-.350	-.355	-.280	-.850	-.770	-.605	-.300	-.170	-.170
.350	-.240	-.258	-.259	-.273	-.268	-.286	-.285	-.309	-.258	-.443	-.791	-.644	-.310	-.161	-.161
.400	-.200	-.220	-.230	-.220	-.220	-.230	-.230	-.230	-.220	-.220	-.780	-.645	-.290	-.120	-.120
.450	-.178	-.166	-.179	-.178	-.173	-.176	-.165	-.164	-.168	-.103	-.434	-.589	-.223	-.027	-.027
.500	-.150	-.155	-.140	-.150	-.120	-.130	-.140	-.130	-.130	-.060	-.210	-.480	-.130	-.080	-.080
.550	-.113	-.111	-.114	-.103	-.093	-.091	-.100	-.104	-.100	-.048	-.081	-.272	-.188	-.223	-.223
.600	-.080	-.090	-.080	-.090	-.070	-.080	-.070	-.070	-.075	-.050	-.030	-.090	-.150	-.355	-.355
.700	-.060	-.070	-.055	-.050	-.040	-.040	-.030	-.040	-.040	-.040	-.020	-.030	-.050	-.440	-.440
.800	.020	-.020	-.010	-.010	-.010	.020	.030	.039	.020	.020	.040	.030	.030	.130	.130
.850	.017	.019	.021	.035	.047	.059	.058	.069	.032	.032	.059	.084	.040	.020	.020
.900	.037	.041	.044	.048	.063	.066	.075	.074	.048	.058	.069	.039	.071	.015	.015

TABLE IIIc.—EXPERIMENTAL LOAD DATA

[NACA 23015 Section Angle of Attack, $\alpha_0 = -2^\circ$]

Station	Values of load parameter, $P = P_1 - P_u$, for different Mach numbers														
	x/c	0.300	0.400	0.500	0.550	0.600	0.625	0.651	0.676	0.701	0.726	0.751	0.777	0.803	0.834
0	0	0	0	0	0	0	0	0	0	0	0	0	0	0	0
0.025	-1.085	-1.150	-1.280	-1.320	-1.350	-1.400	-1.440	-1.490	-1.515	-1.460	-1.420	-1.360	-1.285	-1.210	-1.210
.050	-.520	-.560	-.652	-.685	-.700	-.760	-.793	-.830	-.906	-.960	-1.045	-1.005	-.930	-.870	-.870
.100	-.030	-.050	-.070	-.050	-.070	-.080	-.080	-.085	-.135	-.260	-.265	-.320	-.305	-.270	-.270
.150	.040	-.035	.040	.062	.070	.050	.070	.090	.100	.140	.085	.035	0	.020	.020
.200	.022	-.030	.050	-.027	0	.040	-.030	-.030	-.060	-.030	.123	.130	.110	.095	.095
.250	-.020	-.030	-.060	-.037	-.050	-.070	-.060	-.070	-.100	-.155	-.062	.080	.105	.110	.110
.300	-.045	-.060	-.080	0	-.080	-.060	-.070	-.080	-.090	-.130	-.210	-.030	.100	.110	.110
.350	-.050	-.053	-.064	-.026	-.065	-.060	-.080	-.049	-.072	-.058	-.334	-.118	.045	.068	.068
.400	-.040	-.050	-.060	-.020	-.050	-.040	-.060	-.055	-.060	-.060	-.375	-.290	-.035	.035	.035
.450	-.028	-.019	-.037	-.023	-.048	-.026	-.051	-.064	-.058	-.048	-.159	-.464	-.125	.038	.038
.500	-.010	-.010	-.060	-.040	-.040	-.040	-.050	-.050	-.045	-.030	-.005	-.385	-.070	.055	.055
.550	-.010	.008	-.034	-.028	-.013	-.011	-.020	-.029	-.014	-.018	-.004	-.109	-.235	.078	.078
.600	-.015	.020	.020	-.020	.020	.020	.020	-.015	.010	-.005	.010	.055	-.255	.130	.130
.700	0	-.020	.030	-.015	.020	.010	-.010	-.020	0	-.010	0	.035	-.050	.105	.105
.800	0	-.015	.011	-.010	.020	.008	.010	0	0	0	.010	.020	-.030	.020	.020
.850	.012	.009	.021	.002	.046	.004	.010	.011	.022	.022	.001	.023	.035	.003	.003
.900	.023	.015	.009	.038	.025	.036	.011	.014	.028	.023	.014	.029	.042	-.003	-.003

TABLE III d.—EXPERIMENTAL LOAD DATA

[NACA 23015 Section Angle of Attack, $\alpha_0 = -0^\circ$]

Station x/c	Values of load parameter, $P = P_l - P_u$, for different Mach numbers													
	0.300	0.400	0.500	0.550	0.600	0.625	0.651	0.676	0.701	0.726	0.757	0.780	0.805	0.834
0	0	0	0	0	0	0	0	0	0	0	0	0	0	0
.025	-.260	-.280	-.320	-.355	-.390	-.420	-.450	-.510	-.560	-.600	-.660	-.750	-.850	-.875
.050	.165	.170	.160	.150	.130	.100	.075	.020	-.040	-.100	-.165	-.275	-.830	-.458
.100	.480	.520	.560	.590	.630	.640	.660	.630	.580	.530	.430	.295	.210	.130
.150	.450	.475	.525	.560	.610	.650	.710	.790	.790	.740	.640	.510	.425	.360
.200	.310	.340	.370	.400	.430	.450	.480	.565	.700	.740	.650	.520	.430	.360
.250	.250	.260	.290	.310	.320	.350	.360	.440	.605	.620	.640	.460	.360	.310
.300	.175	.200	.220	.250	.260	.260	.260	.180	.190	.620	.580	.400	.310	.280
.350	.152	.159	.146	.145	.142	.134	.125	.128	.062	.415	.611	.381	.210	.178
.400	.130	.110	.110	.110	.125	.130	.120	.120	.080	.050	.550	.440	.170	.090
.450	.082	.094	.098	.102	.117	.109	.101	.094	.061	-.048	.116	.548	.157	.038
.500	.070	.080	.075	.090	.080	.070	.070	.060	.040	-.020	-.020	.365	-.040	-.085
.550	.057	.069	.078	.087	.089	.069	.075	.066	.042	.022	-.019	.211	-.010	-.252
.600	.050	.050	.090	.100	.085	.100	.090	.100	.045	.060	.020	.080	.050	-.350
.700	.050	.060	.050	.070	.040	.040	.040	.040	.030	.020	-.020	-.045	.060	-.340
.800	.040	.030	.040	.030	.010	-.020	0	0	0	.010	-.020	-.065	.020	-.035
.850	.040	.024	.031	.021	-.001	-.003	-.020	-.029	-.033	-.028	-.059	-.059	-.025	-.002
.900	.012	.011	.014	-.002	-.007	-.010	-.025	-.026	-.032	-.042	-.073	-.041	-.040	-.003

TABLE III e.—EXPERIMENTAL LOAD DATA

[NACA 23015 Section Angle of Attack, $\alpha_0 = 2^\circ$]

Station x/c	Values of load parameter, $P = P_l - P_u$, for different Mach numbers													
	0.300	0.400	0.500	0.550	0.600	0.626	0.651	0.676	0.702	0.728	0.755	0.781	0.807	0.836
0	0	0	0	0	0	0	0	0	0	0	0	0	0	0
.025	.570	.595	.585	.565	.495	.440	.375	.300	.045	.200	-.105	.260	-.405	-.490
.050	.865	.915	.955	.970	.950	.890	.830	.715	.465	.640	.320	-.165	-.015	-.080
.100	1.065	1.065	1.185	1.280	1.410	1.395	1.340	1.210	.970	1.125	.820	-.650	.500	.400
.150	.855	.915	1.005	1.095	1.215	1.330	1.490	1.430	1.155	1.320	1.000	-.825	.675	.580
.200	.655	.700	.780	.850	.990	1.110	1.270	1.265	1.160	1.280	.990	-.800	.660	.565
.250	.540	.580	.620	.655	.630	.540	1.080	1.195	1.040	1.135	.875	-.685	.540	.495
.300	.435	.420	.435	.470	.505	.480	.415	.885	1.030	1.130	.860	-.650	.465	.420
.350	.317	.344	.376	.402	.417	.409	.340	.361	.746	.932	.796	-.604	.370	.318
.400	.280	.300	.315	.335	.340	.350	.320	.225	.615	.375	.580	-.450	.220	.200
.450	.244	.261	.276	.292	.292	.287	.265	.201	.222	.351	.408	-.316	.080	.048
.500	.210	.220	.225	.245	.230	.215	.220	.170	.195	.145	.285	-.230	.020	-.125
.550	.177	.189	.188	.204	.207	.209	.185	.141	.117	.104	.184	-.209	-.018	-.245
.600	.170	.160	.165	.180	.175	.160	.150	.120	.055	.080	.125	-.175	.020	-.325
.700	.120	.095	.095	.105	.110	.095	.085	.075	-.025	.055	.040	-.060	.135	-.440
.800	.055	.060	.060	.055	.050	.030	.030	.010	-.030	0	-.025	0	.065	-.390
.850	.059	.047	.036	.032	.015	.009	.005	-.009	-.018	-.054	-.035	-.019	-.042	-.222
.900	.043	.001	.004	-.015	-.019	-.030	-.025	-.021	-.032	-.062	-.051	-.038	-.033	-.006

TABLE III f.—EXPERIMENTAL LOAD DATA

[NACA 23015 Section angle of attack, $\alpha_0 = 4^\circ$]

Station x/c	Values of load parameter, $P = P_l - P_u$, for different Mach numbers													
	0.300	0.400	0.500	0.550	0.601	0.626	0.652	0.679	0.705	0.731	0.758	0.781	0.809	0.839
0	0	0	0	0	0	0	0	0	0	0	0	0	0	0
.025	1.475	1.510	1.505	1.440	1.270	1.130	.975	.770	.610	.435	.270	.130	-.025	-.110
.050	1.605	1.685	1.775	1.790	1.655	1.535	1.375	1.160	.990	.810	.660	.510	.360	.260
.100	1.550	1.660	1.825	2.010	2.040	1.895	1.730	1.540	1.375	1.190	1.040	.905	.740	.660
.150	1.280	1.370	1.515	1.660	1.915	1.860	1.795	1.560	1.420	1.230	1.105	.945	.860	.770
.200	1.040	1.125	1.260	1.330	1.810	1.720	1.625	1.450	1.300	1.105	.980	.860	.750	.690
.250	.785	.800	.850	.895	.850	1.360	1.470	1.255	1.105	.915	.820	.685	.590	.550
.300	.640	.680	.710	.735	.680	.795	1.050	.965	.880	.730	.645	.530	.460	.440
.350	.532	.569	.609	.619	.587	.564	.709	.736	.688	.584	.511	.376	.265	.271
.400	.465	.490	.515	.530	.505	.450	.510	.545	.530	.470	.415	.300	.150	.110
.450	.395	.417	.436	.452	.427	.382	.365	.396	.407	.382	.336	.251	.090	.008
.500	.335	.350	.360	.370	.350	.300	.275	.295	.310	.305	.280	.225	.070	-.065
.550	.287	.299	.310	.317	.287	.249	.200	.211	.232	.247	.236	.186	.050	-.142
.600	.250	.255	.265	.275	.245	.210	.160	.155	.180	.205	.205	.170	.050	-.175
.700	.160	.155	.160	.150	.140	.100	.050	.050	.080	.095	.120	.140	.100	-.240
.800	.070	.070	.075	.060	.040	.015	-.010	.010	.030	.050	.070	.110	.090	-.250
.850	.037	.034	.029	.030	.007	-.001	-.030	-.021	.017	.020	.046	.089	.070	-.267
.900	.003	.001	.006	.005	-.017	-.022	-.035	-.023	.013	.015	.029	.064	.038	-.260

TABLE IIIg.—EXPERIMENTAL LOAD DATA

[NACA 23015 Section Angle of Attack, $\alpha_0=6^\circ$]

Station	Values of load parameter, $P=P_l-P_u$, for different Mach numbers													
x/c	0.300	0.400	0.500	0.551	0.602	0.629	0.655	0.681	0.708	0.735	0.762	0.788	0.816	0.845
0	0	0	0	0	0	0	0	0	0	0	0	0	0	0
.025	2.350	2.410	2.420	2.220	1.820	1.620	1.380	1.120	.935	.790	.600	.450	.330	.250
.050	2.345	2.470	2.660	2.620	2.250	2.030	1.780	1.490	1.310	1.160	.980	.810	.680	.590
.100	2.100	2.240	2.495	2.760	2.420	2.185	1.900	1.630	1.440	1.340	1.170	1.060	.980	.902
.150	1.745	1.880	2.120	2.450	2.210	1.990	1.720	1.460	1.300	1.210	1.040	.960	.890	.960
.200	1.390	1.340	1.350	1.590	1.990	1.730	1.440	1.210	1.070	.985	.830	.740	.720	.840
.250	1.060	1.120	1.180	1.110	1.430	1.320	1.140	.980	.860	.760	.620	.560	.520	.710
.300	.900	.930	.980	.935	1.060	1.040	.940	.830	.730	.655	.515	.430	.390	.600
.350	.757	.804	.841	.799	.810	.809	.775	.701	.627	.552	.441	.352	.255	.428
.400	.650	.680	.730	.670	.630	.630	.630	.590	.550	.470	.390	.300	.170	.310
.450	.562	.579	.596	.582	.517	.502	.510	.496	.494	.429	.351	.271	.159	.238
.500	.480	.500	.510	.480	.410	.410	.420	.420	.410	.380	.320	.250	.120	.180
.550	.417	.419	.429	.402	.327	.321	.350	.361	.362	.355	.296	.228	.110	.118
.600	.360	.360	.340	.335	.260	.260	.290	.310	.315	.320	.295	.220	.110	.100
.700	.235	.225	.200	.180	.135	.140	.180	.210	.230	.230	.240	.190	.110	.030
.800	.135	.125	.080	.070	.040	.050	.100	.130	.155	.170	.190	.170	.110	-.030
.850	.070	.059	.015	.012	.015	.009	.060	.103	.115	.131	.166	.151	.110	-.032
.900	.033	.006	-.056	-.032	-.007	0	.015	.064	.086	.098	.134	.139	.110	-.023

TABLE IIIh.—EXPERIMENTAL LOAD DATA

[NACA 23015 Section Angle of Attack, $\alpha_0=8^\circ$]

Station	Values of load parameter, $P=P_l-P_u$, for different Mach numbers														
x/c	0.300	0.400	0.501	0.526	0.557	0.578	0.605	0.631	0.658	0.684	0.711	0.738	0.766	0.793	0.821
0	0	0	0	0	0	0	0	0	0	0	0	0	0	0	0
.025	3.280	3.448	3.230	3.060	2.765	2.400	2.120	1.880	1.650	1.460	1.240	1.105	.960	.770	.690
.050	3.110	3.334	3.660	3.490	3.180	2.810	2.490	2.250	2.020	1.810	1.600	1.455	1.320	1.110	1.040
.100	2.650	2.862	3.230	3.220	2.950	2.570	2.270	2.030	1.820	1.630	1.460	1.310	1.210	1.070	1.050
.150	2.270	2.454	3.010	3.090	2.830	2.370	1.960	1.750	1.520	1.380	1.240	1.120	1.050	.940	.910
.200	1.590	1.707	1.670	1.850	2.040	1.760	1.520	1.420	1.230	1.110	.970	.900	.810	.710	.710
.250	1.370	1.448	1.450	1.380	1.490	1.370	1.230	1.180	1.030	.950	.820	.730	.640	.550	.540
.300	1.150	1.143	1.190	1.150	1.140	1.090	1.030	1.010	.910	.840	.730	.640	.560	.440	.425
.350	.965	1.025	1.029	.969	.902	.877	.872	.869	.807	.733	.662	.562	.511	.373	.350
.400	.835	.902	.860	.830	.740	.710	.740	.750	.710	.650	.600	.520	.460	.330	.305
.450	.717	.733	.736	.689	.614	.595	.614	.649	.630	.593	.542	.472	.423	.321	.272
.500	.620	.632	.630	.580	.510	.490	.510	.560	.565	.540	.500	.450	.390	.300	.250
.550	.537	.551	.516	.478	.427	.395	.442	.478	.505	.483	.429	.429	.386	.283	.240
.600	.470	.460	.430	.410	.340	.330	.390	.420	.450	.440	.430	.410	.370	.280	.240
.700	.310	.316	.280	.250	.210	.220	.290	.290	.330	.350	.320	.350	.320	.250	.210
.800	.180	.160	.140	.110	.090	.120	.180	.200	.235	.250	.280	.280	.270	.230	.200
.850	.112	.119	.069	.052	.050	.094	.142	.159	.190	.211	.227	.242	.238	.221	.170
.900	.028	.009	-.018	-.021	-.009	.045	.073	.091	.105	.129	.138	.155	.159	.159	.130

TABLE IIIi.—EXPERIMENTAL LOAD DATA

[NACA 23015 Section Angle of Attack, $\alpha_0=10^\circ$]

Station	Values of load parameter, $P=P_l-P_u$, for different Mach numbers															
x/c	0.300	0.400	0.501	0.528	0.555	0.581	0.608	0.634	0.661	0.688	0.715	0.743	0.771	0.799	0.829	
0	0	0	0	0	0	0	0	0	0	0	0	0	0	0	0	
.025	4.060	4.322	3.690	3.295	2.880	2.570	2.345	2.110	1.910	1.710	1.540	1.420	1.270	1.145	.990	
.050	3.760	4.112	4.030	3.660	3.120	2.730	2.450	2.230	2.020	1.880	1.790	1.590	1.510	1.460	1.310	
.100	3.140	3.477	3.760	3.300	2.740	2.340	2.070	1.860	1.680	1.590	1.570	1.300	1.250	1.300	1.360	
.150	2.430	2.528	3.100	2.635	2.070	1.780	1.620	1.490	1.250	1.280	1.275	1.000	.950	1.120	1.300	
.200	1.910	2.039	1.835	1.810	1.620	1.445	1.360	1.250	1.140	1.060	1.020	.815	.795	.860	1.140	
.250	1.600	1.678	1.470	1.370	1.310	1.230	1.160	1.090	1.020	.935	.875	.710	.675	.710	.890	
.300	1.320	1.390	1.200	1.100	1.085	1.060	1.045	.990	.920	.850	.800	.640	.600	.630	.760	
.350	1.115	1.174	.996	.884	.930	.925	.932	.889	.847	.796	.642	.592	.560	.561	.665	
.400	.950	.994	.820	.730	.800	.810	.820	.820	.770	.740	.690	.555	.520	.520	.600	
.450	.827	.851	.683	.609	.702	.715	.742	.739	.720	.684	.649	.537	.507	.511	.563	
.500	.700	.719	.555	.510	.600	.620	.640	.660	.650	.625	.590	.500	.485	.490	.530	
.550	.599	.618	.456	.429	.532	.545	.587	.609	.600	.591	.562	.492	.471	.476	.510	
.600	.505	.517	.360	.350	.460	.490	.520	.560	.550	.550	.520	.490	.460	.470	.500	
.700	.320	.304	.210	.250	.340	.370	.410	.435	.440	.450	.440	.440	.430	.400	.440	
.800	.170	.160	.105	.175	.260	.270	.300	.330	.330	.360	.330	.380	.380	.370	.410	
.850	.127	.101	.091	.124	.202	.205	.246	.267	.275	.301	.282	.322	.351	.313	.377	
.900	.065	.042	.061	.101	.148	.155	.188	.211	.220	.229	.228	.268	.279	.269	.350	

TABLE IIIj.—EXPERIMENTAL LOAD DATA

[NACA 23015 Section Angle of Attack, $\alpha_0=12^\circ$]

Station	Values of load parameter, $P=P_t-P_u$, for different Mach numbers														
	x/c	0.300	0.401	0.504	0.530	0.557	0.583	0.609	0.636	0.663	0.691	0.719	0.746	0.775	0.806
0	0	0	0	0	0	0	0	0	0	0	0	0	0	0	0
.025	4.800	5.155	3.740	3.340	2.970	2.650	2.390	2.150	2.010	1.905	1.830	1.690	1.540	1.445	1.445
.050	4.355	4.770	3.900	3.310	2.920	2.560	2.270	2.010	1.850	1.790	1.785	1.860	1.645	1.610	1.610
.100	3.610	4.052	3.315	2.540	2.130	1.820	1.730	1.550	1.450	1.435	1.490	1.640	1.420	1.340	1.340
.150	2.720	2.868	2.180	1.900	1.620	1.440	1.390	1.270	1.190	1.155	1.205	1.280	1.160	1.110	1.110
.200	2.130	2.230	1.670	1.540	1.370	1.240	1.210	1.100	1.020	.990	1.010	1.050	.950	.930	.930
.250	1.780	1.839	1.330	1.300	1.180	1.070	1.060	.970	.900	.890	.930	.920	.835	.805	.805
.300	1.460	1.523	1.115	1.130	1.070	.980	.960	.890	.835	.810	.860	.850	.760	.730	.730
.350	1.227	1.242	.951	.982	.959	.900	.882	.829	.778	.761	.802	.802	.706	.678	.678
.400	1.030	1.034	.810	.880	.875	.840	.805	.770	.730	.715	.760	.760	.660	.630	.630
.450	.877	.861	.696	.789	.792	.775	.747	.729	.695	.679	.727	.724	.638	.591	.591
.500	.740	.730	.600	.710	.720	.710	.700	.680	.640	.630	.695	.685	.620	.580	.580
.550	.617	.598	.536	.639	.662	.655	.667	.641	.630	.608	.659	.662	.596	.560	.560
.600	.510	.485	.500	.580	.600	.625	.610	.610	.600	.585	.615	.620	.575	.535	.535
.700	.300	.293	.395	.450	.470	.500	.510	.520	.520	.505	.520	.525	.515	.500	.500
.800	.150	.161	.300	.350	.370	.410	.400	.415	.430	.415	.410	.420	.450	.480	.480
.850	.089	.127	.256	.279	.302	.355	.332	.349	.378	.358	.351	.359	.393	.454	.454
.900	.073	.087	.204	.221	.238	.285	.273	.281	.303	.284	.288	.298	.341	.409	.409

TABLE IIIk.—EXPERIMENTAL LOAD DATA

[NACA 23015 Section Angle of Attack, $\alpha_0=14^\circ$]

Station	Values of load parameter, $P=P_t-P_u$, for different Mach numbers														
	x/c	0.301	0.402	0.506	0.532	0.560	0.586	0.613	0.640	0.668	0.695	0.724	0.752	0.778	0.809
0	0	0	0	0	0	0	0	0	0	0	0	0	0	0	0
.025	5.095	5.086	3.735	3.180	2.845	2.540	2.365	2.115	1.960	1.895	1.925	1.920	1.815	1.690	1.690
.050	4.620	4.701	3.395	2.940	2.610	2.325	2.140	1.900	1.740	1.660	1.700	1.880	2.080	1.730	1.730
.100	3.470	3.241	2.350	2.055	1.900	1.760	1.635	1.470	1.365	1.325	1.360	1.610	1.895	1.500	1.500
.150	2.775	2.460	1.780	1.645	1.550	1.470	1.360	1.250	1.160	1.130	1.150	1.290	1.475	1.320	1.320
.200	2.105	1.871	1.480	1.445	1.395	1.275	1.210	1.090	.995	.970	.975	1.080	1.180	1.140	1.140
.250	1.650	1.383	1.260	1.250	1.195	1.130	1.055	.975	.890	.860	.875	.970	1.025	1.020	1.020
.300	1.305	1.094	1.125	1.130	1.100	1.030	.960	.885	.810	.780	.805	.890	.945	.940	.940
.350	1.027	.903	1.011	1.014	.997	.945	.887	.826	.759	.730	.742	.832	.886	.876	.876
.400	.830	.769	.920	.930	.905	.880	.830	.770	.705	.685	.690	.780	.840	.835	.835
.450	.692	.689	.831	.849	.834	.815	.767	.729	.670	.651	.652	.742	.803	.798	.798
.500	.595	.618	.750	.780	.780	.745	.720	.690	.640	.615	.630	.695	.770	.760	.760
.550	.529	.584	.694	.729	.727	.715	.697	.669	.620	.601	.607	.667	.740	.740	.740
.600	.490	.563	.650	.670	.675	.680	.670	.645	.620	.590	.575	.640	.715	.720	.720
.700	.415	.488	.540	.560	.570	.570	.580	.575	.565	.525	.530	.550	.640	.665	.665
.800	.330	.414	.435	.450	.440	.465	.465	.480	.485	.465	.460	.455	.535	.625	.625
.850	.277	.355	.369	.389	.382	.407	.424	.421	.430	.441	.412	.407	.473	.591	.591
.900	.239	.282	.294	.301	.311	.320	.333	.341	.357	.359	.353	.338	.401	.549	.549

TABLE IIIl.—EXPERIMENTAL LOAD DATA

[NACA 23015 Section Angle of Attack, $\alpha_0=16^\circ$]

Station	Values of load parameter, $P=P_t-P_u$, for different Mach numbers													
	x/c	0.303	0.405	0.508	0.535	0.563	0.589	0.616	0.643	0.670	0.698	0.725	0.755	0.782
0	0	0	0	0	0	0	0	0	0	0	0	0	0	0
.025	4.770	4.799	3.400	2.700	2.520	2.245	2.060	1.970	1.870	1.860	1.850	1.905	2.025	2.025
.050	4.315	4.397	3.095	2.510	2.280	2.055	1.900	1.800	1.720	1.670	1.650	1.685	1.795	1.795
.100	3.040	2.730	2.015	1.805	1.720	1.540	1.460	1.450	1.400	1.415	1.395	1.420	1.565	1.565
.150	2.230	1.954	1.645	1.570	1.470	1.310	1.260	1.260	1.220	1.215	1.200	1.225	1.375	1.375
.200	1.560	1.368	1.420	1.385	1.305	1.160	1.120	1.105	1.060	1.060	1.045	1.090	1.195	1.195
.250	1.175	1.024	1.270	1.260	1.165	1.055	.990	1.005	.950	.955	.940	.980	1.090	1.090
.300	.920	.850	1.170	1.150	1.100	.975	.915	.870	.870	.870	.860	.895	.995	.995
.350	.789	.750	1.078	1.059	1.022	.910	.867	.879	.818	.816	.810	.842	.936	.936
.400	.710	.701	1.000	.995	.970	.860	.815	.825	.760	.770	.755	.790	.880	.880
.450	.670	.674	.929	.926	.902	.818	.790	.807	.735	.739	.732	.744	.838	.838
.500	.630	.632	.860	.860	.850	.775	.750	.770	.700	.705	.680	.700	.805	.805
.550	.607	.604	.814	.819	.817	.760	.737	.757	.697	.684	.665	.682	.776	.776
.600	.590	.603	.760	.790	.785	.740	.710	.740	.670	.665	.640	.665	.760	.760
.700	.550	.546	.635	.675	.690	.680	.660	.685	.605	.590	.575	.600	.680	.680
.800	.470	.460	.515	.530	.575	.570	.570	.600	.530	.535	.505	.535	.625	.625
.850	.407	.399	.436	.464	.505	.480	.497	.519	.470	.476	.472	.499	.601	.601
.900	.338	.332	.347	.371	.411	.407	.410	.421	.390	.394	.400	.448	.546	.546

TABLE IVa.—EXPERIMENTAL LOAD DATA

[NACA 0015 Section Angle of Attack, $\alpha_0=0^\circ$]

Station	Values of load parameter, $P=P_l-P_u$ for different Mach numbers											
x/c	0.400	0.550	0.600	0.625	0.650	0.675	0.701	0.726	0.751	0.777	0.805	0.837
0	0	0	0	0	0	0	0	0	0	0	0	0
.025	-.060	-.065	-.070	-.060	-.060	-.080	-.050	-.050	-.050	-.035	-.030	-.000
.050	-.010	-.010	-.020	-.000	-.015	-.010	-.015	-.065	-.020	-.035	-.055	-.075
.100	-.005	-.055	-.090	-.085	-.095	-.110	-.145	-.110	-.085	-.055	-.065	-.050
.150	-.020	-.025	-.045	-.065	-.065	-.065	-.080	-.080	-.085	-.065	-.275	-.065
.200	-.015	-.030	-.025	-.020	-.025	-.025	-.030	-.030	-.025	-.030	-.020	-.010
.250	-.000	-.020	-.080	-.015	-.025	-.025	-.035	-.035	-.055	-.000	-.015	-.015
.300	-.010	-.035	-.025	-.025	-.040	-.040	-.045	-.055	-.075	-.030	-.000	-.015
.350	-.015	-.030	-.035	-.025	-.055	-.040	-.040	-.065	-.090	-.075	-.015	-.010
.400	-.020	-.020	-.030	-.025	-.015	-.020	-.020	-.015	-.135	-.035	-.010	-.000
.450	-.030	-.035	-.030	-.025	-.035	-.025	-.035	-.090	-.010	-.185	-.015	-.015
.500	-.005	-.015	-.005	-.010	-.015	-.010	-.000	-.000	-.005	-.105	-.010	-.010
.550	-.000	-.000	-.000	-.010	-.000	-.000	-.000	-.000	-.010	-.015	-.065	-.025
.600	-.005	-.000	-.000	-.015	-.000	-.000	-.000	-.060	-.010	-.025	-.075	-.030
.700	-.090	-.000	-.000	-.000	-.000	-.000	-.000	-.010	-.010	-.000	-.070	-.040
.800	-.090	-.000	-.000	-.000	-.000	-.000	-.010	-.000	-.090	-.015	-.010	-.020
.900	-.010	-.030	-.030	-.055	-.020	-.025	-.020	-.020	-.030	-.020	-.230	-.335

TABLE IVb.—EXPERIMENTAL LOAD DATA

[NACA 0015 Section Angle of Attack $\alpha_0=-2^\circ$]

Station	Values of load parameter, $P=P_l-P_u$ for different Mach numbers													
x/c	0.300	0.400	0.500	0.550	0.600	0.625	0.651	0.676	0.701	0.726	0.752	0.779	0.806	0.835
0	0	0	0	0	0	0	0	0	0	0	0	0	0	0
.025	-.860	-.905	-.910	-.935	-.910	-.915	-.900	-.840	-.795	-.700	-.695	-.470	-.410	-.295
.050	-.695	-.730	-.770	-.825	-.820	-.850	-.845	-.775	-.715	-.635	-.515	-.380	-.320	-.210
.100	-.545	-.580	-.610	-.695	-.725	-.745	-.810	-.905	-.820	-.715	-.610	-.455	-.405	-.280
.150	-.415	-.450	-.470	-.540	-.545	-.600	-.650	-.800	-.815	-.730	-.610	-.435	-.360	-.265
.200	-.345	-.370	-.390	-.415	-.435	-.450	-.480	-.590	-.800	-.745	-.620	-.400	-.310	-.230
.250	-.290	-.310	-.330	-.340	-.375	-.400	-.425	-.475	-.670	-.785	-.675	-.420	-.315	-.225
.300	-.245	-.250	-.265	-.240	-.275	-.290	-.300	-.285	-.505	-.705	-.700	-.440	-.275	-.180
.350	-.225	-.210	-.215	-.220	-.230	-.250	-.245	-.240	-.190	-.690	-.695	-.490	-.295	-.185
.400	-.180	-.165	-.175	-.190	-.190	-.200	-.200	-.200	-.150	-.230	-.695	-.500	-.305	-.145
.450	-.150	-.175	-.195	-.185	-.185	-.195	-.195	-.195	-.150	-.095	-.370	-.605	-.280	-.190
.500	-.100	-.110	-.115	-.130	-.150	-.140	-.135	-.130	-.105	-.040	-.135	-.400	-.145	-.045
.550	-.100	-.090	-.090	-.090	-.105	-.105	-.100	-.095	-.090	-.045	-.045	-.235	-.240	-.195
.600	-.075	-.070	-.085	-.085	-.090	-.100	-.105	-.100	-.085	-.050	-.010	-.105	-.190	-.335
.700	-.065	-.065	-.065	-.050	-.060	-.065	-.065	-.045	-.050	-.005	-.030	-.040	-.020	-.430
.800	-.035	-.025	-.025	-.015	-.010	-.010	-.000	-.000	-.015	-.015	-.040	-.080	-.060	-.080
.900	-.020	-.005	-.005	-.030	-.050	-.050	-.020	-.055	-.055	-.050	-.070	-.070	-.060	-.085

TABLE IVc.—EXPERIMENTAL LOAD DATA

[NACA 0015 Section Angle of Attack, $\alpha_0=-4^\circ$]

Station	Values of load parameter, $P=P_l-P_u$ for different Mach numbers													
x/c	0.300	0.400	0.500	0.550	0.600	0.625	0.651	0.676	0.702	0.729	0.755	0.782	0.805	0.837
0	0	0	0	0	0	0	0	0	0	0	0	0	0	0
.025	-1.695	-1.760	-1.760	-1.865	-1.840	-1.765	-1.660	-1.540	-1.415	-1.195	-1.025	-.840	-.668	-.620
.050	-1.415	-1.240	-1.593	-1.660	-1.610	-1.610	-1.515	-1.410	-1.275	-1.065	-.920	-.725	-.722	-.515
.100	-1.080	-1.135	-1.157	-1.725	-1.650	-1.620	-1.570	-1.510	-1.420	-1.160	-.995	-.790	-.643	-.595
.150	-.830	-.875	-.930	-1.030	-1.170	-1.380	-1.515	-1.470	-1.370	-1.145	-.995	-.760	-.579	-.555
.200	-.680	-.730	-.761	-.790	-.765	-.825	-1.360	-1.305	-1.280	-1.100	-.940	-.705	-.569	-.475
.250	-.580	-.575	-.589	-.640	-.680	-.630	-.880	-1.255	-1.195	-1.030	-.885	-.660	-.485	-.460
.300	-.420	-.425	-.494	-.500	-.535	-.520	-.455	-.935	-1.160	-.980	-.810	-.600	-.405	-.420
.350	-.395	-.410	-.420	-.450	-.480	-.465	-.415	-.465	-.735	-.760	-.620	-.475	-.331	-.400
.400	-.335	-.350	-.351	-.385	-.405	-.400	-.350	-.300	-.480	-.530	-.450	-.345	-.183	-.280
.450	-.310	-.315	-.292	-.330	-.340	-.335	-.320	-.265	-.285	-.385	-.365	-.285	-.020	-.175
.500	-.240	-.245	-.257	-.270	-.250	-.245	-.240	-.195	-.190	-.260	-.260	-.195	-.040	-.060
.550	-.160	-.200	-.218	-.185	-.195	-.195	-.190	-.145	-.115	-.155	-.185	-.170	-.084	-.215
.600	-.170	-.175	-.169	-.170	-.150	-.145	-.150	-.130	-.080	-.095	-.120	-.130	-.001	-.315
.700	-.100	-.095	-.099	-.100	-.085	-.080	-.080	-.075	-.040	-.020	-.045	-.100	-.109	-.385
.800	-.045	-.050	-.039	-.040	-.040	-.020	-.035	-.015	-.020	-.040	-.015	-.035	-.049	-.325
.900	-.005	-.052	-.035	-.040	-.055	-.065	-.050	-.050	-.050	-.050	-.035	-.015	-.039	-.060

TABLE IVd.—EXPERIMENTAL LOAD DATA

[NACA 0015 Section Angle of Attack, $\alpha_0 = -6^\circ$]

Station <i>x/c</i>	Values of load parameter, $P = P_t - P_u$, for different Mach numbers													
	0.300	0.400	0.500	0.550	0.601	0.626	0.652	0.678	0.704	0.731	0.757	0.784	0.811	0.839
0	0	0	0	0	0	0	0	0	0	0	0	0	0	0
.025	-2.540	-2.670	-2.825	-2.910	-2.700	-2.540	-2.265	-2.020	-1.775	-1.565	-1.430	-1.220	-1.060	-0.935
.050	-2.075	-2.219	-2.410	-2.490	-2.400	-2.280	-2.025	-1.780	-1.530	-1.350	-1.220	-1.035	-900	-780
.100	-1.580	-1.650	-1.740	-1.755	-2.335	-2.060	-1.835	-1.655	-1.420	-1.290	-1.205	-1.040	-945	-835
.150	-1.245	-1.295	-1.340	-1.290	-2.005	-1.920	-1.735	-1.545	-1.340	-1.220	-1.165	-990	-870	-765
.200	-.950	-.995	-1.085	-1.100	-1.560	-1.840	-1.655	-1.480	-1.210	-1.100	-1.030	-845	-755	-685
.250	-.815	-.860	-.910	-.935	-.850	-1.180	-1.275	-1.125	-.960	-.960	-.890	-760	-640	-590
.300	-.650	-.680	-.750	-.750	-.690	-.790	-.950	-.910	-.775	-.730	-.720	-585	-505	-485
.350	-.595	-.615	-.640	-.650	-.600	-.585	-.700	-.720	-.630	-.580	-.540	-430	-325	-320
.400	-.500	-.520	-.550	-.550	-.520	-.475	-.510	-.550	-.500	-.485	-.440	-330	-200	-170
.450	-.435	-.460	-.455	-.485	-.460	-.405	-.390	-.425	-.420	-.400	-.360	-280	-150	-.095
.500	-.360	-.365	-.375	-.380	-.350	-.315	-.275	-.320	-.335	-.315	-.290	-220	-.090	.020
.550	-.210	-.140	-.290	-.300	-.280	-.255	-.195	-.230	-.260	-.255	-.270	-200	-.080	.070
.600	-.250	-.250	-.225	-.245	-.225	-.190	-.150	-.165	-.210	-.210	-.220	-180	-.095	.125
.700	-.160	-.155	-.135	-.140	-.115	-.110	-.070	-.065	-.110	-.125	-.160	-140	-.120	.175
.800	-.060	-.060	-.045	-.040	-.035	-.025	-.010	0	-.030	-.055	-.110	-115	-.140	.190
.900	.020	.020	.045	.045	.045	.045	.045	.068	.010	-.010	-.060	-.045	-.080	.200

TABLE IVe.—EXPERIMENTAL LOAD DATA

[NACA 0015 Section Angle of Attack, $\alpha_0 = -8^\circ$]

Station <i>x/c</i>	Values of load parameter, $P = P_t - P_u$, for different Mach numbers														
	0.300	0.400	0.500	0.526	0.551	0.576	0.602	0.629	0.655	0.682	0.708	0.735	0.762	0.789	0.817
0	0	0	0	0	0	0	0	0	0	0	0	0	0	0	0
.025	-3.450	-3.686	-4.025	-3.985	-3.705	-3.425	-3.065	-2.790	-2.515	-2.285	-2.065	-1.895	-1.745	-1.570	-1.425
.050	-2.850	-3.042	-3.390	-3.520	-3.405	-3.160	-2.835	-2.555	-2.280	-2.050	-1.850	-1.670	-1.530	-1.345	-1.210
.100	-2.115	-2.300	-2.350	-2.455	-2.790	-2.895	-2.555	-2.300	-2.020	-1.825	-1.640	-1.520	-1.390	-1.270	-1.165
.150	-1.620	-1.723	-1.745	-1.675	-1.885	-2.425	-2.230	-2.000	-1.730	-1.585	-1.420	-1.340	-1.245	-1.150	-1.060
.200	-1.320	-1.376	-1.410	-1.390	-1.300	-1.470	-1.510	-1.410	-1.305	-1.240	-1.165	-1.120	-1.105	-1.000	-.920
.250	-1.110	-1.156	-1.180	-1.165	-1.110	-1.085	-1.100	-1.060	-1.035	-.950	-.880	-.875	-.840	-.800	-.785
.300	-.900	-.943	-.970	-.965	-.910	-.885	-.855	-.830	-.840	-.730	-.700	-.670	-.590	-.560	-.565
.350	-.810	-.822	-.840	-.830	-.770	-.725	-.680	-.665	-.680	-.625	-.590	-.560	-.480	-.430	-.395
.400	-.690	-.695	-.705	-.695	-.650	-.610	-.555	-.545	-.555	-.530	-.505	-.480	-.420	-.370	-.305
.450	-.590	-.595	-.605	-.600	-.555	-.510	-.455	-.460	-.480	-.480	-.460	-.460	-.395	-.335	-.265
.500	-.490	-.496	-.485	-.480	-.440	-.395	-.360	-.370	-.385	-.405	-.405	-.375	-.345	-.285	-.210
.550	-.420	-.397	-.405	-.390	-.350	-.315	-.275	-.300	-.325	-.355	-.345	-.340	-.320	-.265	-.185
.600	-.340	-.340	-.330	-.315	-.280	-.250	-.225	-.240	-.270	-.300	-.305	-.320	-.295	-.250	-.200
.700	-.235	-.212	-.190	-.170	-.150	-.140	-.130	-.150	-.175	-.220	-.230	-.255	-.250	-.235	-.180
.800	-.120	-.085	-.070	-.060	-.055	-.045	-.045	-.080	-.100	-.140	-.155	-.180	-.200	-.190	-.170
.900	-.080	.035	.005	.005	.005	.000	.005	-.035	-.035	-.075	-.080	-.090	-.115	-.125	-.125

TABLE IVf.—EXPERIMENTAL LOAD DATA

[NACA 0015 Section Angle of Attack, $\alpha_0 = -10^\circ$]

Station <i>x/c</i>	Values of load parameter, $P = P_t - P_u$, for different Mach numbers														
	0.300	0.400	0.501	0.527	0.553	0.580	0.606	0.633	0.659	0.685	0.712	0.739	0.766	0.794	0.824
0	0	0	0	0	0	0	0	0	0	0	0	0	0	0	0
.025	-4.280	-4.530	-4.550	-4.210	-3.745	-3.510	-3.170	-2.970	-2.745	-2.565	-2.385	-2.180	-2.035	-1.860	-1.730
.050	-3.290	-3.460	-4.065	-3.755	-3.330	-3.080	-2.775	-2.600	-2.415	-2.280	-2.140	-1.960	-1.760	-1.650	-1.530
.100	-2.425	-2.595	-2.599	-2.821	-2.568	-2.320	-2.118	-2.066	-1.905	-1.859	-1.813	-1.678	-1.474	-1.494	-1.395
.150	-1.975	-2.035	-1.870	-1.860	-1.760	-1.705	-1.620	-1.545	-1.450	-1.465	-1.425	-1.370	-1.195	-1.295	-1.250
.200	-1.595	-1.624	-1.505	-1.425	-1.325	-1.290	-1.245	-1.185	-1.105	-1.115	-1.075	-1.035	-.945	-.990	-1.085
.250	-1.350	-1.361	-1.250	-1.175	-1.080	-1.040	-1.000	-.970	-.910	-.900	-.845	-.780	-.745	-.765	-.855
.300	-1.110	-1.134	-1.020	-.960	-.885	-.860	-.840	-.820	-.770	-.765	-.710	-.635	-.620	-.540	-.565
.350	-.965	-.985	-.860	-.800	-.740	-.735	-.705	-.725	-.675	-.680	-.635	-.555	-.560	-.455	-.440
.400	-.815	-.816	-.720	-.675	-.630	-.630	-.605	-.630	-.600	-.605	-.575	-.520	-.525	-.415	-.390
.450	-.290	-.694	-.595	-.560	-.550	-.540	-.560	-.550	-.565	-.565	-.540	-.510	-.505	-.370	-.380
.500	-.585	-.560	-.470	-.445	-.440	-.450	-.450	-.475	-.480	-.475	-.480	-.455	-.450	-.345	-.315
.550	-.490	-.454	-.360	-.370	-.400	-.400	-.430	-.430	-.440	-.445	-.450	-.425	-.400	-.350	-.300
.600	-.400	-.376	-.285	-.290	-.325	-.335	-.350	-.380	-.390	-.405	-.415	-.415	-.360	-.340	-.290
.700	-.250	-.213	-.155	-.165	-.225	-.250	-.270	-.300	-.320	-.320	-.340	-.350	-.340	-.300	-.270
.800	-.130	-.113	-.065	-.100	-.140	-.180	-.190	-.215	-.240	-.250	-.270	-.290	-.300	-.300	-.270
.900	-.020	-.030	-.016	-.034	-.062	-.095	-.087	-.114	-.130	-.141	-.157	-.182	-.216	-.221	-.215

TABLE IVg.—EXPERIMENTAL LOAD DATA

[NACA 0015 Section Angle of Attack, $\alpha_0 = -12^\circ$]

Station	Values of load parameter, $P = P_1 - P_\infty$, for different Mach numbers														
	0.300	0.401	0.504	0.530	0.557	0.583	0.609	0.635	0.662	0.689	0.713	0.743	0.771	0.800	0.832
0	0	0	0	0	0	0	0	0	0	0	0	0	0	0	0
.025	-5.420	-5.141	-3.940	-3.540	-3.270	-3.100	-2.840	-2.730	-2.605	-2.460	-2.110	-2.230	-2.230	-2.040	-1.970
.050	-3.670	-3.686	-3.380	-3.000	-2.800	-2.670	-2.520	-2.380	-2.260	-2.115	-1.760	-1.970	-2.000	-1.780	-1.780
.100	-2.730	-2.673	-2.185	-1.980	-1.870	-1.860	-1.850	-1.850	-1.780	-1.335	-1.335	-1.580	-1.715	-1.480	-1.607
.150	-2.180	-2.125	-1.600	-1.475	-1.370	-1.380	-1.465	-1.480	-1.435	-1.360	-1.060	-1.300	-1.415	-1.220	-1.470
.200	-1.760	-1.668	-1.280	-1.180	-1.120	-1.125	-1.235	-1.250	-1.225	-1.180	-930	-1.100	-1.000	-1.045	-1.325
.250	-1.475	-1.355	-1.080	-1.010	-970	-980	-1.070	-1.100	-1.090	-1.050	-840	-960	-775	-900	-1.160
.300	-1.205	-1.112	-900	-880	-850	-860	-930	-970	-970	-955	-770	-830	-685	-750	-950
.350	-1.030	-884	-775	-760	-765	-760	-820	-840	-850	-850	-725	-715	-630	-640	-810
.400	-870	-713	-660	-690	-690	-685	-720	-740	-755	-770	-685	-640	-585	-605	-740
.450	-760	-599	-600	-620	-640	-685	-645	-640	-675	-690	-640	-570	-555	-590	-695
.500	-585	-463	-520	-550	-570	-550	-560	-540	-580	-580	-590	-525	-515	-515	-615
.550	-460	-513	-460	-495	-510	-490	-475	-450	-475	-495	-565	-500	-490	-510	-590
.600	-375	-535	-410	-435	-475	-455	-420	-390	-400	-420	-520	-470	-470	-490	-575
.700	-230	-585	-320	-355	-375	-375	-325	-310	-310	-315	-450	-410	-420	-455	-540
.800	-130	-599	-255	-280	-310	-285	-230	-210	-205	-205	-340	-340	-400	-400	-510
.900	-055	-146	-140	-165	-180	-175	-120	-105	-105	-100	-215	-235	-260	-303	-437

TABLE Va.—EXPERIMENTAL LOAD DATA

[NACA 4415 Section Angle of Attack, $\alpha_0 = -6^\circ$]

Station	Values of load parameter, $P = P_1 - P_\infty$, for different Mach numbers													
	0.302	0.401	0.500	0.554	0.603	0.628	0.649	0.681	0.706	0.734	0.759	0.793	0.830	
0	0	0	0	0	0	0	0	0	0	0	0	0	0	
.025	-2.941	-3.100	-3.419	-3.450	-2.979	-2.755	-2.608	-2.359	-2.279	-2.095	-1.964	-1.849	-1.838	
.050	-2.210	-2.405	-2.782	-2.955	-2.578	-2.380	-2.240	-2.025	-1.979	-1.850	-1.880	-1.759	-1.762	
.100	-1.190	-1.290	-1.364	-1.389	-1.638	-1.548	-1.449	-1.368	-1.341	-1.297	-1.258	-1.300	-1.396	
.150	-680	-736	-765	-741	-814	-834	-802	-749	-721	-686	-680	-809	-945	
.200	-351	-372	-374	-359	-395	-445	-430	-420	-372	-349	-353	-440	-573	
.250	-102	-106	-90	-979	-981	-138	-149	-134	-95	-952	-960	-169	-262	
.300	.029	.018	.044	.052	.070	.024	.018	.030	.070	.139	.121	.002	-119	
.350	.105	.117	.143	.166	.198	.170	.165	.189	.222	.293	.305	.180	.040	
.400	.170	.187	.222	.251	.275	.260	.262	.285	.306	.421	.459	.315	.169	
.450	.232	.259	.299	.326	.352	.358	.362	.380	.406	.549	.629	.469	.303	
.500	.227	.244	.275	.289	.335	.339	.359	.363	.390	.499	.650	.500	.353	
.550	.242	.245	.299	.330	.362	.360	.375	.400	.415	.502	.775	.609	.420	
.600	.259	.271	.288	.299	.329	.370	.378	.404	.414	.440	.795	.685	.490	
.700	.275	.275	.299	.323	.370	.362	.375	.379	.385	.364	.438	.732	.565	
.800	.230	.238	.242	.260	.309	.298	.298	.299	.295	.279	.220	.284	.220	
.875	.180	.187	.180	.209	.213	.215	.215	.224	.218	.206	.169	.178	.128	
.900	.155	.160	.154	.200	.199	.199	.191	.205	.200	.190	.164	.148	.113	

TABLE Vb.—EXPERIMENTAL LOAD DATA

(NACA 4415 Section Angle of Attack $\alpha_0 = -4^\circ$)

Station	Values of load parameter $P = P_1 - P_\infty$ for different Mach numbers													
	0.301	0.401	0.499	0.551	0.601	0.627	0.651	0.677	0.701	0.730	0.757	0.787	0.820	0.858
0	0	0	0	0	0	0	0	0	0	0	0	0	0	0
.025	-2.110	-2.215	-2.420	-2.560	-2.550	-2.475	-2.310	-2.170	-2.020	-1.900	-1.780	-1.730	-1.610	-1.450
.050	-1.520	-1.615	-1.776	-1.910	-2.080	-2.240	-2.190	-2.050	-1.910	-1.825	-1.690	-1.640	-1.595	-1.580
.100	-830	-941	-995	-995	-1.040	-1.560	-1.595	-1.485	-1.355	-1.285	-1.190	-1.235	-1.295	-1.325
.150	-330	-360	-402	-415	-415	-390	-530	-725	-765	-785	-775	-895	-1.015	-1.110
.200	-060	-065	-088	-100	.035	-060	-050	-155	-295	-320	-350	-510	-725	-955
.250	.130	.145	.159	.175	.190	.215	.260	.240	.130	.095	.030	-135	-370	-755
.300	.225	.235	.253	.280	.335	.340	.385	.405	.385	.365	.275	.085	-140	-630
.350	.285	.300	.341	.350	.380	.410	.460	.485	.520	.600	.445	.300	.060	-490
.400	.315	.335	.380	.395	.410	.455	.485	.550	.585	.705	.690	.460	.240	-375
.450	.340	.395	.424	.450	.435	.495	.540	.590	.635	.750	.865	.635	.410	-260
.500	.339	.360	.390	.420	.445	.460	.500	.510	.590	.665	.925	.690	.480	-230
.550	.345	.365	.385	.415	.460	.450	.485	.530	.585	.595	.970	.780	.590	-140
.600	.345	.350	.385	.415	.440	.435	.475	.500	.530	.500	.905	.800	.625	-065
.700	.310	.320	.341	.360	.375	.385	.395	.405	.445	.445	.390	.495	.415	.055
.800	.250	.250	.270	.270	.290	.285	.305	.315	.330	.335	.290	.280	.290	-055
.875	.195	.195	.198	.190	.210	.225	.235	.235	.235	.250	.205	.175	.180	-100
.900	.280	.170	.176	.165	.180	.190	.210	.205	.200	.215	.175	.155	.170	-055

TABLE Vc.—EXPERIMENTAL LOAD DATA

NACA 4415 Section Angle of Attack $\alpha_0 = -2^\circ$

Station x/c	Values of load parameter $P = P_l - P_u$ for different Mach numbers													
	0.305	0.402	0.502	0.554	0.601	0.626	0.652	0.677	0.701	0.728	0.756	0.786	0.823	0.850
0	0	0	0	0	0	0	0	0	0	0	0	0	0	0
.025	-1.163	-.310	-1.323	-1.380	-1.491	-1.491	-1.501	-1.540	-1.483	-1.480	-1.461	-1.475	-1.441	-1.395
.050	-.790	-.899	-.924	-.984	-1.138	-1.158	-1.219	-1.339	-1.326	-1.354	-1.367	-1.378	-1.368	-1.311
.100	-.287	-.516	-.345	-.350	-.459	-.519	-.559	-.726	-.858	-.978	-1.081	-1.121	-1.129	-1.098
.150	.031	-.139	.025	.022	.020	.011	0	.004	-.179	-.618	-.730	-.905	-.927	-.901
.200	.283	.280	.305	.345	.329	.342	.376	.361	.380	.241	-.359	-.653	-.750	-.721
.250	.428	.459	.481	.538	.536	.575	.630	.650	.664	.633	.229	-.361	-.554	-.539
.300	.480	.499	.534	.584	.614	.659	.729	.795	.842	.820	.565	.140	-.411	-.406
.350	.509	.530	.563	.611	.651	.682	.742	.801	.998	1.007	.802	.555	-.257	-.271
.400	.503	.549	.578	.609	.657	.690	.732	.778	.899	1.131	.998	.853	-.100	-.161
.450	.500	.560	.594	.640	.661	.722	.741	.798	.930	1.227	1.123	1.031	.140	-.066
.500	.481	.502	.530	.578	.594	.634	.664	.675	.701	1.101	1.086	1.033	.415	-.061
.550	.470	.483	.503	.550	.560	.582	.602	.614	.588	.845	1.070	.991	.589	-.062
.600	.444	.450	.470	.515	.500	.525	.547	.541	.529	.530	.800	.800	.601	-.179
.700	.373	.389	.399	.420	.459	.437	.440	.440	.445	.395	.411	.461	.461	-.408
.800	.300	.291	.298	.300	.479	.309	.320	.309	.300	.287	.222	.245	.300	-.440
.875	.210	.191	.183	.199	.379	.181	.181	.187	.148	.176	.124	.158	.237	-.421
.900	.190	.168	.159	.183	.346	.159	.158	.142	.129	.140	.087	.126	.204	-.417

TABLE Vd.—EXPERIMENTAL LOAD DATA

[NACA 4415 Section Angle of Attack, $\alpha_0 = 0^\circ$]

Station x/c	Values of load parameter, $P = P_l - P_u$, for different Mach numbers													
	0.301	0.397	0.500	0.550	0.600	0.626	0.649	0.672	0.699	0.730	0.757	0.784	0.812	0.843
0	0	0	0	0	0	0	0	0	0	0	0	0	0	0
.025	-.279	-.320	-.365	-.431	-.475	-.500	-.580	-.629	-.719	-.909	-1.000	-1.105	-1.144	-1.166
.050	-.081	-.118	-.145	-.219	-.297	-.282	-.362	-.439	-.450	-.761	-.865	-.989	-1.049	-1.065
.100	.236	.235	.241	.225	.185	.189	.110	.040	-.080	-.341	-.642	-.795	-.845	-.872
.150	.455	.479	.540	.523	.524	.532	.496	.465	.363	.099	-.220	-.598	-.675	-.710
.200	.583	.630	.701	.721	.761	.800	.780	.760	.680	.581	.429	-.340	-.520	-.573
.250	.700	.737	.828	.870	.944	1.002	1.031	1.057	.991	.845	.740	.050	-.303	-.388
.300	.735	.770	.861	.890	.951	1.025	1.120	1.211	1.160	1.022	.909	.571	-.142	-.265
.350	.710	.755	.837	.864	.924	1.020	1.060	1.349	1.310	1.218	1.069	.890	.237	-.119
.400	.682	.725	.801	.838	.908	.931	.999	1.340	1.402	1.303	1.135	1.020	.540	-.026
.450	.664	.705	.785	.821	.879	.891	.881	1.242	1.369	1.300	1.040	1.028	.763	-.001
.500	.640	.666	.710	.719	.749	.755	.750	.791	1.251	1.195	1.002	.874	.772	-.070
.550	.586	.600	.653	.659	.688	.698	.702	.631	.770	.909	.798	.716	.660	-.166
.600	.519	.558	.598	.599	.618	.601	.620	.571	.589	.696	.641	.581	.562	-.259
.700	.448	.482	.498	.498	.482	.480	.481	.460	.411	.408	.401	.425	.442	-.173
.800	.329	.333	.343	.339	.321	.328	.320	.317	.280	.230	.242	.309	.362	-.042
.875	.217	.213	.196	.191	.188	.180	.178	.169	.163	.135	.177	.240	.277	-.081
.900	.181	.170	.180	.156	.141	.131	.130	.137	.125	.109	.159	.229	.260	-.082

TABLE Ve.—EXPERIMENTAL LOAD DATA

[NACA 4415 Section Angle of Attack, $\alpha_0 = 2^\circ$]

Station x/c	Values of load parameter, $P = P_l - P_u$, for different Mach numbers													
	0.302	0.401	0.501	0.551	0.602	0.627	0.649	0.680	0.706	0.734	0.761	0.788	0.817	0.845
0	0	0	0	0	0	0	0	0	0	0	0	0	0	0
.025	.665	.655	.650	.555	.495	.430	.340	.165	-.020	-.285	-.475	-.600	-.675	-.730
.050	.645	.635	.655	.600	.560	.485	.390	.210	.005	-.225	-.455	-.580	-.650	-.695
.100	.780	.795	.890	.860	.850	.815	.740	.570	.380	.160	-.120	-.410	-.510	-.565
.150	.895	.905	1.030	1.025	1.090	1.085	1.020	.855	.705	.500	.250	-.140	-.365	-.420
.200	.950	.990	1.125	1.160	1.240	1.255	1.260	1.140	.980	.815	.630	.255	-.150	-.270
.250	.985	1.035	1.185	1.225	1.350	1.445	1.475	1.345	1.195	1.075	.910	.740	.125	-.100
.300	.985	1.020	1.175	1.200	1.305	1.485	1.620	1.495	1.355	1.210	1.050	.900	.650	.030
.350	.940	.970	1.120	1.135	1.225	1.390	1.605	1.595	1.460	1.285	1.120	.990	.870	.170
.400	.890	.920	1.070	1.075	1.125	1.170	1.560	1.550	1.465	1.330	1.095	1.000	.955	.280
.450	.830	.870	.975	.970	.980	.955	1.170	1.540	1.410	1.310	1.015	.945	.940	.490
.500	.740	.750	.870	.860	.860	.855	.800	1.660	1.240	1.135	.855	.815	.835	.565
.550	.675	.715	.780	.785	.780	.775	.735	.770	.890	.865	.715	.680	.685	.600
.600	.625	.645	.705	.700	.695	.695	.660	.590	.660	.715	.605	.595	.575	.565
.700	.520	.520	.555	.535	.530	.520	.500	.415	.385	.440	.455	.455	.460	.485
.800	.365	.360	.385	.350	.335	.325	.310	.270	.240	.280	.345	.370	.380	.420
.875	.235	.220	.240	.195	.245	.235	.175	.165	.155	.215	.305	.345	.335	.390
.900	.200	.195	.230	.160	.235	.235	.240	.220	.140	.190	.280	.310	.300	.345

TABLE Vf.—EXPERIMENTAL LOAD DATA

[NACA 4415 Section Angle of Attack, $\alpha_0=4^\circ$]

Station	Values of load parameter, $P=P_l-P_u$, for different Mach numbers														
	x/c	0.302	0.401	0.501	0.549	0.596	0.627	0.651	0.682	0.705	0.736	0.760	0.787	0.818	0.844
0	0	0	0	0	0	0	0	0	0	0	0	0	0	0	0
.025	1.455	1.430	1.480	1.390	1.250	1.120	.855	.620	.390	.165	0	0	-.195	-.350	-.445
.050	1.360	1.360	1.465	1.405	1.305	1.080	.930	.690	.470	.245	.060	-.150	-.300	-.370	-.370
.100	1.295	1.315	1.470	1.515	1.500	1.395	1.170	.960	.750	.525	.350	.095	-.140	-.235	-.235
.150	1.285	1.330	1.515	1.570	1.650	1.575	1.390	1.190	.995	.790	.625	.380	.055	-.135	-.135
.200	1.275	1.315	1.545	1.590	1.815	1.755	1.585	1.385	1.205	1.035	.875	.675	.355	-.055	-.055
.250	1.265	1.300	1.505	1.560	1.830	1.915	1.760	1.555	1.375	1.220	1.070	.905	.785	.295	.295
.300	1.215	1.255	1.450	1.490	1.740	1.850	1.740	1.545	1.390	1.260	1.125	.990	.910	.655	.655
.350	1.150	1.165	1.360	1.415	1.695	1.845	1.735	1.550	1.395	1.250	1.135	1.000	.935	.870	.870
.400	1.075	1.065	1.195	1.180	1.360	1.715	1.705	1.435	1.265	1.140	1.010	.905	.905	.975	.975
.450	.970	.990	1.120	1.115	1.120	1.055	1.305	1.175	1.060	.955	.875	.770	.825	.945	.945
.500	.865	.880	.985	.975	.985	.865	1.000	.965	.890	.820	.765	.675	.710	.835	.835
.550	.790	.800	.885	.885	.885	.795	.770	.795	.770	.730	.700	.640	.645	.715	.715
.600	.720	.725	.795	.775	.765	.700	.625	.640	.655	.650	.635	.600	.600	.645	.645
.700	.565	.565	.600	.580	.565	.520	.435	.425	.495	.520	.535	.525	.505	.545	.545
.800	.375	.375	.385	.370	.350	.320	.280	.290	.355	.405	.450	.490	.460	.505	.505
.875	.235	.240	.250	.200	.210	.200	.180	.220	.285	.330	.390	.445	.425	.480	.480
.900	.190	.200	.210	.170	.160	.155	.160	.185	.255	.330	.355	.400	.405	.425	.425

TABLE Vg.—EXPERIMENTAL LOAD DATA

[NACA 4415 Section Angle of Attack, $\alpha_0=6^\circ$]

Station	Values of load parameter, $P=P_l-P_u$, for different Mach numbers														
	x/c	0.301	0.400	0.501	0.550	0.601	0.628	0.654	0.684	0.709	0.739	0.763	0.792	0.820	0.850
0	0	0	0	0	0	0	0	0	0	0	0	0	0	0	0
.025	2.287	2.339	2.321	2.217	1.871	1.564	1.288	1.010	.837	.601	.421	.264	.093	-.040	-.040
.050	2.077	2.115	2.244	2.211	1.920	1.621	1.331	1.064	.891	.655	.481	.310	.059	-.011	-.011
.100	1.795	1.891	2.070	2.220	2.002	1.746	1.478	1.251	1.068	.851	.675	.515	.290	.129	.129
.150	1.696	1.793	1.952	2.174	2.149	1.918	1.646	1.460	1.287	1.072	.920	.761	.544	.305	.305
.200	1.600	1.699	1.875	2.059	2.259	2.041	1.819	1.605	1.442	1.250	1.103	.964	.762	.567	.567
.250	1.546	1.630	1.792	1.965	2.160	1.975	1.770	1.629	1.469	1.290	1.178	1.060	.926	.835	.835
.300	1.460	1.539	1.689	1.860	2.135	1.976	1.761	1.583	1.460	1.274	1.162	1.080	.990	.980	.980
.350	1.339	1.370	1.457	1.501	2.049	1.859	1.618	1.408	1.277	1.129	1.083	.991	.981	1.049	1.049
.400	1.190	1.245	1.305	1.360	1.373	1.406	1.285	1.189	1.097	.931	.875	.794	.880	1.080	1.080
.450	1.128	1.169	1.236	1.267	1.093	1.111	1.044	1.024	.944	.826	.782	.711	.776	1.078	1.078
.500	.988	1.020	1.064	1.097	.968	.911	.879	.902	.855	.767	.719	.680	.704	1.055	1.055
.550	.889	.919	.949	.978	.830	.769	.745	.799	.776	.722	.699	.663	.666	1.000	1.000
.600	.791	.819	.835	.848	.724	.648	.644	.716	.700	.670	.659	.663	.670	.900	.900
.700	.618	.619	.615	.610	.510	.459	.480	.570	.580	.591	.600	.601	.590	.750	.750
.800	.400	.397	.364	.369	.309	.309	.352	.449	.476	.505	.538	.563	.565	.709	.709
.875	.209	.204	.198	.191	.191	.221	.280	.369	.389	.430	.449	.509	.492	.670	.670
.900	.191	.181	.153	.159	.155	.185	.238	.344	.353	.380	.426	.460	.465	.620	.620

TABLE Vh.—EXPERIMENTAL LOAD DATA

[NACA 4415 Section Angle of Attack, $\alpha_0=8^\circ$]

Station	Values of load parameter, $P=P_l-P_u$, for different Mach numbers															
	x/c	0.301	0.400	0.500	0.525	0.551	0.577	0.604	0.630	0.656	0.683	0.712	0.741	0.766	0.796	0.833
0	0	0	0	0	0	0	0	0	0	0	0	0	0	0	0	0
.025	3.040	3.299	3.185	2.995	2.860	2.597	2.220	1.962	1.728	1.449	1.229	1.040	.857	.683	.508	.508
.050	2.721	2.895	3.080	2.990	2.913	2.640	2.260	2.000	1.760	1.478	1.264	1.066	.879	.713	.536	.536
.100	2.271	2.360	2.687	2.764	2.875	2.670	2.320	2.295	1.868	1.601	1.398	1.200	1.021	.857	.669	.669
.150	2.030	2.130	2.420	2.469	2.742	2.710	2.360	2.160	1.941	1.699	1.540	1.359	1.201	1.038	.858	.858
.200	1.906	1.990	2.259	2.285	2.611	2.595	2.320	2.119	1.938	1.720	1.570	1.404	1.264	1.146	1.030	1.030
.250	1.816	1.873	2.086	2.054	2.362	2.558	2.227	2.039	1.858	1.642	1.530	1.375	1.270	1.190	1.115	1.115
.300	1.621	1.665	1.807	1.770	1.670	2.295	1.929	1.668	1.540	1.375	1.205	1.103	1.060	1.137	1.125	1.125
.350	1.489	1.517	1.614	1.584	1.560	1.584	1.561	1.369	1.320	1.218	1.021	.940	.875	.969	1.070	1.070
.400	1.349	1.368	1.441	1.424	1.399	1.299	1.298	1.169	1.169	1.100	.940	.851	.809	.870	.938	.938
.450	1.249	1.265	1.320	1.280	1.269	1.156	1.095	1.038	1.044	.999	.880	.815	.765	.797	.852	.852
.500	1.076	1.055	1.126	1.195	1.086	1.000	.941	.918	.959	.918	.856	.795	.742	.763	.805	.805
.550	.959	.963	.971	.950	.940	.869	.837	.806	.877	.846	.806	.764	.730	.740	.762	.762
.600	.840	.840	.859	.826	.832	.756	.745	.731	.808	.809	.800	.759	.741	.745	.769	.769
.700	.610	.605	.570	.539	.524	.486	.528	.560	.625	.651	.671	.661	.665	.662	.665	.665
.800	.334	.351	.310	.291	.286	.308	.388	.440	.501	.550	.590	.592	.620	.629	.670	.670
.875	.200	.236	.248	.223	.228	.220	.300	.399	.439	.486	.520	.548	.583	.584	.650	.650
.900	.157	.151	.072	.160	.165	.189	.266	.347	.391	.441	.472	.500	.532	.536	.619	.619

TABLE Vi.—EXPERIMENTAL LOAD DATA

[NACA 4415 Section Angle of Attack, $\alpha_0=10^\circ$]

Station	Values of load parameter, $P=P_l-P_u$, for different Mach numbers															
	x/c	0.301	0.401	0.502	0.525	0.551	0.580	0.605	0.637	0.658	0.687	0.714	0.748	0.775	0.808	0.841
0	0	0	0	0	0	0	0	0	0	0	0	0	0	0	0	0
.025	3.668	3.562	3.762	3.520	3.198	2.844	2.537	2.259	2.059	1.823	1.539	1.363	1.190	1.039	.918	.918
.050	3.278	3.345	3.731	3.539	3.221	2.888	2.577	2.300	2.199	1.858	1.566	1.363	1.209	1.060	.923	.923
.100	2.660	2.761	3.168	3.360	3.211	2.830	2.580	2.290	2.114	1.910	1.667	1.469	1.310	1.154	1.029	1.029
.150	2.319	2.389	2.585	3.090	2.990	2.670	2.455	2.208	2.040	1.870	1.682	1.528	1.392	1.275	1.169	1.169
.200	2.089	2.133	2.222	2.238	2.929	2.449	2.295	2.008	1.890	1.757	1.598	1.497	1.482	1.318	1.298	1.298
.250	1.959	2.016	2.112	1.975	2.335	2.079	1.915	1.770	1.652	1.485	1.283	1.243	1.224	1.280	1.373	1.373
.300	1.742	1.771	1.838	1.789	1.718	1.631	1.506	1.508	1.399	1.240	1.019	.976	.905	1.038	1.403	1.403
.350	1.567	1.604	1.591	1.551	1.444	1.415	1.327	1.387	1.303	1.155	.962	.912	.850	.924	1.387	1.387
.400	1.400	1.413	1.386	1.340	1.251	1.230	1.166	1.260	1.217	1.100	.925	.880	.815	.860	1.300	1.300
.450	1.268	1.288	1.205	1.177	1.091	1.080	1.039	1.154	1.130	1.040	.896	.851	.798	.838	1.219	1.219
.500	1.086	1.093	.992	.962	.929	.939	.926	1.064	1.068	1.009	.865	.838	.786	.827	1.144	1.144
.550	.940	.942	.818	.791	.780	.828	.845	.971	1.004	.977	.858	.818	.776	.810	1.086	1.086
.600	.803	.765	.656	.620	.631	.720	.748	.889	.935	.938	.829	.820	.788	.825	1.066	1.066
.700	.539	.498	.451	.423	.441	.535	.597	.720	.785	.807	.740	.740	.716	.759	.989	.989
.800	.311	.316	.352	.339	.320	.420	.494	.579	.640	.685	.715	.675	.686	.740	.952	.952
.875	.211	.217	.286	.260	.266	.349	.392	.497	.558	.591	.688	.679	.700	.721	.940	.940
.900	.175	.165	.242	.230	.222	.303	.346	.440	.473	.527	.675	.600	.627	.671	.898	.898

TABLE Vj.—EXPERIMENTAL LOAD DATA

[NACA 4415 Section Angle of Attack, $\alpha_0=12^\circ$]

Station	Values of load parameter, $P=P_l-P_u$, for different Mach numbers													
	x/c	0.404	0.502	0.521	0.556	0.581	0.605	0.638	0.662	0.696	0.720	0.748	0.778	0.819
0	0	0	0	0	0	0	0	0	0	0	0	0	0	0
.025	4.260	4.229	3.860	3.455	3.145	2.895	2.620	2.370	2.120	1.880	1.705	1.555	1.385	1.385
.050	3.772	4.158	3.845	3.415	3.140	2.870	2.725	2.385	2.140	1.910	1.725	1.560	1.385	1.385
.100	3.012	3.613	3.520	3.190	2.925	2.690	2.475	2.270	2.095	1.905	1.775	1.620	1.450	1.450
.150	2.497	2.332	3.325	2.880	2.590	2.400	2.225	2.035	1.915	1.770	1.670	1.565	1.450	1.450
.200	2.250	2.216	2.180	2.245	2.030	1.955	1.805	1.675	1.505	1.385	1.290	1.505	1.460	1.460
.250	2.040	2.013	1.840	1.820	1.700	1.685	1.590	1.445	1.265	1.125	1.080	1.150	1.325	1.325
.300	1.762	1.699	1.605	1.520	1.435	1.460	1.415	1.300	1.145	1.040	.990	1.030	1.110	1.110
.350	1.508	1.414	1.370	1.340	1.300	1.365	1.325	1.230	1.105	1.005	.955	.980	1.065	1.065
.400	1.275	1.144	1.175	1.150	1.175	1.255	1.260	1.185	1.080	.970	.930	.945	1.000	1.000
.450	1.065	.908	.980	1.005	1.050	1.135	1.170	1.130	1.020	.945	.900	.925	.990	.990
.500	.847	.731	.815	.880	.960	1.065	1.105	1.085	.995	.925	.885	.910	.965	.965
.550	.705	.610	.680	.785	.895	.995	1.035	1.055	.970	.905	.870	.900	.950	.950
.600	.593	.550	.600	.695	.800	.920	.960	.970	.915	.875	.845	.880	.925	.925
.700	.488	.478	.480	.570	.685	.800	.835	.890	.850	.820	.795	.835	.885	.885
.800	.412	.429	.415	.475	.580	.675	.710	.760	.760	.760	.750	.785	.845	.845
.875	.345	.352	.365	.420	.495	.560	.610	.635	.690	.680	.675	.705	.770	.770
.900	.315	.324	.345	.365	.420	.500	.560	.565	.600	.600	.630	.650	.730	.730

TABLE Vk.—EXPERIMENTAL LOAD DATA

[NACA 4415 Section Angle of Attack, $\alpha_0=14^\circ$]

Station	Values of load parameter, $P=P_l-P_u$, for different Mach numbers													
	x/c	0.404	0.503	0.530	0.559	0.586	0.611	0.636	0.661	0.693	0.722	0.757	0.783	0.825
0	0	0	0	0	0	0	0	0	0	0	0	0	0	0
.025	4.499	4.514	3.938	3.579	3.295	3.080	2.782	2.617	2.395	2.220	2.015	1.835	1.598	1.598
.050	3.973	4.263	3.788	3.405	3.107	2.938	2.686	2.553	2.379	2.240	2.008	1.830	1.600	1.600
.100	2.928	3.778	3.319	2.890	2.580	2.468	2.332	2.231	2.145	2.055	1.911	1.785	1.625	1.625
.150	2.477	2.227	2.338	2.115	1.928	1.822	1.705	1.630	1.595	1.664	1.698	1.645	1.665	1.665
.200	2.149	2.001	1.867	1.705	1.616	1.518	1.425	1.359	1.265	1.246	1.250	1.297	1.749	1.749
.250	1.844	1.694	1.608	1.495	1.445	1.398	1.306	1.270	1.195	1.160	1.168	1.145	1.795	1.795
.300	1.514	1.381	1.357	1.289	1.305	1.281	1.226	1.205	1.138	1.100	1.099	1.089	1.820	1.820
.350	1.214	1.096	1.178	1.198	1.225	1.228	1.185	1.150	1.107	1.069	1.071	1.046	1.828	1.828
.400	1.013	.923	1.030	1.082	1.148	1.168	1.144	1.102	1.073	1.058	1.042	1.010	1.807	1.807
.450	.810	.794	.918	1.008	1.064	1.107	1.081	1.066	1.042	1.020	1.006	.994	1.777	1.777
.500	.720	.743	.829	.969	1.005	1.040	1.032	1.015	1.015	.992	.994	.969	1.724	1.724
.550	.660	.701	.775	.912	.955	1.009	1.018	.993	.995	.994	.965	.960	1.665	1.665
.600	.629	.669	.727	.858	.900	.950	.966	.964	.970	.972	.931	.930	1.617	1.617
.700	.562	.624	.629	.720	.776	.830	.861	.857	.890	.899	.880	.881	1.519	1.519
.800	.510	.557	.565	.650	.689	.738	.767	.780	.815	.838	.834	.850	1.450	1.450
.875	.441	.481	.497	.560	.572	.627	.647	.661	.699	.745	.754	.797	1.382	1.382
.900	.408	.446	.450	.492	.515	.561	.572	.599	.645	.688	.680	.741	1.325	1.325

TABLE VI.—EXPERIMENTAL LOAD DATA

[NACA 4415 Section Angle of Attack, $\alpha_0=16^\circ$]

Station x/c	Values of load parameter, $P=P_l-P_u$, for different Mach numbers										
	0.301	0.399	0.507	0.535	0.559	0.587	0.613	0.640	0.665	0.692	0.719
0	0	0	0	0	0	0	0	0	0	0	0
.025	4.475	4.680	4.213	3.818	3.399	3.100	2.760	2.781	2.629	2.590	2.460
.050	3.975	4.275	3.938	3.498	3.075	2.804	2.440	2.495	2.399	2.444	2.417
.100	2.900	2.932	2.766	2.511	2.197	2.056	1.837	1.773	1.831	2.053	2.100
.150	2.337	2.377	2.024	1.927	1.725	1.701	1.558	1.384	1.551	1.598	1.476
.200	1.962	1.973	1.677	1.604	1.500	1.480	1.421	1.330	1.388	1.380	1.326
.250	1.625	1.613	1.413	1.391	1.369	1.377	1.338	1.278	1.308	1.278	1.249
.300	1.275	1.222	1.188	1.235	1.240	1.251	1.250	1.214	1.235	1.205	1.211
.350	.962	.960	1.050	1.125	1.180	1.218	1.210	1.148	1.208	1.175	1.155
.400	.813	.810	.962	1.030	1.115	1.159	1.149	1.100	1.152	1.138	1.120
.450	.738	.750	.885	.970	1.047	1.097	1.088	1.065	1.106	1.089	1.081
.500	.700	.720	.841	.924	.990	1.045	1.046	1.036	1.050	1.049	1.059
.550	.663	.675	.814	.878	.940	.997	1.016	1.004	1.015	1.015	1.021
.600	.650	.660	.770	.820	.879	.930	.950	.949	.955	.970	1.000
.700	.625	.623	.709	.731	.790	.837	.838	.876	.865	.899	.939
.800	.588	.555	.643	.659	.697	.729	.740	.775	.773	.820	.869
.875	.513	.458	.561	.562	.610	.635	.621	.675	.670	.726	.800
.900	.475	.405	.512	.491	.539	.561	.549	.595	.602	.641	.711

TABLE VI.—NACA 65₂-215 ($\alpha=0.5$)

[Stations and ordinates given in percent of airfoil chord]

Upper surface		Lower surface	
Station	Ordinate	Station	Ordinate
0	0	0	0
.370	1.185	.630	-1.047
.605	1.445	.895	-1.251
1.086	1.841	1.414	-1.547
2.311	2.575	2.689	-2.057
4.786	3.679	5.214	-2.797
7.276	4.547	7.724	-3.359
9.774	5.274	10.226	-3.822
14.783	6.448	15.217	-4.552
19.806	7.344	20.194	-5.096
24.835	8.024	25.165	-5.500
29.871	8.519	30.129	-5.783
34.912	8.838	35.088	-5.952
39.958	8.984	40.042	-6.012
45.009	8.925	44.991	-5.929
50.076	8.638	49.924	-5.698
55.131	8.112	54.869	-5.326
60.154	7.396	59.846	-4.834
65.157	6.546	64.643	-4.256
70.147	5.589	69.853	-3.607
75.127	4.568	74.873	-2.916
80.100	3.509	79.900	-2.203
85.069	2.455	84.931	-1.497
90.039	1.450	89.961	-.836
95.013	.572	94.987	-.284
100.000	0	100.000	0

L. E. radius: 1.505. Slope of radius through L. E.: 0.116

TABLE VII.—NACA 66₂-215 ($\alpha=0.6$)

[Stations and ordinates given in percent of airfoil chord]

Upper surface		Lower surface	
Station	Ordinate	Station	Ordinate
0	0	0	0
.379	1.168	.621	-1.038
.616	1.413	.884	-1.231
1.101	1.777	1.399	-1.499
2.329	2.466	2.671	-1.978
4.807	3.496	5.193	-2.664
7.298	4.313	7.702	-3.191
9.794	5.019	10.206	-3.645
14.801	6.150	15.199	-4.352
19.818	7.030	20.182	-4.892
24.842	7.721	25.158	-5.307
29.871	8.245	30.129	-5.617
34.904	8.622	35.096	-5.836
39.910	8.862	40.060	-5.968
44.979	8.969	45.021	-6.021
50.021	8.934	49.979	-5.986
55.069	8.738	54.931	-5.850
60.132	8.336	59.868	-5.584
65.179	7.658	64.821	-5.148
70.186	6.695	69.814	-4.493
75.170	5.575	74.830	-3.723
80.139	4.352	79.861	-2.874
85.099	3.087	84.901	-1.999
90.057	1.838	89.943	-1.136
95.020	.725	94.980	-.395
100.000	0	100.000	0

L. E. radius: 1.384. Slope of radius through L. E.: 0.110

TABLE VIII.—NACA 0015

[Stations and ordinates given in percent of airfoil chord]

Station	Ordinate
0	0
1.250	2.367
2.500	3.268
5.000	4.443
7.500	5.250
10.000	5.853
15.000	6.681
20.000	7.172
25.000	7.427
30.000	7.502
40.000	7.254
50.000	6.618
60.000	5.704
70.000	4.580
80.000	3.279
90.000	1.810
95.000	1.008
100.000	(.158)
100.000	0

L. E. radius: 2.48

TABLE IX.—NACA 23015

[Stations and ordinates given in percent of airfoil chord]

Station	Upper surface	Lower surface
0	0	0
1.25	3.34	-1.54
2.50	4.44	-2.25
5.00	5.89	-3.04
7.50	6.91	-3.61
10.00	7.64	-4.09
15.00	8.52	-4.84
20.00	8.92	-5.41
25.00	9.08	-5.78
30.00	9.05	-5.96
40.00	8.59	-5.92
50.00	7.74	-5.50
60.00	6.61	-4.81
70.00	5.25	-3.91
80.00	3.73	-2.83
90.00	2.04	-1.59
95.00	1.12	-.90
100.00	(.16)	(-.16)
100.00	0	0

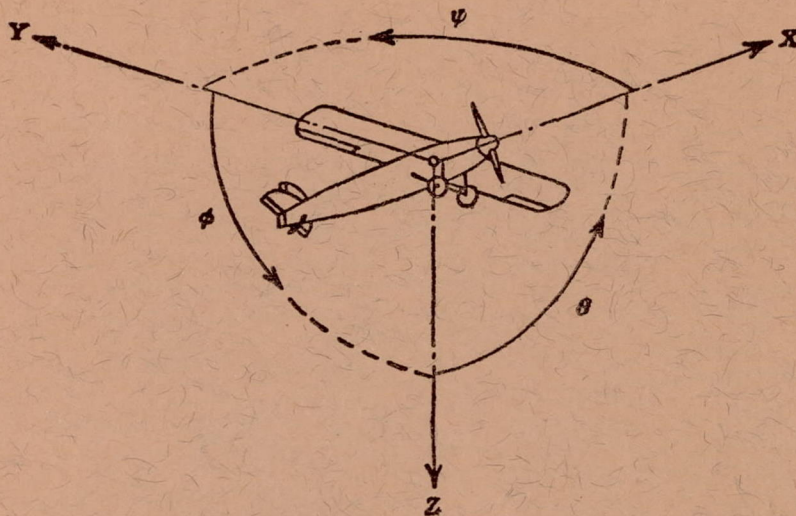
L. E. radius: 2.48. Slope of radius through L. E.: 0.305

TABLE X.—NACA 4415

[Stations and ordinates given in percent of airfoil chord]

Station	Upper surface	Lower surface
0	0	0
1.25	3.07	-1.79
2.50	4.17	-2.48
5.00	5.74	-3.27
7.50	6.91	-3.71
10.00	7.84	-3.98
15.00	9.27	-4.18
20.00	10.25	-4.15
25.00	10.92	-3.98
30.00	11.25	-3.75
40.00	11.25	-3.25
50.00	10.53	-2.72
60.00	9.30	-2.14
70.00	7.63	-1.55
80.00	5.55	-1.03
90.00	3.08	-.57
95.00	1.67	-.36
100.00	(.16)	(-.16)
100.00	-----	0

L. E. radius: 2.48. Slope of radius through L. E.: 0.200



Positive directions of axes and angles (forces and moments) are shown by arrows

Axis		Force (parallel to axis) symbol	Moment about axis			Angle		Velocities	
Designation	Sym- bol		Designation	Sym- bol	Positive direction	Designa- tion	Sym- bol	Linear (compo- nent along axis)	Angular
Longitudinal.....	X	X	Rolling.....	L	Y→Z	Roll.....	φ	u	p
Lateral.....	Y	Y	Pitching.....	M	Z→X	Pitch.....	θ	v	q
Normal.....	Z	Z	Yawing.....	N	X→Y	Yaw.....	ψ	w	r

Absolute coefficients of moment

$$C_l = \frac{L}{qbS} \quad C_m = \frac{M}{qcS} \quad C_n = \frac{N}{qbS}$$

(rolling) (pitching) (yawing)

Angle of set of control surface (relative to neutral position), δ . (Indicate surface by proper subscript.)

4. PROPELLER SYMBOLS

D	Diameter	P	Power, absolute coefficient $C_P = \frac{P}{\rho n^3 D^5}$
p	Geometric pitch	C_s	Speed-power coefficient $= \sqrt[5]{\frac{\rho V^5}{P n^2}}$
p/D	Pitch ratio	η	Efficiency
V'	Inflow velocity	n	Revolutions per second, rps
V_s	Slipstream velocity	Φ	Effective helix angle $= \tan^{-1} \left(\frac{V}{2\pi r n} \right)$
T	Thrust, absolute coefficient $C_T = \frac{T}{\rho n^2 D^4}$		
Q	Torque, absolute coefficient $C_Q = \frac{Q}{\rho n^2 D^5}$		

5. NUMERICAL RELATIONS

1 hp = 76.04 kg-m/s = 550 ft-lb/sec
 1 metric horsepower = 0.9863 hp
 1 mph = 0.4470 mps
 1 mps = 2.2369 mph

1 lb = 0.4536 kg
 1 kg = 2.2046 lb
 1 mi = 1,609.35 m = 5,280 ft
 1 m = 3.2808 ft